technische universität dortmund

fakultät für chemie und chemische biologie

NOVEL HYPERCOORDINATED ELEMENT COMPOUNDS. CONTRIBUTIONS TO CONTEMPORARY MAIN GROUP ELEMENTS CHEMISTRY

A dissertation submitted to the faculty of

Chemistry and Chemical Biology

in partial fulfillment of the requirements for the

degree of

Doctor Rerum Naturalium

(Dr. rer. nat.)

By

M. Sc. Hazem Alnasr

Dortmund, Germany

Approved by

Prof. Dr. KLAUS JURKSCHAT

Prof. Dr. NORBERT KRAUSE

TO MY PARENTS…

TO MY SISTERS…

TO MY BROTHERS…

ACKNOWLEDGMENT

To my advisor **PROF. DR. KLAUS JURKSCHAT** I would like to express my sincere gratitude for the support of my Ph.D course, the immense knowledge, for the motivation and the patience. Without his guidance during all the time of research I couldn't have imagined to complete this thesis.

Next to my advisor, I would like to express my gratitude to my thesis committee, especially **PROF. DR. NORBERT KRAUSE** for agreeing to be my second examiner.

I would like to express my gratitude to **DR. WOLF HILLER**, **MR. BENJAMIN KISSEL**, and **MR. JAN SCHONERT** for measuring the NMR samples, **MRS. SYLVIA MARZIAN** and **MR. MARKUS HÜFFNER** for the ESI-MS and the CHN elemental analysis.

To **DR. CHRISTINA KRABBE**, and **DR. MICHAEL Lutter** I am deeply grateful for the support concerning crystallography. To **CHRISTINA** I want like to show my greatest appreciation for her help in the experimental and the theoretical background of the crystallography.

My special thanks goes also to **DR. MATTHIAS GAWRON** for the nice time that we spent together.

I am deeply grateful to **B. SC. ANDRÉ PLATZEK**, **MRS. LAURA SCHNEIDER** and **MR. MARVIN VON KÖLLN** for their support in the laboratory.

I would like to offer my special thanks to **MRS. HELGA SCHULTE** and **MRS. PEGGY SIEG** for their help in managing the bureaucratic and the organization stuff.

Last but not least, I would like to show my greatest appreciation to my family for the infinite support during my study and my life in general.

Say not, "I have found the truth," but rather, "I have found a truth."

Say not, "I have found the path of the soul." Say rather, "I have met the soul walking upon my path."

GIBRAN KAHLIL GIBRAN,

The Prophet

INDEX

ABBREVIATIONS

a, b, c	Cell parameter
Ad	Adamantyl
α, β, γ	Cell Parameter (Angels)
Eq.	Equivalents
wB97XD	The latest functional from Head-Gordon
COSY	Correlated Spectroscopy
DEPT	Distortionless Enhancement by Polarization Transfer
Dipp	2,6-Di*iso*propylphenyl
DMAP	4-(Dimethylamino)-pyridin
DFT	Density Functional Theory
DOSY	Diffusion Ordered Spectroscopy
d	Doublet
dd	Doublet of Doublet
dt	Doublet of Triplett
ESI	Electrospray
Et	Ethyl
h	Hour
HR	High resolution
Hz	Hertz
i	ipso-Position of the aromatic ring
IR	Infrared spectroscopy
INEPT	Insensitive Nuclei Enhanced by Polarization Transfer
iPr	*Iso*Propyl
^{n}J	Coupling Constant in Hz over n bonds
L	Ligand
LDA	Lithiumdi*iso*propylamide
MS	Mass spectrometry
Me	Methyl
m	meta-Position of the aromatic ring
ρ	Density
Z	Number of molecules in unit cell

Mes	Mesityl
m	Multiplet
NPA	Natural Population Analysis
NHC	N Heterocyclic Carbene
NMR	Nuclear Magnetic Resonance Spectroscopy
NOESY	Nuclear Overhauser Enhancement Spectroscopy
NBO	Natural Bond Orbital
OAc	Acetat
o	Ortho-Position of the Aromatic Ring
ppm	Parts Per Million
Ph	Phenyl
p	Para-Position of the aromatic ring
q	Quartet
RT	Room temperature
s	Singlet
sept	Septet
m.p.	Melting point
T	Temperature
THF	Tetrahydrofuran
*t*Bu	*Tert*Butyl
t	Triplett
UV	Ultraviolet
Vis	Visible
$\nu_{1/2}$	Full Width at Half Maximum in Hz
δ	Chemical shift in ppm
$\widetilde{\nu}$	Wavenumber in cm^{-1}
2D	Two dimensional
m/z	Mass/Charge
Å	Ångström
σ	Standard Deviation
°	Grad
V	Volume of Unit Cell

GENERAL INTRODUCTION

Over many decades, the chemistry of carbon was dominated by compounds containing this element in its tetravalent state. The chemistry of divalent carbon got momentum when ARDUENGO published his N-heterocyclic carbene (NHC) in 1990 (**A**, Chart 1).[1] Since then, several review articles summarized the achievement in this domain of chemistry.[2]

The heavier group 14 elements adopt the divalent state more easily, which is explained by the simple model of the inert electron pair.[3,4] And this effect is more pronounced for tin than for silicon.

There are two general strategies to stabilized Sn(II) compounds. The first one involves the use of bulky substituents which make the corresponding compounds kinetically inert towards polymerization. A classic example for this is LAPPERTS SnR_2 where (R = $CH(SiMe_3)_2$) which is monomeric in the solution but dimeric in the solid state[5] (**B**, Chart 1) and the first tin(II) amide (**C**, Chart 1) where (R = $N(SiMe)_3$).[6] The same concept of steric protection was also used by P. P. POWER to establish his outstanding position in the domain of low-valent main group element chemistry (**D**, Chart 1).[4,7]

The second concept is that of thermodynamic stabilization. It involves the use of substituents bearing heteroatoms capable of donating electron density into vacant orbitals at the low-valent elements. There is plethora for such compounds and selected examples are shown in chart 1.[8]

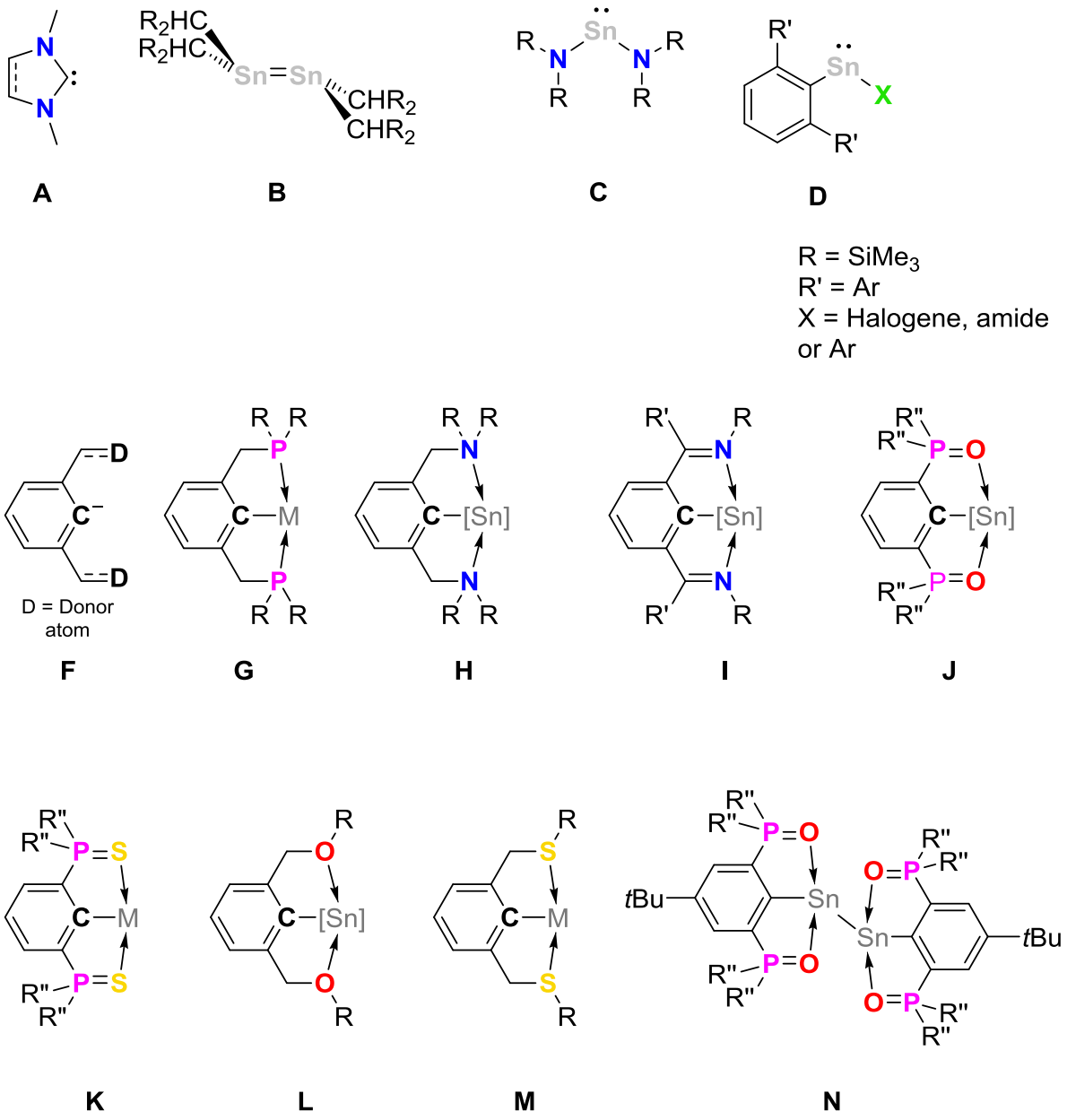

Chart 1. Examples of classic tin(II) derivatives including some Pincer-type ligands.

Sometimes a combination of both kinetic and thermodynamic stabilization is used. And for this reason a pincer compounds are applied, which are compound based on phenyl moiety and donor atoms (N, P, O[9] and S[10] atoms) bridged with CH_2, CH groups at C2 and C6. The donor atoms stabilize a metal-carbon bond thermodynamically by the formation of intramolecular coordination between the lone pair of the donor and the empty orbital of the metal.[11]

The first pincer-type proligand was reported by SHAW *et. al.* in 1976. It was synthesized by the treatment of 1,3-bis(bromomethyl)benzene with tBu$_2$PH.[12] This

pincer compound reacts with $PtCl_2L_2$, $PdCl_2L_2$, $RhCl_3 \cdot 3H_2O$ and $IrCl_3 \cdot xH_2O$ (L = C_6H_5CN) under mild conditions, according to the principle of hard and soft acids and bases (HSAB)[13], to give Pt(PCP)Cl, Pd(PCP)Cl, Rh(PCP)HCl and Ir(PCP)HCl, respectively (PCP = 1,3-bis[(di-*t*butylphosphino)methyl) benzene]) (**G**, Chart 1). VAN KOTEN *et. al.* reported the Pt(PCP)X and Pd(PCP)X where PCP = 1,3-bis[(*di*methylamino)methyl) benzene] and X = Cl, Br and I (**H**, Chart 1).[14] The later compounds were synthesized by the deprotonation of 1-bromo-2,6-bis[(*di*methylamino)methyl) benzene] with elemental lithium in diethyl ether[15] followed be the addition of the electrophile MX_2L_2 (M = Pt and Pd; X = Cl, Br and I; L = SEt_2 and 1,5-COD). And from the same team the first pincer-tin(IV) compound was reported in 1991,[16] while ZUCKERMAN *et. al.* reported the first Sn(II) with the same pincer compound in 1981 (**H**, Chart 1).[17]

Another class of pincer-precursor ligands were reported by JURKSCHAT *et. al.,* in which the donor groups are P=O and/or P=S (**J** and **K**, Chart 1) functional groups. MEHRING synthesized 1,3-$[P(O)R_2]_2C_6H_4$ (R = Ph or OEt) according to TAVS reaction[18] by heating di-bromophenyl and alkyl phosphite with $NiBr_2$ as a catalyst. The deprotonation of the compounds with lithiumdi*iso*propyl amide (LDA) followed by the addition of the corresponding electrophile produces {1-[M]-2,6-$[P(O)R_2]_2$}C_6H_3 or {1,5-di[M_2]-2,4-$[P(O)R_2]_2$}C_6H_2 (M = $SnPh_3$ or $SiMe_3$).[19]

To improve the later ligand precursors, *tert*butyl group was added to the phenyl ring and $(iPrO)_2P(O)$ instead of $(EtO)_2P(O)$ to produce 4-*t*Bu-2,6-$[P(O)(OiPr)_2]_2C_6H_2$- which allows the selective deprotonation with LDA at *ortho* position in respect to the both P=O functional groups. The *in situ* synthesized LiR reacts with $SnCl_2$ to obtain SnRCl (R = 4-*t*Bu-2,6-$[P(O)(OiPr)_2]_2C_6H_2$).[20,21] The reactivity of this compound was intensively studied toward transition metals such as $M(CO)_x$ (M = Cr, Fe and W); $PtCl_2L_2$, the oxidation with halogens and the reduction with KC_8.[21,22] The reduction product RSnSnR (**N**, figure 1) is instable in room temperature and decompose according to first order reaction to give the unique SnR_2 and elemental tin. In the molecular structure of SnR_2 it was found that the tin atom is stabilized thermodynamically by two P=O's that belong to both organic substitutions (Chart 2).

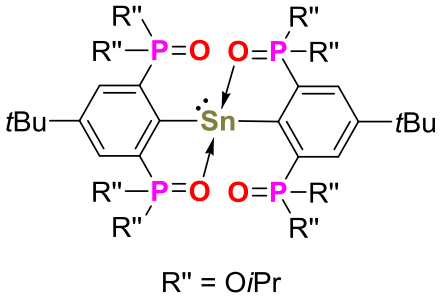

Chart 2. The diorganotin(II) compound obtained from the disproportionation of RSnSnR (R = 4-*t*Bu-2,6-[P(O)(O*i*Pr)$_2$]$_2$C$_6$H$_2$).

The (P=S) pincer compound 4-*t*Bu-2,6-[P(S)Ph$_2$]$_2$C$_6$H$_3$ (**K**, Chart 1) was synthesized by the lithium-halogen exchange of 1,3-dibromo-5-*t*Bu benzene with *n*BuLi at –78 °C, subsequent addition of PPh$_2$Cl and oxidation with S$_8$. The compounds PtRCl and PdRCl (R = 4-*t*Bu-2,6-[P(S)Ph$_2$]$_2$C$_6$H$_2$) are produced by C-H activation of the phenyl group with PtCl$_2$L$_2$ and PdCl$_2$L$_2$.[23]

LITERATURE

[1] a) H. W. Wanzlick, E. Schikora, *Chem. Ber.* **1961**, *94*, 2389; b) H. W. Wanzlick, E. Schikora, *Angew. Chem.* **1960**, *72*, 494; c) A. J. Arduengo III, R. L. Harlow, M. Kline, *J. Am. Chem. Soc.* **1991**, *113*, 361.

[2] a) F. E. Hahn, M. C. Jahnke, *Angew. Chem. Int. Ed.* **2008**, *47*, 3122; b) R. Hoffmann, R. Gleiter, F. B. Mallory, *J. Am. Chem. Soc.* **1960**, *92*, 1460; c) A. Nemirowski, P. R. Schreiner, *J. Org. Chem.* **2007**, *72*, 9533.

[3] D. S. Russell, *J. Phys. Chem.* **1958**, *62*, 353.

[4] P. P. Power, *Chem. Rev.* **1999**, *99*, 3463.

[5] a) P. J. Davidson and M. F. Lappert, *J. Chem. Soc., Chem. Comm* **1973**, 317; b) D. E. goldberg, P. B. hitchcock, M. F. Lappert and M. Thomas, *J. Chem. Soc., Dalton Trans.* **1986**, 2387; c) D. E. goldberg, D. H. Harris, M. F. Lappert and M. Thomas, *J. Chem. Soc., Chem. Comm* **1976**, 261.

[6] a) C. D. Schaeffer, L. K. Myers, M. S. Coley, J. C. Otter and C. H. Yoder, *J. Chem. Ed.* **1990**, *67*, 347; b) D. H. Harris and M. F. Lappert, *J. Chem. Soc., Chem. Comm* **1974**, 895.

[7] a) B. E. Eichler, L. Pu, M. Stander and P. P. Power, *Polyhedron* **2001**, *20*, 551; b) B. E. Eichler, P. P. Power, *Inorg. Chem.* **2000**, *39*, 5444; c) Y. Peng, R. C. Fischer, W. A. Merrill, J. Fischer, L. Pu, B. D. Ellis, J. C. Fettinger, R. H. Herber, P. P. Power, *Chem. Sci.* **2010**, *1*, 461; d) P. D. Andrew, S. Hino and P. P. Power, *J. Am. Chem. Soc.* **2003**, *125*, 7520;
e) R. S. Simons, L. Pu, M. M. Olmstead and P. P. Power, *Organometallics* **1997**, *16*, 1920; f) L. Pu, M. M. Olmstead, P. P. Power, *Organometallics* **1998**, *17*, 5602.

[8] a) *Organometallchemie*, Vieweg+Teubner, Wiesbaden, **2008**; b) B. G. McBurnett, A. H. Cowley, *Chem. Commun.* **1999**, 17; c) J.-L. Fauré, H. Gornitzka, R. Réau, D. Stalke, G. Bertrand, *Eur. J. Inorg. Chem.* **1999**, *1999*, 2295; d) S. K. Mandal, H. W. Roesky, *Chem. Commun.* **2010**, *46*, 6016; e) A. Tzschach, M. Scheer, K. Jurkschat, A. Zschunke and C. Mügge, *Z. Anorg. Allg. Chem.* **1983**, *502*, 158; f) M. Huang, E. K. Lermontova, K. V. Zaitsev, A. V. Churakov, Y. F. Oprunenko, J. A. Howard, S. S. Karlov, G. S. Zaitseva, *J. Organomet. Chem.* **2009**, *694*, 3828; g) L. Iovkova-Berends, T. Berends, T. Zöller, G. Bradtmöller, S. Herres-Pawlis, K. Jurkschat, *Eur. J. Inorg. Chem.* **2012**, *2012*, 3191;

h) W. P. Neumann, *Chem. Rev.* **1991**, *91*, 311; i) Y. Mizuhata, T. Sasamori, N. Tokitoh, *Chem. Rev.* **2009**, *109*, 3479; j) M. Asay, C. Jones, M. Driess, *Chemical reviews* **2011**, *111*, 354; k) V. Y. Lee, A. Sekiguchi, *Organometallic compounds of low-coordinate Si, Ge, Sn and Pb*. *From phantom species to stable compounds / by Vladimir Ya. Lee, Akira Sekiguchi*, Wiley, Oxford, **2010**; l) A. V. Zabula, F. E. Hahn, *Eur. J. Inorg. Chem.* **2008**, *2008*, 5165; m) M. Weidenbruch, *J. Organomet. Chem.* **2002**, *646*, 39.

[9] a) R. Jambor, L. Dostál, A. Růžička, I. Císařová, J. Brus, M. Holčapek, J. Holeček, *Organometallics* **2002**, *21*, 3996; b) L. Dostál, R. Jambor, A. Růžička, R. Jirásko, I. Císařová, J. Holeček, *J. Organomet. Chem.* **2006**, *691*, 35.

[10] a) C. A. Kruithof, H. P. Dijkstra, M. Lutz, A. L. Spek, Gebbink, Robertus J. M. Klein, G. van Koten, *Organometallics* **2008**, *27*, 4928; b) J. E. Kukowski, J. R. Lamb, V. A. Stepanova, I. P. Smoliakova, *Inorganic Chemistry Communications* **2012**, *26*, 64; c) N. Lucena, J. Casabó, L. Escriche, G. Sánchez-Castelló, F. Teixidor, R. Kivekäs, R. Sillanpää, *Polyhedron* **1996**, *15*, 3009.

[11] M. Albrecht and G. van Koten, *Angew. Chem. Int. Ed.* **2001**, *40*, 3750.

[12] C. J. Moulton, B. L. Shaw, *J. Chem. Soc., Dalton Trans.* **1976**, 1020.

[13] a) A. A. Tishkov, H. Mayr, *Angew. Chem. Int. Ed.* **2004**, *44*, 142; b) R. G. Pearson, *J. Am. Chem. Soc.* **1963**, *85*, 3533; c) R. G. Pearson, *J. Chem. Ed.* **1968**, *45*, 643; d) R. G. Pearson, *J. Chem. Ed.* **1968**, *45*, 581; e) R. D. Hancock, *Chem. Rev.* **1989**, *89*, 1875.

[14] D. M. Grove, G. Van Koten, J. N. Louwen J. G. Noltes, A. L. Spek, H. J. C. Ubbels, *J. Am. Chem. Soc.* **1982**, *104*, 6609.

[15] J. T. B. H. jastrzebski, G. Van koten, M. Konijn, C. H. Stam, *J. Am. Chem. Soc.* **1982**, *104*, 5490.

[16] a) J. T. Jastrzebski, E. Wehman, J. Boersma, G. van Koten, K. Goubitz, D. Heijdenrijk, *J. Organomet. Chem.* **1991**, *409*, 157; b) P. Steenwinkel, Jastrzebski, Johann T. B. H., B.-J. Deelman, D. M. Grove, H. Kooijman, N. Veldman, W. J. J. Smeets, A. L. Spek, G. van Koten, *Organometallics* **1997**, *16*, 5486; c) J. T. Jastrzebski, J. Boersma, G. van Koten, *J. Organomet. Chem.* **1991**, *413*, 43; d) J. T. Jastrzebski, van der Schaaf, Paul A., J. Boersma, G. van Koten, M. de Wit, Y. Wang, D. Heijdenrijk, C. H. Stam, *J. Organomet. Chem.* **1991**, *407*, 301.

[17] M. P. Bigwood, P. J. Corvan, J. J. Zuckerman, *J. Am. Chem. Soc.* **1981**, *103*, 7643.

[18] P. Tavs, *Chem. Ber.* **1970**, *103*, 2428.

[19] a) M. Mehring, *Neue intramolekulare Donorliganden zur Synthese hyperkoordinierter Organoelementverbindungen*; b) M. Mehring, C. Löw, M. Schürmann, K. Jurkschat, *Eur. J. Inorg. Chem.* **1999**, 887; c) M. Mehring, M. Schürmann, K. Jurkschat, *Organometallics* **1998**, *17*, 1227; d) M. Mehring, C. Löw, M. Schürmann, F. Uhlig, K. Jurkschat, B. Mahieu, *Organometallics* **2000**, *19*, 4613; e) M. Mehring, C. Löw, I. Vrasidas, M. Schürmann, K. Jurkschat, *Phosphorus, Sulfur Silicon Relat. Elem.* **1999**, *150*, 311.

[20] a) M. Henn, *Neue intramolekular koordinierte Organoelementverbindungen des Zinns und Antimons unter Verwendung O,C,O-Koordinierender Zangenliganden*, **2004**; b) M. Wagner, K. Dorogov, M. Schürmann, K. Jurkschat, *Dalton Trans.* **2011**, *40*, 8733;

c) M. Henn, K. Jurkschat, R. Ludwig, M. Mehring, K. Peveling, M. Schürmann, *Z. Anorg. Allg. Chem.* **2002**, *628*, 2940; d) K. Peveling, M. Henn, C. Löw, M. Mehring, M. Schürmann, B. Costisella, K. Jurkschat, *Organometallics* **2004**, *23*, 1501.

[21] M. Wagner, M. Henn, C. Dietz, M. Schürmann, M. H. Prosenc, K. Jurkschat, *Organometallics* **2013**, *32*, 2406.

[22] a) M. Wagner, C. Dietz, M. Bouška, L. Dostál, Z. Padělková, R. Jambor, K. Jurkschat, *Organometallics* **2013**, *32*, 4973; b) M. Wagner, C. Dietz, S. Krabbe, S. G. Koller, C. Strohmann, K. Jurkschat, *Inorg. Chem.* **2012**, *51*, 6851; c) S. Krabbe, M. Wagner, C. Löw, C. Dietz, M. Schürmann, A. Hoffmann, S. Herres-Pawlis, M. Lutter, K. Jurkschat, *Organometallics* **2014**, *33*, 4433; d) M. Henn, M. Schürmann, B. Mahieu, P. Zanello, A. Cinquantini, K. Jurkschat, *J. Organomet. Chem.* **2006**, *691*, 1560; e) M. Henn, V. Deáky, S. Krabbe, M. Schürmann, M. H. Prosenc, S. Herres-Pawlis, B. Mahieu, K. Jurkschat, *Z. anorg. allg. Chem.* **2011**, n/a-n/a; f) M. Wagner, T. Zoller, W. Hiller, M. H. Prosenc, K. Jurkschat, *Chem. Commun.* **2013**, *49*, 8925; g) M. Wagner, T. Zöller, C. Dietz, K. Jurkschat, *Main Group Met. Chem.* **2015**, *38*; h) M. Wagner, T. Zoller, W. Hiller, M. H. Prosenc, K. Jurkschat, *Chem. Eur. J* **2013**, *19*, 9463; i) M. Wagner, M. Lutter, C. Dietz, M. H. Prosenc, K. Jurkschat, *Eur. J. Inorg. Chem.* **2015**, *2015*, 2152.

[23] a) J. Fischer, M. Schürmann, M. Mehring, U. Zachwieja, K. Jurkschat, *Organometallics* **2006**, *25*, 2886; b) J. Fischer, *Diplom thesis*, **2003**; c) B. Piorr, *Synthese und Charakterisierung von Zangenligandstabilisierten Organoelementverbindungen – Struktur und Reaktionsverhalten*. *Piorr - 2016 - Dissertation*, **2016**;

d) J. Fischer, *Neue intramolekular koordinierte Organoelementverbindungen des Zinns und Palladiums unter Verwendung unsymmetrischer C,Y– und Y,C,Y'–koordinierender Zangenliganden*, **2007**.

CHAPTER 1

1.1 INTRODUCTION

In the team of JURKSCHAT a large number of *O*,*C*,*O* and *O*,*N*,*O*-coordinating pincer-type compounds were synthesized and studied intensively. Some of these compounds are listed in figure 1. The P=O-coordinating containing pincer-type compounds were synthesized by the Tavs reaction or via lithium halogen exchange followed by the addition of the corresponding electrophile and/or the oxidation with H_2O_2 (**A** – **G**, Figure 1).[1–3]

The deprotonation of these compounds is successful with lithiumdi*iso*propyl amide (LDA) to give the compounds (**H - K**, Figure 1), in which the mono- or the di-substituted compounds are obtained at C3 or C5 (**H** and **I**, Figure 1) or C3 and C5 (**J** and **K**, Figure 1) using one or two molar equivalents of LDA, respectively. The substitution of the proton at the C4 atom (**E - G**, Figure 1) allows the selective deprotonation of the C1 atom (**L - N**, Figure 1).[1,3,4]

In this chapter two different pyridine-based *O*,*N*,*O*-coordinating pincer-type ligands are synthesised and characterized (**1** and **2**, Scheme 1). The reactions of these products with *n*BuLi, *t*BuLi, and LDA followed by the addition of $SnPh_3Cl$ as an electrophile, and the functionalization of the products obtained with elemental iodine were studied. Furthermore, the substitution of **1** with elemental bromine and the ability to generate the corresponding free carbene (1,3-(P(O)(O*i*Pr)$_2$C$_5$H$_2$N) of **1**·pyridinium derivative in addition to the platinum derivative [1,3-(P(O)(O*i*Pr)$_2$C$_5$H$_3$NMe][PtCl$_3$] were also investigated**.**

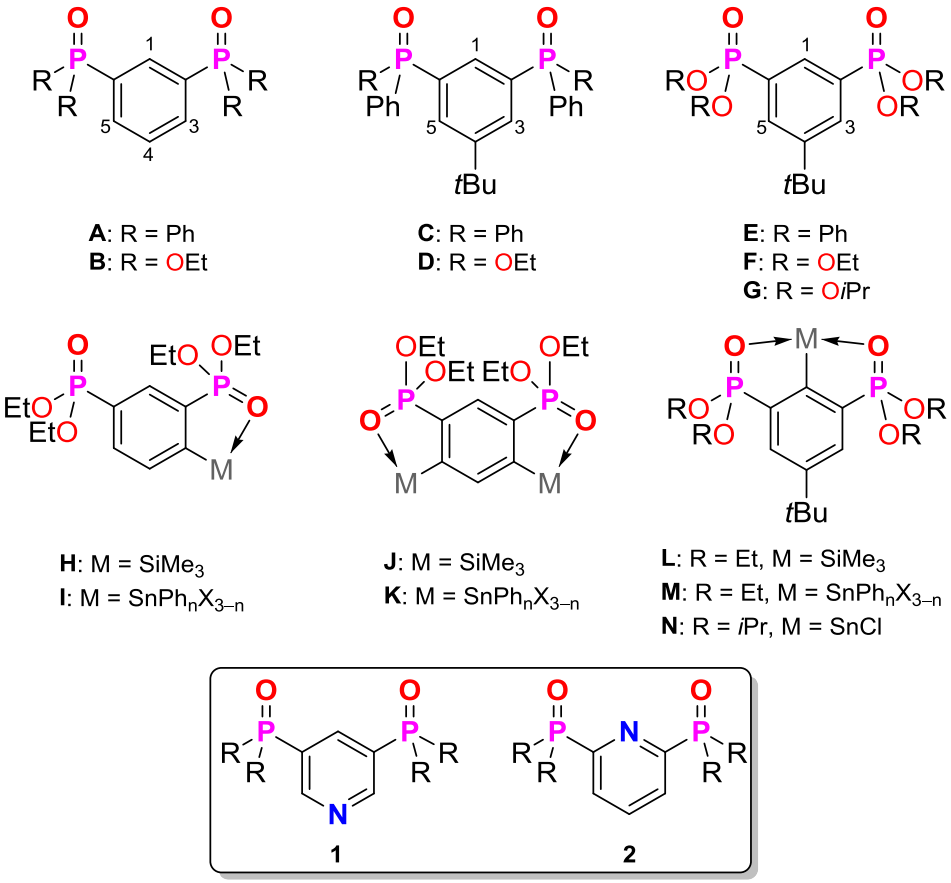

Figure 1. Some of the synthesized *O,C,O*-coordinating Pincer-type compounds and their derivatives.

1.2 RESULTS AND DISCUSSION

1.2.1 The syntheses of the ligand precursors

The compounds **1**-**4** were synthesized according to the Hirao cross-coupling reaction[5] in one step for **1**-**3**, and two steps for **4.** The corresponding pyridine derivatives were heated with di*iso*propyl phosphite, triethyl amine, palladium acetate and dppf (1,1'-Bis(diphenylphosphino)ferrocene) in acetonitrile at 90 °C for 24 h (Scheme 1).

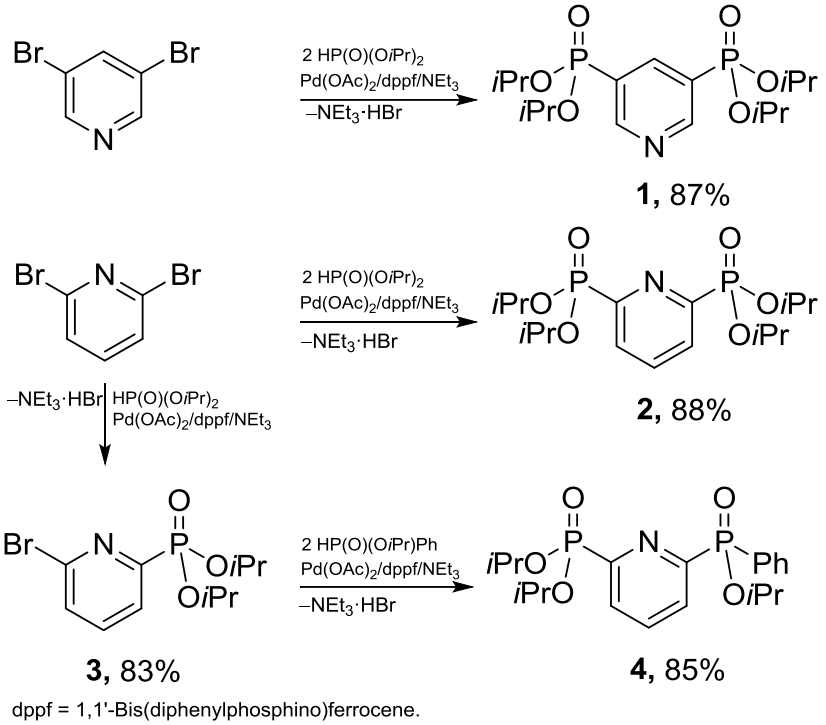

Scheme 1. The syntheses of the ligands **1** - **4**.

The compounds **1**-**4** are brown solids. They are soluble in common organic solvents such as hexane, THF and toluene. They are air and moisture stable in solution and in the solid state. Table 1 contains the $^{31}P\{^{1}H\}$ NMR, IR-spectroscopic data of compounds **1**-**4** and the P=O distances of **1** and **3**. The $^{31}P\{^{1}H\}$ NMR chemical shifts of **1, 2** and **3** are δ 13.4, 8.8 and 6.5, respectively. Compound **4** contains two non-equivalent phosphorus atoms which resonate at δ 6.4 for (P(O)(O*i*Pr)$_2$) and 23.3 for (P(O)O*i*PrPh. The $^{31}P\{^{1}H\}$ NMR chemical shifts of **1** and **2** are similar to those of 3-P(O)(OEt)$_2$C$_5$H$_4$N and 2-P(O)(OEt)$_2$C$_5$H$_4$N at δ 12.7 and 8.0, respectively.[6] They are high field-shifted in comparison with 5-*t*Bu-1,3-[P(O)(O-*i*Pr)$_2$]$_2$C$_6$H$_3$ **5** (δ 17.3).[7] The IR spectra show that the

P=O donor is not effected by the position at the pyridine moiety. The $\tilde{\nu}$(P=O) range from 1243 to 1247 cm^{-1}. The $\tilde{\nu}$(P=O) of 5-*t*Bu-1,3-[P(O)(O-*i*Pr)$_2$]$_2$C$_6$H$_3$ is 1250 cm^{-1}.[7]

Table 1. Analytic data of compounds 1 – 4.

Compound	^{31}P NMR [ppm]	P=O [cm^{-1}]	P=O [Å]
1	13.4	1243	1.472(6)
2	8.8	1247	-
3	6.5	1244	1.4584(17)
4	23.3[a] and 6.4[b]	1246[b] and 1232[a]	-
B [7]	17.3	1250	1.468

[a] P(O)PhO*i*Pr, [b] of P(O)(O*i*Pr)$_2$

The compound **1** crystalizes from ethyl acetate and hexane in the triclinic space group $P\bar{1}$ with two molecules per unit cell. Figure **2** shows the molecular structure of **1**. Selected interatomic distances and angles are given in the figure caption. There are no intermolecular interactions at distances shorter than the sums of the van der Waals radii of the atoms involved.[8] The phosphorus atoms have a distorted tetrahedral environment with angles ranging between 101.8 and 113.8°. The C(3)–P(1) (1.799(7)) and C(5)–P(2) (1.801(8) Å) distances are typical for a P–C bond , are P(2)–O(2), 1.457(6) and P(1)–O(1), 1.472 (6) Å. The O(1) and O(2) atoms point to the hydrogen atoms bound to C(2) and C(6), respectively. The O(1)···H(6) and O(2)···H(2) distances of 2.591(6) and 2.640(7) Å, respectively, are equal to the sum of vdw. radii of oxygen 1.52 Å and hydrogen Å.[8] The P=O bonds are not in the plane defined by the pyridine ring and show O(1)–P(1)–C(5)–C(6) and O(2)–P(2)–C(3)–C(2) torsion angles of 0.5(8) and 24.9(8)°, respectively. The molecular structure of **1**, has the same formation of **B** with P=O bond length 1.470(3) and 1.466(3) Å and torsion angle 17.6(4) and 11.1(4) between P=O and the phenyl ring.[7]

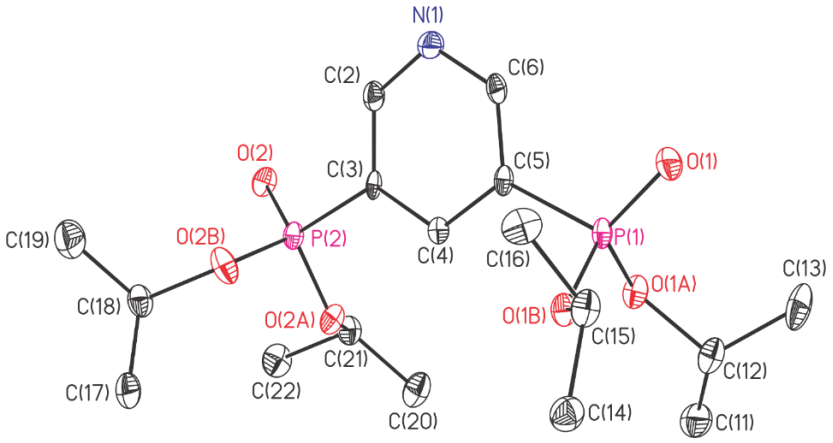

Figure 2. Ellipsoid plot and numbering scheme of the molecular structure of **1**. The hydrogen atoms were omitted for clarity; ellipsoids are set at 30 % probability. Selected bond lengths [Å]

and angles [°]: P(1)–O(1) 1.472(6), P(1)–O(1A) 1.568(6), P(1)–C(5) 1.801(8), P(2)–O(2) 1.457(6), P(1)–O(2B) 1.561(6), P(1)–O(2A) 1.579(6), P(1)–C(3) 1.799(7), C(2)–N(1)–C(6) 115.2(7), C(5)–P(1)–O(1) 112.5(4), O(1B)–P(1)–O(1) 114.8(3), O(1B)–P(1)–C(5) 106.4(3), O(1)–P(1)–O(1A) 117.8(4), O(1A)–P(1)–C(5) 100.8(3), C(3)–P(2)–O(2) 112.6(4), O(2B)–P(2)–O(2) 116.5(4), O(2B)–P(2)–C(3) 101.8(3), O(2)–P(2)–O(2A) 113.8(4) and O(2A)–P(2)–C(3) 107.1(3).

Compound **3** crystalizes from ethyl acetate and *iso*hexane in the monoclinic space group $P\ 2_1/\ n$ with four molecules per unit cell. The molecular structure is shown in Figure **3**. Selected interatomic distances and angles are given in the figure caption. The phosphorus atom shows a tetrahedral environment with angles ranging between 101.16(2) and 114.63(2)°. The C(6)–P(1) and O(1)–P(1) distances are 1.803(2) and 1.458(2) Å, respectively. The O(1)–P(1)–C(6)–C(5) torsion angle of 11.4(2) ° is similar to **A** with torsion angle 11.1(4) and 17.6(4) ° than **1** with torsion angle 0.5(8) and 24.9(8)°. The O(1)–H(5) distance is 2.744(2) Å. For **B** there are such distances of 2.718(5) and 2.693(4) Å. The bromine atom is bound to the pyridine ring at a Br(1)–C(2) distance of 1.895(2) Å. This distance between is similar to that reported for 1-Br-4-*t*Bu-2,6[P(O)OEtO$_2$]$_2$C$_6$H$_2$, 1.893(3) Å. [2]

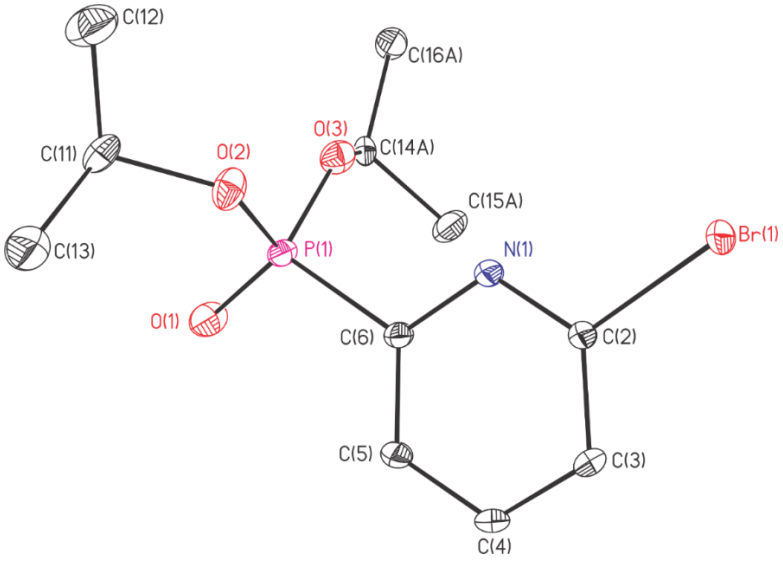

Figure 3. Ellipsoid plot and numbering scheme of the molecular structure of **3**. The hydrogen atoms were omitted for clarity; ellipsoids are set at 30 % probability. Selected bond lengths [Å] and angles [°]: Br(1)–C(2) 1.895(2), P(1)–C(6) 1.803(2), P(1)–O(1) 1.4584(17), P(1)–O(2) 1.5598(17), P(1)–O(3) 1.5702(17), N(1)–C(2)–Br(1) 115.07(14), C(2)–N(1)–C(6) 117.04(16), C(6)–P(1)–O(1) 113.42(9), O(1)–P(1)–O(2) 117.18(11), O(1)–P(1)–O(3) 114.64(11), C(5)–C(6)–P(1) 120.77(16), N(1)–C(6)–P(1) and 116.07(14).

1.2.2 The metalation of compound 2,6-{P(O)(O*i*Pr)$_2$}C$_5$H$_5$N and 3,5-{P(O)(O*i*Pr)$_2$}C$_5$H$_5$N:

The research of MEHRING[3] and HENN[2] about the lithiation of the pincer-type proligands (5-*t*Bu-1,3-[P(O)(OEt)$_2$]$_2$C$_6$H$_3$) and (5-*t*Bu-1,3-[P(O)Ph$_2$]$_2$C$_6$H$_3$) showed that *n*BuLi and *t*BuLi make a nucleophilic attack at the phosphorus atoms while the much less nucleophilic LDA deprotonates the phenyl ring.

On the other hand, HAASE *et al.*[9] studied the reactions of alkyl pyridinyl phosphonates with different bases and at different temperatures. The study reveals that the phosphorus centre is attacked nucleophilically by the amide anion, according to scheme 2.

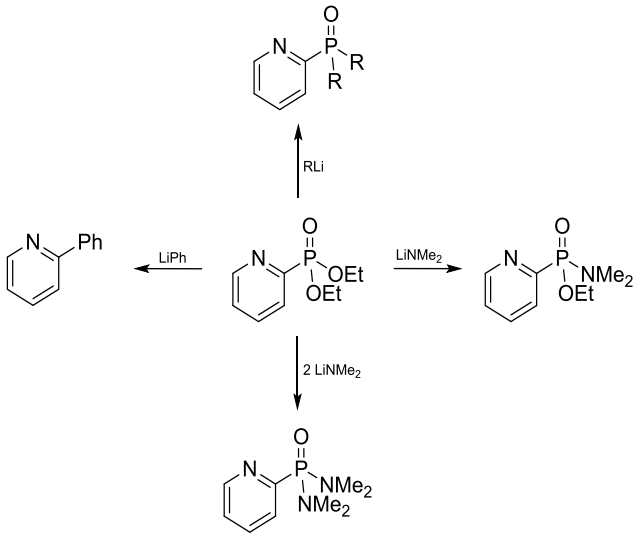

Scheme 2. The reactions of pyridine diethylphosphonate (pyridinyl phosphonic diethyl ester) with different lithium bases.

In order to study its deprotonation, compound **1** was stirred for 6h at different temperatures (–60, –40, –30, –20 and 0 °C) with LDA, *t*BuLi and *n*BuLi, respectively. In all experiments the solution became highly viscose with no change in the color. After addition of the electrophile Ph$_3$SnCl the reaction mixtures were stirred overnight. The ^{31}P{^{1}H} NMR spectra of the crude reaction mixtures exclusively showed the signal of compound **1** apparently, no reaction took place. The reason that makes the LDA not able to deprotonate compound **1** is may be traced back to the complexation of RLi compounds via the P=O functional group or the nitrogen of the pyridine as the reaction reported by WARREN *et al.*[10] (**1**, Scheme 3).

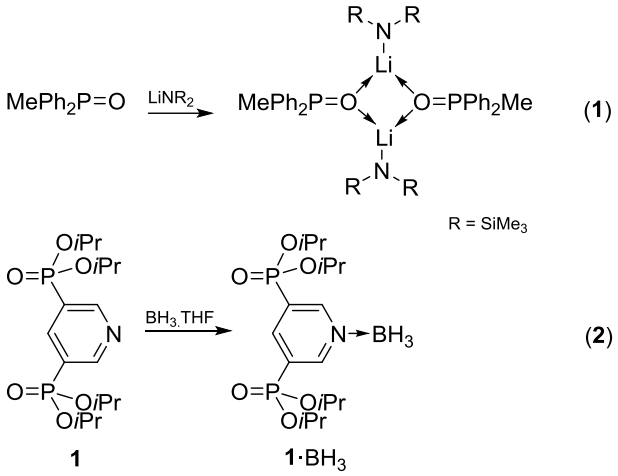

Scheme 3. The coordination of methyldiphenyl phosphine oxide at lithium hexamethyldisilylamide and the reaction of **1** with BH_3·THF.

To avoid the coordination of the donor atoms at the RLi, compound **1** and BH_3·thf complex were stirred at room temperature for 15 min (**2**, Scheme 3). The solution of the reaction mixture turns to yellow and a $^{31}P\{^1H\}$ NMR spectrum of the reaction mixture showed a singlet at δ 9.4. The signals of the Py-protons in the ^1H NMR spectra are downfield shifted from δ 7.97 - 7.89 (m), 7.08 - 6.95 (m) for **1** to 9.36 (d, $^3J(^1H, ^1H)$ = 8 Hz), 8.83 (d, $^3J(^1H, ^1H)$ = 12 Hz) for **1**·BH3. The BH_3 protons resonate as a broad signal centred at 3.60 ($\nu_{1/2}$= 170 Hz).

To deprotonate **1**·BH_3, LDA was added to the *in situ* synthesized 3,5[P(O)(O*i*Pr)$_2$]$_2$C$_5$H$_2$N·BH_3 at –20 °C and stirred for 3h (Scheme 4), after which triphenyltin chloride, Ph_3SnCl, was added. The reaction mixture was warmed to room temperature. The $^{31}P\{^1H\}$ NMR of the crude reaction mixture shows resonances at δ 38.7(2%), 31.2(2%), 30.1(2%), 24.3 (d, $J(^{31}P, ^{31}P)$ = 10 Hz, $J(^{31}P, ^{117/119}Sn)$ = 16 Hz; 45%), 22.7(2%), 20.9(2%), and 18.8 (d, $J(^{31}P, ^{31}P)$ = 10 Hz, $^3J(^{31}P, ^{117/119}Sn)$ = 16 Hz; 45%). The doublets at 24.3 ($J(^{31}P, ^{31}P)$ = 10 Hz, $J(^{31}P, ^{117/119}Sn)$ = 16 Hz) and 18.8 ($J(^{31}P, ^{31}P)$ = 10 Hz, $^3J(^{31}P, ^{117/119}Sn)$ = 16 Hz) refer to two different phosphorus atoms that couple with each other. They are tentatively assigned to the $SnPh_3$-substituted compound **1a** (Scheme 4). Attempts to isolating this compound from the reaction mixture by column chromatography (SiO_2, hexane/ethyl acetate), failed, however.

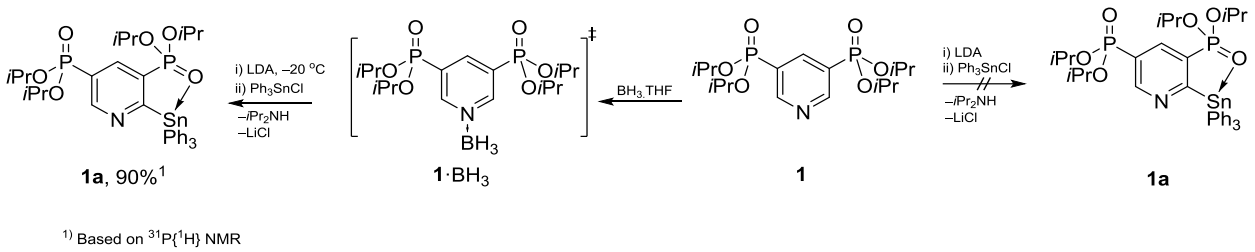

Scheme 4. The metalation conditions of compounds **1** and **2.**

The same procedures were used to deprotonate compound **2**. It was stirred for 3h with LDA, *t*BuLi and *n*BuLi, respectively, at –60, –40, –30, –20 and 0 °C (in all experiments the solution turns to dark red) after which the electrophile (Ph_3SnCl) was added and the reaction mixtures were stirred overnight. The $^{31}P\{^1H\}$ NMR shows the signal of compound **2**, in the reactions that took place at –40 °C or below but above –20 °C apparently, a reaction at the $P(O)(OiPr)_2$ moieties take place. Finally, the reaction at –30 °C of compound **2** with one molar equivalent of LDA gave a crude reaction mixture a ^{31}P NMR spectrum of which showed a doublet at δ 13.2 $J(^{31}P, ^{31}P)$ = 2 Hz; $^3J(^{31}P, ^{117/119}Sn)$ = 16 Hz, 15%) a broad resonance at δ 10.6 ($\nu_{1/2}$ = 1100 Hz, 60%) and anther rather broad resonance at 9.5 ($\nu_{1/2}$ = 20 Hz, 25%). After extraction and purification with column chromatography (SiO_2, ethyl acetate and hexane) the compounds **5** and **6** were isolated from this reaction mixture as colourless solid materials. They are air and moisture stable in the solid state and in the solution. Compounds **5** and **6** are soluble in common organic solvents such as ethyl acetate, acetone, tetrahydrofuran, and toluene. A $^{31}P\{^1H\}$ NMR spectrum of compound **5** (Figure 4) shows two doublets at δ = 10.3 (d, $J(^{31}P, ^{31}P)$ = 2 Hz, $J(^{31}P, ^{117/119}Sn)$ = 23/26 Hz) and 13.4 (d, $J(^{31}P, ^{31}P)$ = 2 Hz, $J(^{31}P, ^{117/119}Sn)$ = 14/18 Hz). These signals are shifted downfield in comparison with 2,6-bis(diisopropoxy phosphoryl) pyridine **2**. The coupling constants are similar to the compounds H – M (Figure 1) described by MEHRING[3] and PIORR[11] with $J(^{31}P, ^{31}P)$ = 4 Hz and $J(^{31}P, ^{117/119}Sn)$ = 16 and 27 Hz; $J(^{31}P, ^{31}P)$ = 8 Hz and $J(^{31}P, ^{117/119}Sn)$ = 16 and 24 Hz, respectively. A $^{119}Sn\{^1H\}$ NMR spectrum shows a doublet of doublet resonance at δ = –160 ($J(^{119}Sn, ^{31}P)$= 16, 25 Hz). For 2,6-$P(O)(OiPr)_2$-3-$SnPh_3C_6H_3$[11] and 2,6-$P(O)(OEt)_2$-3-$SnPh_3C_6H_3$[3] signals at δ –150 (dd, $J(^{119}Sn, ^{31}P)$= 16, 27 Hz) and δ –151 (AA'XX' system), respectively, were observed. An IR spectrum shows $\tilde{\nu}_{P=O}$ absorbtions at 1251 and 1227 cm^{-1}.

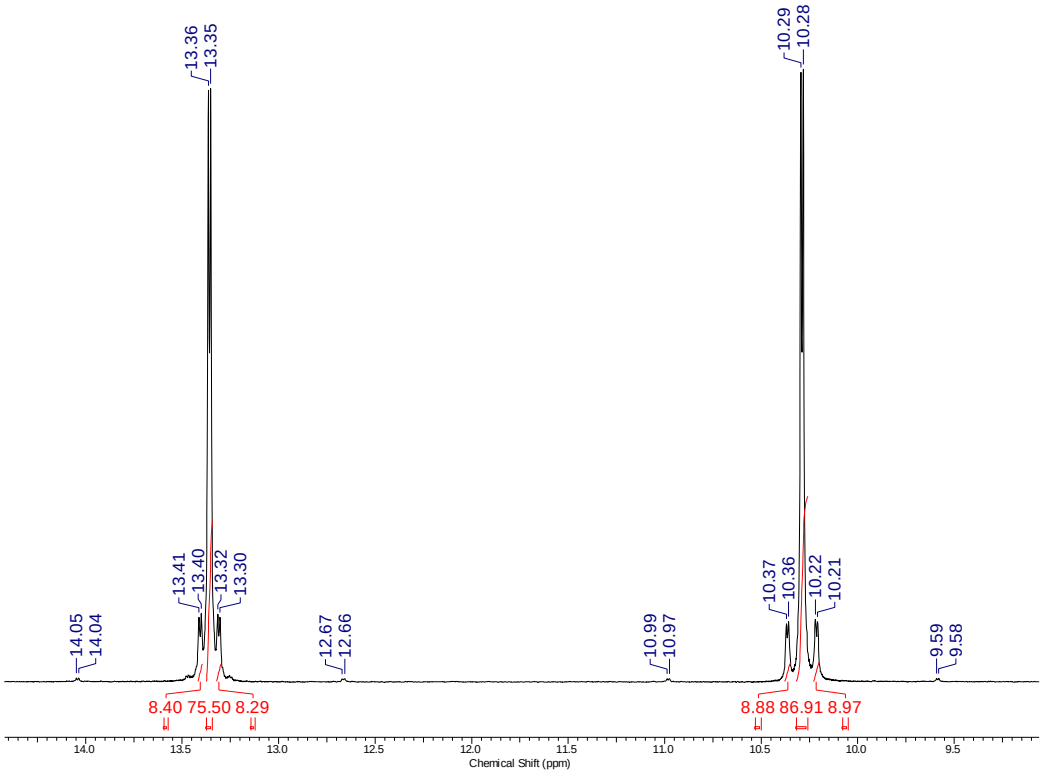

Figure 4. $^{31}P\{^{1}H\}$NMR spectrum of compound **5.**

A $^{31}P\{^{1}H\}$ NMR spectrum of compound **6** shows a singlet with two sets of tin satellites at δ = 13.4, $J(^{31}P$, $^{117/119}Sn)$ = 27/29 Hz, $J(^{31}P$, $^{117/119}Sn)$ = 10/12 Hz and in the $^{119}Sn\{^{1}H\}$ NMR spectrum appears a doublet of doublet resonance at δ = –159 ($J(^{119}Sn$, $^{31}P)$ = 11, 30 Hz).

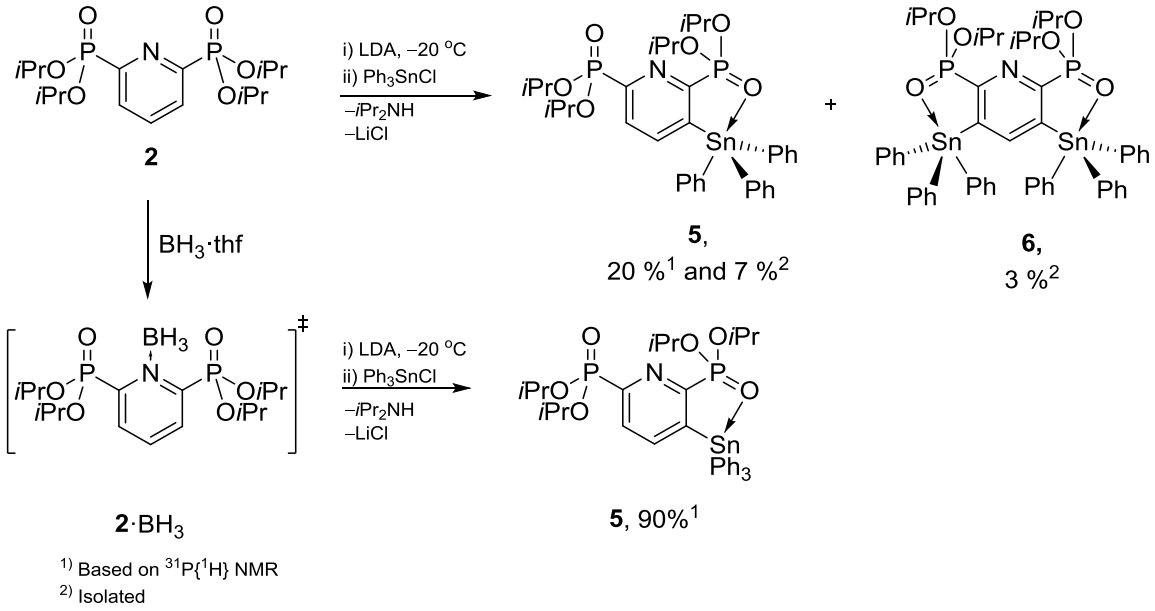

Scheme 5. The synthesis of compounds **5** and **6**.

Compound **5** crystalizes from ethyl acetate and hexane in the triclinic crystal system with space group $P\bar{1}$ and two molecules per unit cell (Figure 5). The tin center is [4+1] coordinate and it shows a distorted trigonal bipyramidal environment. The oxygen atom O(1) approaches the tin atom via the tetrahedral face defined by C(1), C(31), C(41) at a distance of 2.7012(16) Å. It is the same distance as reported by PIORR[11] for 2,6-P(O)(O*i*Pr)$_2$-3-SnPh$_3$C$_6$H$_3$. The P(1)–O(1) distance (1.475(2) Å) is longer than the P(2)–O(6) one (1.442(2) Å). This difference is traced back to the P=O→Sn coordination.

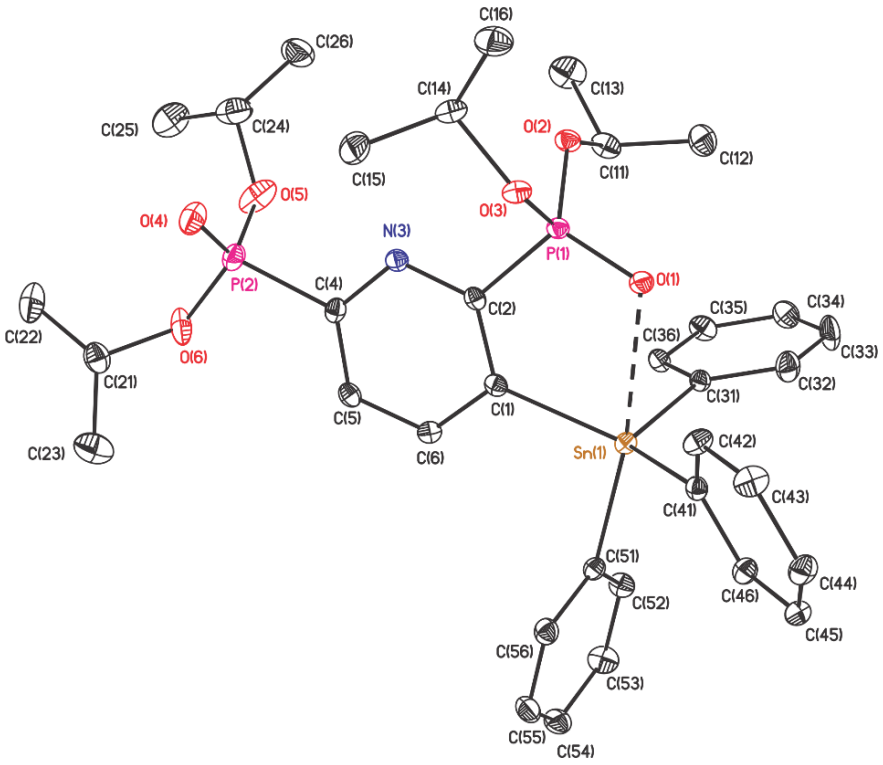

Figure 5. Ellipsoid plot and numbering scheme of the molecular structure of **5.** The hydrogen atoms were omitted for clarity; ellipsoids are set at 30 % probability. Selected bond lengths [Å] and angles [°]: Sn(1)–C(1) 2.167(2), Sn(1)–C(31) 2.1511(10), Sn(1)–C(41) 2.1564(10), Sn(1)–C(51) 2.1956(10), Sn(1)–O(1) 2.7012(16), P(1)–C(2) 1.812(2), P(1)–O(1) 1.4749(18), P(2)–O(2) 1.5647(17), P(2)–O(3) 1.5672(17) and N(1)–C(2)–P(1) 115.10(17), C(2)–C(1)-Sn(1) 124.93(16), C(2)–P(1)–O(1) 108.06(10), P(1)–C(2)–C(1) 119.43(17), C(1)–Sn(1)–C(31) 107.83(7), O(1)–Sn(1)–C(1) 73.99(7), C(1)–Sn(1)–C(51) 99.04(7), C(1)–Sn(1)–C(41) 123.99(7), C(31)–Sn(1)–C(41) 117.46(6), C(31)–Sn(1)–C(51) 111.61(10) and C(41)–Sn(1)–C(51) 99.70(6).

The compound **6** crystalizes from ethyl acetate and hexane in the monoclinic crystal system with space group *C*1/c and four molecules per unit cell (Figure 6). Again, the tin atom is [4+1] coordinate and shows a distorted trigonal bipyramidal environment.

The oxygen atom O(1) approaches the Sn(1) atom via the tetrahedral face defined by C(1), C(21), C(41) at a distance of 2.767(2) Å, being slightly longer than the corresponding distance observed for compound **5**. The P(1)–O(1) distance is 1.471(2) Å.

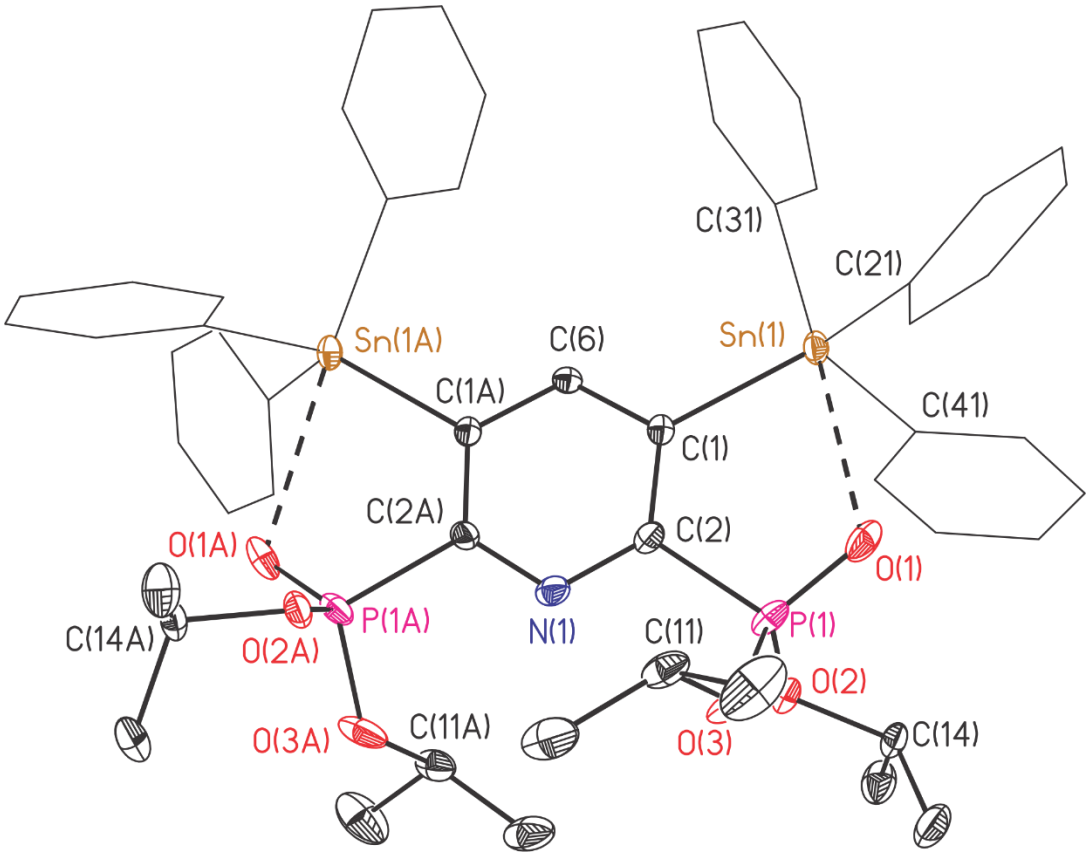

Figure 6. Ellipsoid plot and numbering scheme of the molecular structure of **6.** The hydrogen atoms were omitted for clarity; ellipsoids are set at 30 % probability. Selected bond lengths [Å] and angles [°] : Sn(1)–C(1) 2.174(2), Sn(1)–C(21) 2.138(3), Sn(1)–C(31) 2.168(3), Sn(1)–C(4) 2.143(3), Sn(1)–O(1) 2.7672(23), P(1)–C(2) 1.812(3), P(1)–O(1) 1.471(2), P(2)–O(2) 1.569(2), P(2)–O(3) 1.568(2) and N(1)–C(2)–P(1) 115.13(19), C(2)–P(1)–O(1) 108.95(12), C(2)–C(1)–Sn(1) 123.21(18), P(1)–C(2)–C(1) 120.1(2), C(1)–Sn(1)–C(21) 121.83(10), O(1)–Sn(1)–C(1) 74.555(81), C(1)–Sn(1)–C(41) 111.02(10), C(1)–Sn(1)–C(31) 103.63(10), C(21)–Sn(1)–C(31) 101.74(11), C(21)–Sn(1)–C(41) 111.61(10) and C(31)–Sn(1)–C(41) 104.74(11).

Attempts to functionalize the pyridine ring of **1** by reaction with elemental bromine failed (Path **B**, Scheme 6). With the idea to improve the reaction of **1** with elemental bromine, PdL_2Cl_2 (L = 3,5-P(O)(O*i*Pr)$_2$C$_5$H$_3$N) **7**, was synthesized by stirring a solution (CH_2Cl_2/CH_3CN, 10:1) containing **1** and $PdCl_2$ at room temperature. In the $^{31}P\{^1H\}$ NMR spectrum of **7** appears a singlet at δ 8.3 that is high field-shifted with respect to the signal of compound **1** at δ 13.4.

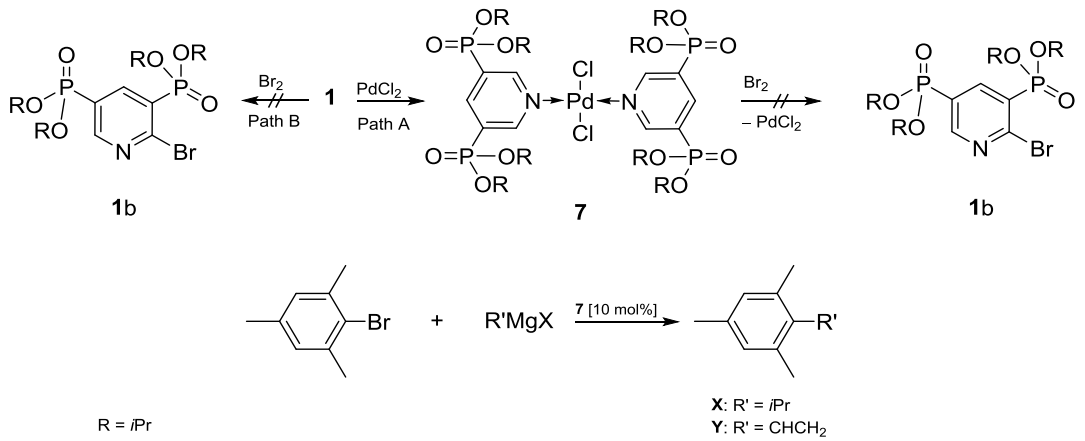

Scheme 6. The reaction of compound **1** with $PdCl_2$ and Br_2 and Kumada coupling using **7** as a catalyst.

The palladium complex **7** was obtained by crystallisation from the mother liquor as a yellow crystalline material. It dissolves in acetonitrile, dichloromethane and tetrahydrofuran**.** Single crystals suitable for X-ray diffraction of **7**, as its water solvate **7**·H_2O, were obtained from its solution in acetonitrile and dichloromethane. It crystallized in the triclinic crystal system with the space group $P\bar{1}$ and two molecules per unit cell. The molecular structure is shown in figure 7, and selected interatomic distances and angles are given in the figure caption. In the molecular structure it was found that two molecules of **1** coordinate at one molecule $PdCl_2$. The palladium center has a square planar geometry, in which the chloride ligands are trans. The angle Cl(1)–Pd(1)–Cl(2) is 179.29(2) °. The Pd(1)–Cl(1), Pd(1)–Cl(2), Pd(1)–N(1), Pd(1)–N(7) distances are 2.2879(6), 2.2844(6), 2.0208(17) and 2.0170(17) Å, respectively. The pyridine rings lay in a plane. The torsion angle Cl(1)–Pd(1)–N(1)–C(2) is 51.509(4)°.

Compound **7** and elemental bromine were stirred at room temperature according to the procedure described by PARASKEWAS[12] (Path **A**, Scheme 6). After a reaction time of 16 h a $^{31}P\{^1H\}$ NMR spectrum exclusively showed the signal of the starting material indicating that no reaction had occurred. This may be traced back to the high positive charge caused by the P(O)(O*i*Pr)$_2$ moiety in comparison to the pyridine.

To test the ability of complex **7** to catalyse a cross coupling reaction between ArX (MesBr) and RMgX (Kumada coupling), mesityl bromide, allylmagnesium chloride ($CH_2CHMgCl$), *iso*propylmagnesium chloride (CH_3CHCH_3MgCl) and **7** in toluene was stirred at 100 °C for 12h. After extraction and distillation, 2,4,6-trimethylstyrene (**Y**,

Scheme 6) and 1-*iso*propyl-2,4,6-trimethylbenzene (**X,** Scheme 6) are obtained with yield 75% and 80%, respectively.

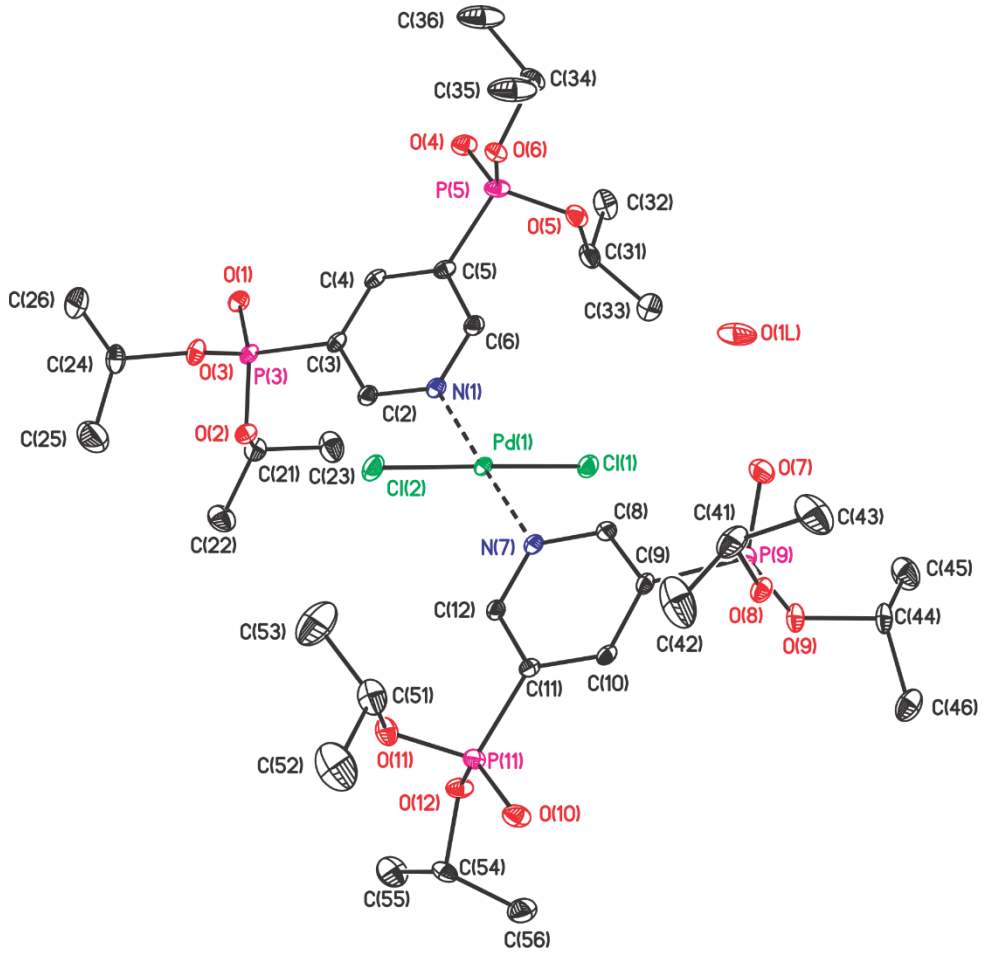

Figure 7. Ellipsoid plot and numbering scheme of the molecular structure of **7**. The hydrogen atoms were omitted for clarity, ellipsoids are set at 30 % probability. Selected bond lengths [Å] and angles [°]: Pd(1)–N(1) 2.0208(17), Pd(1)–N(7) 2.0170(17), Pd(1)–Cl(1) 2.2879(6), Pd(1)–Cl(2) 2.2844(6), C(3)–P(3) 1.807(2), C(5)–P(5) 1.799(2), C(9)–P(9) 1.804(2), P(3)–O(1) 1.4584(16), P(5)–O(4) 1.4558(16) P(9)–O(7), 1.4621(18) P(11)–O(11) 1.4625(16), C(11)–P(11) 1.798(2), N(1)–Pd(1)–N(7) 117.33(7), Cl(1)–Pd(1)–Cl(2) 179.29(2), N(1)–Pd(1)–Cl(1) 89.63(5), N(1)–Pd(1)–Cl(2) 89.60(5), N(7)–Pd(1)–Cl(1) 89.98(5) and N(7)–Pd(1)–Cl(2) 89.82(5).

1.2.3 The reactivity of compounds 2,6-{P(O)(O*i*Pr)$_2$}C$_5$H$_2$NSnPh$_3$ toward halide:

2,6-bis(diisopropoxy phosphoryl)-3-triphenyl tin pyridine **5** reacts with one equivalent iodine and two equivalents in dichloromethane at room temperature (Scheme 7) to give 2,6-bis(diisopropoxy phosphoryl)-3-iododiphenyl tin pyridine (**8**) and 2,6-bis(diisopropoxy phosphoryl)-3-diiodophenyl tin pyridine (**9**), respectively.

Compounds **8** and **9** are bright yellow solid materials which dissolve in polar solvents such as dichloromethane, acetonitrile and tetrahydrofuran.

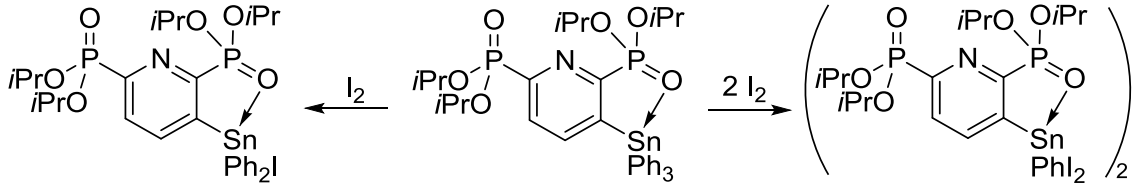

8 **5** **9**

Scheme 7. Functionalization of compound **5** with iodine.

A $^{31}P\{^{1}H\}$ NMR spectrum of **8** shows signals at δ 14.3 (d, $J(^{31}P, ^{31}P)$ = 2 Hz, $J(^{31}P, ^{117/119}Sn)$ = 53/57 Hz) and 7.1 (d, $J(^{31}P, ^{31}P)$ = 2 Hz, $J(^{31}P, ^{117/119}Sn)$ = 29/32 Hz). A $^{119}Sn\{1H\}$ NMR spectrum shows a doublet of doublet resonance at δ –196 (dd, $J(^{119}Sn, ^{31}P)$= 57 Hz, $J(^{119}Sn, ^{31}P)$= 32 Hz).

Compound **9** crystalizes from dichloromethane and hexane in the monoclinic space group $P2_1/c$ with two molecules per unit cell (Figure 8). The molecular structure is shown in Figures 8 and 9, and selected interatomic distances and angles are given in the figure caption. In the solid state compound **9** forms a centrosymmetric head-to-tail dimer (with I(1) and I(1A) trans) induced by intermolecular P=O→Sn interaction at a Sn(1)–O(4) distance of 2.414(7) Å. The distance between the centres of the pyridine rings is 3.86 Å. This is in the range of a π-stacking "π-π interaction" (3.8 Å).[13] The pyridine rings are offset and the angle N(3), X(1A), X(1B) is 72.8° (X1A and X1B are the centroids of the pyridine ring C(1) to C(6) and C(1A) to C(6A), respectively), which allow to calculate the offset, which is 1.2 Å. This kind of formation, antiparallel-displaced is more stable than antiparallel-sandwich formation, because of a difference in the energy of about 1 kcal.mol^{-1}.[14] The tin centers are six-coordinate and show a slightly distorted octahedral environment. The interatomic Sn(1)–I(1), Sn(1)–I(2), Sn(1)–C(1), Sn(1)–C(31) and Sn(1)–O(1) distances are 2.8331(11), 2.7914(12), 2.175(10), 2.198(11) and 2.352(7) Å, respectively.

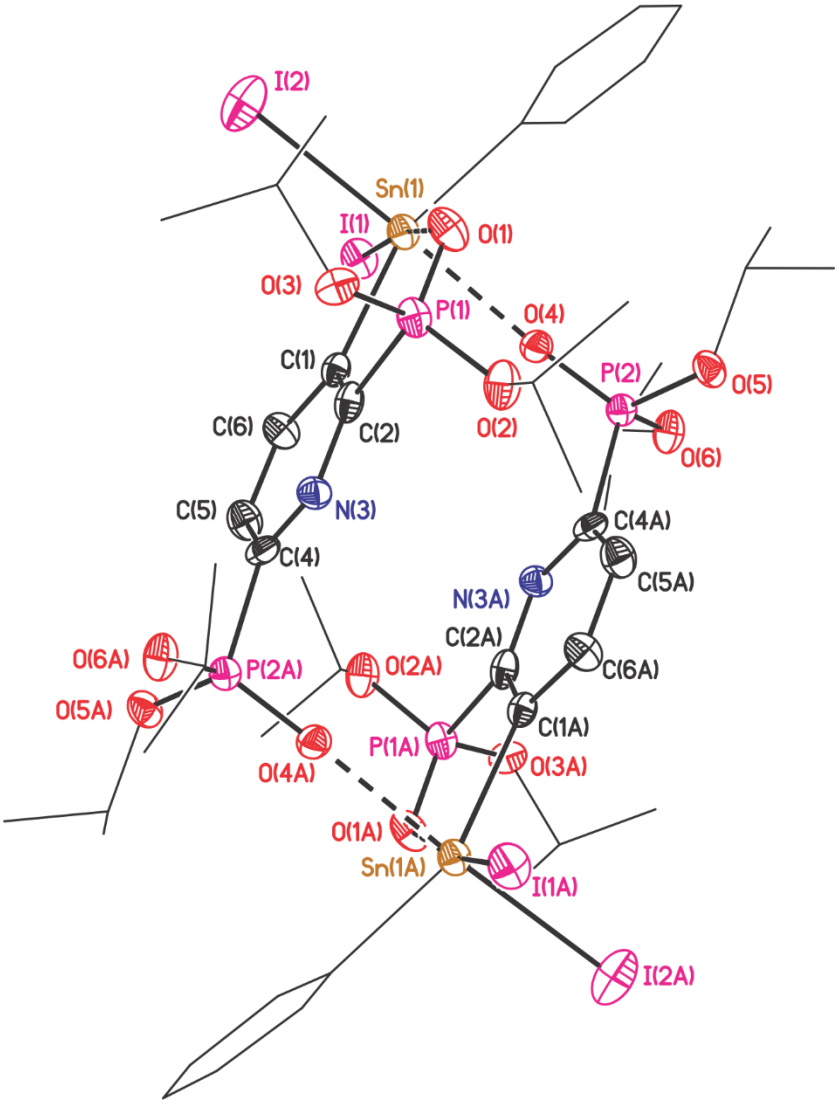

Figure 8. Ellipsoid plot and numbering scheme of the molecular structure of **9**. The hydrogen atoms were omitted for clarity, ellipsoids are set at 30 % probability. Selected bond lengths [Å] and angles [°]: Sn(1)–C(1) 2.175(10), Sn(1)–C(31) 2.198(11), Sn(1)–O(1) 2.352(7), Sn(1)–O(4) 2.414(7), Sn(1)–I(1) 2.8331(11), Sn(1)–I(2) 2.7914(12), P(1)–O(1) 1.471(2), P(2) – O(4) 1.463(8), P(2)–O(2) 1.569(2) P(2)–O(3), 1.568(2) P(1)–C(2) 1.812(3), C(1)–Sn(1)–O(1) 78.3(3), I(1)–Sn(1)–I(2) 96.30(4), O(4)–Sn(1)–I(1) 88.50(17), O(4)–Sn(1)–I(2) 174.29(17), O(1)–Sn(1)–I(2) 89.0(2), C(31)–Sn(1)–I(2) 99.8(3), O(1)–Sn(1)–O(4) 86.0(3), C(1)–Sn(1)–I(1) 96.4(3), O(1)–Sn(1)–I(1) 173.0(2), C(1–Sn(1)–O(4) 78.6(3) and C(31)–Sn(1)–O(4) 82.5(3).

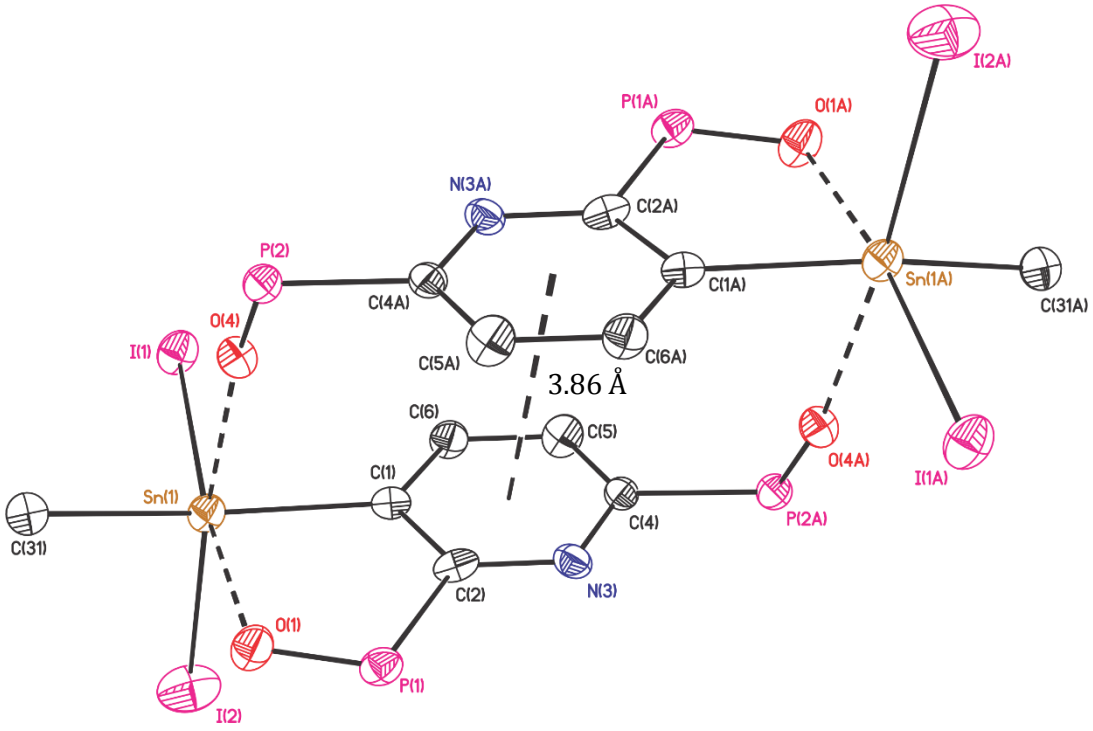

Figure 9. Simplified Ellipsoid plot and numbering scheme of the molecular structure of **9** showing the head-to-tail dimer**.** The *i*OPr, the rest of the phenyl ring and the hydrogen atoms were omitted for clarity. Selected bond lengths [Å] and angles [°]: Sn(1)–C(1) 2.175(10), Sn(1)–C(31) 2.198(11), Sn(1)–O(1) 2.352(7), Sn(1)–O(4) 2.414(7), Sn(1)–I(1) 2.8331(11), Sn(1)–I(2) 2.7914(12), P(1)–O(1) 1.471(2), P(2) –O(4) 1.463(8), P(2)–O(2) 1.569(2) P(2)–O(3), 1.568(2).

A $^{31}P\{^{1}H\}$ NMR of compound **9** shows two doublets with tin satellites at δ 13.7, $J(^{31}P, ^{31}P)$ = 2 Hz, $J(^{31}P, ^{117/119}Sn)$ = 65 Hz), and at δ 6.3, $J(^{31}P, ^{31}P)$ = 2 Hz, $J(^{31}P, ^{117/119}Sn)$ = 40 Hz), respectively. The latter signal is high field-shifted in comparison with the starting compound.

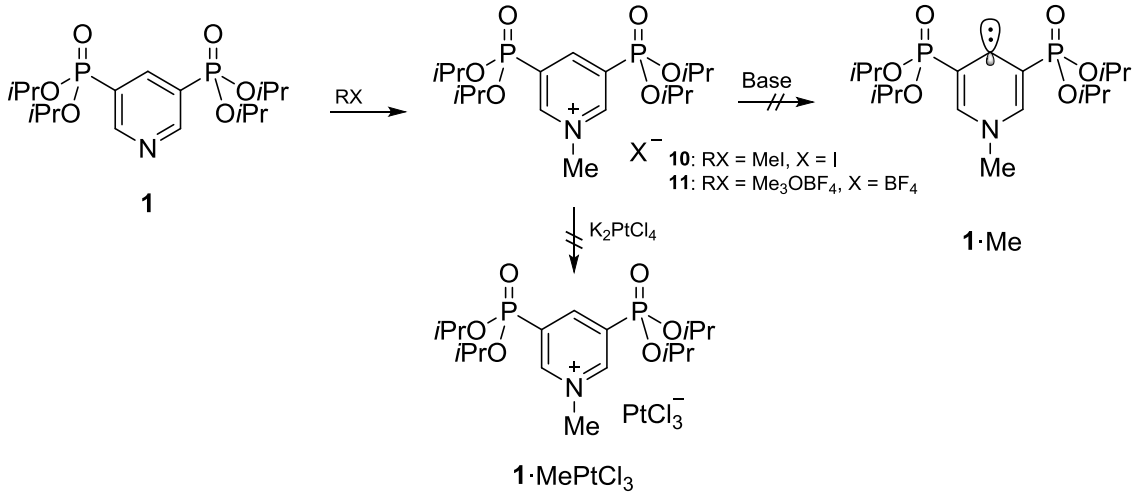

Scheme 8. The methylation of compound **1** with different methylation reagents.

The general procedures to produce stable carbenes is to deprotonate ammonium salts of the general formula $[(R_2N)_2CH]^+X^-$, in which the free electron pair is located in sp^2 hybrid orbital and the empty p_z orbital is thermodynamically stabilized by the lone pair of the nitrogen atom.

To synthesise the corresponding ammonium salt of compound **1**, two different alkylation reagents were used; methyl iodide and trimethyloxonium tetrafluoroborate (Scheme 8). Compound **1** reacts with methyl iodide in acetonitrile at 40 °C over 1h (Scheme 8). After removing the volatiles under reduced pressure, the methylated compound **10** was isolated as a yellow solid. It dissolves in polar organic solvents such as THF, dichloromethane and acetonitrile. The $^{31}P\{^1H\}$ NMR spectrum of **10** shows a singlet at (δ 4.7) which is high field-shifted with respect to **1**.

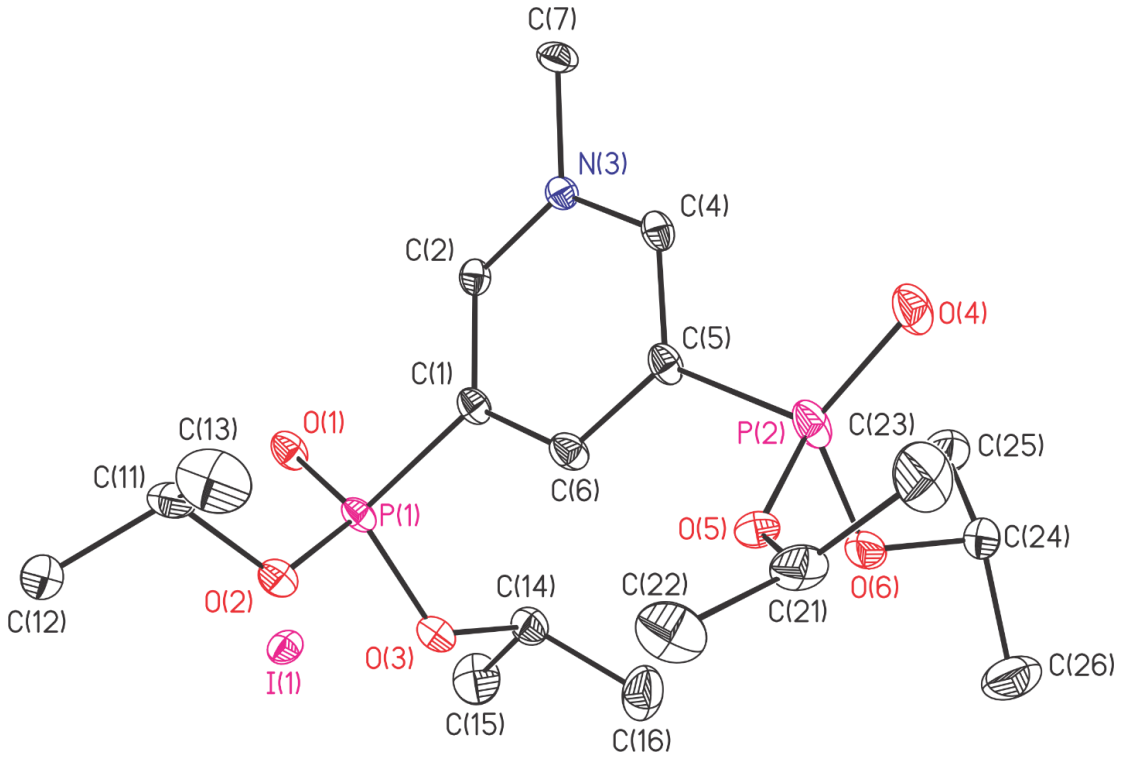

*Figure **10**.* Ellipsoid plot and numbering scheme of the molecular structure of **10**. The hydrogen atoms were omitted for clarity, ellipsoids are set at 30% probability. Selected bond lengths [Å] and angles [°]: N(3)–C(7) 1.480(3), P(1)–C(1) 1.805(2), P(1)–O(1) 1.4653(16), P(1)–O(2) 1.5641(15) P(1)–O(3), 1.5632(16) P(2)–C(5) 1.804(2), P(2)–O(4) 1.4622(17), P(2)–O(5) 1.522(5), P(2)–O(6) 1.5615(19), C(4)–N(3)–C(7) 119.34(17), C(7–N(3)–C(2) 119.34(17), C(2)–N(3)–C(4) 121.64(18), C(2)–N(3)–C(7) 119.01(17), C(5)–P(2)–O(4) 111.33(10), C(4)–C(5)–P(2)

119.84(16), O(4)–P(2)–O(5) 123.18(19), O(4)–P(2)–O(6) 117.15(10), C(1)–P(1)–O(1) 110.56(9), O(1)–P(1)–O(2) 117.48(9), O(1)–P(1)–O(3) 118.44(9).

Compound **10** crystalizes from ethyl acetate and hexane in the monoclinic space group $P\,2_1/n$ and four molecules per unit cell. The molecular structure reveals that the phosphorus atoms are attached to the pyridine ring at C(1) and C(5) with distances of 1.805(2) and 1.804(2) Å, respectively. The methyl carbon atom C(7) group is bound to the nitrogen atom N(3) of the pyridine ring at a distance of 1.480(3) Å. The O(1)–H(2) and O(4)–H(4) distances are 2.67 and 2.63 Å, respectively. The oxygen atom O(1) and O(4) lay in the plane defined by the pyridine ring while O(2) is displayed from that plane with a torsion angle O(2)–P(1)–C(1)–C(6) of 59°. The phosphorus atoms have a tetrahedral geometry with angles ranging between 97.72(4) and 119.89(4)°. The P(1)–O(1) and P(2)–O(2) distances are 1.4653(16) and 1.4622(17) Å, respectively.

Compound **1** reacts with trimethyloxonium tetrafluoroborate in dichloromethane at room temperature over 6h to give compound **11**. After removing the volatiles under reduced pressure, compound **11** was obtained as a white solid, which dissolves in polar solvents such as dichloromethane, acetonitrile and tetrahydrofuran. In a $^{31}P\{^1H\}$ NMR spectrum the phosphorus nucleus resonates as a singlet at δ 4.9. A $^{19}F\{^1H\}$ NMR spectrum reveals a signal at δ –152.6, while a $^{11}B\{^1H\}$ NMR spectrum shows a signal at δ –1.5.

The deprotonation of compounds **10** and **11** was not successful although the experiments were performed with different bases (*t*BuOK, *n*BuLi and *t*BuLi) under different conditions. The reason that the carbene was not obtained is not clear. It may be traced back to the high lattice enthalpy of the salt or the dimerization of the product.

In 2014 ALCARAZO *et al.* reported a new kind of cationic ligands based on methyl pyridinium moiety and a phosphine moiety bound at C2. The weak σ-donor and strong π-acceptor character gives Pt(II) and Au(I) more π-acidity, which improve them to activate alkynes toward nucleophilic attacks. To change the counter anion (BF_4^-) for ($PtCl_3^-$) and to test it for $C_{aromatic}$–C_{alkyne} coupling[15], K_2PtCl_4 was added to **11** in dimethyl sulfoxide (DMSO). The mixture was stirred for 18 h. A $^{31}P\{^1H\}$ NMR spectrum of the reaction mixture exclusively showed the signal of **11** indicating that no reaction had occurred.

1.3. EXPERIMENTAL SECTION:

All reactions were carried out under argon 4.6 atmosphere using standard Schlenk line technique, unless otherwise specified. The argon was dried by passing through a glass column filled with phosphorus pentoxide and the glassware was dried by flame under reduced pressure. All solvents were dried according to the standard procedures fresh distilled and stored over molecular sieve.[16]

The NMR spectroscopy data was measured on the spectrometers Bruker AV 400 Avance III HD NanoBay, AV 500 Avance III HD, AV 600 Avance III HD, AV 700 Avance III HD and Agilent Technologies DD2. The NMR chemical shifts (δ) are given in ppm and the coupling constants *J* in Hz. ^{1}H and $^{13}C\{^{1}H\}$ NMR were referenced at $SiMe_4$ via the chemical shift of the solvents (C_6D_6 ^{1}H 7.16, ^{13}C 128.39, CD_2Cl_2 ^{1}H 5.32, ^{13}C 54.00, $CDCl_3$ ^{1}H 7.26, ^{13}C 77.16, CD_3CN ^{1}H 1.94, ^{13}C 1.39, CD_3OD ^{1}H 3.31, ^{13}C 49.00). The reference of ^{31}P, 85% H_3PO_4, ^{119}Sn, $SnMe_4$, ^{11}B, $BF_3.OEt_2$ and ^{19}F, $CFCl_3$. The IR spectra (cm^{-1}) are measured as a solid or oil by ATR Perkin Elmer Spectrum two.

The melting point (°C) is measured Büchi M-560 using an opened capillary. The elementary analysis was measured on CHNS-932 of the firm Leco, the measurements were carried out without inert atmosphere. The electrospray-mass spectroscopy was measured by the gadget Thermoquest Finnigan Instrument, which is thermoquest-finnigan device, the mobile phase is acetonitrile or dichloromethane with flow rate 10 µL/min. The concentration is c = 0.1 mg · mL^{-1}, the source voltage is 3.8 kV, the capillary voltage is 41 V (tube lens: 140 V) and the capillary temperature is 275 °C.

3,5-{P(O)(O*i*Pr)$_2$}C$_5$H$_4$N (1)

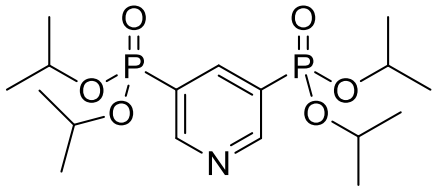

To 3,5-Dibromopyridine (80.00 g, 337.70 mmol), diisopropyl phosphite (134.67 g, 810.48 mmol) and triethylamine (85.43 g, 844.26 mmol) in acetonitrile (1000 mL) was added palladium(II)acetate (0.76 g, 3.38 mmol) and dppf (1.87 g, 3.38 mmol) at RT. The reaction mixture was heated at 90 °C over 48h. The solid was filtered, the solvent was removed under reduced pressure and the residues were dissolved in ethyl acetate (100 mL). Water (100 mL) was added and the organic layer was separated. The aqueous layer was extracted (3x, 100 mL) with ethyl acetate. The organic layers were collected, dried over $MgSO_4$ and concentrated to dryness. The crude product was purified with chromatography (silica gel, hexane : ethyl acetate from 9:1 to 1:1 and Et_3N 5%) followed by crystallization with hexane to obtain a white solid (119.69 g, 293.80 mmol, 87%) which melts at 52.11 °C and decomposes at 227.29 °C. **IR**: $\tilde{\nu}$ = 566 (s), 969 (vs, ν_{as} (PO*i*Pr)), 1245 (m, ν_s (PO)), 2979 (w) cm^{-1}, **^{1}H NMR** (200 MHz, C_6D_6): δ = 7.97 - 9.89 (m, 2H, *o*-Py), 7.08 – 6.95 (m, 1H, *p*-Py), 4.69 - 4.73 (m, 4H, OCH), 1.24 (d, ^3J(^{1}H , ^{1}H) = 6 Hz, 12H, OCH_3), 1.17 (d, ^3J(^{1}H , ^{1}H) = 6 Hz, 12H, CH_3), **^{13}C{^{1}H} NMR** (100.6 MHz, C_6D_6): δ = 155.6-155.8 (m, 2C, *o*-Py), 143.0 (t, 1C, ^2J(^{13}C , ^{31}P) = 8.8 Hz, *p*-Py), 128.1 (d, ^1J(^{13}C , ^{31}P) = 187.6 Hz, *m*-Py), 128.0 (d, ^1J(^{13}C , ^{31}P) = 187.8 Hz, *m*-Py), 71.6 – 71.7 (m, OCH), 24.3 (m, CH3), 24.0 – 24.1 (m, CH3), **^{31}P{^{1}H} NMR** (81 MHz, C_6D_6): δ = 13.4 (s). **Elemental Analyses.** Calcd. for $C_{17}H_{31}NO_6P_2$ 407.38 [g/mol]: C, 50.1 %, H, 7.7 %, N, 3.4%. Found: C, 50.3 %, H, 7.6 %, N, 3.2%, **ESI-MS**(70 eV): m/z (%): 408.2 (90) [M+H$^+$]

2,6-{P(O)(O*i*Pr)$_2$}C$_5$H$_4$N (2)

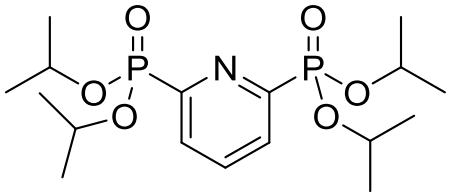

To 2,6-Dibromopyridine (20.00 g, 84.4 mmol), di*iso*propyl phosphite (33.70 g, 202.6 mmol) and triethylamine (42.70 g, 422.0 mmol) in acetonitrile (500 mL) was added palladium(II)acetate (0.19 g, 0.8 mmol) and dppf (0.51 g, 0.9 mmol) at rt. The reaction mixture was heated at 100 °C for 48h. The solid was filtered, the solvent was removed under reduced pressure and the residues were dissolved in ethyl acetate (50 mL). Water (100 mL) was added and the organic layer was separated. The aqueous layer was extracted with ethyl acetate (3x, 50

mL). The organic layers were collected, dried over $MgSO_4$ and concentrated to dryness. The crude product was purify with chromatography (ethyl acetate as eluent) to obtain a brown solid (30.55 g, 88%). **m.p.** 53.80 °C and decomposes at 228.13 °C , **IR**: $\tilde{\nu}$ = 559 (s), 971 (vs, ν_{as} (PO*i*Pr)), 1247 (m, ν_s (PO)), 1372 (w), 2979 (w) cm^{-1}, **^{1}H NMR** (400 MHz, CD_2Cl_2): δ = 8.02 – 7.99 (m, 2H, *m*-Py), 7.92 – 7.86 (m, 1H, *p*-Py), 4.84 – 4.73 (m, 4H, OCH), 1.35 (d, $^3J(^1H, ^1H)$ = 6 Hz, 12H, CH_3), 1.27 (d, $^3J(^1H, ^1H)$ = 6 Hz, 12H, CH_3), **^{13}C{^{1}H} NMR** (100 MHz, CD_2Cl_2): δ = 156.0 (d, $^2J(^{13}C, ^{31}P)$ = 22 Hz, $C_{3,5}$), 153.7 (d, $^2J(^{13}C, ^{31}P)$ = 22 Hz, $C_{3,5}$), 136.7 (t, $^3J(^{13}C, ^{31}P)$ = 11 Hz, C_4), 129.7 (d, $^1J(^{13}C, ^{31}P)$ = 29 Hz, $J(^{13}C, ^{31}P)$ = 21 Hz, $C_{2,6}$), 71.8 (d, $^2J(^{13}C, ^{31}P)$ = 6 Hz, OCH), 24.4 – 24.3 (m, CH_3), 24.2 – 24.1 (m, CH_3), **^{31}P{^{1}H} NMR** (162 MHz, CD_2Cl_2): δ = 7.31 (s). **Elemental Analyses.** Calcd. for $C_{17}H_{31}NO_6P_2$ 407.38 [g/mol]: C, 50.1 %, H, 7.7 %, N, 3.4%. Found: C, 49.9 %, H, 7.6 %, N, 3.2%. **ESI-MS** (70 eV): m/z (%): 408.2 (90) [$M+H^+$].

6-Br-2-{P(O)(O*i*Pr)$_2$}C$_5$H$_4$N (3)

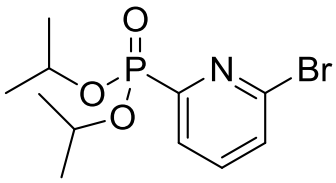

To 2,6-dibromopyridine (10.00 g, 42.1 mmol), di*iso*propyl phosphite (7.01 g, 42.1 mmol) and triethylamine (13.00 g, 126.6 mmol) in acetonitrile (250 mL) was added palladium(II)acetate (0.1 g, 0.4 mmol) and dppf (0.25 g, 0.4 mmol) at rt. The reaction mixture was heated at 100 °C for 48h. The solid was filtered, the solvent was removed under reduced pressure and the residues were dissolved in ethyl acetate (20 mL). Water (50 mL) was added and the organic layer was separated. The aqueous layer was extracted with ethyl acetate (3x, 20 mL). The organic layers were collected, dried over $MgSO_4$ and concentrated to dryness. The crude product was purified with chromatography (ethyl acetate as eluent) to obtain a brown solid (11.29 g, 83%). **^{1}H NMR** (200 MHz, C_6D_6): δ = 7.91 – 7.87 (m, 1H, *p*-Py), 7.65 – 7.56 (m, 2H, *m*-Py), 4.89 – 4.78 (m, 2H, OCH), 1.38 ($^3J(^1H, ^1H)$ = 6 Hz, 12H, CH_3), 1.32 ($^3J(^1H, ^1H)$ = 6 Hz, 12H, CH_3), **^{13}C{^{1}H} NMR** (100.6 MHz, C_6D_6): δ = 154.5 (d, $^1J(^{13}C, ^{31}P)$ = 226.6 Hz, CP), 142.9(s, CBr), 138.2 (d,

$^{2}J(^{13}C\ ,\ ^{31}P)$ = 12.3 Hz, *m*C), 130.4 (s, *m*C), 126.7 (s, *p*C), 72.2 (s, OC), 24.0 (s, CH_3), 23.7 (s, CH_3), **$^{31}P\{^{1}H\}$ NMR** (162 MHz, C_6D_6): δ = 6.5 (s).

2-{P(O)(O*i*Pr)$_2$}-6-{P(O)(O*i*Pr)Ph}C_5H_4N (4)

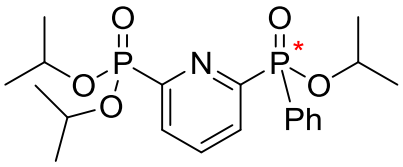

To 2-(diisopropyl phosphonato)-6-bromo pyridine (10.00 g, 31.0 mmol), *iso*propyl phenyl phosphite (5.72 g, 31.0 mmol) and triethylamine (6.00 g, 31.0 mmol) in acetonitrile (250 mL) was added palladium(II)acetate (0.1 g, 0.4 mmol) and dppf (0.25 g, 0.4 mmol) at rt. The reaction mixture was heated at 100 °C for 48h. The solid was filtered, the solvent was removed under reduced pressure and the residues were dissolved in ethyl acetate (20 mL). Water (50 mL) was added and the organic layer was separated. The aqueous layer was extracted with ethyl acetate (3x, 20 mL). The organic layers were collected, dried over $MgSO_4$ and concentrated to dryness. The crude product was purify with chromatography (ethyl acetate as eluent) to obtain a brown solid (8.50 g, 85%). **^{1}H NMR** (200 MHz, C_6D_6): δ = 8.16 (br, 1H), 7.93 – 7.83 (m, 4H), 4.42 – 4.34 (m, 3H), 4.68 – 4.55 (m, 3H, OCH),1.26 – 1.22 (m, 9H)1.14 – 1.11 (m, 6H) 1.08 – 1.05 (m, 3H), **$^{31}P\{^{1}H\}$ NMR** (162 MHz, C_6D_6): δ = 6.4 (s), 23.3 (s).

5-$SnPh_3$-2,6-{P(O)(O*i*Pr)$_2$}C_5H_2N (5)

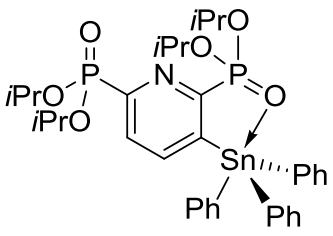

To 2,6-diisopropyl phosphite pyridine (5.00 g, 21.27 mmol) in THF was added LDA (12.76 mL, 25.53 mmol, 2M) at –60 °C and the mixture was stirred for 6h at –30 °C. The volatiles were removed under reduced pressure. The residue was suspended in water and extracted with ethylacetate (100 mL, 3x). The combined organic layers were dried over $MgSO_4$, filtered and concentrated to dryness. The crude product was purified with column chromatography (SiO_2, cyclohexane: ethyl acetate, 9:1 to 5:1) to give the product as a colourless solid (0.7g, 7%). **m.p.** 116.6 °C , **IR**: $\tilde{\nu}$ = 456 (s), 548 (s), 699 (s), 977 (vs, ν_{as} (PO*i*Pr)), 1227 (w, ν_s (PO)) cm^{-1}, **^{1}H NMR** (400 MHz, C_6D_6): δ = 8.10 – 8.05 (m, 1H, Py), 7.87 – 7.85 (m, 6H, Ph) 7.71 – 7.67 (m, 1H, Py), 7.27 – 7.17 (m, 9H, Ph), 4.97 – 4.86 (m, 2H, CH), 4.40 – 4.29 (m, 2H, CH), 1.26 (d, $^{3}J(^{1}H\ ,\ ^{1}H)$ = 6 Hz, 6H, CH_3), 1.22 (d, $^{3}J(^{1}H\ ,\ ^{1}H)$ = 6 Hz, 6H, CH_3), 1.04 (d, $^{3}J(^{1}H\ ,\ ^{1}H)$ = 6 Hz, 6H, CH_3), 0.94 (d, $^{3}J(^{1}H\ ,\ ^{1}H)$ = 6 Hz, 6H, CH_3). **$^{31}P\{^{1}H\}$ NMR** (162.0 MHz, C_6D_6): δ = 10.3 (d, $J(^{31}P\ ,\ ^{31}P)$ = 2 Hz, $J(^{31}P\ ,\ ^{117/119}Sn)$= 23/ 26 Hz), 13.4

(d, J(^{31}P , ^{31}P) = 2 Hz, J(^{31}P , $^{117/119}$Sn)= 14/ 18 Hz). **^{119}Sn{^{1}H} NMR** (162.0 MHz, C_6D_6): δ = –160 (dd, J(^{119}Sn , ^{31}P)= 16 Hz, J(^{119}Sn , ^{31}P)= 25 Hz. **Elemental Analyses.** Calcd. for $C_{17}H_{31}NO_6P_2$ 407.38 [g/mol]: C, 55.6 %, H, 6.0 %, N, 1.9 %. Found: C, 55.6 %, H, 6.0 %, N, 1.8 %. ESI-MS: m/z = 512.0 [M–Ph –4*i*Pr+4H], 554.1 [M–Ph –3*i*Pr+ 3H], 596.1 [M–Ph –2*i*Pr+ 2H], 638.1 [M–Ph –*i*Pr+ H], 680.2 [$C_{29}H_{40}NO_6P_2Sn$ (M–Ph)].

5,3-SnPh$_3$-2,6-{P(O)(O*i*Pr)$_2$}C$_5$H$_1$N (6)

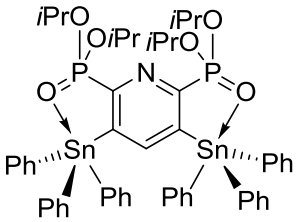

^{1}H NMR (400 MHz, C_6D_6): δ = 3.93 (t, ^{4}J(^{1}H , ^{31}P) = 5 Hz, ^{3}J(^{1}H , $^{117/119}$Sn) = 44/46 Hz, 1H, Py), 7.67 – 7.52 (m, 12H, *o*-Ph) 7.48 – 7.35 (m, 4H, Ph), 6.96 (s, 14H, Ph), 4.27 – 4.16 (m, 4H, OCH), 0.88 (d, ^{3}J(^{1}H , ^{1}H) = 6 Hz, 6H, CH_3), 0.77 (d, ^{3}J(^{1}H , ^{1}H) = 6 Hz, 6H, CH_3), 1.04 (d, ^{3}J(^{1}H , ^{1}H) = 6 Hz, 6H, CH_3), 0.94 (d, ^{3}J(^{1}H , ^{1}H) = 6 Hz, 6H, CH_3). **^{31}P{^{1}H} NMR** (C_6D_6, 162.0 MHz): δ = 13.4 (s, ^{5}J(^{31}P , $^{117/119}$Sn) = 27/29 Hz, ^{3}J(^{31}P , $^{117/119}$Sn) = 10/12 Hz).

PdCl$_2$[3,5-{P(O)(O*i*Pr)$_2$}C$_5$H$_4$N]$_2$ (7)

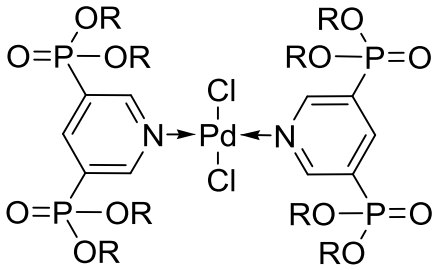

A dichloromethane and acetonitrile solution (1:10) of compound **1** (0.50 g, 1.23 mmol) and $PdCl_2$ (0.11 g, 0.61 mmol) was stirred for 2h at room temperature. From this solution, yellow crystals precipitated during 2 days. The crystals were separated, washed with dichloromethane and dried under reduced pressure. Yield 0.59 g, (97%). **m.p.** 140.8 °C, **IR**: $\tilde{\nu}$ = 974 (vs, ν_{as} (PO*i*Pr)), 1268 (m, ν_s (PO)) cm^{-1}, **^{1}H NMR** (400 MHz, $CDCl_3$): δ = 9.27 – 9.24 (m, 2H, *o*-Py), 8.60 – 8.53 (m, 1H, *p*-Py), 4.85 – 4.74 (m, 4H, OCH), 1.35 (d, ^{3}J(^{1}H , ^{1}H) = 6 Hz, 12H, OCH_3), 1.25 (d, ^{3}J(^{1}H , ^{1}H) = 6 Hz, 12H, CH_3), **^{13}C{^{1}H} NMR** (400 MHz, $CDCl_3$): δ = 157.9 (2C, *o*-Py), 144.8 (1C, *p*-Py), 130.1 (d, ^{1}J(^{13}C , ^{31}P) = 11 Hz, *m*-Py), 128.0 (d, ^{1}J(^{13}C , ^{31}P) = 11 Hz, *m*-Py), 72.8 (m, OCH), 24.1 (m, CH_3), **^{31}P{^{1}H} NMR** (162.0 MHz, $CDCl_3$): δ = 8.3. **Elemental Analyses.** Calcd. for

$C_{17}H_{31}NO_6P_2$ 407.38 [g/mol]]: C, 41.2 %, H, 6.3 %, N, 2.8%. Found: C, 41.1 %, H, 6.4 %, N, 2.8 %.

2,4,6-trimethylstyrene

To a mixture of 7 (0.5 g, 0.50 mmol) and mesityl bromide (1 g, 5.02 mmol) was added allylmagnesium chloride (3 mL 1.7M in THF, 5.02 mmol). The solution was stirred at 80 °C for 12h, after which the volatiles were removed under reduced pressure. The residues were dissolved in water and extracted with ethylacetate. The combined organic layers were dried over $MgSO_4$ filtered and concentrated to dryness under vacuum. The crude product was distilled (52 °C, 1 mbar) to obtain the product as a colourless oil (0.55 g, 75%), **^{1}H NMR** (400 MHz, $CDCl_3$): δ = 6.88 (s, 2H, Mes), 5.96 - 5.86 (m, 1H, C*H*CH_2), 5.01 (dq, ^3J(^{1}H , ^{1}H) = 10 Hz, ^6J(^{1}H , ^{1}H) = 2 Hz), 1H, CHCH_2), 4.89 (dq, ^3J(^{1}H , ^{1}H) = 17 Hz, ^6J(^{1}H , ^{1}H) = 2 Hz), 1H, CHCH_2), 2.29 (s, 9H, CH_3)

5-$SnPh_2I$-2,6-{P(O)(O*i*Pr)$_2$}C_5H_2N (8)

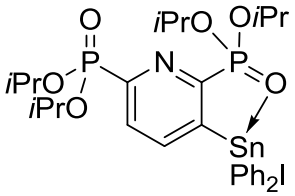

2,6-bis(diisopropyl phosphonato)-3-triphenyl tin pyridine (0.15 g, 0.20 mmol) and iodine (0.05 g, 0.20 mmol) in dichloromethane was stirred at room temperature for 16h. The volatiles were removed under reduced pressure and the residues were recrystallized with chloroform/hexane to obtain the product as a pale yellow crystals (0.15 g, 80%) **m.p.** 134.3 °C ;**^{1}H NMR** (400 MHz, $CDCl_3$): δ = 9.29 – 9.25 (m, 1H, Py), 8.19 – 8.15 (m, 1H, Py), 8.07 – 7.86 (m, 4H, Ph), 7.73 – 7.70 (m, 2H, Ph), 7.44 – 7.36 (m, 4H, Ph), 4.91 – 4.83 (m, 2H, OCH), 4.38 – 4.30 (m, 2H, OCH), 1.40 (d, ^3J(^{1}H , ^{1}H) = 6 Hz, 6H, CH_3), 1.33 (d, ^3J(^{1}H , ^{1}H) = 6 Hz, 6H, CH_3) 1.15 (d, ^3J(^{1}H , ^{1}H) = 6 Hz, 6H, CH_3), 1.02 (d, ^3J(^{1}H , ^{1}H) = 6 Hz, 6H, CH_3). **^{13}C{^{1}H} NMR** (100.6 MHz, $CDCl_3$): δ = 147.5 (s), 142.4 (s), 137.5 (s),136.4 (s), 130.3 (s), 129.37 (s), 128.3 (s), 127.5 (s), 74.2 (d, ^1J(^{13}C , ^{31}P) = 7 Hz, OCH), 72.1 (d, ^1J(^{13}C , ^{31}P) = 7 Hz, OCH), 24.1 (d, ^3J(^{13}C , ^{31}P) = 5 Hz, CH_3), 23.9(d, ^3J(^{13}C , ^{31}P) = 5 Hz, CH_3), 23.5 (d, ^3J(^{13}C , ^{31}P) = 5 Hz, CH_3), 23.4 (d, ^3J(^{13}C , ^{31}P) = 5 Hz, CH_3), **^{31}P{^{1}H} NMR** (162.0 MHz, $CDCl_3$): δ = 14.3 (d, J(^{31}P , ^{31}P) = 2 Hz, J(^{31}P , $^{117/119}$Sn) = 53/57 Hz), 7.1 (d, J(^{31}P , ^{31}P)

= 2 Hz, $J(^{31}P, ^{117/119}Sn)$ = 29/32 Hz) **^{119}Sn{^{1}H} NMR** (162.0 MHz, $CDCl_3$): δ = –196 (dd, $J(^{119}Sn, ^{31}P)$= 57 Hz, $J(^{119}Sn, ^{31}P)$= 32 Hz).

5-SnPhI$_2$-2,6-{P(O)(O*i*Pr)$_2$}C$_5$H$_2$N (9)

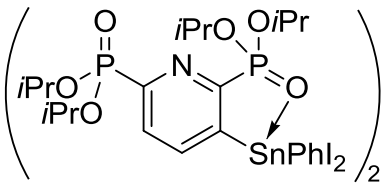

2,6-bis(diisopropyl phosphonato)-3-triphenyl tin pyridine (0.15 g, 0.20 mmol) and iodine (0.10 g, 0.40 mmol) in dichloromethane was stirred at room temperature for 16h. The volatiles were removed under reduced pressure and the residues were recrystallized with chloroform/hexane to obtain the product as a pale yellow crystals (0.13 g, 75%) **m.p.** 165.3 °C **^{1}H NMR** (400 MHz, $CDCl_3$): δ = 9.13 – 8.87 (m, 1H, Py), 8.17 – 8.14 (m, 1H, Py), 7.88 – 7.85 (m, 1H, Ph), 7.38 – 7.25 (m, 4H, Ph), 4.84 – 4.76 (m, 2H, OCH), 4.65 – 4.57 (m, 2H, OCH), 1.33 (d, $^{3}J(^{1}H, ^{1}H)$ = 6 Hz, 6H, CH_3), 1.26 (d, $^{3}J(^{1}H, ^{1}H)$ = 6 Hz, 6H, CH_3) 1.23 (d, $^{3}J(^{1}H, ^{1}H)$ = 6 Hz, 6H, CH_3), 1.11 (d, $^{3}J(^{1}H, ^{1}H)$ = 6 Hz, 6H, CH_3). **^{31}P{^{1}H} NMR** (162.0 MHz, $CDCl_3$): δ = 13.7 (d, $J(^{31}P, ^{31}P)$ = 2 Hz, $^{3}J(^{31}P, ^{117/119}Sn)$ = 65 Hz), 6.2 (d, $J(^{31}P, ^{31}P)$ = 2 Hz, $J(^{31}P, ^{117/119}Sn)$ = 40 Hz) **^{119}Sn{^{1}H} NMR** (162.0 MHz, $CDCl_3$): δ = –448 (dd, $J(^{119}Sn, ^{31}P)$= 40 Hz, $J(^{119}Sn, ^{31}P)$= 65 Hz).

3,5-{P(O)(O*i*Pr)$_2$}C$_5$H$_4$NMe·I (10)

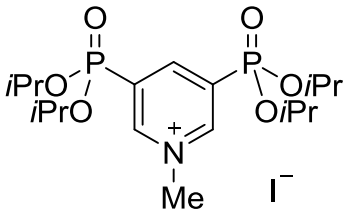

To a solution of **1** (10.00 g, 24.55 mmol) in acetonitrile (250 mL) was added methyl iodide (6.97 g, 49.09 mmol). The solution was stirred at room temperature for 16 h followed by heating at 40 °C for 4 h. The volatiles were removed under reduced pressure, the residues were washed with hexane (10 mL), filtered and dried, to obtain the product as a yellow amorphous powder (5.60 g, 77%), which was recrystallized from EE/DCM. **m.p.** 115 °C, **IR**: 1253 (s, P=O), 980 (vs, PO*i*Pr) cm^{-1}, **^{1}H NMR** (600 MHz, $CDCl_3$): δ = 9.37 (m, 2H, *o*-Py), 8.82 (t, 1H, $^{2}J(^{1}H, ^{1}H)$ = 12 Hz, *p*-Py), 4.93 (m, 4H, OC*H*), 4.88 (s, 3H, NCH_3), 1.44 (d, 12H, CCH_3, $^{2}J(^{1}H, ^{1}H)$ = 6 Hz), 1.34 (d, 12H, CCH_3, $^{2}J(^{1}H, ^{1}H)$ = 6 Hz)**, ^{13}C{^{1}H} NMR** (150 MHz, $CDCl_3$): δ = 149.9 (*o*-Py), 149.4 (*o*-Py), 133.5 (*p*-Py), 132.2 (*m*-Py), 74.2 (O*C*H), 51.4 (NCH_3), 24.1 (C*C*H_3), 24.0 (C*C*H_3)**, ^{31}P{^{1}H} NMR** (250 MHz, $CDCl_3$): δ = 4.7 (s)**, Elemental Analyses.**

Calcd. for $C_{18}H_{34}NO_6P_2I$ 549.09 [g/mol]: C, 39.36%, H, 6.24%, N, 2.55%, found: C, 38.00%, H, 6.40%, N, 2.30%, **ESI-MS (70 eV, positive mode)**: m/z (%): 422.2 (100) [M + H^+].

3,5-{P(O)(O*i*Pr)$_2$}C_5H_4NMe·BF_4: (11)

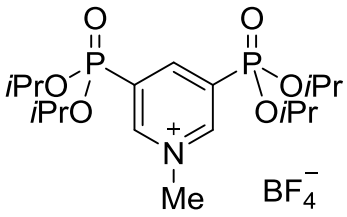

To **1** (4.20 g, 10.31 mmol) in dichloromethane was added trimethyloxonium tetrafluoroborate (1.52 g, 10.31 mmol) at room temperature. The reaction mixture was stirred over 18h and the volatiles were removed under reduced pressure, to obtain the product as a white solid (4.7 g, 89 %). **M.p.** 115 °C, **^{1}H NMR** (400 MHz, $CDCl_3$): δ = 9.12 (d, ^4J(^{1}H , ^{1}H)= 9 Hz, 2H, *o*-Py), 8.88 (t, ^4J(^{1}H , ^{1}H)= 12 Hz, 1H, *m*-Py), 4.89 – 4.82 (m, 4H, OC*H*), 4.65 (s, NCH_3), 1.43 (d, ^2J(^{1}H , ^{1}H) = 6 Hz, 12H, CCH_3), 1.31 (d, ^2J(^{1}H – ^{1}H) = 6 Hz, 12H, CCH_3), **^{13}C{^{1}H} NMR**(100 MHz, $CDCl_3$): δ = 149.9 (m, Py), 149.1 (s, Py), 133.9 (d, J(^{13}C , ^{31}P) = 11 Hz, Py), 132.0 (d, J(^{13}C , ^{31}P) = 11 Hz, Py), 74.1 (s, O*C*H), 49.9 (s, N*C*H_3), 24.0 (s, C*C*H_3). **^{31}P{^{1}H} NMR** (162 MHz, $CDCl_3$): δ = 4.6 (s), **^{19}F{^{1}H} NMR** (250 MHz, $CDCl_3$): δ = –152.6 (s), **^{11}B{^{1}H} NMR** (377 MHz, $CDCl_3$): δ = –1.5 (s).

1.4 CONCLUSION

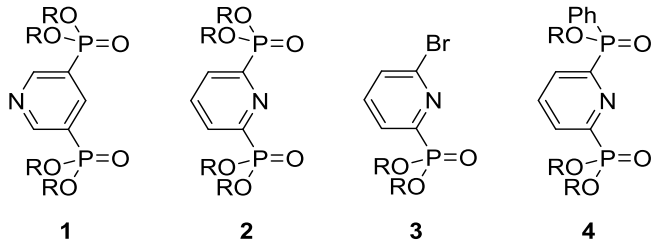

Scheme 9. The synthesised ligands.

In this chapter the syntheses of novel *O*,*C*,*O*-and *O*,*N*,*O*-coordinating pincer-type ligands is reported (Scheme **10**). The compounds were prepared by Hirao cross coupling reactions between the corresponding *di*-bromo pyridine derivate and di*iso*propyl phosphite. The products were isolated in good yields and listed in (Scheme **10**).

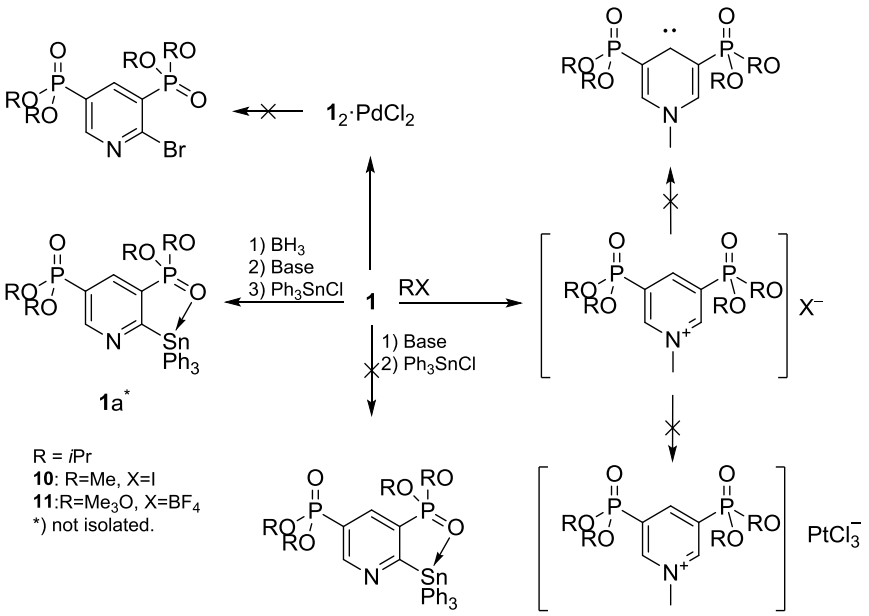

Scheme 10. Reactivity of compound **1**.

Compound **1** is stable toward *n*BuLi, *t*BuLi and LDA because it complexes RLi, while the deprotonation of **1**·BH_3 with LDA followed by the addition of $SnPh_3Cl$ gives to **1a** which was, however, not isolated (Scheme 10). The reaction of **1** with alkylation reagents (MeI and Me_3OBF_4) provides the corresponding pyridinium salts **10** and **11**. The reaction of **10** and **11** with base to produce the corresponding carbene, the change of BF_4^- with $PtCl_3^-$, and the addition of elemental bromine to the pyridine ring to achieve selective bromination failed.

Compound **2** reacts with LDA to produce the corresponding lithium compound, which reacts with Ph_3SnCl to give 2,6-di-P(O)(O*i*Pr)$_2$C$_5$H$_2$N-3-SnPh$_3$ and 2,6-di-P(O)(O*i*Pr)$_2$C$_5$H$_2$N-3,5-(SnPh$_3$)$_2$.

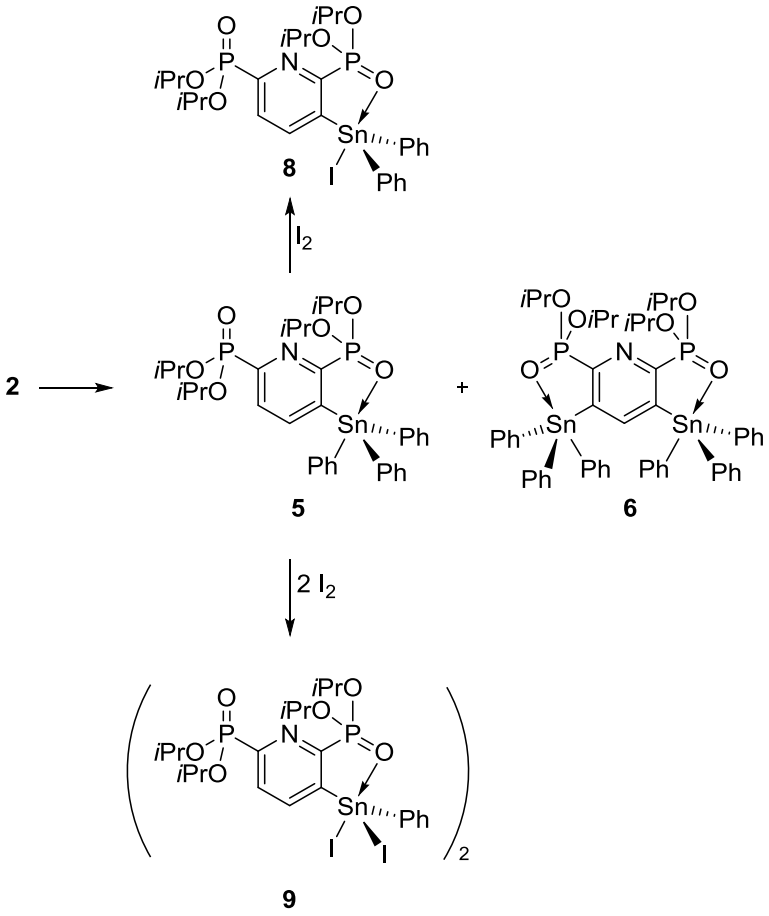

Scheme 11. Reactivity of compound **2**.

Compound 2,6-di-P(O)(O*i*Pr)$_2$C$_5$H$_2$N-3-SnPh$_3$ reacts with elemental iodine in 1:1 and 1:2 stoichiometric ratios to give 2,6-di-P(O)(O*i*Pr)$_2$C$_5$H$_2$N-3-SnPh$_2$I **8** and 2,6-di-P(O)(O*i*Pr)$_2$C$_5$H$_2$N-3-SnPhI$_2$ **9** (Scheme 11).

1.5. LITERATURE

[1] M. Mehring, M. Schürmann, K. Jurkschat, *Organometallics* **1998**, *17*, 1227.

[2] H. Markus, *Neue intermolekular koordination organoelmentverbindugen des Zinns undAntimons unter verwendung O,C,O-koordinierende Zangenligand*, **2004**.

[3] M. Mehring, *Neue intramolekulare Donorliganden zur Synthese hyperkoordinierter Organoelementverbindungen*, Shaker, Aachen, **1998**.

[4] a) M. Mehring, C. Löw, M. Schürmann, F. Uhlig, K. Jurkschat, *Organometallics* **2000**, *19*, 4613; b) M. Wagner, K. Dorogov, M. Schürmann, I. Vrasidas, K. Jurkschat, *Phosphorus, Sulfur, and Silicon and the Related Elements* **1999**, *150*, 311; c) M. Wagner, K. Dorogov, M. Schürmann K. Jurkschat, *Dalton Trans.* **2011**, *40*, 8733; d) M. Wagner, M. Henn, C. Dietz, M. Schürmann, M. Prosenc, K. Jurkschat, *Organometallics* **2013**, *32*, 2406; e) K. Peveling, M. Henn, C. Löw, M. Mehring, M. Schürmann, B. Costisella, K. Jurkschat, *Organometallics* **2004**, *23*, 1501; f) M. Wagner, C. Dietz, M. Bouska, L. Dostal, Z. Padelkova, R. Jamor, K. Jurkschat, *Organometallics* **2013**, *32*, 4973; g) M. Wagner, C. Dietz, S. Krabbe, S. Koller, C. Strohmann,K. Jurkschat, *Inorg. Chem.* **2012**, *51*, 6851; h) S. Krabbe, M. Wagner, C. Löw, C. Dietz, M. Schürmann, A. Hoffmann, S. Herres-Pawlis, M. Lutter, K. Jurkschat, *Organometallics* **2014**, *33*, 4433; i) M. Henn, M. Schürmann, B. Mahieu, P. Zanello, A. Cinquantini, K. Jurkschat, *J. Organomet. Chem.* **2006**, *691*, 1560; j) Wagner, Zoller, Hiller, Prosenc, Jurkschat, *Chem. Commun.* **2013**, *49*, 8925; k) M. Wagner, T. Zöller, C. Dietz, K. Jurkschat, *Main Group Met. Chem.* **2015**, *38*; l) M. Wagner, T. Zoller, W. Hiller, M. H. Prosenc. K. Jurkschat, *Chem. Eur. J.* **2013**, *19*, 9463; m) M. Wagner, M. Lutter, C. Dietz, M. H. Prosenc, K. Jurkschat, *Eur. J. Inorg. Chem.* **2015**, *2015*, 2152; n) M. Henn, K. Jurkschat, R. Ludwig, M. Mehring, K. Peveling M. Schüemann, *Z. Anorg. Allg. Chem.* **2002**, *628*, 2940; o) K. Peveling, M. Schürmann, K. Jurkschat, *Z. Anorg. Allg. Chem.* **2002**, *628*, 2435; p) M. Mehring, C. Löw, M. Schürmann, K. Jurkschat, *Eur. J. Inorg. Chem.* **1999**, 887.

[5] Y. Belabassi, S. Alzghari, J.-L. Montchamp, *J. Organomet. Chem.* **2008**, *693*, 3171.

[6] J. J. Bulot, E. E. Aboujaoude, N. Collignon, P. Savignac, *Phosphorus, Sulfur Silicon Relat. Elem.* **2006**, *21*, 197.

[7] M. Henn, V. Deáky, S. Krabbe, M. Schürmann, M. H. Prosenc, S. Herres-Pawlis, B. Mahieu, K. Jurkschat, *Z. Anorg. Allg. Chem.* **2011**, *637*.

[8] M. Mantina, A. C. Chamberlin, R. Valero, C. J. Cramer, D. G. Truhlar, *J. Phys. Chem., A* **2009**, *113*, 5806.

[9] M. Haase, W. Günter, H. Görls and E. Anders, *Synthesis* **1999**, *1999*, 2071.

[10] D. R. Armstrong, M. G. Davidson, R. P. Davies, H. J. Mitchell, R. M. Oakley, P. R. Raithby, R. Smith and S. Warren, *Angew. Chem.* **1996**, *108*, 2071.

[11] Benedikt Piorr, *Synthese und Charakterisierung von Zangenligandstabilisierten Organoelementverbindungen –Struktur und Reaktionsverhalten*, **2016**.

[12] S. Paraskewas, *Synthesis* **1980**, *5*, 378.

[13] J. Christoph, *J. Chem. Soc., Dalton Trans.* **2000**, 3885.

[14] D. B. Ninkovic, J. M. Andric, S. D. Zaric, *Chemphyschem* **2013**, *14*, 237.

[15] H. Tinnermann, C. Wille, M. Alcarazo, *Angew. Chem. Int. Ed.* **2014**, *53*, 8732.

[16] W. L. F. Armarego, C. L. L. Chai, *Purification of laboratory chemicals*, Elsevier/Butterworth-Heinemann, Amsterdam, Boston, **2009**.

[17] a) D. W. Stephan, G. Erker, *Angew. Chem. Int. Ed.* **2015**, *54*, 6400; b) D. W. Stephan, *Science* **2016**, *354*; c) D. W. Stephan, *J. Am. Chem. Soc.* **2015**, *137*, 10018.

[18] a) P. Jutzi, K. Leszczyńska, A. Mix, B. Neumann, W. W. Schoeller, H.-G. Stammler, *Organometallics* **2009**, *28*, 1985; b) P. Jutzi, K. Leszczynska, B. Neumann, W. W. Schoeller, H.-G. Stammler, *Angew. Chem. Int. Ed.* **2009**, *48*, 2596; c) P. Jutzi, G. Reumann, *J. Chem. Soc., Dalton Trans.* **2000**, 2237; d) P. Jutzi, A. Mix, B. Rummel, W. W. Schoeller, B. Neumann, H.-G. Stammler, *Science* **2004**, *305*, 849.

[19] A. P. Singh, H. W. Roesky, E. Carl, D. Stalke, J.-P. Demers, A. Lange, *J. Chem. Soc., Dalton Trans.* **2012**, *134*, 4998.

[20] a) M. Bouska, L. Dostal, M. Lutter, B. Glowacki, Z. Ruzickova, D. Beck, R. Jambor, K. Jurkschat, *Inorganic chemistry* **2015**, *54*, 6792; b) M. Bouška, L. Dostál, A. Růžička, R. Jambor, *Organometallics* **2013**, *32*, 1995.

[21] J. C. Avery, M. A. Hanson, R. H. Herber, K. J. Bladek, P. A. Rupar, I. Nowik, Y. Huang, K. M. Baines, *Inorg. Chem.,* **2012**, *51*, 7306.

[22] M. J. Frisch, G. W. Trucks, H. B. Schlegel, G. E. Scuseria, M. A. Robb, J. R. Cheeseman, G. Scalmani, V. Barone, G. A. Petersson, H. Nakatsuji, X. Li, M. Caricato, A. Marenich, J. Bloino, B. G. Janesko, R. Gomperts, B. Mennucci, H. P. Hratchian, J. V. Ortiz, A. F. Izmaylov, J. L. Sonnenberg, D. Williams-Young, F. Ding, F. Lipparini, F. Egidi, J. Goings, B. Peng, A. Petrone, T. Henderson, D. Ranasinghe, V. G. Zakrzewski, J. Gao, N. Rega, G. Zheng, W. Liang, M. Hada, M. Ehara, K. Toyota, R. Fukuda, J.

Hasegawa, M. Ishida, T. Nakajima, Y. Honda, O. Kitao, H. Nakai, T. Vreven, K. Throssell, J. A. Montgomery, Jr., J. E. Peralta, F. Ogliaro, M. Bearpark, J. J. Heyd, E. Brothers, K. N. Kudin, V. N. Staroverov, T. Keith, R. Kobayashi, J. Normand, K. Raghavachari, A. Rendell, J. C. Burant, S. S. Iyengar, J. Tomasi, M. Cossi, J. M. Millam, M. Klene, C. Adamo, R. Cammi, J. W. Ochterski, R. L. Martin, K. Morokuma, O. Farkas, J. B. Foresman, and D. J. Fox, *Gaussian 09, Revision E.01*, Gaussian, Inc. Wallingford CT, 2016.

[23] J.-D. Chai, M. Head-Gordon, *Phys. Chem. Chem. Phys.* **2008**, *10*, 6615.

[24] a) F. Weigend, R. Ahlrichs, *Phys. Chem. Chem. Phys.* **2005**, *7*, 3297; b) B. Metz, H. Stoll, M. Dolg, *J. Chem. Phys.* **2000**, *113*, 2563.

[25] R. Krishnan, J. S. Binkley, R. Seeger, J. A. Pople, *J. Chem. Phys.* **1980**, *72*, 650.

[26] [Cannot display reference #27, because the template "Bibliography - Journal Article - (Default template)" contains only fields that are empty in this reference.]

[27] B. R. Kim, H.-G. Lee, S.-B. Kang, G. H. Sung, J.-J. Kim, J. K. Park, S.-G. Lee, Y.-J. Yoon, *Synthesis* **2012**, *44*, 42.

[28] Li Shen, Juliane Haufe and Martin K. Patel, *Product Overview and Market Projection of Emerging Bio-based Plastics*, **2009**, Utrecht.

[29] J. Majid, T. Elmira Arab, M. Imran, M. Jacquot, S. Desobry, *Comprehensive Reviews in Food Science and Food Safety* **2010**, *9*, 552.

[30] a) D. S. McGuinness, E. L. Marshall, V. C. Gibson, J. W. Steed, *J. Polym. Sci., Polym Chem.* **2003**, *41*, 3798; b) S. Csihony, T. T. Beaudette, A. C. Sentman, G. W. Nyce, R. M. Waymouth, J. L. Hedrick, *Adv. Syn. Catal.* **2004**, *346*, 1081; c) A. Bhaw-Luximon, D. Jhurry, N. Spassky, S. Pensec, J. Belleney, *Polymer* **2001**, *42*, 9651; d) C. Stere, M. Iovu, A. Boborodea, D. S. Vasilescu, I. S. Fazakas-Anca, *Polym. Advan. Technol.* **1998**, *9*, 322.

[31] N. Emig, H. Nguyen, H. Krautscheid, R. Reau, J. Cazaux and G. Bertrand, *Organometallics* **1998**, *17*, 3599.

[32] a) E. L. Marshall, V. C. Gibson, H. S. Rzepa, *J. Am. Chem. Soc.* **2005**, *127*, 6048; b) A. Kowalski, A. Duda, S. Penczek, *Macromolecules* **2000**, *33*, 7359.

[33] M. S. Stanford, A. Dove, *Chem. Soc. Rev.* **2010**, *39*, 486.

[34] K. Izod, *Coordination Chemistry Reviews* **2012**, *256*, 2972.

[35] M. J. S. Gynane, D. H. Harris, M. F. Lappert, P. P. Power, P. Rividre, M. Rividre-Baudet, *J. CHem. Soc. Dalton Trans.* **1977**, 2004.

[36] W. W. Du Mont, M. Grenz, *Chem. Ber.* **1985**, *118*, 1045.

[37] R. Janoschek, H. Pritzkow, S. Rell, U. Winkler, M. Driess, *Angew. Chem. Int. Ed.* **1995**, *34*, 1614.

[38] K. Izod, J. Stewart, E. R. Clark, W. McFarlane, B. Allen, W. Clegg, R. W. Harrington, *Organometallics* **2009**, *28*, 3327.

[39] K. Izod, J. Stewart, W. Clegg, R. W. Harrington, *Organometallics* **2010**, *29*, 108.

[40] T. Řezníček, L. Dostál, A. Růžička, R. Jambor, *Eur. J. Inorg. Chem.* **2012**, *2012*, 2983.

[41] a) S. M. Mansell, C. A. Russell, D. F. Wass, *Inorg. Chem.,* **2008**, *47*, 11367; b) M. Huang, M. M. Kireenko, E. K. Lermontova, A. V. Churakov, Y. F. Oprunenko, K. V. Zaitsev, D. Sorokin, K. Harms, J. Sundermeyer, G. S. Zaitseva et al., *Z. anorg. allg. Chem.* **2013**, *639*, 502; c) K. Jurkschat, M. Scheer, A. Tzschach, *Z. Anorg. Allg. Chem.* **1984**, *515*, 147; d) J. Faure, H. Gornitzka, R. Reau, D. Stalke, G. Bertrand, *Eur. J. Inorg. Chem.* **1999**, *1999*, 2295.

[42] W. W. du Mont, *Polyhedron* **1988**, *7*, 1317.

[43] M. Driess, S. Martin, K. Merz, V. Pintchouk, H. Pritzkow, H. Griitzmacher, M. Kaupp, *Angew. Chem. Int. Ed.* **1997**, *36*, 1894.

[44] a) V. M. D'yakov, A. F. Makarov, A. M. Kir'yanova, S. I. Androsenko, *J. Gen. Chem. USSR (Engl. Transl.)* **1992**, *62*, 285; b) M. G. Voronkov, A. I. Albanov, E. A. Grebneva, O. M. Trofimova, N. F. Chernov, N. N. Chipanina, *Russ. J. Gen. Chem.* **2006**, *76*, 1854; c) M. A. Pudovik, S. A. Terent'eva, A. N. Pudovik, *J. Gen. Chem. USSR (Engl. Transl.)* **1983**, *55*, 2185; d) A. A. Selina, S. S. Karlov, G. S. Zaitseva, *Chem. Heterocycl. Compd.* **2006**, *42*, 1518.

[45] M. Lutter, L. Iovkova-Berends, C. Dietz, V. Jouikov, K. Jurkschat, *Main Group Metal Chemistry* **2012**, *35*.

[46] A. Helßer, S. Kuchen, O. Stelzer, W. S. Sceldrick, *J. Organomet. Chem.* **1998**, *553*, 39.

[47] S. Molitor, J. Becker, V. H. Gessner, *J. Am. Chem. Soc.,* **2014**, *136*, 15517.

CHAPTER 2

2.1. INTRODUCTION

The cations of low valent group 14 elements have, in addition to the empty orbital, a positive charge which causes a high electrophilic character. In addition, the lone electron pair gives them a nucleophile character, which forms frustrated lewis pairs (FLP) compounds.[1]

The first tin(II) cation, {[$Me_2Si(Me_4C_5H)[Sn(\eta^5\text{-}C_5Me_5)]$]}$^+$, as its CF_3SO_3, BF_4 salt, was reported by JUTZI *et al.* (Figure 1). It was obtained from the reaction of $Me_2Si(Me_4C_5H)(Me_4C_5Li)$ with tin(II)halide followed by the addition of HX (X = CF_3SO_3, BF_4).[2] In 2012 ROESKY *et al.* and in 2015 JAMBOR *et al.* reported the autoionization of $SnCl_2$ to obtain $SnCl^+$and $SnCl_3^-$ via a *N*,*N*,*N*-ligand[3] **B** and *N*,*N*-ligand[4] **C**, respectively. BAINES *et al.* reported cryptand[2.2.2]SnX][SnX_3] (X = Cl, Br and I) and [cryptand[2.2.2]Sn][OTf]$_2$ by the stirring a solution of SnX_2 and 2.2.2-cryptand at room temperature.[5]

In the last two decades, Jurkschat *et al.* systematically studied intramolecularly coordinated low-valent tin compounds of types **E** and **F**.[4–6] They also reported a [SnCl]$^+$ cation of type **G** stabilized by ferrocene-backboned P=O donor ligands. Looking at compounds of type **E** and **F**, and thinking isoelectronically, the formal replacement of the *O,C,O*-coordinating pincer-type ligand by a corresponding pyridine-based *O,N,O*-coordinating ligand should allow the synthsis of the complexes **1** - **4**. Indeed, this chapter reports the syntheses and complete characterisation of these compounds. In addition, the reactivity toward the LEWIS acid $WD_x(CO)_{6-x}$ (D = THF or MeCN; X = 1 and 2) is also reported.

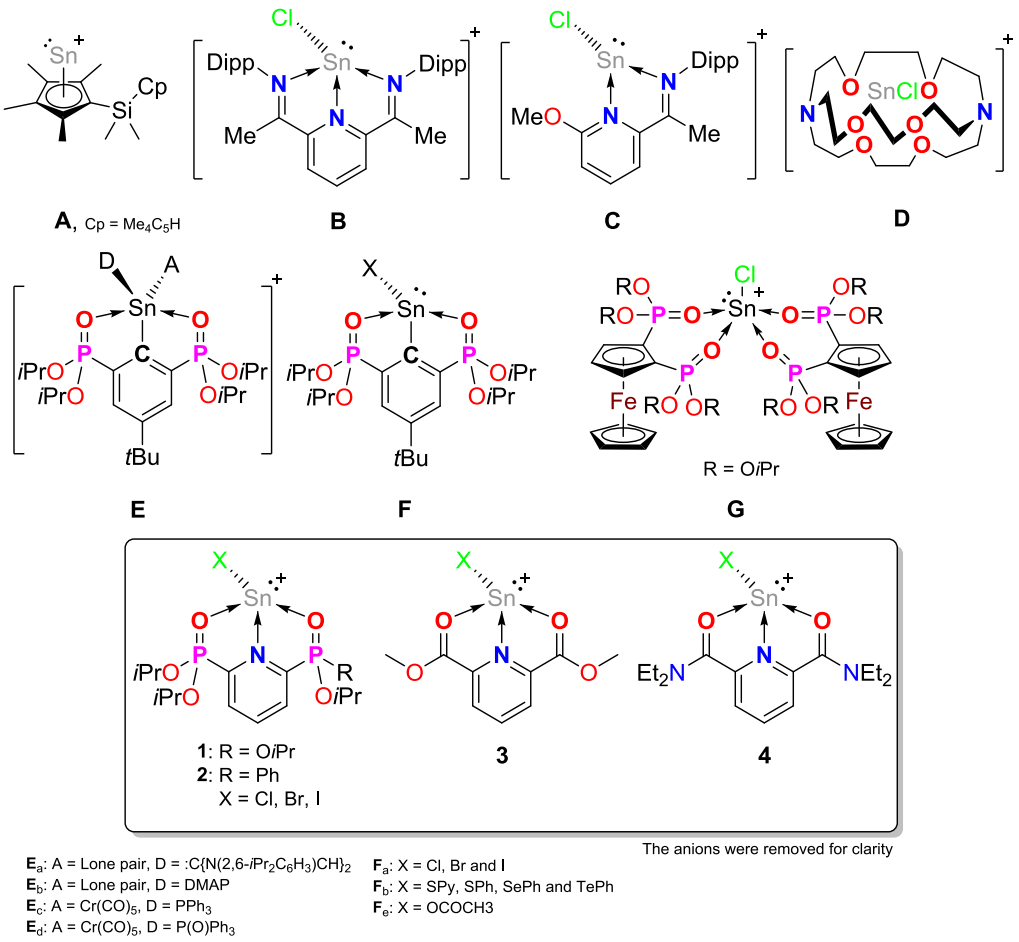

Figure 1. Selected examples of tin(II) cations and of the novel compounds reported in this thesis.

2.2 RESULTS AND DISCUSSION

2.2.1 The synthesis and characterization of compound [2,6-{P(O)(O*i*Pr)$_2$}C$_5$H$_5$NSnX]SnX$_3$

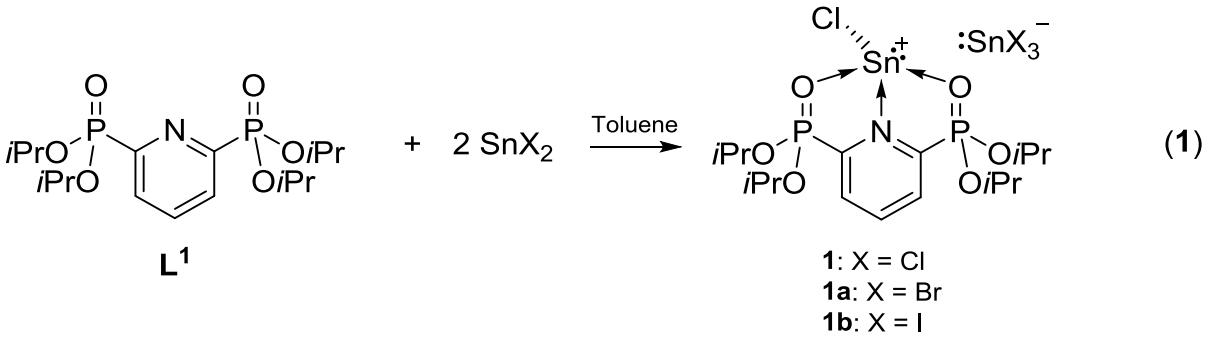

(1)

The ligand **L**^{1} was treated with $SnCl_2$ in toluene at room temperature in a ratio of 1:2 under an argon atmosphere (Equation 1). After 15 min of magnetical stirring, the $SnCl_2$ had completely dissolved. A $^{31}P\{^1H\}$NMR spectrum of the crude reaction mixture showed a singlet at δ 16.9.

Compound **1** was isolated in good yield (86%) as colourless air-stable crystalline material from its saturated toluene solution. It is soluble in toluene, benzene and tetrahydrofuran. A ^1H NMR spectrum of a solution of compound **1** in toluene-d$_8$ shows the *para* proton of the pyridine moiety shifted downfield (δ 8.63) in comparison to the ligand **L**^{1} (δ 7.99). A $^{31}P\{^1H\}$ NMR spectrum (in toluene-d$_8$) shows the phosphorus atoms of complex **1** to resonate downfield (δ 16.5) in comparison to the free ligand (δ 8.8). This downfield shift is traced back to the coordination of the P=O oxygen atoms to the $SnCl^+$.

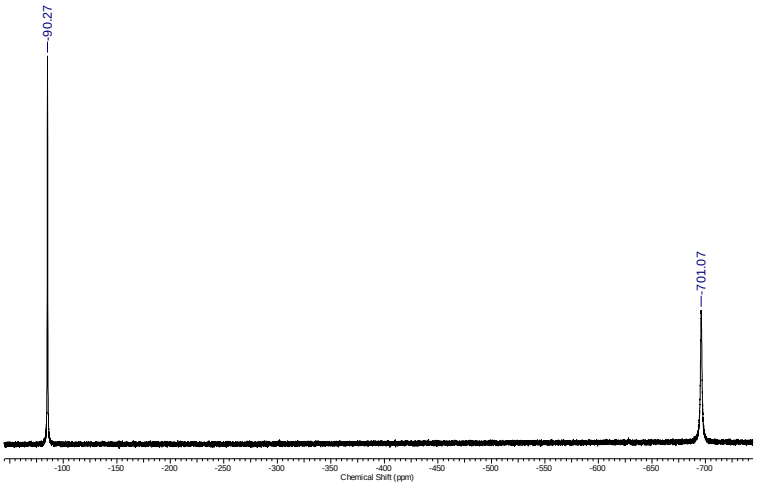

Figure 2. $^{119}Sn\{^1H\}$ NMR spectrum of a solution of compound **1** toluene-d$_8$ at –80 °C.

A $^{119}Sn\{^{1}H\}$ NMR spectrum at 298 K revealed no signals indicating kinetic lability on the ^{119}Sn NMR time scale. However, at 193 K two equally intense resonances at δ –90 ($SnCl_3^-$) and δ –701 ($SnCl^+$) were observed (Figure 2). In comparison with compounds **B** ($\delta_{^{119}Sn}$ –60 and –435) and **C** ($\delta_{^{119}Sn}$ –73 and –330) synthesized by ROESKY *et al.* and JAMBOR *et al.*, respectively, compound **1** shows the most high field shift. This high field shift for **1** is traced back to an increased shift of electron density from the P=O functional group to the tin centre (see below).

Single crystals of **1** suitable for X-ray diffraction analysis were obtained from its toluene solution at room temperature. On the other hand, at 263 K compound **1** crystalizes as its toluene solvate **1**·C_7H_8. Figure 3 shows the molecular structures of both **1** (left) and **1**·C_7H_8 (right).

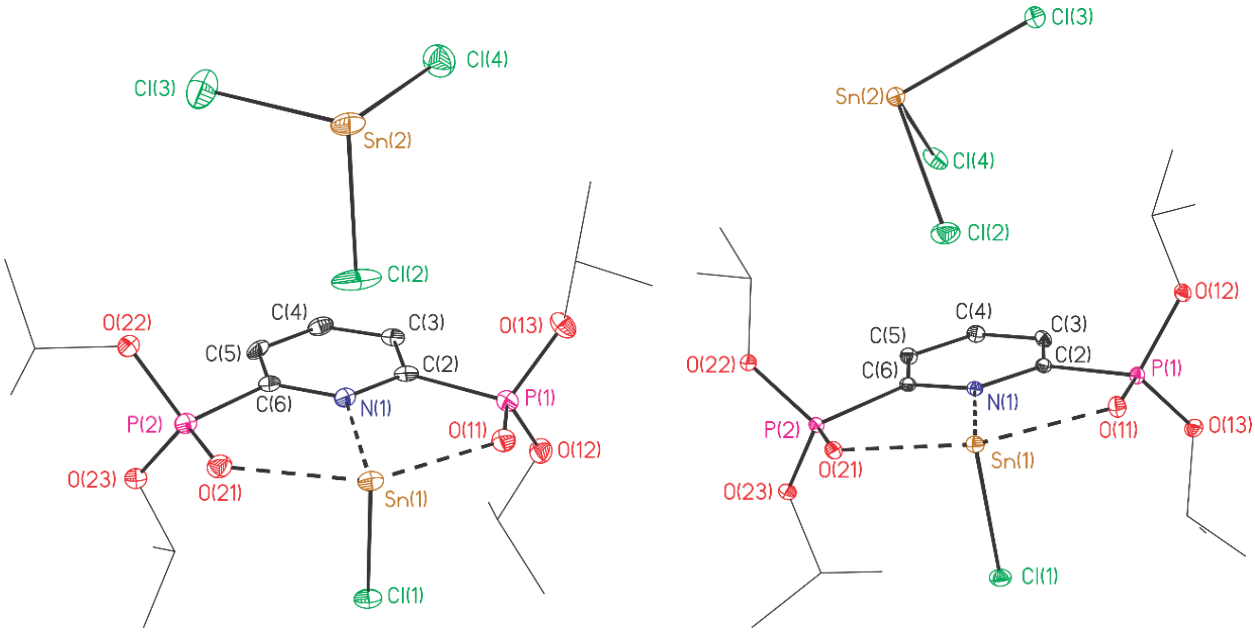

Figure 3. Ellipsoid plot and numbering scheme of the molecular structure of **1** crystallized at room temperature (left) and of **1**·C_7H_8 (right) crystallised at 263 K. The hydrogen atoms were omitted for clarity; ellipsoids are set at 30% probability. Selected interatomic distances [Å] : Sn(1)–Cl(1) 2.4967(15), 2.4643(4); Sn(1)–Cl(2) 3.156(4), 3.307(5); Sn(1)–O(21) 2.375(4), 2.3755(12); Sn(1)–O(11) 2.401(4), 2.3535(12); Sn(1)–N(1) 2.527(5), 2.4276(14); Sn(2)–Cl(2) 2.5547(18), 2.4856(5); Sn(2)–Cl(3) 2.4680(18), 2.4670(5); Sn(2)–Cl(4) 2.4973(18), 2.4647(5). Selected interatomic angles [°]:Cl(1)–Sn(1)–N(1) 81.89(11), 82.96(3); O(11)–Sn(1)–N(1) 87.63(10), 72.67(4); O(21)–Sn(1)–O(11) 140.76(10), 144.92(4); O(21)–Sn(1)–N(1) 70.53(14), 72.27(4); O(11)–Sn(1)–Cl(1) 86.95(10), 87.30(3); Cl(2)–Sn(2)–Cl(3) 92.06(7), 94.425(17); Cl(3)–Sn(2)–Cl(4) 93.80(7), 95.068(16); Cl(4)–Sn(2)–Cl(2) 89.39(7), 91.003(17).

Compound **1** crystalizes in the orthorhombic space group *Pbca*. The molecular structure of **1** reveals that one cation $SnCl^+$ and one anion $SnCl_3^-$ are present in the crystal

lattice. Considering the lone electron pair at Sn(1) being stereochemically active, the Sn(1) centre is pseudo-five coordinate and shows a distorted square pyramidal environment. The N(1), O(11), O(21) atoms and the lone electron pair occupy the equatorial positions. The Cl(1) atom occupies the axial position. However, when taking the Sn(1)–Cl(2) distance of 3.154(2) Å into account, the Sn(1) centre shows a strongly distorted pseudo-octahedral environment with Cl(1), Cl(2) and O(11), O(21) being trans with angles of 1.56.16(7) and 140.72(5) °, respectively. There are further Sn(1)···Cl and Sn(1)···Sn(2A) interactions at distances of 3.466(5) (Sn1–Cl4A), 3.706(5) (Sn1–Cl3A), and 4.200(7) Å, respectively. These distances are shorter than the sum of the van der Waals radii of Sn (2.17 Å) and Cl (1.75 Å). Connected to two oxygen atoms and one nitrogen atom and one chlorine atom. The oxygens, nitrogen, and tin atoms form a plane. The geometry of the tin atom in the cation is distorted octahedral when the electron pair is considered. The chlorine and the oxygen atoms occupy the corners of the square, in which the chlorine atoms are trans to each other. This formation between the tin in the cation and the ligand leads to two five-membered rings. The Sn(1)–O(1), Sn(1)–O(4) and Sn(1)–N(1) interatomic distances are 2.375(4), 2.400(4) and 2.531(5) Å, respectively. The chlorine atom of $SnCl^+$ is closely perpendicular to the plane determined by O(1), N(6), O(4) and the tin center, Sn(1)–Cl(1) is 2.4971(15), and the N(6)–Sn(1)–Cl(1) is 81.92(14)°. The angles of the five-membered rings determined by N(6)–Sn(1)–O(1) and N(6)–Sn(1)–O(4) are 70.52 (14), 70.23 (13)°. The geometry of tin center in the anion is trigonal pyramidal and the average of Sn–Cl bond is 2.505(2). A four membered ring is formed between Cl···Sn···Cl···Sn (Figure 4, top), this formation can be the reason behind the Cl–Sn···Cl change, which makes the system fast to record $^{119}Sn\{^1H\}$NMR at room temperature. The bond distance Cl···Sn is 3.269(2) while Sn···Cl is 3.618(2) Å (vdw. Radii of Sn–Cl is 3.92 Å)[6].

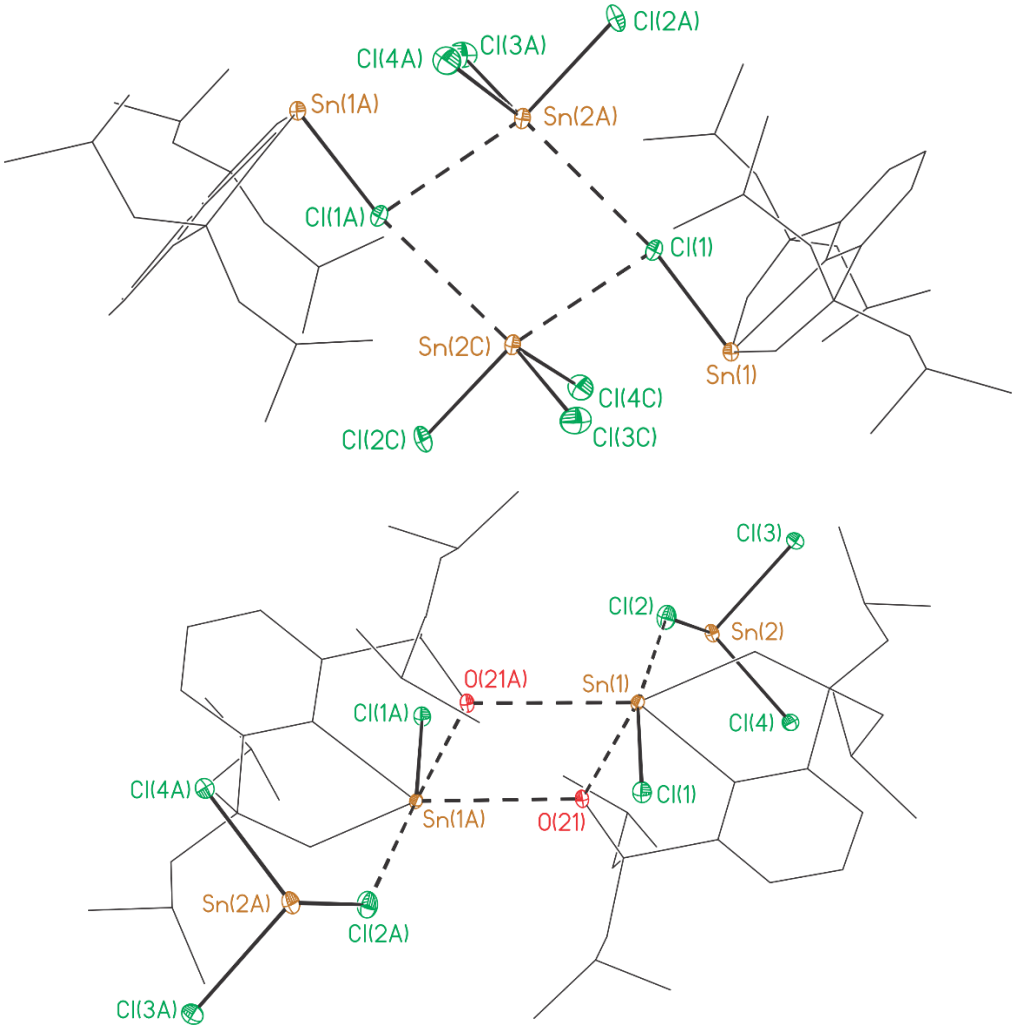

Figure 4. Comparison between the coordination environments of **1** and **1**·C_7H_8.

On the other hand, at 263 K compound **1** crystalizes as its toluene solvate **1**·C_7H_8 in the triclinic crystal system with space group $P\bar{1}$ and two molecules in the unit cell (figure 3, left). The bond length are almost the same but the dimeric structure is presented by the inter coordination bond Sn···O, in which a four-membered ring is formed between O···Sn···O···Sn (Figure 4, bottom). The O(21)–Sn(1A) distance is 3.101(1) Å which is shorter than the sum of the van der Waals radii of Sn and O(3.69 Å)[6]. Dissolving the crystals of **1**·C_7H_8 and keeping the solution at room temperature for 24 h give crystals of **1** without toluene.

2.2.1.1 Comparison between 1, 1·C_7H_8 and B, G

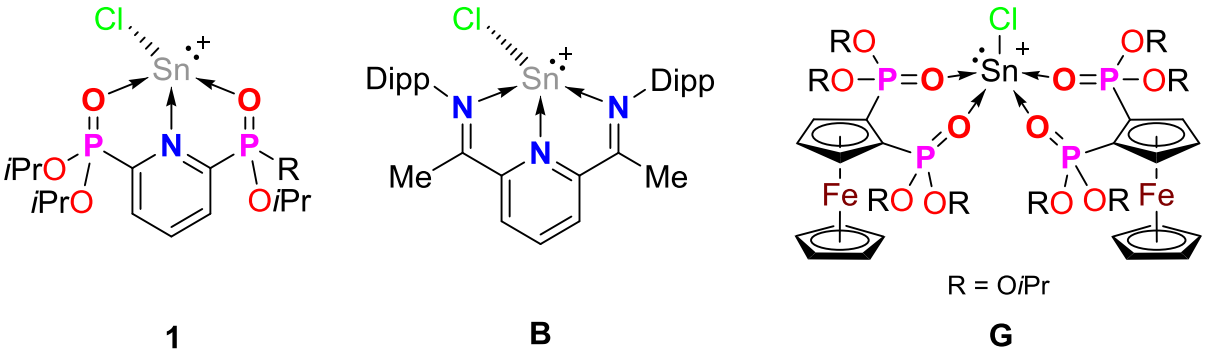

Figure 5. The compounds **1**, **B** and **G**.

Table (1) contains selected interatomic distances and angles of **1**, **1**·C_7H_8, **B** and **G** (Figure **5**). D(1) is N(1) for **1**, **1**·C_7H_8 and **B**; O(1) for **G**. D(2) is O(11) for **1**, **1**·C_7H_8; N(2) for **B** and O(4) for **G**. D(3) is O(21) for **1**, **1**·C_7H_8; N(3) for **B** and O(7) for **G**. The Sn(1)–N(1) distances vary between 2.527(5) Å (**1**) and 2.286(2) Å (**B**). While the longest Sn(1)···O has compound **G** with 2.603(2) Å. The Sn(1)–Cl(1) distance is the longest in compound **1** (2.497(2) Å) and the shortest in compound **G** (2.429(1) Å). The longest average Sn–Cl distance in the $SnCl_3^-$ anion is 2.507(2) Å in **1** and 2.448(2) Å in **G** and.

The largest angles between Sn(1)–D is in compound **1**·C_7H_8 with 72.67(4), 72.27(4) and 144.92(4)° for D(1)–Sn(1)–D(2), D(1)–Sn(1)–D(3)and D(2)–Sn(1)–D(3). In compound **B** was found the largest N(1)–Sn(1)–Cl(1) angle with 88.31(6)°. While the biggest Cl–Sn–Cl average is for **G** with 95.01(5)°.

Table 1. Comparison between selected bond length and angles of **1**, **1**·C_7H_8, **B** and **G**.

	1	**1**·C_7H_8	**B**	**G**
	D(1)=N(1), D(2)=O(11) and D(3)=O(21)		D(1)=N(1), D(2)=N(2) and D(3)=N(3)	D(1)=O(1), D(2)=O(4) and D(3)=O(7)
Sn(1)–D(1)	2.527(5)	2.428(1)	2.286(2)	2.603(2)
Sn(1)–D(2)	2.401(4)	2.354(1)	2.403(2)	2.353(2)
Sn(1)–D(3)	2.375(4)	2.376(1)	2.411(2)	2.263(2)
Sn(1)–Cl(1)	2.497(2)	2.464(4)	2.436(1)	2.429(1)
Sn(2)–Cl(2)	2.555(2)	2.486(5)	2.480(8)	2.440(1)
Sn(2)–Cl(3)	2.468(2)	2.467(5)	2.519(9)	2.447(1)
Sn(2)–Cl(4)	2.497(2)	2.465(5)	2.487 (8)	2.457(1)
D(1)–Sn(1)–D(2)	70.23(1)	72.67(4)	68.71(7)	77.88(8)
D(1)–Sn(1)–D(3)	70.53(1)	72.27(4)	68.79(7)	160.04(9)
D(2)–Sn(1)–D(3)	140.76(1)	144.92(4)	136.87(7)	82.58(9)
D(1)–Sn(1)–Cl(1)	81.90(1)	82.96(3)	88.31(6)	85.61(6)

D(2)–Sn(1)–Cl(1)	87.00(1)	87.30(3)	86.18(6)	91.29(6)
D(3)–Sn(1)–Cl(1)	87.63(1)	87.30(3)	85.59(6)	90.82(7)
Cl(2)–Sn(2)–Cl(3)	92.06(7)	94.4(2)	93.03(3)	93.11(5)
Cl(3)–Sn(2)–Cl(4)	93.80(7)	91.00 (2)	94.24(3)	96.23(5)
Cl(4)–Sn(2)–Cl(2)	89.39(7)	95.07(2)	95.69(3)	95.68(4)

2.2.1.2 Compounds 1a and 1b

The compounds **1a** and **1b** were synthesised by stirring the ligand L1 with the corresponding tin(II)halide in toluene at room temperature and obtained as a yellow crystalline materials (eq 1). In the $^{31}P\{^{1}H\}$ NMR spectrum appears a singlet resonance at δ 16.3 ppm for both **1a** and **1b**. However, no resonances where observed in the $^{119}Sn\{^{1}H\}$ NMR spectra at room temperature.

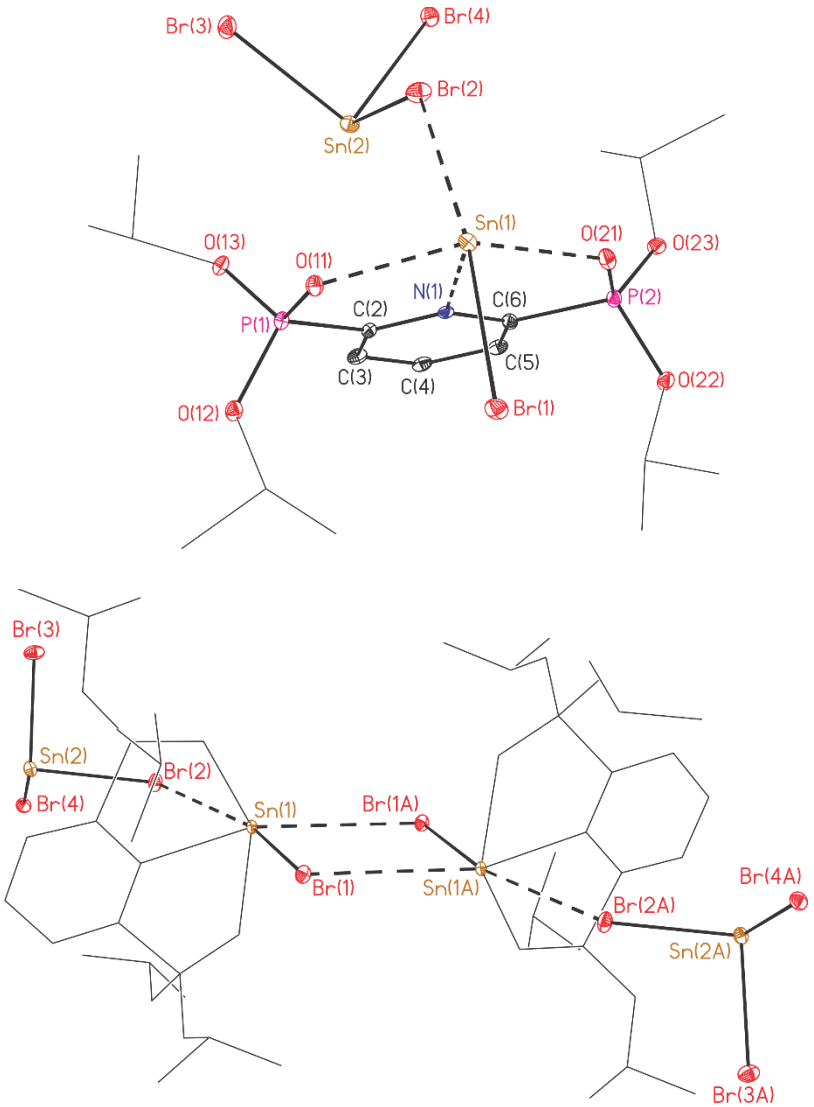

Figure 6. Ellipsoid plot and numbering scheme of the molecular structure of **1a.** The hydrogen atoms were omitted for clarity; ellipsoids are set at 30 % probability. Selected bond lengths [Å]

and angles [°]: Sn(1)–Br(1) 2.6473(5), Sn(1)–Br(2) 3.319(6), Sn(1)–O(21) 2.371(3); Sn(1)–O(11) 2.354(3); Sn(1)–N(1) 2.454(4); Sn(2)–Br(2) 2.6987(6); Sn(2)–Br(3) 2.6477(6); Sn(2)–Br(4) 2.6438(6); Br(1)–Sn(1)–N(1) 90.34(8); O(11)–Sn(1)–N(1) 71.98(11); O(11)–Sn(1)–O(21) 143.28(10); O(21)–Sn(1)–N(1) 71.94(11); O(11)–Sn(1)–Br(1) 85.96(7); Br(2)–Sn(2)–Br(3) 94.227(18); Br(3)–Sn(2)–Br(4) 92.208(18); Br(4)–Sn(2)–Br(2) 92.951(18).

Compound **1a** crystalizes in the monoclinic crystal system with space group $C\,2/c$. Figure **6** shows its molecular structure and selected interatomic distances and angles are given in the figure caption. The molecular structure of **1a** reveals that one cation $SnBr^+$ and one anion $SnBr_3^-$ are presented in the crystal lattice. The tin center is connected to two oxygen atoms and one nitrogen atom and one bromine atom. The oxygen, nitrogen, and tin atoms form a plane. The geometry of the tin atom in the cation is distorted octahedral when the electron pair is considered. The bromine atom and the oxygen atoms occupy the corners of the square, in which the bromine atoms are trans to each other. The distortion of the octahedral geometry is expressed by the O(11)–Sn(1)–O(21) and Br(1)–Sn(1)–Br(2) angles of 143.28(10) and 163.07(11), respectively. This formation between the tin in the cation and the ligand lead to two five-membered rings. The Sn1–O(11), Sn(1)–O(21) and Sn(1)–N(1) distances are 2.354(3), 2.371(3) and 2.454(4) Å, respectively. The bromine atom of $SnBr^+$ is perpendicular to the plane determined by O(11), N(1), O(21) and the tin center. The Sn(1)–Br(1) distance is 2.6473(5) Å. It is 2.8664(1) Å to the Sn–Br distance in $SnBr_2$. The N(1)–Sn(1)–Br(1) angle of 90.34(8)° indicate high s-character of the lone electron pair at the tin centre. The of the five membered-rings N(1)–Sn(1)–O(11) and N(1)–Sn(1)–O(21) angles are 71.98 (11), 71.94 (11)°, respectively. The geometry of tin center in the anion is trigonal pyramidal and the average of Sn–Br bond is 2.662. The angles average of Br–Sn– Br in the anion $SnBr_3^-$ is 93.13°.

The dimeric structure of compound **1a** (Figure 5) has a Sn(2)···Br(2) four-membered ring as central motif. The Br···Sn bond distance is 3.745(4) Å.

2.2.2 The synthesis and the characterization of compound [2-{P(O)(OiPr)$_2$}-6-{P(O)(OiPr)$_2$}C$_5$H$_5$NSnCl]SnCl$_3$

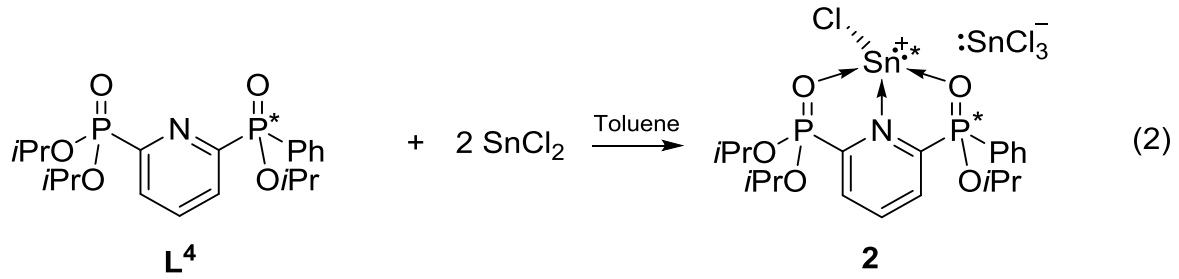

L^4 2

In analogy to the procedure described for the preparation of **1**, compound **2** was synthesized by the addition of $SnCl_2$ to the ligand **L4** in toluene at room temperature (eq 1). The reaction mixture was stirred until the $SnCl_2$ had completely dissolved. **2** precipitates as colourless crystalline material from a saturated toluene solution. It dissolves in toluene, acetonitrile and tetrahydrofuran. In a ^{1}H NMR spectrum, the OC*H* protons resonate as a multiplet centred at δ 5.07 ppm. Six doublets at δ 1.52, 1.50, 1.47, 1.37, 1.33 and 1.27ppm with $^3J(^1H, ^1H)$ = 6 Hz are observed for the CH_3 protons. In a $^{31}P\{^1H\}$ NMR spectrum at room temperature two singlets are found (δ 35.8 and 15.7), which are shifted downfield as compared to the signals of **L4** (δ 23.3 and 6.4). This deshielding is caused by the coordination of the P=O donor at $SnCl^+$. At 193 K, decoalescence of the resonance at 35.8 ppm into two almost equally intense signals at δ 37.4 and 36.8 ppm takes place. No ^{119}Sn NMR signal is observed at room temperature but at 193 K three signals appear at δ –89, –673 and –681 ppm. The results are interpreted in terms of compound **2** existing in two diastereomers the epimerization of which is fast at room temperature but slow at 193 K on the corresponding NMR time scales.

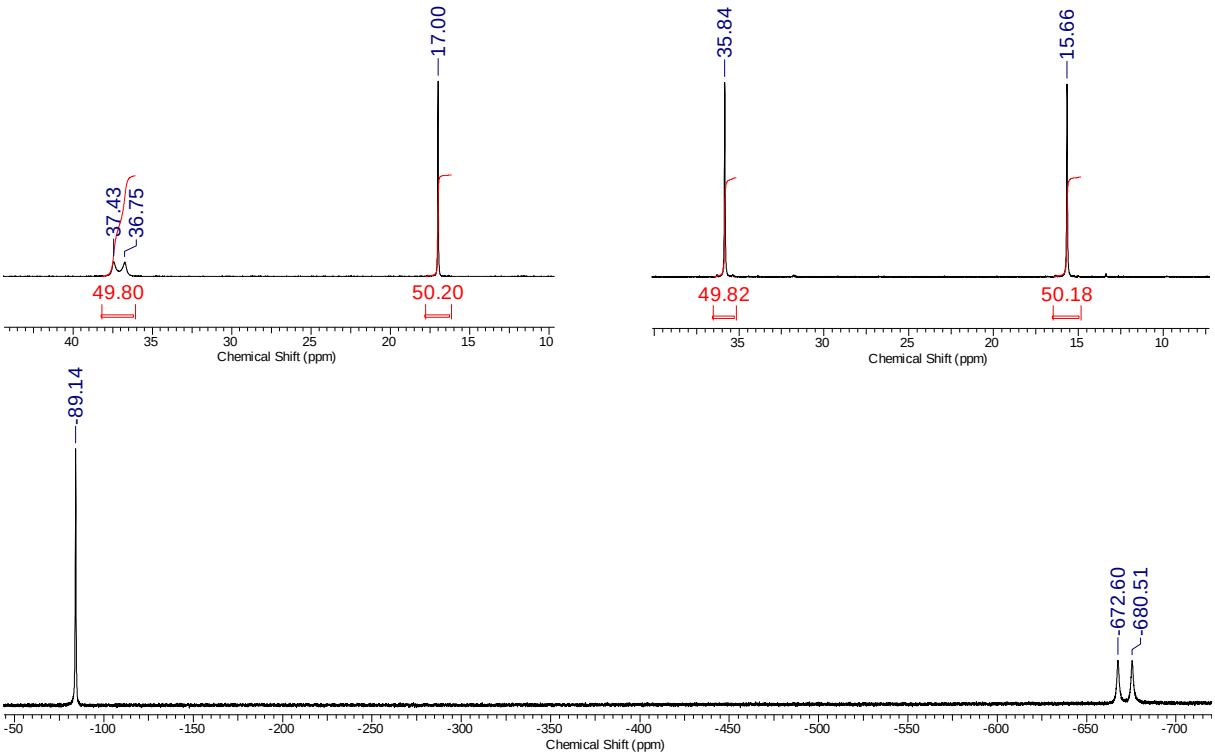

Figure 7. The $^{31}P\{^{1}H\}$ NMR spectrum at –80 °C (top left); $^{31}P\{^{1}H\}$ NMR spectrum at 25 °C (top right) and $^{119}Sn\{^{1}H\}$ NMR spectrum at –80 °C (down) of compound **2**.

Compound **2** crystalizes from toluene in the monoclinic crystal system with the *Pc* space group containing two molecules in the unit cell. Figure 7 shows its molecular structure and selected interatomic distances and angles are given in the figure caption. The molecular structure of **2** contains one cation $SnCl^{+}$ and one anion $SnCl_3^{-}$ in the crystal lattice. The Sn(1) centre is coordinated by N(1), O(11), O(21), Cl(1), and Cl(2) in a distorted pseudo-octahedral environment at distances ranging between 2.294(9) (Sn1–O21) and 3.215(4) Å (Sn1–Cl2). The structure resembles that of the complex **1** with the essential difference that in **2** the Sn(1)–O(21) distance is much shorter than the Sn(1)–O(11) distance of 2.408(9) Å. This observation indicates the superior donor capacity of the PhP(O)(O*i*Pr) versus the P(O)(O*i*Pr)$_2$ moiety. An interesting aspect is the σ-π interaction between Sn(2), and the phenyl ring with distances to the carbon atoms C(34), C(35) and C(36) of 3.798(10), 3.671(10) and 3.741(9) Å, respectively. These distances are shorter than the sum of the van der Waals radii of tin and carbon (3.87 Å[6]). This interaction is also observed in solution. Thus, a ^{1}H NMR spectrum of **2** shows downfield shifts for the phenyl protons (δ 8.63 – 8.57, 1H, *p*-Ph; 8.30 – 8.24, 2H, *o,m*-Ph···SnCl$_3$; 8.16 – 8.12, 2H, *o*',*m*'-Ph) as compared with the chemical shifts of the ligand **L4** (δ 8.16, 1H, *p*-Ph; 7.93 – 7.83, 4H, *o,m*-Ph). This downfield shift maybe traced back to the donation of

electronic density from the π-bonds of the phenyl ring to a sigma star orbital of the Sn(2)–Cl(2) bond.

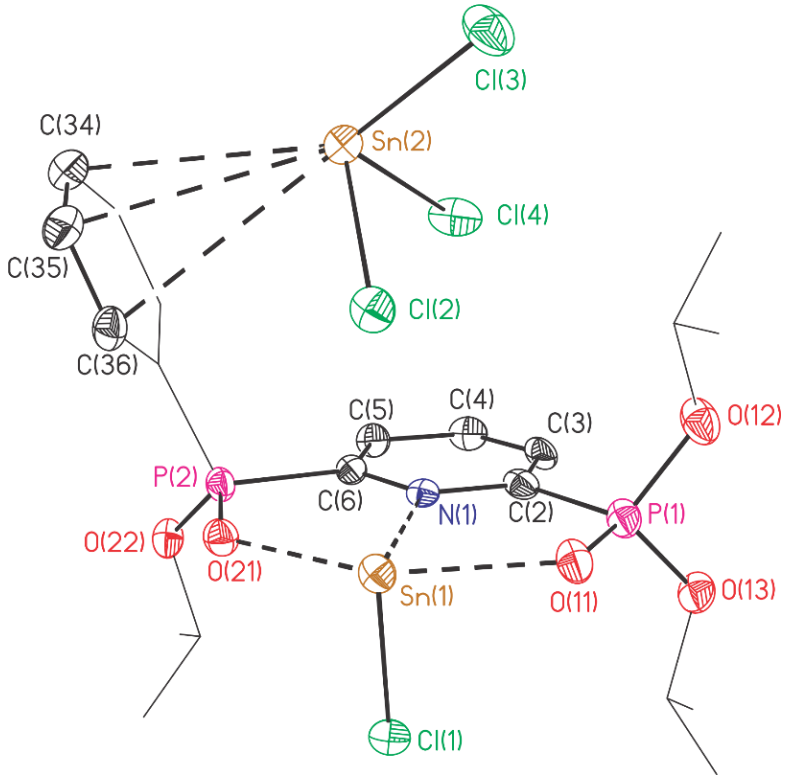

Figure 8. Ellipsoid plot and numbering scheme of the molecular structure of **2**. The hydrogen atoms were omitted for clarity; ellipsoids are set at 30 % probability. Selected bond lengths [Å] and angles [°]: Sn(1)–Cl(1), 2.478(3); Sn(1)–Cl(2) 3.214(4), Sn(1)–O(11), 2.408(9); Sn(1)–O(21), 2.294(9); Sn(1)–N(1), 2.406(9); Sn(2)–Cl(2), 2.530(4); Sn(2)–Cl(3), 2.456(4); Sn(2)–Cl(4), 2.454(4); Sn(1)–C(34), 3.798(9); Sn(1)–C(35), 3.669(9); Sn(1)–C(36), 3.740(9); O(11)–Sn(1)–Cl(1), 88.5(2); N(1)–Sn(1)–O(21), 73.4(3); O(11)–Sn(1)–O(21), 87.7(2), 146.1(3); Cl(4)–Sn(2)–Cl(2), 92.38(12); Cl(4)–Sn(2)–Cl(3), 94.48, (14); Cl(3)–Sn(2)–Cl(2), 94.37(16).

2.2.3 The reaction of [2,6-{P(O)(O*i*Pr)$_2$}C$_5$H$_5$NSnCl]SnCl$_3$ with W(CO)$_5$thf

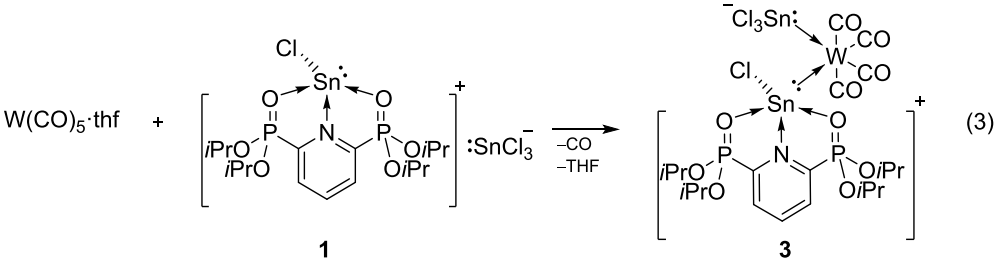

To study the reactivity of **1** towards transition metals, it was added to a solution of the tungsten pentacarbonyl-THF complex in THF and the mixture was stirred for 18h (equation 3). A $^{31}P\{^{1}H\}$NMR spectrum of the reaction mixture showed a signal at δ 13.4. The yellow solution was evaporated in vacuo to dryness and the residual W(CO)$_6$ was

sublimated. The residue was dissolved in THF and after one month few colourless crystals had been formed. Single crystal X-ray diffraction analysis showed the crystal to be compound **3**.

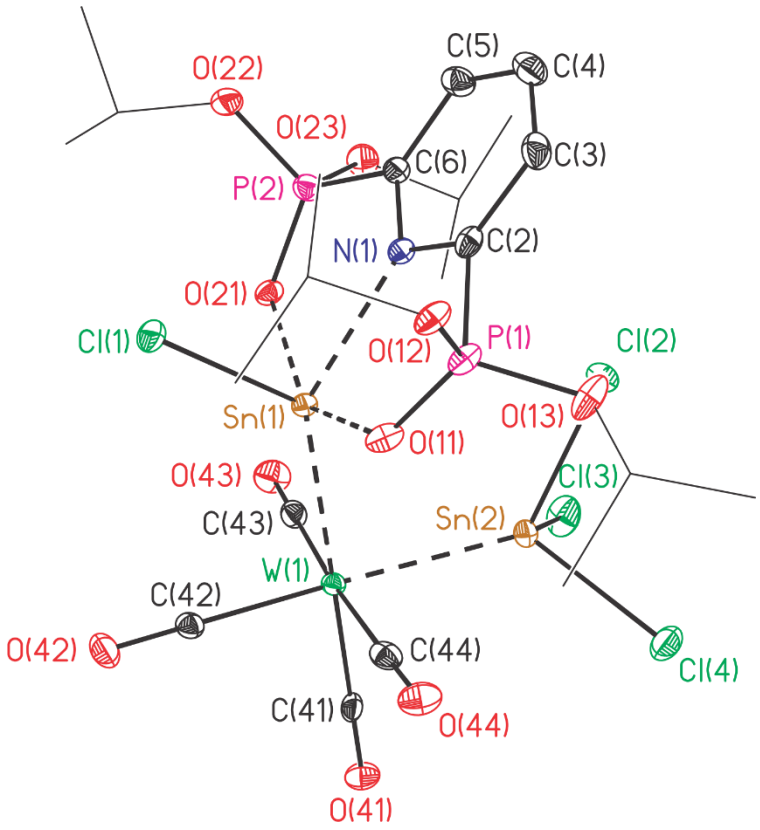

Figure 9. Ellipsoid plot and numbering scheme of the molecular structure of **3.** The hydrogen atoms were omitted for clarity; ellipsoids are set at 30 % probability. Selected bond lengths [Å] and angles [°]:O(12)–P(1) 1.545(3), O(13)–P(1) 1.541(4), O(21)–P(2) 1.486(3), O(22)–P(2) 1.552(4), W(1)–Sn(1) 2.7069(4), W(1)–Sn(2) 2.6909(4), Sn(1)–Cl(1) 2.3656(12), Sn(1)–O(11) 2.232(3), Sn(1)–N(1) 2.335(4), Sn(1)–O(21) 2.291(3), Sn(2)–Cl(2) 2.3914(13), Sn(2)–Cl(3) 2.4004(14), Sn(2)–Cl(4) 2.3900(14) and Cl(2)–Sn(2)–W(1) 121.91(4), Cl(2)–Sn(2)–Cl(3) 96.56(5), Cl(3)–Sn(2)–W(1) 118.42(4), Cl(4)–Sn(2)–W(1) 121.06(4), Cl(4)–Sn(2)–Cl(2) 97.02(5), Cl(4)–Sn(2)–Cl(3) 96.03(5), Sn(2)–W(1)–Sn(1) 91.082(11), Cl(1)–Sn(1)–W(1) 130.95(3), O(11)–Sn(1)–W(1) 101.85(8), O(11)–Sn(1)–Cl(1) 88.47(9), O(11)–Sn(1)–O(21) 148.29(11), N(1)–Sn(1)–Cl(1) 90.72(10), O(21)–Sn(1)–W(1) 104.21(8), O(21)–Sn(1)–N(1) 74.04(12).

Compound **3** crystalizes in the triclinic crystal system ($P\bar{1}$ space group, two molecules per unit cell). Figure 9 shows its molecular structure and selected interatomic distances and angles are given in the figure caption. The W(1) centre is, in a distorted octahedral environment, coordinated by four carbon monoxide ligands (C41-C44), the $SnCl_3^-$ anion and the L$SnCl^+$ cation with the two latter being cis. To the best of our knowledge, this is the first such case in which a tin(II) stannate anion and a tin(II)

stannylium cation simultaneously coordinate to a transition metal centre. The Sn(1)–W(1) and Sn(2)–W(1) distances of 2.7069(4) and 2.6909(4) Å are almost equal. The Sn(1)–O(11), Sn(1)–O(21), Sn(1)–N(1), and Sn(1)–Cl(1) distances of 2.232(3), 2.291(3), 2.335(4), and 2.366(1) Å, respectively, are shorter as compared to the corresponding distances in the parent compound **1**. The Sn(2) atom has a distorted tetrahedral geometry $\bar{A}_{SnCl_3^-}$ is 104 ° and the $\overline{D}_{SnCl_3^-}$ is 2.39 Å.

2.2.4 [2,6-{C(O)OMe}C_5H_5NSnX]SnX_3

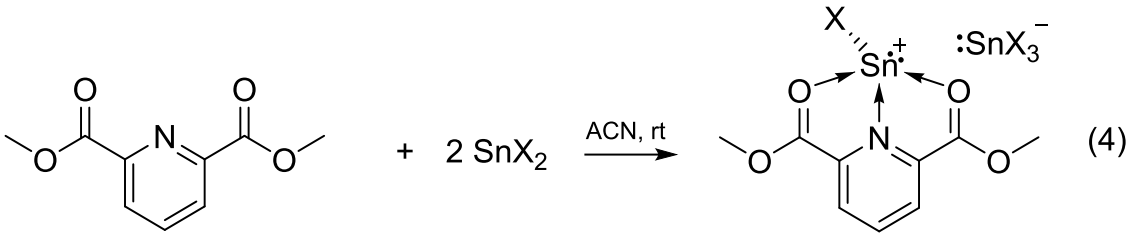

(4)

4: X = Cl
4a: X = Br
4b: X = I

Compounds **4**-**4b** were synthesized according to the general procedures described for **1** with acetonitrile as a solvent (Equation 3). The compounds are yellow (**4**, **4a**) red (**4b**) crystalline materials that dissolve in polar solvents such as methanol and acetonitrile. The ^{1}H NMR spectrum of **4** is identical with the pyridine carboxylic ester. The *m*-Py protons resonate at δ 8.31 (d, $^3J(^1H, ^1H)$ = 7.4 Hz), the *p*-Py proton resonance appears at δ 8.08 (t, $^3J(^1H, ^1H)$ = 7.8 Hz), and the methoxy protons show a singlet resonance at δ 4.02 (s). A ^{119}Sn{^{1}H} NMR spectrum shows a broad signal at δ –222 ($\Delta\nu_{1/2}$ = 712 Hz). Apparently, compound **4** is kinetically labile on the ^{119}Sn NMR time scale. Attempts at recording a ^{119}Sn NMR spectrum at low temperature failed as the compound precipitated upon cooling the solution.

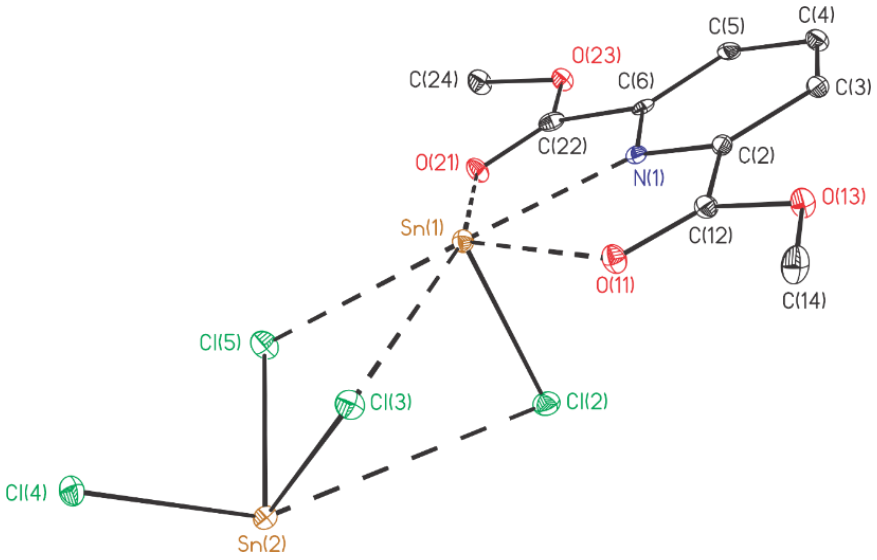

Figure 10. Ellipsoid plot and numbering scheme of the molecular structure of **4**. The hydrogen atoms were omitted for clarity; ellipsoids are set at 30 % probability. Selected bond lengths [Å] and angles [°]: Sn(1)–Cl(2) 2.4799(9), Sn(1)–O(11) 2.478(3), Sn(1)–O(21) 2.554(3), Sn(1)–N(1) 2.460(3), Sn(2)–Cl(2) 2.6517(10), Sn(2)–Cl(3) 2.4595(10), Sn(2)–Cl(4) 2.4852(10), O(11)–C(12) 1.221(4), O(21)–C(22) 1.216(5), O(11)–Sn(1)–Cl(1); 88.5(2), N(1)–Sn(1)–O(21) 73.4(3), O(11)–Sn(1)–O(21), Cl(4)–Sn(2)–Cl(2) 88.02(3), Cl(4)–Sn(2)–Cl(3) 93.47(3), Cl(3)–Sn(2)–Cl(2) 87.34(3).

Yellow single crystals of compound **4** suitable for X-ray diffraction measurement were obtained from acetonitrile (Figure 10). They crystallize in the orthorhombic space group *P*bca with eight molecules per unit cell. The Sn(1) cation is coordinated by N(1), O(11), O(21), and Cl(2) at distances of 2.460(3), 2.478(3), 2.554(3), and 2.4799(9) Å, respectively. In addition, there are weak Sn(1)–Cl(3) (2.994(3) Å) and Sn(1)–Cl(5) (3.151(3) Å) interactions giving, under participation of its lone electron pair, the Sn(1) a distorted pentagonal bipyramidal geometry with Cl(2) and the lone electron pair occupying the axial positions and the Sn(1)–Cl(2) bond length is 2.6517(10) Å. The Sn(2) centre of the $SnCl_3^-$ anion is tetracoordinate by Cl(2) - Cl(4) and show, under participation of the lone electron pair, a pseudo-trigonal bipyramidal geometry. The Sn–Cl distances range between 2.4595(10) and 2.6517(10) Å. $\overline{A}_{SnCl_3^-}$ = 89.6°.

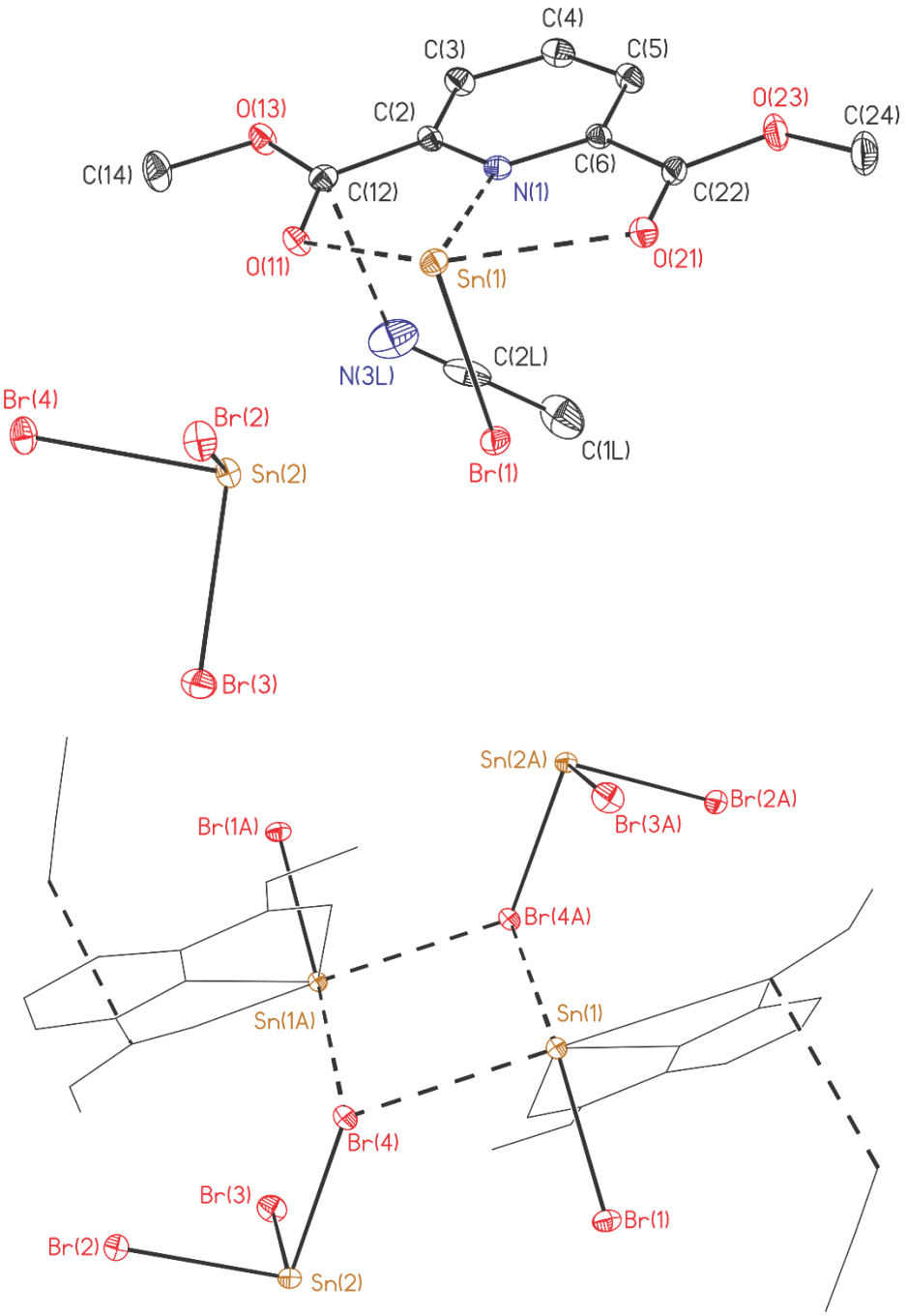

Figure 11. Ellipsoid plot and numbering scheme of the molecular structure of **4a**.The hydrogen atoms were omitted for clarity; ellipsoids are set at 30 % probability. Selected bond lengths [Å] and angles [°]: Sn(1)–Br(1) 2.6330(5), Sn(1)–Br(4) 3.248(10), Sn(1)–O(11) 2.549(3), Sn(1)–O(21) 2.478(3), Sn(1)–N(1) 2.397(3), Sn(2)–Br(2) 2.6486(6), Sn(2)–Br(4) 2.6939(5), Sn(2)–Br(3) 2.6680(6) and O(11)–Sn(1)–Br(1) 86.29(7), O(21)–Sn(1)–Br(1) 80.56(7), O(21)–Sn(1)–O(11) 130.99(10), N(1)–Sn(1)–Br(1) 86.39(8), N(1)–Sn(1)–O(11) 65.69(10), N(1)–Sn(1)–O(21) 66.51(10), Br(2)–Sn(2)–Br(4) 91.510(17), Br(2)–Sn(2)–Br(3) 93.610(19), Br(3)–Sn(2)–Br(4) 93.281(19).

Compound **4a** crystalizes as its acetonitrile solvate **4a**·CH_3CN in the monoclinic space group $P\,2_1/c$ with four molecules in the unit cell. Figure 11 shows its molecular structure and the figure caption collects selected interatomic distances and angles. The Sn(1) centre is coordinated by N(1), O(11), O(21), and Br(1) at distances of 2.397(3), 2.549(3), 2.478(3), and 2.6330(5) Å, respectively, giving it a distorted pseudo-square pyramidal environment with N(1), O(11), O(21) and the lone electron pair in the tin centre is connected to two oxygen atoms and one nitrogen atom and one bromine atom. The oxygen, nitrogen, and tin atoms form a plane. The geometry of the tin atom in the cation is distorted trigonal bipyramidal when the electron pair is considered. The formation between the tin in the cation and the ligand lead to two five-membered rings. The Sn1–O(11), Sn(1)–O(21) and Sn(1)–N(1) bond distance are 2.549(3), 2.478(3) and 2.397(3) Å, respectively. The bromine atom of $SnBr^+$ is perpendicular to the plane determined by O(11), N(1), O(21) and the tin centre, Sn(1)–Br(1) is 2.6330(5) Å and the N(1)–Sn(1)–Br(1) is 86.39(8)°. The angles of the five membered-rings determined by N(1)–Sn(1)–O(11) and N(1)–Sn(1)–O(21) are 65.69(10) and 66.51(10)°. The geometry of tin centre in the anion is tetrahedral and $\bar{D}_{SnCl_3^-}$is 2.670(6). The $\bar{A}_{Br-Sn-Br}$ in the anion $SnBr_3^-$ is 92.80(2)°.Oddly, the nitrogen atom in acetonitrile coordinate to the carbonyl functional group and the bond distance N(3L)–C(12) 3.085(7) Å.

The molecular **4a**·CH_3CN crystalize as a dimer, in which Sn···Br···Sn···Br form a four membered ring. The bond distance between Sn···Br is 3.248(5) and 3.823(5) Å.

2.2.5 [2,6-{C(O)NEt$_2$}C$_5$H$_5$NSnX]SnX$_3$

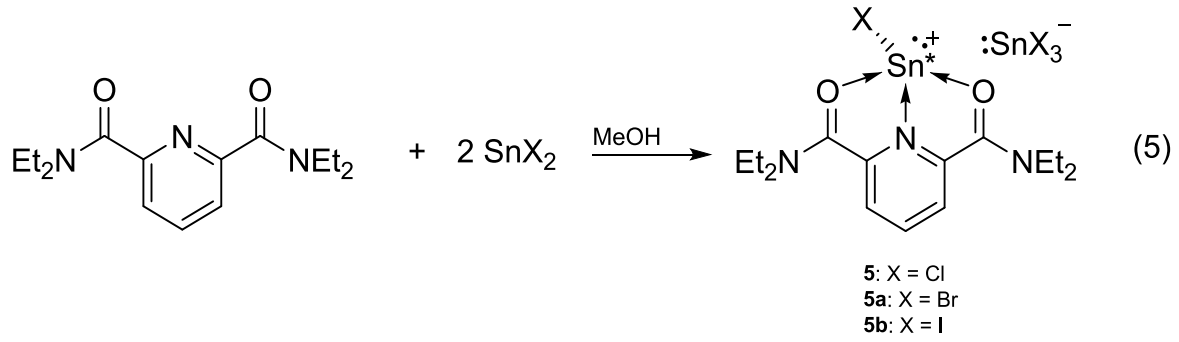

(5)

5: X = Cl
5a: X = Br
5b: X = I

Compound **5** was synthesized according the general procedures described in **1** with methanol as a solvent (equation 5). **5** and **5a** is a colourless solid and **5b** is red, which dissolves in polar solvents like methanol and warm acetonitrile. In the ^{1}H NMR spectrum the chemical shifts of **4** is downfield shifted in comparison with the starting material, in

which δ 8.13 (d, $^3J(^1H, ^1H)$ = 7.8 Hz); 7.71 (t, $^3J(^1H, ^1H)$ = 7.8 Hz); 7.43 (q, $^3J(^1H, ^1H)$ = 7.0 Hz); 3.36 (q, $^3J(^1H, ^1H)$ = 7.0 Hz); 3.15 (t, $^3J(^1H, ^1H)$ = 7.3 Hz) and 1.06 (t, $^3J(^1H, ^1H)$ = 7.3 Hz). A $^{119}Sn\{^1H\}$ NMR spectrum shows a broad signal at δ −300 ($\nu_{1/2}$= 355 Hz), very likely indicating an exchange process that is fast on the $^{119}Sn\{^1H\}$ NMR time scale at room temperature.

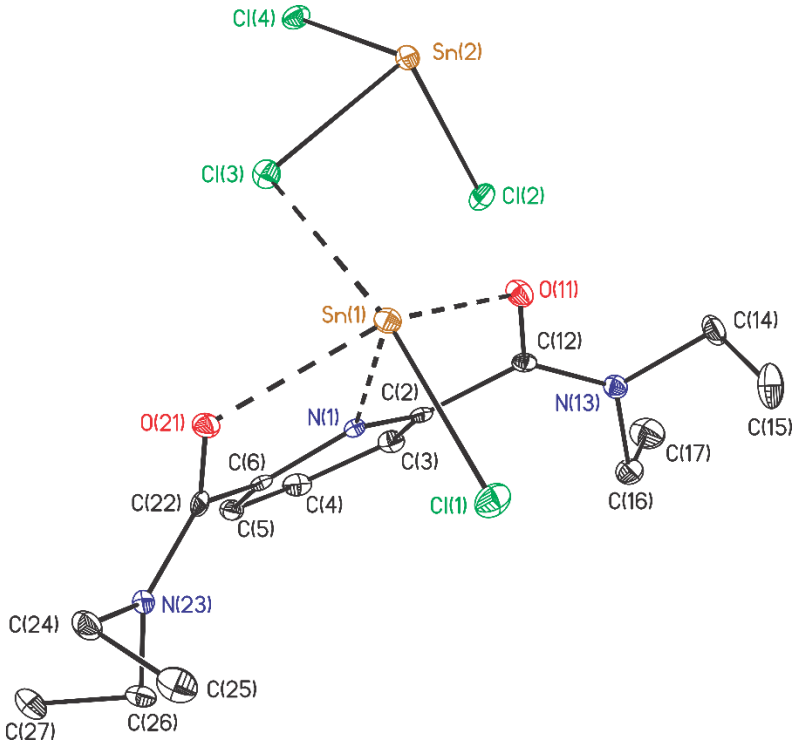

Figure 12. Ellipsoid plot and numbering scheme of the molecular structure of **5**. The hydrogen atoms were omitted for clarity; ellipsoids are set at 30 % probability. Selected bond lengths [Å] and angles [°]: Sn(1)–Cl(1) 2.4738(7), Sn(1)–Cl(3) 3.322(1), Sn(1)–O(11), 2.246(2); Sn(1)–O(21), 2.4054(19); Sn(1)–N(1), 2.315(2); Sn(2)–Cl(2), 2.5103(7); Sn(2)–Cl(3), 2.5156(7); Sn(2)–Cl(4), 2.4650(7); O(11)–C(12), 1.256(3); O(21)–C(22), 1.257(3); O(11)–Sn(1)–Cl(1), 90.71(5); N(1)–Sn(1)–O(21), 67.46(7); O(11)–Sn(1)–O(21), 136.98(7); Cl(4)–Sn(2)–Cl(2), 89.22(2); Cl(4)–Sn(2)–Cl(3), 92.06(2); Cl(3)–Sn(2)–Cl(2), 95.36(2).

Compound **5** crystalizes from methanol as a colourless crystal in the monoclinic space group $P2_1/n$ with four molecules per unit cell. Figure 12 shows its molecular structure and the figure caption collects selected interatomic distances and angles. The cation Sn(1) is coordinated by N(1), Cl(1), O(11), O(21) and Cl(3) at distances of 2.315(2), Sn(1)–Cl(1), 2.246(2), 2.4054(19), and 3.322(1) Å, respectively, in a distorted pseudo-octahedral environment when considering the lone electron pair at Sn(1) . These coordinations form two five-membered rings between the ligand and the cation $SnCl^+$. The Sn(2) centre in the $SnCl_3^-$ anion is tetrahedral when the electron pair is considered.

The Sn(2)–Cl(2), Sn(2)–Cl(3) and Sn(2)–Cl(4) distances are 2.5103(7), 2.5156(7) and 2.4650(7) Å, respectively. The $\bar{A}_{Cl-Sn-Cl}$ in the anion $SnCl_3^-$ is 95.2(2)°.

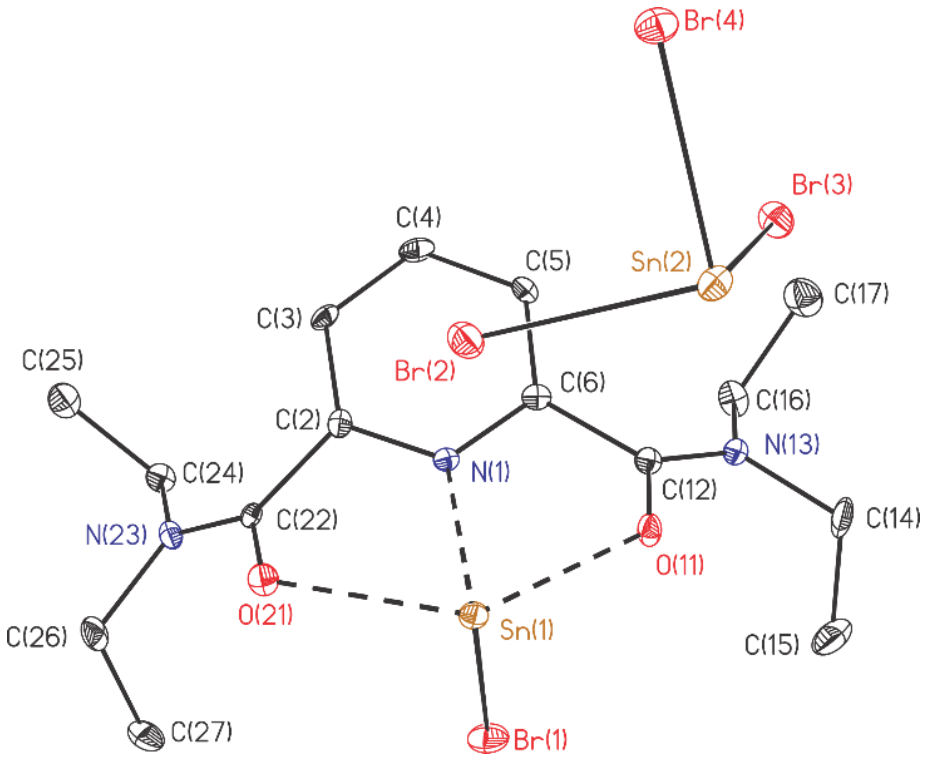

Figure 13. Ellipsoid plot and numbering scheme of the molecular structure of **5a**. The hydrogen atoms were omitted for clarity; ellipsoids are set at 30 % probability. Selected bond lengths [Å] and angles [°]: Sn(1)–Br(1) 2.6332(7), Sn(1)–O(11) 2.244(3), Sn(1)–O(21) 2.429(3), Sn(1)–N(1) 2.319(4), Sn(2)–Br(4) 2.6221(6), Sn(2)–Br(2) 2.6722(6), Sn(2)–Br(3) 2.6625(7) and O(11)–Sn(1)–Br(1) 88.99(9), O(11)–Sn(1)–O(21) 136.88(11), O(11)–Sn(1)–N(1) 69.38(11), O(21)–Sn(1)–Br(1) 89.14(8), N(1)–Sn(1)–Br(1) 85.16(9), N(1)–Sn(1)–O(21) 67.54(12), Br(4)–Sn(2)–Br(2) 92.299(19), Br(4)–Sn(2)–Br(3) 89.90(2), Br(3)–Sn(2)–Br(2) 95.61(2).

Compound **5a** crystalizes from methanol as a yellow crystal in monoclinic crystal system with the space group $P\,2_1/n$ and four molecules in the unit cell. Figure 13 shows its molecular structure and the figure caption collects selected interatomic distances and angles. The Sn(1) cation is coordinated by N(1), Br(1), O(12), O(22) and Br(3) at distance of 2.319(4), 2.6332(7), 2.244(3), 2.429(3) Å in a distorted pseudo-octahedral environment when considering the free electron pair at Sn(1). These coordinations form two five-membered rings between the ligand and the cation $SnCl^+$. The Sn(2) centre in the $SnBr_3^-$ anion is tetrahedral when the electron pair is considered. The Sn(2) centre in the $SnBr_3^-$ anion is tetrahedral when the electron pair is considered. The $\bar{D}_{SnBr_3^-}$ is 2.652(6). The $\bar{A}_{Br-Sn-Br}$ in the anion $SnBr_3^-$ is 92.60(2)°.

2.2.6 Comparison between 1, 4, 5 and their derivatives

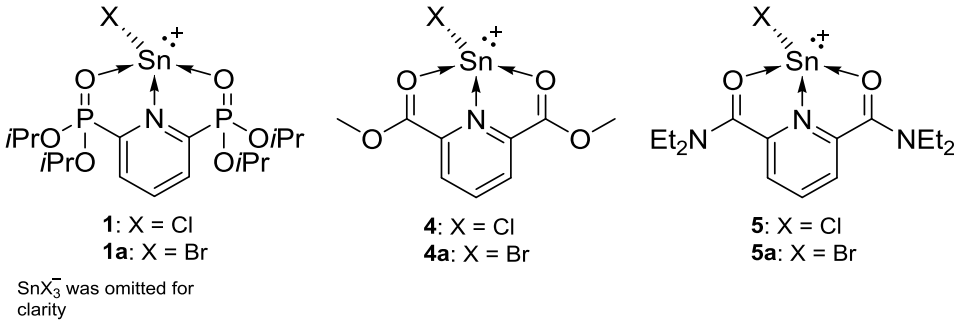

Figure 14. Compare between **1a, 4a** and **5a.**

Table 2 collects selected interatomic distances and angles of **1**, **1a**, **4**, **4a**, **5** and **5a**. The Sn(1)–N(1) distances fall in the range between 2.527(5) (**1**) and 2.315(2) Å (**5**) while the Sn(1)–O distances show variations between 2.554(3) (**4**) and 2.244(3) Å (**5a**). This is remarkable and illustrate the different donor strength of the pyridine-backboned ligands. The Sn(1)–Cl(1)/Sn(1)–Br(1) distances are rather similar and vary only between 2.4967(2) (**1**)/2.6476(3) (**1a**) and 2.4738(7)(**5**)/ 2.6330(5) Å (**4a**). The N(1)–Sn(1)–X(1) angles vary between 81.90(1) (**1**, X = Cl) and 90.34(8)° (**1a**, X = Br). With caution, it suggests the lone electron pair at the tin atom to be most stereochemically active for compound **1**. (The longest $SnCl_3^-$ bonds average is found in compound **3**, $\bar{D}_{SnCl_3^-}$ is 2.532(1) Å and the largest $\bar{A}_{SnCl_3^-}$ is 92.21(2)° for compound **5**.

In comparison between **1a**, **4a** and **5a**, compound **1a** has the longest Sn(1)–N(1) 2.458(2) Å and the largest N(1)–Sn(1)–O(11), N(1)–Sn(1)–O(21), O(11)–Sn(1)–O(21) and N(1)–Sn(1)–Br(1) 73.00(1), 71.94(1), 143.28(1) and 90.34(8)°, respectively. The longest Sn(1)–O(11) and Sn(1)–O(12) are found in compound **4a** 2.354(3) and 2.371(3)Å, while the largest O(11)–Sn(1)–Br(1) and O(21)–Sn(1)–Br(1) 90.71(5) and 89.07(5)° are found in compound **5a**. The longest $\bar{D}_{SnBr_3^-}$is 2.670(6) for **4a** and the largest $\bar{A}_{SnBr_3^-}$ is 93.13(2) for **1a.**

Table 2. Selected bonds lengthes of compound **1**, **1a**, **4**, **4a**, **5** and **5a**.

	1 (X = Cl)	**1a** (X = Br)	**4** (X = Cl)	**4a** (X = Br)	**5** (X = Cl)	**5a** (X = Br)
Sn(1)–N(1)	2.527(5)	2.458(2)	2.460(3)	2.397(3)	2.315(2)	2.319(4)
Sn(1)–O(11)	2.401(4)	2.354(3)	2.478(3)	2.549(3)	2.246(2)	2.244(3)
Sn(1)–O(21)	2.375(4)	2.371(3)	2.554(3)	2.478(3)	2.405(2)	2.429(3)
Sn(1)–X(1)	2.4967(2)	2.6476(3)	2.4799(9)	2.6330(5)	2.4738(7)	2.6332(7)
Sn(2)–X(2)	2.555(2)	2.6987(6)	2.652(1)	2.6486(6)	2.5103(7)	2.6722(6)

Sn(2)–X(3)	2.468(2)	2.6477(6)	2.460(1)	2.6680(6)	2.5156(7)	2.6625(7)
Sn(2)–X(4)	2.497(2)	2.6438(6)	2.485(1)	2.6939(5)	2.4650(7)	2.6221(6)
N(1)–Sn(1)–O(11)	70.23(1)	73.00(1)	65.44(9)	65.69(1)	69.76(7)	69.38(1)
N(1)–Sn(1)–O(21)	70.53(1)	71.94(1)	64.75(9)	66.51(1)	67.46(7)	67.54(1)
O(11)–Sn(1)–O(21)	140.76(1)	143.28(1)	118.7(2)	130.99(1)	136.98(7)	136.88(1)
N(1)–Sn(1)–X(1)	81.90(1)	90.34(8)	84.67(7)	86.39(8)	83.70(5)	85.16(9)
O(11)–Sn(1)–X(1)	87.00(1)	85.96(7)	84.66(6)	86.29(7)	90.71(5)	88.99(9)
O(21)–Sn(1)–X(1)	87.63(1)	87.66(7)	85.55(6)	80.56(7)	89.07(5)	89.14(8)
X(2)–Sn(2)–X(3)	92.06(7)	94.23(2)	87.34(3)	93.61(2)	95.36(2)	95.61(2)
X(3)–Sn(2)–X(4)	93.80(7)	92.21(2)	93.47(3)	93.28(2)	89.22(2)	89.90(2)
X(4)–Sn(2)–X(2)	89.39(7)	92.95(2)	88.02(3)	91.51(2)	92.06(2)	92.30(2)

2.2.7 The thermal stability of the compounds 1 – 4:

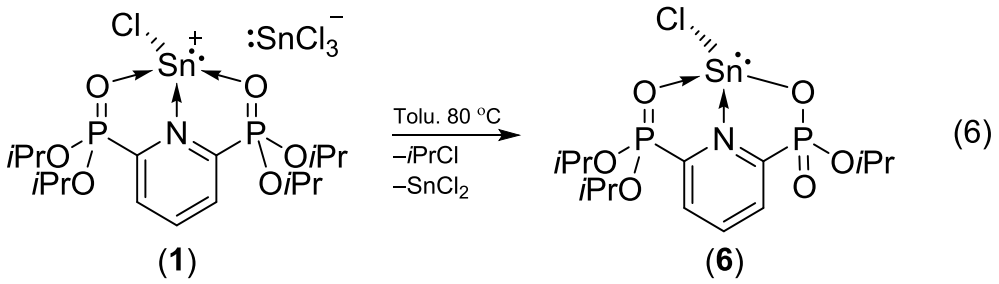

(6)

When **1** is heated in toluene solution at 80 °C, compound **1** gives the heterocyclic compound **6**, $SnCl_2$ and 2-chloropropane (Equation 6)**.** Most remarkably, upon this reaction a stereogenic centre at the phosphorus atom involved in the cyclization is formed. In the ^{1}H NMR spectrum of the reaction mixture resonate the OC*H* group as multiplet from δ 4.93 to 4.85 and ClC*H* from δ 3.79 to 3.70 (septett, $^3J(^1H, ^1H)$ = 6.4 Hz) (3:1) while the OCH(CH_3)$_2$ and ClCH(CH_3)$_2$ protons resonate as doublets at 1.17 ($^3J(^1H, ^1H)$ = 6.4 Hz) and 0.96 ppm($^3J(^1H, ^1H)$ = 6.4 Hz), respectively, with an integral ratio of 18:6. In a $^{31}P\{^1H\}$ NMR spectrum appear two singlet δ 19.2 and 13.4. After removing the volatiles the product was isolated as a colourless micro-crystalline solid material. It dissolves in toluene.

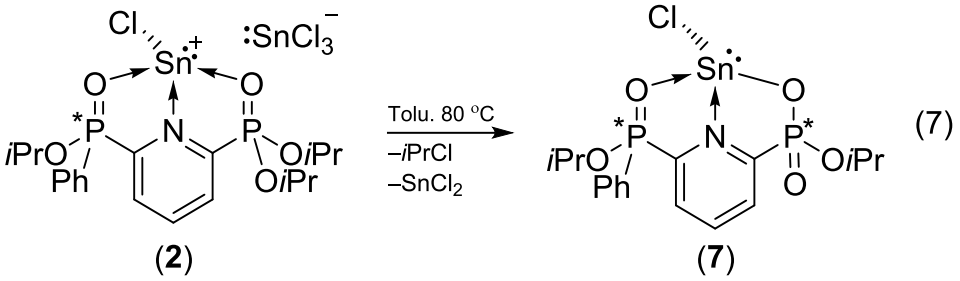

(2) (7) (7)

Compound **2** gives when it is heated in toluene at 80 °C compound **7**, $SnCl_2$ and 2-chloropropane (Equation 7)**.** In the ^{1}H NMR spectrum of the reaction mixture resonate the OC*H* group as broad signal (δ 5.02), as septet from (δ 4.94, $^{3}J(^{1}H, ^{1}H)$ = 6.2 Hz), doublet (δ 1.28, $^{3}J(^{1}H, ^{1}H)$ = 6.2 Hz) and ClC*H* from δ 3.79 to 3.70 (septett, $^{3}J(^{1}H, ^{1}H)$ = 6.4 Hz) (1:1:1), δ 1.00 to 0.96 (m). In the $^{31}P\{^{1}H\}$ NMR spectrum at room temperature appears four signals δ 34.1, 27.3, 16.3 and 10.2 (3:2:2:3) but in the $^{31}P\{^{1}H\}$ NMR spectrum at –80 °C appears six signals δ 34.9, 34.1, 27.9, 17.1, 14.0 and 11.1 (1:2:2:2:2:1)

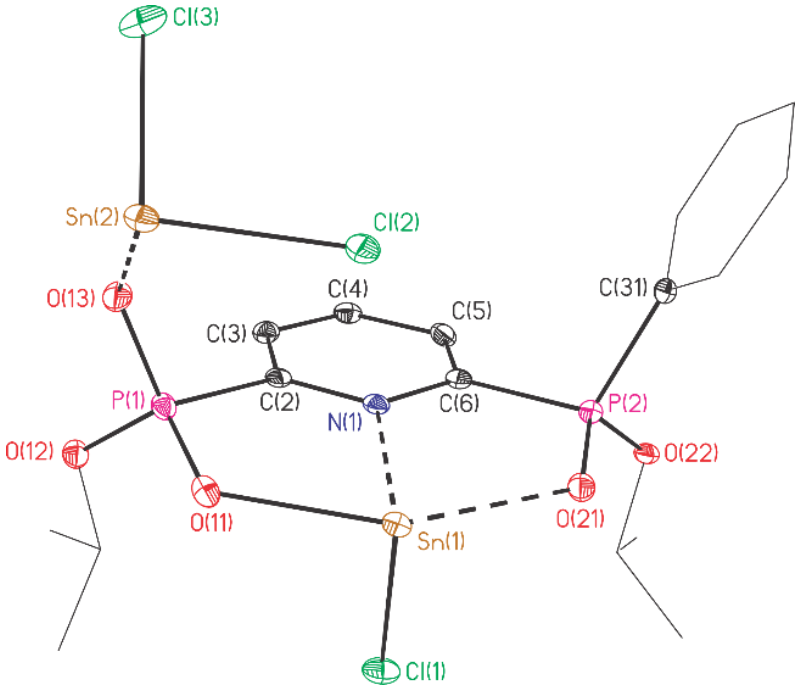

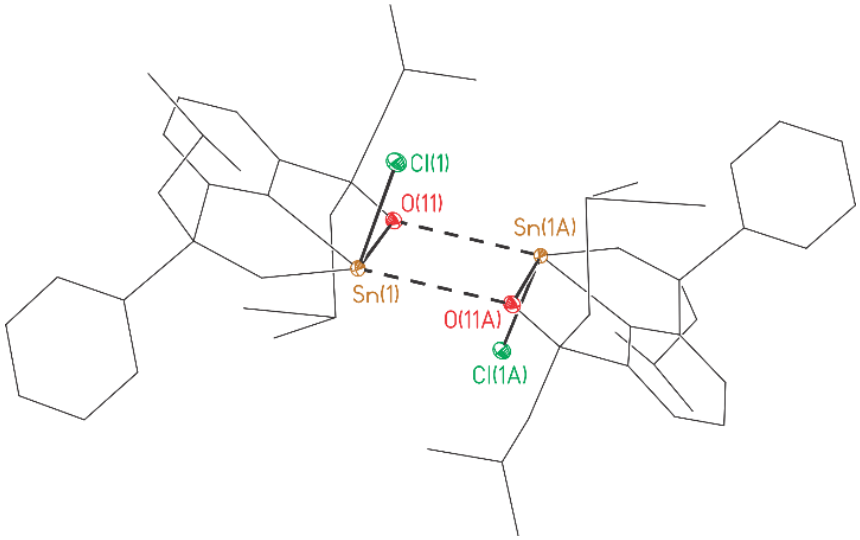

Figure 15. Ellipsoid plot and numbering scheme of the molecular structure of **7**. The hydrogen atoms were omitted for clarity; ellipsoids are set at 30 % probability. Selected interatomic distances [Å] and angles [°]: Sn(1)–Cl(1) 2.5025(8), Sn(1)–N(1) 2.425(2), Sn(1)–O(11) 2.265(2), Sn(1)–O(21) 2.430(2), Sn(1)–O(11A) 3.232(1), Sn(2)–O(13) 2.239(2), Sn(2)–Cl(2) 2.497(1), Sn(2)–Cl(3) 2.462(1), P(1)–O(11) 1.503(2), P(1)–O(12) 1.570(2), P(1)–O(13) 1.504(2), Sn(2)–O(13) 2.239(2), P(2)–O(21) 1.485(2) and N(1)–Sn(1)–Cl(1) 83.46(6), N(1)–Sn(1)–O(21) 71.98(8), O(11)–Sn(1)–Cl(1) 89.22(6), O(11)–Sn(1)–N(1) 74.03(8), O(11)–Sn(1)–O(21) 146.01(7), O(21)–Sn(1)–Cl(1) 86.54(6).

Compound **7** crystalizes from toluene as a colourless crystal, in triclinic crystal system the $P\bar{1}$ space group and two molecules per unit cell *R*,*R* and *S*,*S* (Figure 15). In the crystal lattice was found that P(1)–O(13) coordinates at $SnCl_2$ and SnCl forms a bond with P(1)–O(11). The bonds lengths Sn(2)–O(13), O(13)–P(1), P(1)–O(11) and O(11)–Sn(1) are 2.239(2), 1.504(2), 1.503(2) and 2.265(2) Å. The O(21) and N(1) coordinate at SnCl and form two five-membered rings. N(1)–Sn(1) is 2.435(2) Å and O(21)–Sn(1) is 2.430(2) Å. The Sn(1) centre has distorted square pyramidal geometry, when the lone pair is considered and Sn(2) centre is tetrahedral. O(11), O(21) Sn(1) And N(1) are in a plane and Cl(1) atom forms 83.46(6)° angle with N(1) and Sn(1).

While the addition of the Lewis acid $W(THF)(CO)_5$ to **3** followed by the heating at 80 °C lead form the heterocycle **8**.

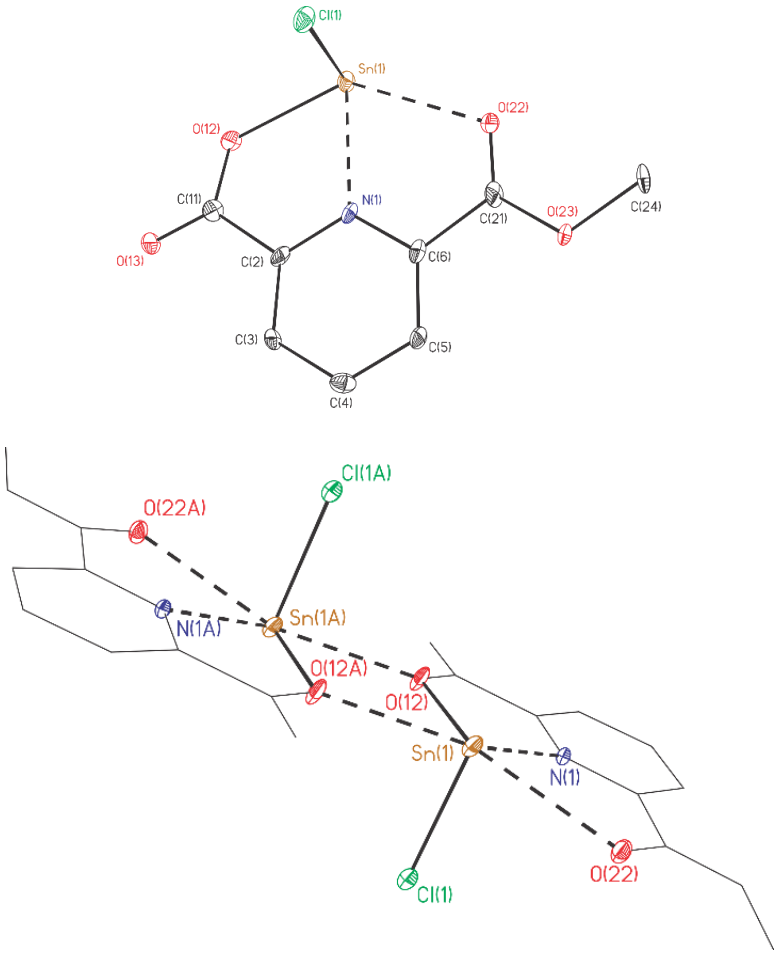

Figure 16. Ellipsoid plot and numbering scheme of the molecular structure of **8**. The hydrogen atoms were omitted for clarity; ellipsoids are set at 30 % probability. Selected bond lengths [Å] and angles [°]: Sn(1)–N(1) 2.419(5), Sn(1)–Cl(1) 2.4447(18), Sn(1)–O(12) 2.230(5), Sn(1)–O(12A) 2.517(4), C(11)–O(12) 1.287(8), C(11)–O(13) 1.209(8), C(21)–O(22) 1.201(8), C(21)–O(23) 1.313(8) and N(1)–Sn(1)–Cl(1) 85.93(13), O(12)–Sn(1)–N(1) 68.90(16), O(12)–Sn(1)–Cl(1) 89.42(13), C(2)–N(1)–Sn(1) 115.5(4), O(12)–C(11)–C(2) 114.5(6), O(13)–C(11)–C(2) 119.5(6), Sn(1)–O(12)–Sn(1A) 115.24(18), C(11)–O(12)–Sn(1) 125.2(4).

Compound **8** crystalizes from THF as a colourless crystal in triclinic crystal system the $P\bar{1}$ space group and two molecules per unit cell (Figure 16). The molecular structure reveals that one Sn(II) atom is in presented in the crystal lattice. This tin atom is connected to Cl(1), O(12), O(12A) and N(1). The bond lengths are Sn(1)–N(1) 2.419(5), Sn(1)–Cl(1) 2.4447(18), Sn(1)–O(12) 2.230(5) and C(11)–O(12) 1.287(8) Å. The tin centre is stabilized via intermolecular coordination between Sn(1) and O(12A) in which the Sn(1)–O(12A) is 2.517(4) Å Figure **16**. The ligand forms with the tin centre two five-membered rings in which the chlorine atom is perpendicular on the plane defined by rest of the molecule and the angle Cl(1)–Sn(1)–N(1) is 85.93(13)°. In the dimeric structure the chlorine atoms are in trans position to each other.

2.2.8 DFT Calculations

To gain a deeper understanding of the electronic structure of **1**, **4** and **5**, natural bond orbital analyses (NBO) of the (L)$SnCl^{+}$complexes were performed. The Geometry optimizations were performed with the Gaussian 09 suite of program E.01[7].

A brief benchmarking exercise showed that the meta-hybrid wB97Xd functional outperformed both the popular b3LYP and BP86 hybrid function in generating an optimized geometry which correlated with the data obtained by X-ray crystallography. In view of this, ground state optimization of the cation $[(L)SnCl]^{+}$ was applied using the wB97XD[8] hybrid functional; def2TZVP[9] (on Sn) and 6-311+G(d) (on H, C, N, O and Cl) basis sets.

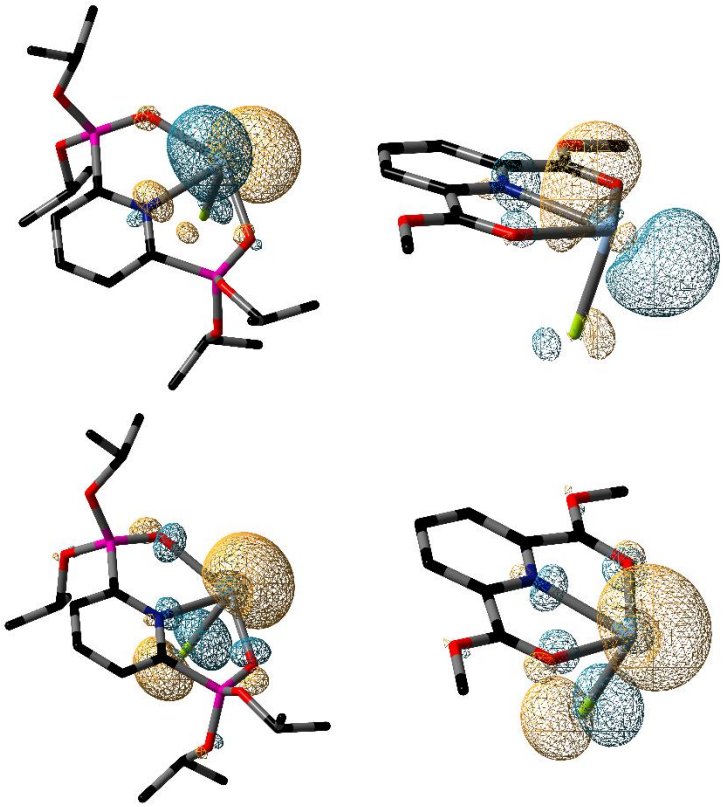

Figure 17. Selected NBOs of compounds **1** (left) and **3** (right). **A** occupied lone pair on Sn (bottom) and **B** unoccupied orbital on Sn (top). The isosurface value for all plots is 0.05 $electron \cdot bohr^{-3}$. Hydrogen atoms were omitted for clarity.

The results of the NBO calculations indicate that the Sn atom has a nonbonding electron density (lone pair), which has 93% 5s orbital character on **1**, 92% on **4** and 89% on **5.** Each of the σ_{SnCl} bonds consists of a *p*-rich hybrid orbital from the Cl atom and a 5p

atomic orbital (AO) from the Sn atom. The bond is strongly polarized toward the Cl atom (85.4% for **1**, 83.1% for **4**, and 84.0% for **5**). The vacant p-orbital on the Sn atom makes it a strong Lewis acid which is capable of accepting electron density from the N and O donor atoms. The NBO analysis predicts noncovalent interactions between the lone pairs of oxygen and nitrogen atoms and the empty orbitals of Sn centre with ΔE^2 values of 18, 21 and 36 kcal/mol for **1**, 19, 22 and 43 kcal/mol for **4** and 20, 22 and 46 kcal/mol for **5**, respectively. The natural population analysis of the (L)$SnCl^+$ complex at the wB97XD/ def2TZVP (on Sn)/6-311+G(d)(on H, C, N, O and Cl) reveals a relatively high residual charge of +1.36 on Sn for **1** +1.29 for **4** and +1.28 for **5**, despite of the donor/acceptor interaction with the O,N,O-ligand. The Wiberg bond indices[11] calculated using the natural atomic orbital basis are 0.19 (**1**), 0.21(**4**), and 0.23 (**5**) for the Sn–N interactions, 0.17(**1**), 0.13(**4**), and 0.18(**5**) for the Sn–O(3) and 0.17(**1**), 0.15(**4**), and 0.20(**5**) for the Sn–O(5) interactions. These values are smaller than the bond index of 1.00 expected for a single bond.

Table 3. Comparison between NBO analysis data of **1**, **3**, **5**, **A** and **B**.

	5S [%]	WBI			Natural charge	ΔE^2 [kcal/mol]			
		D(1) → Sn	D(2) → Sn	D(3) → Sn		LP D(1) → LP* Sn	LP D(2) → LP* Sn	LP D(3) → LP* Sn	
1	93	0.19	0.17	0.17	1.36	36	21	18	
3	92	0.21	0.13	0.15	1.29	43	22	19	D(1) = N and D(2), D(3) = O
5	89	0.23	0.18	0.20	1.28	46	22	20	
A	93	0.16	0.15	0.15	1.52	49	34	34	D(1) = D(2) = D(3) = N
B	93	0.21	0.21	-	1.47	60	59	-	D(1) = D(2)= N

In Table 3 summarizes the NBO analysis data. The 5s lone pair character is the same in compounds **1**, **A** and **B** while in compound **3** and **5** more p character is presented in the free electrons 5s 92% and 89%; 5p 8% and 11% respectively. The interaction between the donor atoms and the Sn centre is between 0.23 and 0.15 and the values are small to form a single bond, because WBI for single bond is 1.00. The ΔE^2 refers to the second-order perturbative, which estimates of donor-acceptor (bond-antibond) interactions. The nitrogen atom of the pyridine ring found to form the strongest interaction because of the angle C–N···Sn is close to 120° which is suitable for sp^2 lone pair symmetry in comparison with the nitrogen of the amine. In case of oxygen tin interaction, it is weaker than that of the amine because of the angle P=O···Sn is larger than 109°, which is suitable for sp^3 lone pair of the oxygen.

The Mulliken charges show that the highest tin positive charge is found in compounds **A** and **B**, and that may be traced back to the strong electron withdrawing $CF_3SO_3^-$ group.

2.3 EXPERIMENTAL SECTION

All reactions were carried out under argon 4.6 atmosphere using standard Schlenk-line technique, unless otherwise specified. The argon was dried by passing through a glass column filled with phosphorus pentoxide and the glassware was dried by flame under reduced pressure. All solvents were dried according to the standard procedures, fresh distilled and stored over molecular sieve.[12]

The NMR spectroscopy data was measured on the spectrometers Bruker AV 400 Avance III HD NanoBay, AV 500 Avance III HD, AV 600 Avance III HD, AV 700 Avance III HD and Agilent Technologies DD2. The NMR chemical shifts (δ) are given in ppm and the coupling constants *J* in Hz. ^{1}H and $^{13}C\{^{1}H\}$ NMR were referenced at $SiMe_4$ via the chemical shift of the solvents (C_6D_6 ^{1}H 7.16, ^{13}C 128.39; CD_2Cl_2 ^{1}H 5.32, ^{13}C 54.00; $CDCl_3$ ^{1}H 7.26, ^{13}C 77.16; CD_3CN ^{1}H 1.94, ^{13}C 1.39; CD_3OD ^{1}H 3.31, ^{13}C 49.00). The reference of ^{31}P, 85% H_3PO_4; ^{119}Sn, $SnMe_4$; ^{11}B, $BF_3.OEt_2$ and ^{19}F, $CFCl_3$. The IR spectra (cm^{-1}) are measured as a solid or oil by ATR Perkin Elmer Spectrum two.

The melting point (°C) was measured with a Büchi M-560 using an open capillary. The elemental analysis was performed on a CHNS-932 of the company Leco. The measurements were carried out without inert atmosphere. The electrospraymass spectra were measured by the gadget Thermoquest Finnigan Instrument, which is thermoquest-finnigan device, the mobile phase is acetonitrile or dichloromethane with flow rate 10 µL/min. The concentration is c = 0.1 mg · mL^{-1}, the source voltage is 3.8 kV, the capillary voltage is 41 V (tube lens: 140 V) and the capillary temperature is 275 °C.

General procedures

Compounds **1** - **4** were synthesized in 85 - 90% yield by stirring $SnCl_2$ with the corresponding ligand (molar ratio 2:1) at room temperature in toluene (for **1** and **2**), acetonitrile (for **3**) and methanol (for **4**).

[2,6-{P(O)(O*i*Pr)$_2$}C$_5$H$_5$NSnCl]SnCl$_3$ (1)

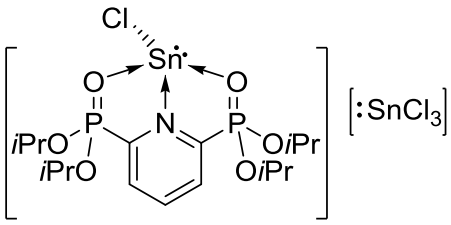

Isolated as a colourless crystals **m**.**p**. 71 °C; **IR**: $\tilde{\nu}$ = 547 (vs), 996 (vs, PO*i*Pr), , 1166 (s), 1207 (s, P=O), cm^{-1}; **^{1}H NMR** (400 MHz, CD_2Cl_2): δ = 8.62 (m, 1H, *p*-Py), 8.30 (m, 2H, *m*-Py), 5.08 (m, 4H, OC*H*), 1.49 (d, 12H, CC*H*$_3$, ^3J(^{1}H , ^{1}H) = 4 Hz), 1.31 (d, 12H, CC*H*$_3$, ^3J(^{1}H , ^{1}H) = 4 Hz); **^{13}C{^{1}H} NMR** (240 MHz, CD_2Cl_2): δ = 148.6 (*o*-Py), 146.5 (*o*-Py), 142.8 (*p*-Py), 132.6 (*m*-Py), 77.1 (O*C*H), 23.7 (C*C*H$_3$); **^{31}P{^{1}H} NMR** (162 MHz, CD_2Cl_2): δ = 16.54 (s); **^{31}P{^{1}H} NMR** (162 MHz, CD_2Cl_2, T = 193 K): δ = 17.87 (s); **^{119}Sn{^{1}H} NMR** (149 MHz, CD_2Cl_2, T = 193 K): δ = −90.28 (s, *Sn*Cl$_3^-$); −701.06 (s, *Sn*Cl$^+$); **Elemental analysis** calcd. for $C_{17}H_{31}Cl_4NO_6P_2Sn_2$ 786.84 [g/mol]: C, 26.0%; H, 4.0%; N, 1.8%, found: C, 25.9%; H, 4.0%; N, 1.8%; **ESI-MS** (70 eV, positive mode): m/z (%): 385.1 [$C_{14}H_{28}N_1O_7P_2$]; (negative mode): 482.7 [$C_5H_9N_1O_7P_2Sn_1Cl_3$].

[2,6-{P(O)(O*i*Pr)$_2$}C$_5$H$_5$NSnBr]SnBr$_3$ (1a)

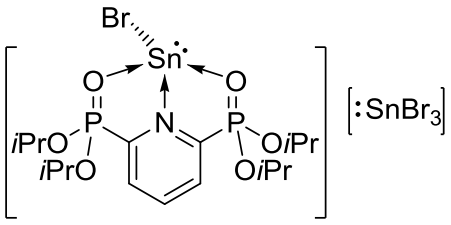

Isolated as pale yellow solid, **m**.**p**. 123 °C decompose; **IR:** $\tilde{\nu}$ = 718 (s), 1001 (s, PO*i*Pr), 1100 (s, P=O), 1600 (b), 2981 (br) cm^{-1}; **^{1}H NMR** (400 MHz, CD_2Cl_2): δ = 8.55 (m, 1H, *p*-Py)**,** 8.22 (m, 2H, *o,m*-Py), 5.04 (m, 4H, OC*H*), 1.42 (d, 12H, CC*H*$_3$, ^3J(^{1}H , ^{1}H) = 4 Hz), 1.25 (d, 12H, CC*H*$_3$, ^3J(^{1}H , ^{1}H) = 4 Hz); **^{13}C{^{1}H} NMR** (240 MHz, CD_2Cl_2): δ = 149.7 (*o*-Py), 147.6 (*o*-Py), 143.3 (*p*-Py), 133.3 (*m*-Py), 77.9 (O*C*H), 24.5 (C*C*H$_3$); **^{31}P{^{1}H} NMR** (162 MHz,

CD_2Cl_2): δ = 16.3 (s). **Elemental analysis** calcd. for $C_{17}H_{31}Br_4NO_6P_2Sn_2$ 786.84 [g/mol]: C, 21.2%; H, 3.2%; N, 1.5%, found: C, 21.4%; H, 3.3%; N, 1.4%;

[2,6-{P(O)(O*i*Pr)$_2$}C$_5$H$_5$NSnI]SnI$_3$ (1b)

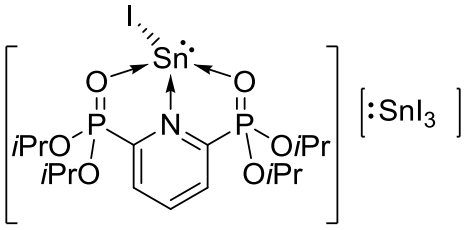

Isolated as red solid, **m**.**p**. 275 °C; **IR:** $\tilde{\nu}$ = 563 (s), 991 (w, PO*i*Pr), 1171 (s, P=O), 2977 (br) cm^{-1}; **^{1}H NMR** (400 MHz, CD_2Cl_2): δ = 8.56 (m, 1H, *p*-Py)**,** 8.26 (m, 2H, *o,m*-Py), 5.16 (m, 4H, OC*H*), 1.50 (d, 12H, CC*H*$_3$, ^3J(^{1}H , ^{1}H) = 4 Hz), 1.35 (d, 12H, CC*H*$_3$, ^3J(^{1}H , ^{1}H) = 4 Hz); **^{13}C{^{1}H} NMR** (240 MHz, CD_2Cl_2): δ = 149.7 (*o*-Py), 147.6 (*o*-Py), 143.3 (*p*-Py), 133.3 (*m*-Py), 77.9 (O*C*H), 24.5 (C*C*H$_3$); **^{31}P{^{1}H} NMR** (162 MHz, CD_2Cl_2): δ = 16.3 (s). The amount of the obtained substance was small to perform an elemental analysis.

[2-{P(O)(OiPr)$_2$}-6-{P(O)(OiPr)$_2$}C$_5$H$_5$NSnCl]SnCl$_3$ (2)

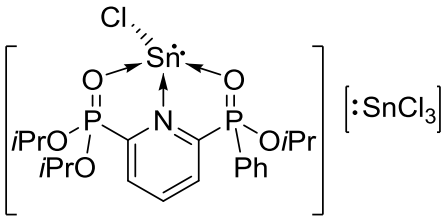

Isolated as a colorless crystals **m**.**p**. 114 °C; **IR**: $\tilde{\nu}$ = 541 (vs), 533 (vs), 976 (s, POR), 1006 (vs, POR), 1157 (s, P=O), 1174 (s, P=O); **^{1}H NMR** (400 MHz, CD_2Cl_2): δ = 8.63 – 8.57 (m, 1H, *p*-Ph), 8.30 – 8.24 (m, 2H, *o*,*m*-Ph), 8.16 – 8.12 (m, 2H, *o*,*m*-Ph), 7.76 – 7.72 (m, 2H, *p*-Py), 7.67 – 7.62 (m, 2H, *p*-Py), 5.15 – 5.01 (m, 3H, OC*H*), 1.52 (d, 3H, ^3J(^{1}H , ^{1}H) = 6 Hz, CH$_3$), 1.50 (d, 3H, ^3J(^{1}H , ^{1}H) = 6 Hz, CH$_3$), 1.47 (d, 3H, ^3J(^{1}H , ^{1}H) = 6 Hz, CH$_3$), 1.37 (d, 3H, ^3J(^{1}H , ^{1}H) = 6 Hz, CH$_3$), 1.33 (d, 3H, ^3J(^{1}H , ^{1}H) = 6 Hz, CH$_3$), 1.27 (d, 3H, ^3J(^{1}H , ^{1}H) = 6 Hz, CH$_3$); **^{13}C{^{1}H} NMR** (240 MHz, CD_2Cl_2): δ = 149.7 (s, *i*-Ph), 143.1 (s, *p*-Ph), 135.5 (s, *p*-Py), 133.5 – 132.7 (m, *m,p*-Ph), 130.1 (d, ^2J(^{13}C , ^{31}P) = 14.7, *m*-Py), 125.4 (d, ^1J(^{13}C , ^{31}P) = 151.8, *o*-Py), 77.6 – 77.39 (m, OCH), 24.7 – 24.1 (m, CH$_3$); **^{31}P{^{1}H} NMR** (162 MHz, CD_2Cl_2): δ = 36.7 (s, P(O)PhO*i*Pr), 15.8 (s, P(O)(O*i*Pr)$_2$); **^{31}P{^{1}H} NMR** (162 MHz, CD_2Cl_2, T = 193 K): δ = 37.4 (s, P(O)PhO*i*Pr), 36.7 (s, P(O)PhO*i*Pr), 17.0 (s, P(O)(O*i*Pr)$_2$); **^{119}Sn{^{1}H} NMR** (149 MHz, CD_2Cl_2, T = 193 K): δ = −89 (s, *Sn*Cl$_3^-$), −673 (s, *Sn*Cl$^+$), −680 (s, *Sn*Cl$^+$); **Elemental analysis** calcd. for $C_{20}H_{30}Cl_4NO_5P_2Sn_2$ 786.84 [g/mol]: C, 29.8%; H, 3.8%; N,

1.7%, found: C, 29.9%; H, 3.7%; N, 1.6%; **ESI-MS** (70 eV, negative mode): m/z (%): 300.1 [L–3*i*Pr+2H], 570.0 [L– *i*Pr+$SnCl_2$]

[2,6-{C(O)OMe}C_5H_5NSnCl]$SnCl_3$ (3)

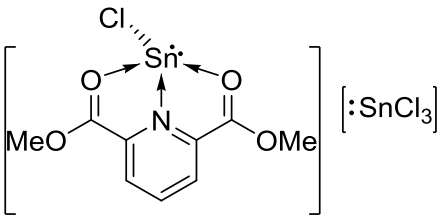

Isolated as a yellow solid, which is crystalizes from acetonitrile as a yellow crystals. **m.p**. 113 °C, **IR**: $\tilde{\nu}$ = 756 (vs), 988 (vs), 1280 (s), 1680 (br, C=O) cm^{-1}; **^{1}H NMR** (400 MHz, CD_2Cl_2): δ = 8.31 (d, 2H, $^3J(^1H, ^1H)$ = 4 Hz, *m*-Py)**,** 8.08 (t, 1H, $^3J(^1H, ^1H)$ = 4 Hz, *p*-Py), 4.02 (s, 6H, OCH_3); **^{13}C{^{1}H} NMR** (100 MHz, CD_2Cl_2): δ = 166.1 (*o*-Py), 148.5 (*m*-Py), 139.8 (*p*-Py), 129.1 (*C*=O), 54.1 (O*C*H_3); **^{119}Sn{^{1}H} NMR** (150 MHz, CD_2Cl_2): δ = −223 (br, $\Delta\nu_{1/2}$= 670 Hz); **Elemental analysis** calcd. for $C_9H_9Cl_4NO_4Sn_2$ 786.84 [g/mol]: C, 18.82%; H, 1.58%; N, 2.44%, found: C, 25.3%; H, 2.5%; N, 4.4%; **ESI-MS (70 eV, positive mode)**: m/z (%): 350.0 (100) [(L)$SnCl^+$], 220.0 [L_c – Me + MeCN].

[2,6-{C(O)OMe}C_5H_5NSnBr]$SnBr_3$ (3a)

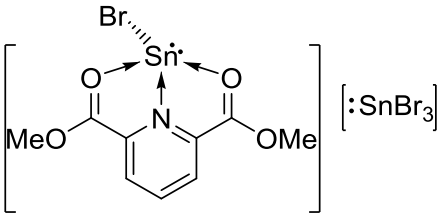

Isolated as a yellow solid, which is crystalizes from acetonitrile as a yellow crystals. **m.p**. 93.4 °C, **IR**: $\tilde{\nu}$ = 681 (s), 755 (vs), 986 (s), 1281 (vs), 1336 (vs), 1591 (s), 1664 (s, C=O), 1679 (s, C=O); **^{1}H NMR** (400 MHz, CD_3CN): δ = 8.43 – 8.41 (m, 2H, *m*-Py)**,** 8.38 – 8.34 (m, 1H, *p*-Py), 4.03 (s, 6H, OCH_3); **^{13}C{^{1}H} NMR** (100 MHz, CD_3CN): δ = 167.0 (*o*-Py), 147.5 (*m*-Py), 140.0 (*p*-Py), 129.1 (*C*=O), 54.6 (O*C*H_3); **^{119}Sn{^{1}H} NMR** (150 MHz, CD_2Cl_2): no resonances were observed; **Elemental analysis** calcd. for $C_9H_9Br_4NO_4Sn_2$ (CH_3CN) 791.56 [g/mol]: C, 16.7%; H, 1.5%; N, 3.5%, found: C, 16.3%; H, 1.4%; N, 3.5%.

[2,6-{C(O)OMe}C_5H_5NSnI]SnI_3 (3b)

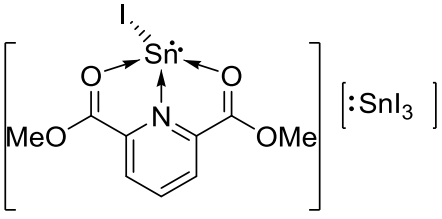

Isolated as a red micro crystals, **m.p**. 145 °C, **IR**: $\tilde{\nu}$ = 751 (vs), 1011 (vs), 1080 (vs), 1280 (w), 1337 (w), 1425 (w), 1581 (w), 1658 (w), 1671 (w) cm^{-1}; **^{1}H NMR** (400 MHz, CD_2Cl_2): δ = 8.18 – 8.32 (m, 3H) 3.97 (s, 6H, OCH_3); **^{13}C{^{1}H} NMR** (100 MHz, CD_2Cl_2): δ = 166.1 (*o*-

Py), 148.5 (*m*-Py), 139.8 (*p*-Py), 129.1 (*C*=O), 54.1 (O*C*H$_3$); **^{119}Sn{^{1}H} NMR** no resonances were observed; **Elemental analysis** calcd. for $C_9H_9I_4NO_4Sn_2$ 742.48 [g/mol]: C, 11.50%; H, 0.96%; N, 1.49%, found: C, 25.3%; H, 2.5%.

[2,6-{C(O)NEt$_2$}C$_5$H$_5$NSnCl]SnCl$_3$ (4)

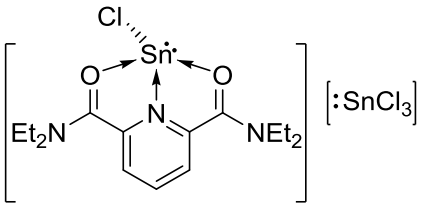

N,N,N',N'-tetraethyl-2,6-pyridinedicarboxamide was synthesis according to the modified literature[13] procedures. **4** was isolated as a colorless crystals. **^{1}H NMR** (400 MHz, CD_3OD): δ = 8.13 (t, 1H, $^3J(^1H, ^1H)$ = 8 Hz, *p*-Py)**,** 7.72 (d, 2H, $^3J(^1H, ^1H)$ = 8 Hz, *p*-Py), 3.57 (q, 2H, $^3J(^1H, ^1H)$ = 7 Hz, NC*H*$_2$), 3.39 (q, 2H, $^3J(^1H, ^1H)$ = 7 Hz, C*H*$_3$); **^{13}C{^{1}H} NMR** (100 MHz, CD_3OD): δ = 168.6 (Py), 153.0 (Py), 139.0 (Py), 123.4 (CO), 43.5 (N*C*H$_2$), 40.3 (N*C*H$_2$), 13.1 (CH$_2$*C*H$_3$), 11.6 (CH$_2$*C*H$_3$); **^{119}Sn{^{1}H} NMR** (150 MHz, CD_3OD): δ = −300 (br, $\nu_{1/2}$= 355 Hz), **^{119}Sn{^{1}H} NMR** (150 MHz, CD_3OD, 193 K): δ = −303 (br, $\nu_{1/2}$= 3525 Hz) **Elemental analysis** calcd. for $C_{15}H_{23}Cl_4N_3O_2Sn_2$ 656.6 [g/mol]: C 27.4%; H 3.5%; N 6.4%, found: C 27.1%; H 3.7%; N 6.6%.

[2,6-{C(O)NEt$_2$}C$_5$H$_5$NSnBr]SnBr$_3$ (4a)

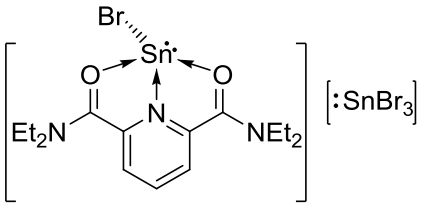

Isolated as a yellow solid, which is crystalizes from acetonitrile as a yellow crystals. **m.p**. 136 °C, **IR**: $\tilde{\nu}$ = 422 (vs), 1021 (vs), 1445 (w), 1567 (s)1586 (vs) cm^{-1}; **^{1}H NMR** (400 MHz, CD_3OD): δ = 8.06 (t, 1H, $^3J(^1H, ^1H)$ = 8 Hz, *p*-Py), 7.64 (d, 2H, $^3J(^1H, ^1H)$ = 8 Hz, *p*-Py), 3.57 (q, 4H, $^3J(^1H, ^1H)$ = 7 Hz, NC*H*$_2$), 3.36 (m, 4H), 1.28 (t, 6H, $^3J(^1H, ^1H)$ = 7 Hz, C*H*$_3$), 1.17 (t, 6H, $^3J(^1H, ^1H)$ = 7 Hz, C*H*$_3$); **^{13}C{^{1}H} NMR** (100 MHz, CD_3OD): δ = 169.0 (Py), 152.5 (Py), 139.0 (Py), 124.3 (CO), 44.6 (N*C*H$_2$), 41.3 (N*C*H$_2$), 14.4 (CH$_2$*C*H$_3$), 12.9 (CH$_2$CH$_3$); **^{119}Sn{^{1}H} NMR** (150 MHz, CD_3OD): no resonances were observed. The amount of the obtained substance was small to perform an elemental analysis.

[2,6-{C(O)NEt$_2$}C$_5$H$_5$NSnI]SnI$_3$ (4b)

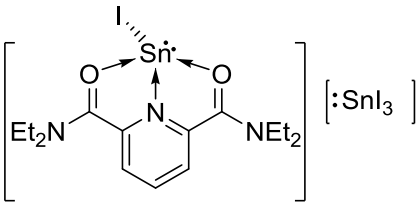

Isolated as a red micro crystals. . **m**.**p**. decompose 98 °C, **IR**: $\tilde{\nu}$ = 1008 (vs), 1067 (vs), 1441 (br), 1595 (br) cm^{-1}; **^{1}H NMR** (400 MHz, CD_3OD): δ = 8.06 (t, 1H, $^3J(^1H, ^1H)$ = 8 Hz, *p*-Py)**,** 7.64 (d, 2H, $^3J(^1H, ^1H)$ = 8 Hz, *p*-Py), 3.59 (q, 4H, $^3J(^1H, ^1H)$ = 7 Hz, NC*H*$_2$), 3.36 (br, 2H, NC*H*$_2$), 1.28 (t, 6H, $^3J(^1H, ^1H)$ = 7 Hz, C*H*$_3$), 1.17 (t, 6H, $^3J(^1H, ^1H)$ = 7 Hz, C*H*$_3$); **^{13}C{^{1}H} NMR** (100 MHz, CD_3OD): δ = 169.0 (Py), 160.0 (Py), 133.8 (Py), 124.9 (CO), 45.3 (N*C*H$_2$), 42.0 (N*C*H$_2$), 15.0 (CH$_2$*C*H$_3$), 13.05 (CH$_2$*C*H$_3$); **^{119}Sn{^{1}H} NMR** (150 MHz, CD_3OD): δ = no resonances were observed. The amount of the obtained substance was small to perform an elemental analysis**.**

2-{P(O)(O*i*Pr)$_2$-6-{P(O)(O*i*Pr)SnCl}C$_5$H$_5$N (5)

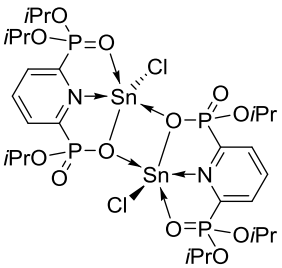

A toluene solution of **1** (0.80 g, 1 mmol) was heated at 80 °C over 16 h. The reaction mixture was filtered and the volatiles were removed under reduced pressure to obtain **5** as a colourless solid (0.46 g, 88%). **^{1}H NMR** (400 MHz, C_6D_6): δ = 8.05 – 8.01 (m, 1H, *m*-Py), 7.32 – 7.28 (m, 1H, *m*-Py), 7.13 – 7.12 (m, 1H, *p*-Py), 5.09 – 4.72 (m, 3H, OC*H*), 1.14 (d, 12H, $^3J(^1H, ^1H)$ = 6 Hz, CH_3), 0.94 (d, 6H, $^3J(^1H, ^1H)$ = 6 Hz, CH_3); **^{13}C{^{1}H} NMR** (100 MHz, C_6D_6): δ = 152.7 (dd, $J(^{13}C, ^{31}P)$ = 201/17 Hz, *o*-Py), 147.0 (dd, $J(^{13}C, ^{31}P)$ = 209/16 Hz, *o*-Py), 140.4 (t, $J(^{13}C, ^{31}P)$ = 10 Hz, *p*-Py), , 133.4 (d, $J(^{13}C, ^{31}P)$ = 19 Hz, *m*-Py), 130.8 (d, $J(^{13}C, ^{31}P)$ = 19 Hz, *m*-Py), 75.8 (d, $J(^{13}C, ^{31}P)$ = 4 Hz, O*C*H, O*C*H), 73.8 (d, $J(^{13}C, ^{31}P)$ = 4 Hz, O*C*H), 24.2 (s, CH_3), 23.9 (s, CH_3); **^{31}P{^{1}H} NMR** (162 MHz, C_6D_6): δ = 19.0 (s), 13.4 (s); **^{119}Sn{^{1}H} NMR** (150 MHz, C_6D_6): δ = –587 (br, $\nu_{1/2}$= 414 Hz). **Elemental analysis** calcd. for $C_{14}H_{24}Cl_1N_1O_6P_2Sn_1$+0.5$C_7H_8$ 564.5 [g/mol]: C, 32.4%; H, 4.7%; N, 2.7%, found: C, 35.2%; H, 5.2%; N, 2.6%.

2-{P(O)(O*i*Pr)Ph-6-{P(O)(O*i*Pr)SnCl}C$_5$H$_5$N (6)

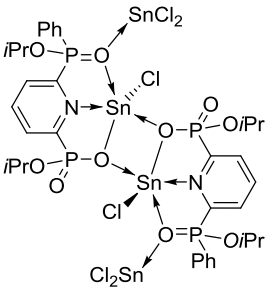

A toluene solution of **2** (0.64 g, 0.8 mmol) was heated at 80 °C over 16 h. The reaction mixture was filtered and the volatiles were removed under reduced pressure to obtain **5** as a colourless solid (0.34 g, 79%). **^{1}H NMR** (400 MHz, toluene-d_8): δ = 8.31-8.26 (m, 1H, Py), 8.06 (m, 1H, Ph)7.83 (t, $^3J(^1H, ^1H)$ = 7 Hz, 1H, Py), 7.70 (t, $^3J(^1H$

, ^{1}H) = 7 Hz, 1H, Py), 7.33-7.32 (m, 1H, Ph), 7.31 (s, 2H, Ph), 7.29 (s, 1H, Ph) 5.02 (br, $\nu_{1/2}$= 30 Hz, 1H, OC*H*), 4.97-4.89 (m, 1H, OC*H*), 1.17 (d, ^{3}J(1H , 1H) = 6 Hz, 12H, CH_3); **^{31}P{^{1}H} NMR** (162 MHz, toluene-d_8): δ = 34.1, 27.3, 18.3 and 10.2 ($\nu_{1/2}$ = 55 Hz) (1:1:1:1); **^{31}P{^{1}H} NMR** (162 MHz, toluene-d_8, 193 K): δ = 34.9, 34.1, 27.9, 17.1, 14.0 and 11.1 (1:2:2:2:2:1); **^{119}Sn{^{1}H} NMR** (150 MHz, toluene-d_8, 193 K): δ = –248 (br, $\nu_{1/2}$= 1140 Hz), –262 (br, $\nu_{1/2}$= 1145 Hz), –588 (br, $\nu_{1/2}$= 775 Hz) and –637 (br, $\nu_{1/2}$= 1640 Hz). **Elemental analysis** calcd. for $C_{17}H_{22}Cl_1N_1O_5P_2Sn_1$+$SnCl_2$+0.5$C_7H_8$ 772.8 [g/mol]: C 31.9%; H 3.4%; N 1.8%, found: C 32.3%; H 3.9%; N 1.8%.

2.4 CONCLUSION

In this chapter the reactions of SnX_2 (X = Cl, Br and I) with the phosphorus-substituted pyridine derivatives L_1, L_2, L_3 and L_4 are described giving salts of the type $[(L)SnCl]SnCl_3$ (Scheme 1).

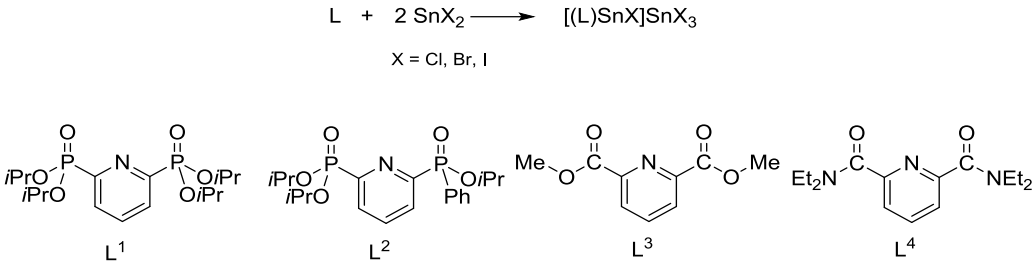

Scheme 1. The reaction of SnX_2 with P-substituted pyridine derivatives.

On $^{119}Sn\{^1H\}$ NMR time scale, the complexes are kinetically labile with the consequence that no ^{119}Sn resonances were observed. At –80 °C, however, the exchange processes are slow and single resonances are observed for both the cation $[(L)SnCl]^+$ (δ –701) and the anion $SnCl_3^-$ (δ –90). Two diastereomers are observed for $[(L\_2)SnCl]SnCl_3$.

The reaction of $[(L)SnCl]SnCl_3$ with $[W(CO)_5(thf)]$ gave the unprecedented $[(L)SnCl]W(CO)_4SnCl_3$, in which not only the anion $SnCl_3^-$ but also the cation $[(L_1)SnCl]^+$coordinate to the $W(CO)_4$ moiety

2.5 LITERATURE

[1] a) D. W. Stephan, *J. Am. Chem. Soc.* **2015**, *137*, 10018; b) D. W. Stephan, *Science* **2016**, *354*; c) D. W. Stephan, G. Erker, *Angew. Chem. Int. Ed.* **2015**, *54*, 6400.

[2] a) P. Jutzi, G. Reumann, *J. Chem. Soc., Dalton Trans.* **2000**, 2237; b) P. Jutzi, A. Mix, B. Rummel, W. W. Schoeller, B. Neumann, H.-G. Stammler, *Science* **2004**, *305*, 849; c) P. Jutzi, K. Leszczyńska, A. Mix, B. Neumann, W. W. Schoeller, H.-G. Stammler, *Organometallics* **2009**, *28*, 1985; d) P. Jutzi, K. Leszczynska, B. Neumann, W. W. Schoeller, H.-G. Stammler, *Angew. Chem. Int. Ed.* **2009**, *48*, 2596.

[3] A. P. Singh, H. W. Roesky, E. Carl, D. Stalke, J.-P. Demers, A. Lange, *J. Chem. Soc., Dalton Trans.* **2012**, *134*, 4998.

[4] a) M. Bouška, L. Dostál, A. Růžička, R. Jambor, *Organometallics* **2013**, *32*, 1995; b) M. Bouska, L. Dostal, M. Lutter, B. Glowacki, Z. Ruzickova, D. Beck, R. Jambor, K. Jurkschat, *Inorg. Chem.* **2015**, *54*, 6792.

[5] J. C. Avery, M. A. Hanson, R. H. Herber, K. J. Bladek, P. A. Rupar, I. Nowik, Y. Huang, K. M. Baines, *Inorg. Chem.***2012**, *51*, 7306.

[6] M. Mantina, A. C. Chamberlin, R. Valero, C. J. Cramer, D. G. Truhlar, *J. Phys. Chem. A* **2009**, *113*, 5806.

[7] M. J. Frisch, G. W. Trucks, H. B. Schlegel, G. E. Scuseria, M. A. Robb, J. R. Cheeseman, G. Scalmani, V. Barone, G. A. Petersson, H. Nakatsuji, X. Li, M. Caricato, A. Marenich, J. Bloino, B. G. Janesko, R. Gomperts, B. Mennucci, H. P. Hratchian, J. V. Ortiz, A. F. Izmaylov, J. L. Sonnenberg, D. Williams-Young, F. Ding, F. Lipparini, F. Egidi, J. Goings, B. Peng, A. Petrone, T. Henderson, D. Ranasinghe, V. G. Zakrzewski, J. Gao, N. Rega, G. Zheng, W. Liang, M. Hada, M. Ehara, K. Toyota, R. Fukuda, J. Hasegawa, M. Ishida, T. Nakajima, Y. Honda, O. Kitao, H. Nakai, T. Vreven, K. Throssell, J. A. Montgomery, Jr., J. E. Peralta, F. Ogliaro, M. Bearpark, J. J. Heyd, E. Brothers, K. N. Kudin, V. N. Staroverov, T. Keith, R. Kobayashi, J. Normand, K. Raghavachari, A. Rendell, J. C. Burant, S. S. Iyengar, J. Tomasi, M. Cossi, J. M. Millam, M. Klene, C. Adamo, R. Cammi, J. W. Ochterski, R. L. Martin, K. Morokuma, O. Farkas, J. B. Foresman, and D. J. Fox, *Gaussian 09, Revision E.01*, Gaussian, Inc. Wallingford CT, 2016.

[8] J.-D. Chai, M. Head-Gordon, *Phys. chem. chem. phys.* **2008**, *10*, 6615.

[9] a) B. Metz, H. Stoll, M. Dolg, *J. Chem. Phys.* **2000**, *113*, 2563; b) F. Weigend, R. Ahlrichs, *Phys. chem. chem. phys.* **2005**, *7*, 3297.

[10] R. Krishnan, J. S. Binkley, R. Seeger, J. A. Pople, *J. Chem. Phys.* **1980**, *72*, 650.

[11] [Cannot display reference #27, because the template "Bibliography - Journal Article - (Default template)" contains only fields that are empty in this reference.]

[12] W. L. F. Armarego, C. L. L. Chai, *Purification of laboratory chemicals*, Elsevier/Butterworth-Heinemann, Amsterdam, Boston, **2009**.

[13] B. R. Kim, H.-G. Lee, S.-B. Kang, G. H. Sung, J.-J. Kim, J. K. Park, S.-G. Lee, Y.-J. Yoon, *Synthesis* **2012**, *44*, 42.

CHAPTER 3

3.1 INTRODUCTION

The dependence of mankind on petrochemicals decreases. This is the result of the increasing price, the limitation and the global warming. Today the demand to new resources leads to relaying on regenerating bio-resources.[1] One of these bio resources is lactic acid which can be obtained from corn starch fermentation using lactobacillus. The lactic acid can be directly polymerized or through condensation reaction giving lactide which can polymerize according to ring opening polymerization (ROP). The ROP is applied using metal-based catalysts or enzymes to get polylactide (PLA) with higher molecular weight, selectivity and melting point than that of the lactide acid polymerization product (Figure 1). The PLA decomposes into CO_2 and H_2O which is adsorbed from plants to close the lifecycle.[2]

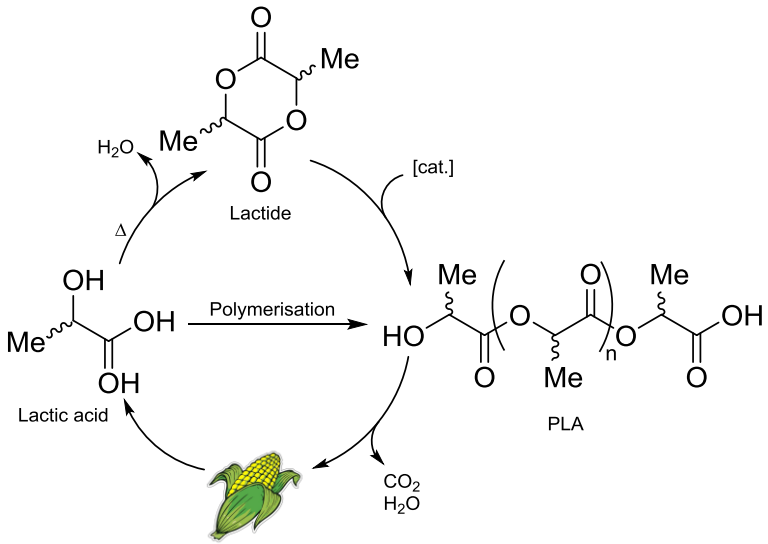

Figure 1. The lifecycle of PLA

The ring opening polymerization is applied via anionic[3], cationic[4] or coordination-insertion mechanism.[5] The coordination-insertion mechanism is described in scheme 1, the lactide coordinates at the Lewis acidic tin center **A**, followed by the rearrangement of the substituents **B**, cleavage of C–O bond and the cycle is closed by the re-coordination of a new lactide unit.

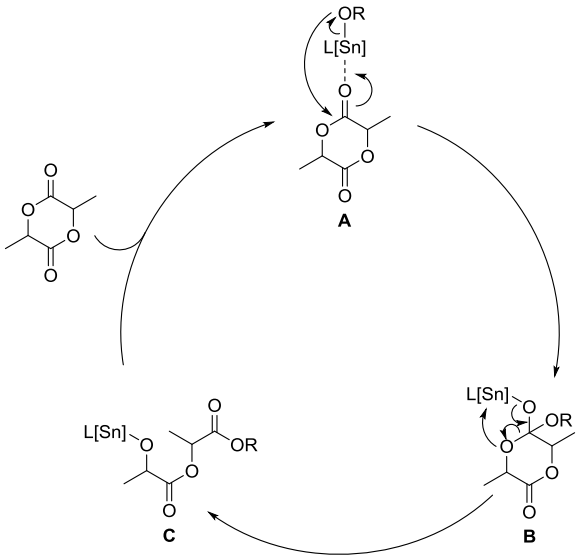

Scheme 1. ROP of Lactide

The lactide is commercially available in three pure diastereomers *R*,*R* (*D*-lactide), *S*,*S* (*L*-lactide) and *R*,*S* (*meso*-lactide). Because of the stereogenic centres, it polymerizes in different diastereomers which affect the physical properties of the product (Scheme 2)

The ROP of the pure *D*- or *L*-lactide results in isotactic polylactide along the chain of the polymer in which all stereogenic centres are *RR...* or *SS*… (isotactic chiral) but in case of the polymerization of a racemic Lactide the resulting polymer is syndiotactic (i.e. *RSRSR*…). In one case a heterotactic polymer is obtained by the ROP of a mixture of a *D*- and *L*-lactide and the result is *SSRR*… polymer.[6]

Another two kind of isotactic polymers are presented isotactic diblock and isotactic multiblock via the polymerization of a mixture of *D*- and *L*-lactide. The isotactic diblock polymer has a chain consists of $(SS)_n(RR)_m$ but in the case of isotactic multiblock the chain has $[(SS)_n(RR)_m]_x$.

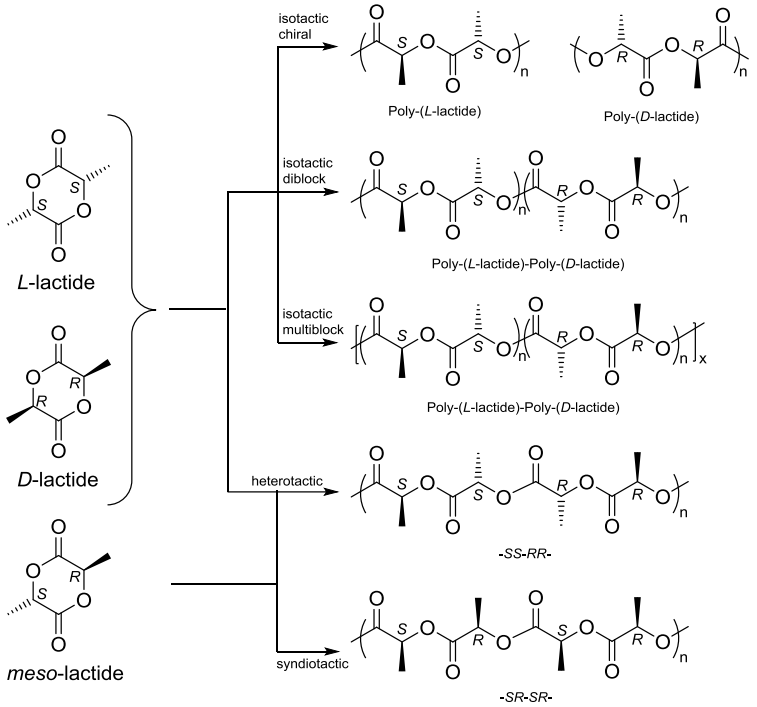

Scheme 2. The possibilities for the stereoselctive polymerisation of lactide

In this chapter the polymerization of lactide catalysed by $[C_5H_3N(C(O)N(C_2H_5)_2)_2SnCl]SnCl_3$ was studied via ^1H NMR spectroscopy at room temperature, and after 48h at 90 °C. On the other hand the polymerization of hexamethylenediisocyanate and triethyl glycol monomethyl ether was tested under neutral and acidic conditions with different concentrations.

3.2 RESULTS AND DISCUSSION

3.3 Lactide polymerization

To study the reactivity of lactide toward methanol and diethyl amine, lactide was stirred in methanol and *di*ethyl amine at room temperature and 90 °C, respectively (Scheme 3). After 1h the volatiles were removed under reduced pressure and ^{1}H NMR spectroscopy shows that the lacide ring is opened to obtain compound **1** in case of methanol and **3** in case of *di*ethyl amine.

Compound **1,** or **3**, **HN_3** and lactide in the ratio 1:1:10 in acetonitrile were stirred at room temperature for 18 h and a ^{1}H NMR spectrum recorded from the reaction solution showed that the reaction had not taken place. The reaction solution was heated at reflux for 48h, the volatiles were removed under reduced pressure. The conversion of the monomer was determined from the integrations of a slandered ^{1}H NMR spectrum (Figure 4) and in agreement with lit.[7]

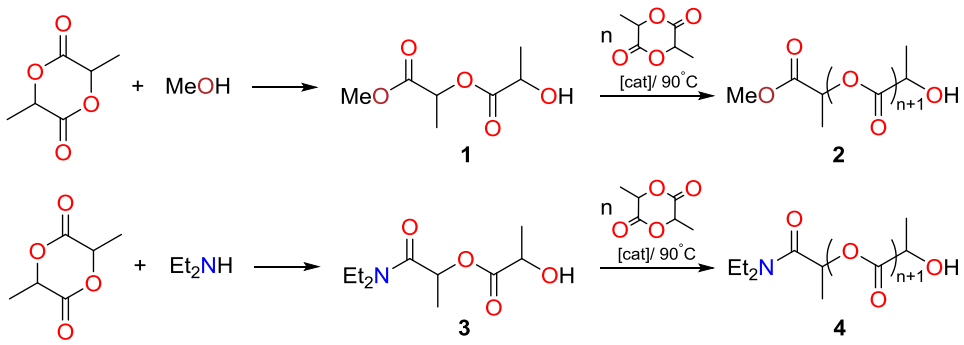

Scheme 3. The ring opening of lactide and the ROP of lactide.

In the ^{1}H NMR spectrum of **4** (Figure 2) appear the resonances for the pyridine protons at δ 8.07 (t, ^3J(^{1}H , ^{1}H) = 8 Hz), 7.67 (t, ^3J(^{1}H , ^{1}H) = 8 Hz), 5.13 (m, (^3J(^{1}H , ^{1}H) = 7 Hz, SnOC*H*), from 5.04 to 4.99 (m, (OC*H*)$_9$),4.28 – 4.23 (q, (^3J(^{1}H , ^{1}H) = 7 Hz, OC*H* of the monomer), 3.55 – 3.50 (q, (^3J(^{1}H , ^{1}H) = 7 Hz, NCH_2), 3.24 – 3.16 (q, (^3J(^{1}H , ^{1}H) = 7 Hz, NCH_2), 1.44 (d, ^3J(^{1}H , ^{1}H) = 7 Hz, CH_3 of the monomer), 1.25 (d, ^3J(^{1}H , ^{1}H) = 7 Hz, CH_3), 1.17 (d, ^3J(^{1}H , ^{1}H) = 7 Hz, (CH_3)$_9$), 1.08 (t, ^3J(^{1}H , ^{1}H) = 7 Hz, NCH$_2$CH_3) and 0.98 (t, ^3J(^{1}H , ^{1}H) = 7 Hz, NCH$_2$CH_3).

The ROP reaction using HN_3 as a catalyst shows a 50% conversion (the integration of signals 1, 2 and 8 in figure 2) and building a polymer unit of 10 monomers (the integration of signals 1 and 2 in figure 2) after 48 h and heating to 80 °C.

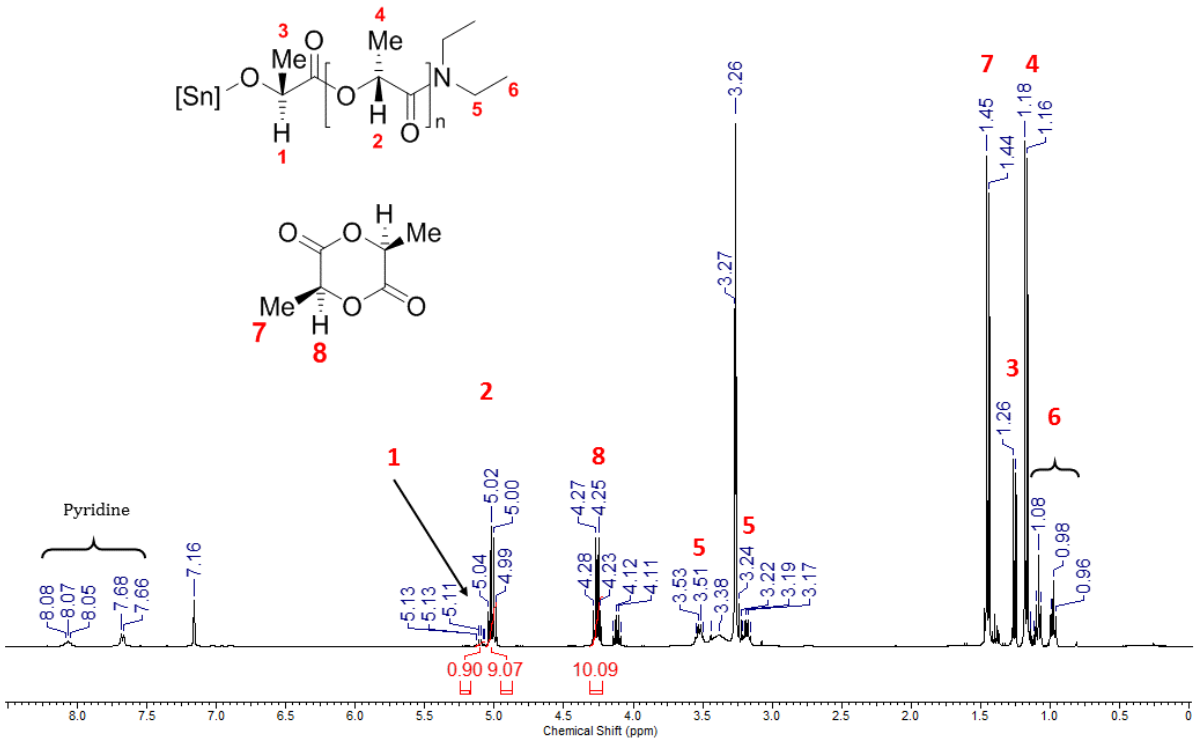

Figure 2. ^{1}H NMR of the polymerisation reaction.

3.4 The poylerisation of hexamethylene diisocyanate and triethylene glycol monomethyl ether

To study the catalytic activity and the delayed action effect of **HN_1**, **HN_2** and **HN_3** (Figure 3) in the polymerization of two components was used the COVESTRO standard protocol. In this reaction, hexamethylenediisocyanate and triethyl glycol monomethyl ether are used as starting materials (scheme 3).

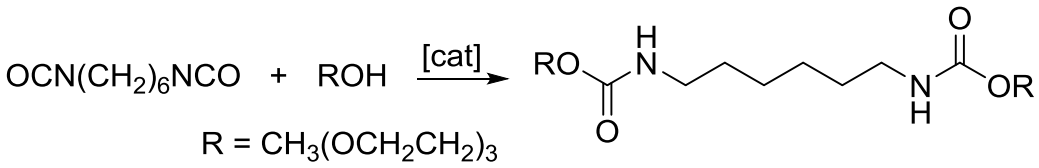

Scheme 3. The reaction between hexamethylenediisocyanate and triethyl glycol monomethyl ether.

The reaction mixture was stirred for 2 h at 30 °C. A sample is taken each 20 min, followed by increasing the temperature to 50 °C and stirring for 24 h. In the heating phase, a sample was taken every 10 min. To determine the amount of the remained

isocyanate, the samples were diluted with acetone, 10 mL of di-*n*butylamine was added and titrated with HCl.

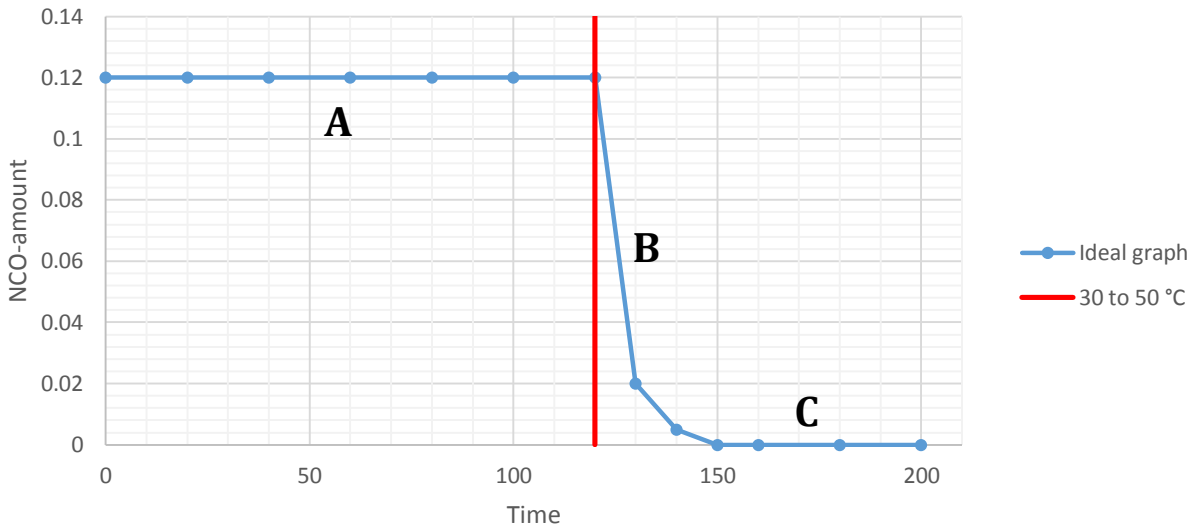

Chart 1. The plot of an ideal polymerization by a catalyst with delayed action effect.

The graph of an ideal catalyst is shown in Chart 1. In area **A** of the ideal graph appears no catalytic activity at 30 °C and the amount of the isocyanate is stable (delayed action effect). When the temperature is increased to 50 °C (the red line), the amount of the isocyanate is decreased rapidly, area **B**. In this area **B**, the catalyst has high activity and the amount of the isocyanate in short time is zero, area **C**.

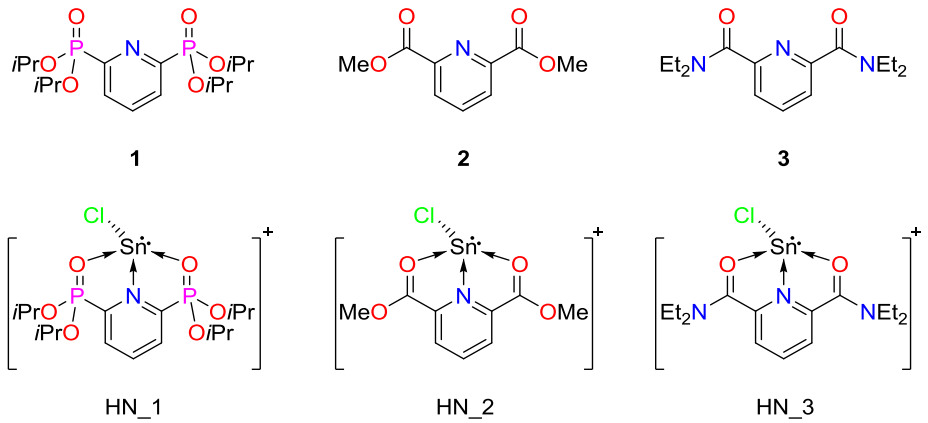

Figure 3. The tested catalysts, the counter anion $SnCl_3^-$ is omitted for clarity.

The results of the polymerization reactions in neutral and acidic conditions are shown in Charts 2 to 4. In all charts the isocyanate amount is plotted versus the time. In the reactions without DBTL (di-butyl tin di-laurate) the amount of isocyanate stays stable

until the reaction is heated to 50 °C and then the amount of isocyanate starts to decrease. But after 24h it remains about 50% of the isocyanate amount not reacted.

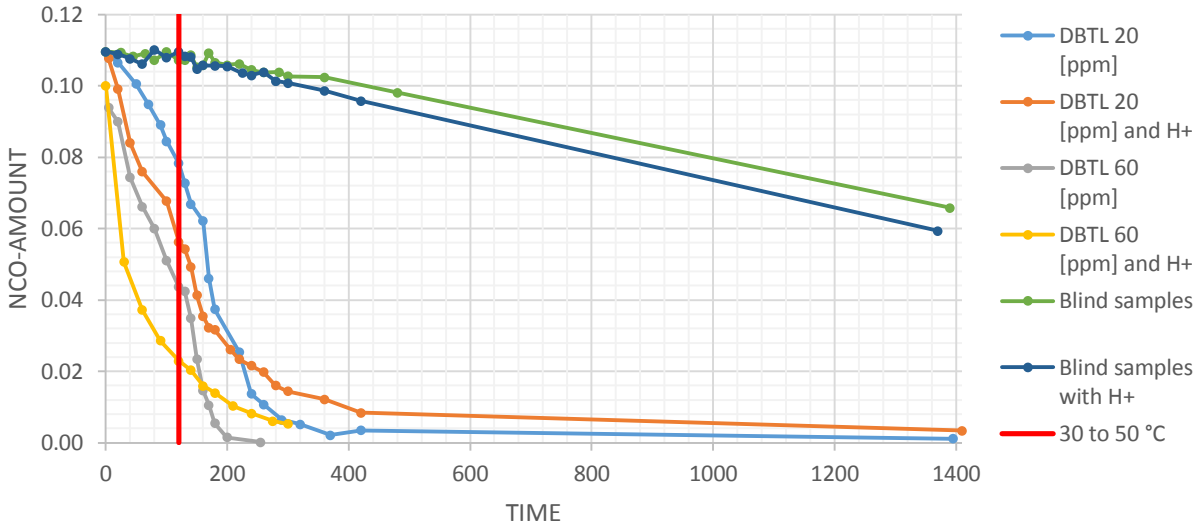

Chart 2. Using DBTL as a catalyst in different concentrations.

Using DBTL (60 ppm) as a catalyst in the reaction shows that the polymerization reaction is faster under neutral conditions than acidic conditions and after about 6h the isocyanate amount is about 0%. While using DBTL (20 ppm) shows less catalytic activity than DBTL (60 ppm) and after 24h a small amount of isocyanate was found in the reaction mixture.

In Chart 2 the 2,6-di-*iso*propylphosphoryl pyridine **1** and **HN_1** (figure 3) are shown in acidic and neutral conditions. Compound **1** shows no catalytic activity, and it works better in 20 than 60 ppm concentration, and better in acidic than neutral conditions. When using 60 ppm,**HN_1** shows higher activity than with 20 ppm. In acidic conditions it reduces the amount of the isocyanate to about 0% after 6h.

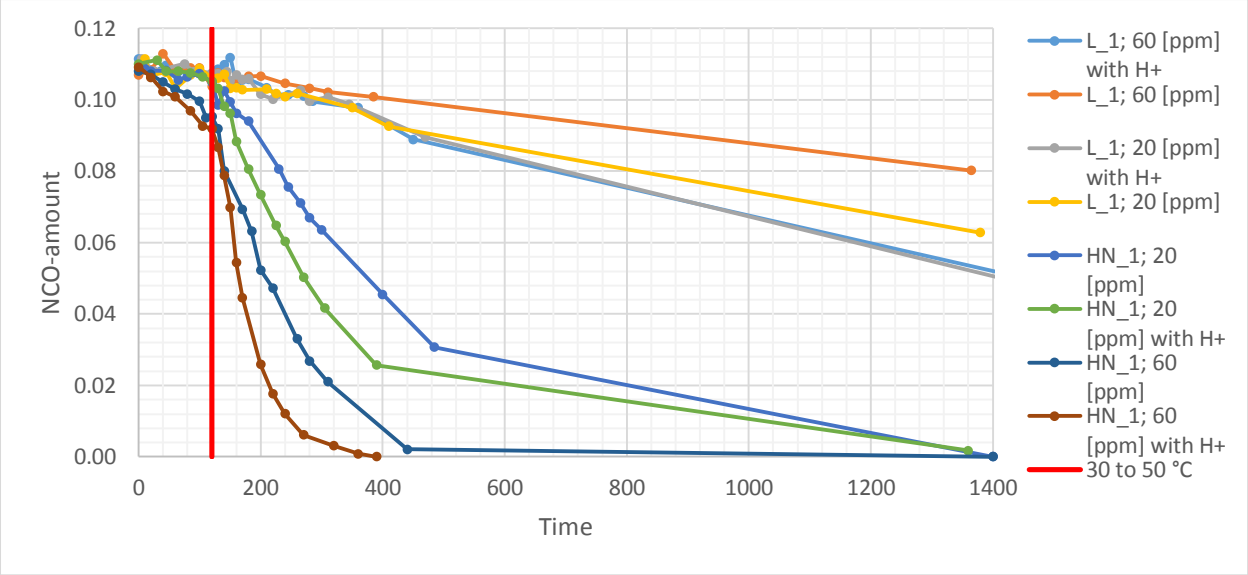

Chart 3. Comparison between L_1 and HN_1 in different concentrations.

In Chart 3 the **HN_2** and **HN_3** (Figure 3) are shown for 20 and 60 ppm; in neutral and acidic conditions. In all conditions the amount of isocyanate after 24h the amount is about 0%. The catalysts are more active in 60 ppm than 20 ppm and in acidic conditions than neutral medium. In case of **HN_3** (60 ppm) in acidic medium the amount of the isocyanate is reduced to about 0% in 3h.

In Chart 4, a comparison is made between **HN_1** (60 ppm), **HN_2** (60 ppm), **HN_3** (60 ppm) in acidic medium and DBTL in neutral medium. **HN_3** in acidic medium and DBTL show high catalytic activity. After 3h the amount of the isocyanate is about 0%. On the other hand, the **HN_1**, **HN_2** and **HN_3** have a better delayed action effect as compared with DBTL.

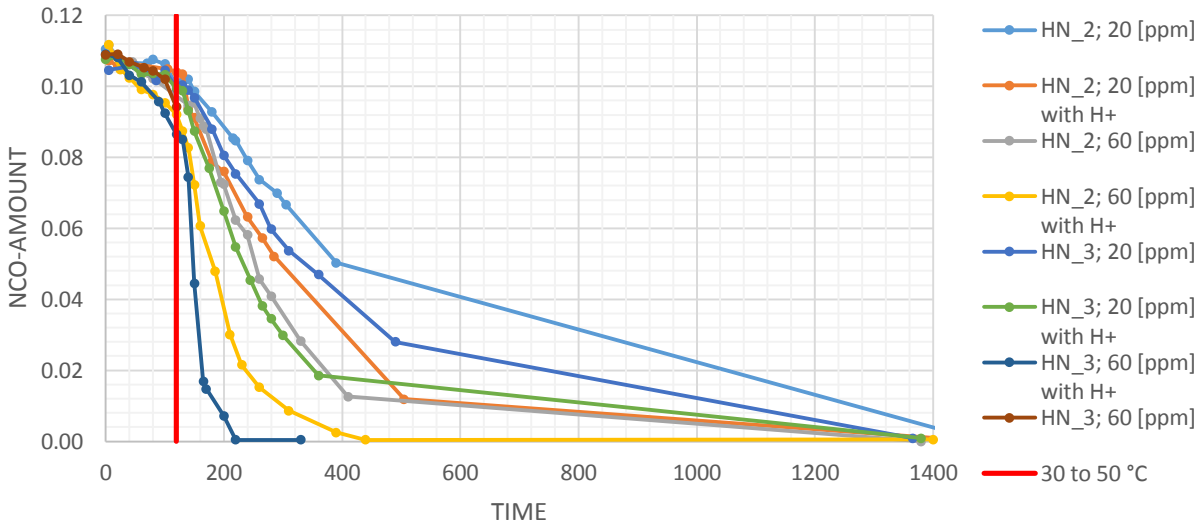

Chart 4. Comparison between **HN_2** and **HN_3** as catalysts in different concentrations.

3.5 CONCLUSION

In Chart 4, a comparison is shown between **HN_1** (60 ppm), **HN_2** (60 ppm), **HN_3** (60 ppm) in acidic medium and DBTL in neutral medium. **HN_3** in acidic medium and DBTL show high catalytic activity, in which after 3h the amount of the isocyanate is about 0%. On the other hand the **HN_1**, **HN_2** and **HN_3** show a better delayed action effect as compared with DBTL.

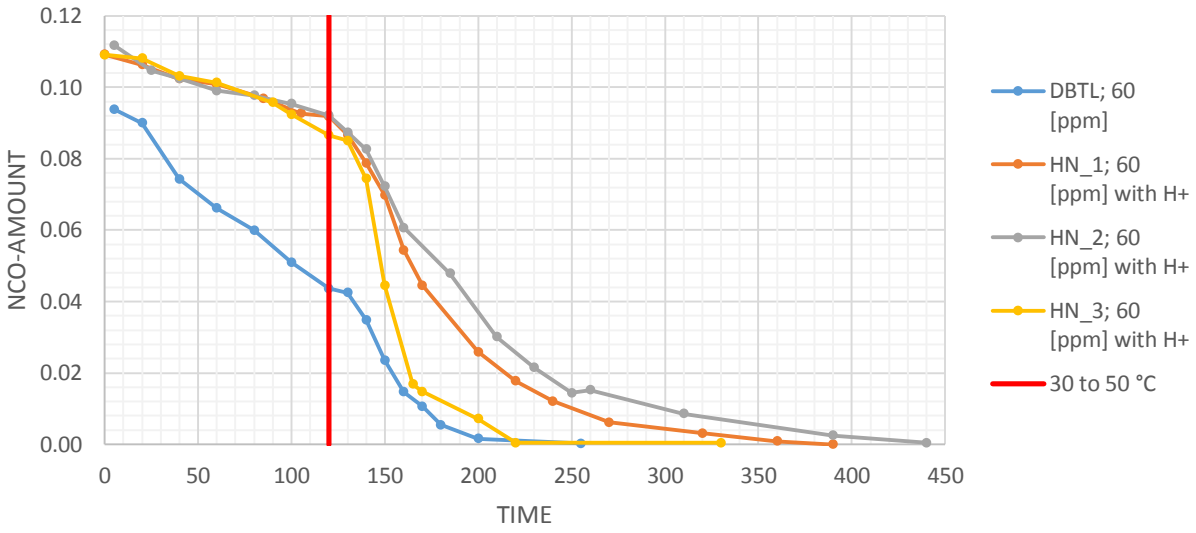

Chart 5. Comparison between **HN_1**, **HN_2** and **HN_3**.

3.6 LITERATURE

[1] L. Shen, J. Haufe and M. K. Patel, *Product Overview and Market Projection of Emerging Bio-based Plastics*, **2009**, Utrecht.

[2] M. Jamshidian, E. A. Tehrany, M. Imran, M. Jacquot and S. Desobry, *Comprehensive Reviews in Food Science and Food Safety* **2010**, *9*, 552.

[3] a) D. S. McGuinness, E. L. Marshall, V. C. Gibson, J. W. Steed, *J. Polym. Sci., Polym Chem.* **2003**, *41*, 3798; b) S. Csihony, T. T. Beaudette, A. C. Sentman, G. W. Nyce, R. M. Waymouth, J. L. Hedrick, *Adv. Syn. Catal.* **2004**, *346*, 1081; c) A. Bhaw-Luximon, D. Jhurry, N. Spassky, S. Pensec, J. Belleney, *Polymer* **2001**, *42*, 9651; d) C. Stere, M. Iovu, A. Boborodea, D. S. Vasilescu, I. S. Fazakas-Anca, *Polym. Advan. Technol.* **1998**, *9*, 322.

[4] N. Emig, H. Nguyen, H. Krautscheid, R. Reau, J. Cazaux and G. Bertrand, *Organometallics* **1998**, *17*, 3599.

[5] a) E. L. Marshall, V. C. Gibson, H. S. Rzepa, *J. Am. Chem. Soc.* **2005**, *127*, 6048; b) A. Kowalski, A. Duda, S. Penczek, *Macromolecules* **2000**, *33*, 7359.

[6] M. S. Stanford, A. Dove, *Chem. Soc. Rev.* **2010**, *39*, 486.

[7] P. Lewinski, S. Sosnowski, S. Kazmierski and S. Penczek, *Polym*. *Chem*., **2015**, *6*, 4353–4357.

CHAPTER 4

4.1 Introduction

The subvalent carbon homologues diphosphatetrylenes $(R_2P)_2E$, E = Si, Ge, Sn and Pb (carbene analogues) have a LEWIS acid and Lewis base reactivity.[1] They have been studied much less extensively than diaminotetrylenes $(R_2N)_2E$, the first example of which was reported by LAPPERT *et al.*in 1977.[2] The first bis(diorganophospha)stannylene $(^tBu_2P)_2Sn$ **A** was reported by DU-MONT in 1985.[3] It is a dimer in solution. Kinetically inert monomeric derivatives of the types **C** and **D** were reported in 1995 using bulky substituents.[4] Another class of tin(II) compounds are intramolecularly coordinated derivatives such as types **E**[5], **G**[6] **H**[7] and **J.**[8] The enhanced stability of this class of compounds relies on the intramolecular coordination makes these compounds strong σ-donors (correspondingly weak π-acceptor) and more stable. The heteroleptic compounds of tin(II) such as **F** and **B**[9] were synthesized by the addition of tin(II) chloride to the corresponding R_2PLi while **I** was synthesized by the addition of the tin(II) chloride to the corresponding R_2PH[10] and the elimination of HCl.

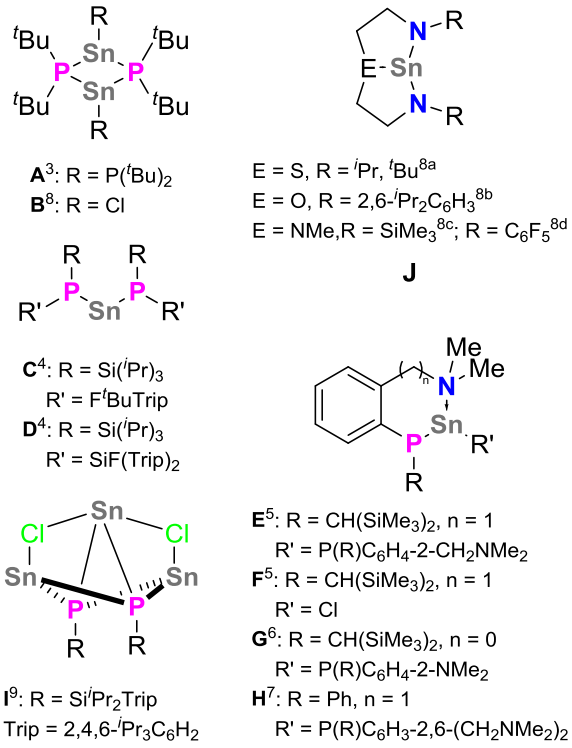

Figure 1. Examples for homo- and heteroleptic Sn(II) compounds.

Herein, two novel potentially *P,N,P*-coordinating ligands are reported. They were used for the syntheses of the corresponding hetero and homoleptic tin(II) compounds. The reactivity of the tin(II) compounds toward $W(CO)_5$(thf) and by PhSSPh is also reported.

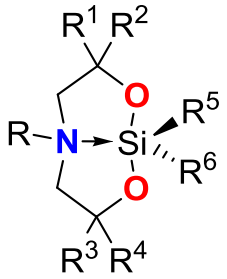

R = alkyl, vinyl, aryl
$R^1 = R^3$ = H and Me
$R^2 = R^4$ = H and Me
$R^5 = R^6$ = alkyl, vinyl, aryl

Figure 2. Examples for silicon derivatives of amino alcohols.

A representative selection of the published silicon derivatives of amino alcohols [11] are listed in figure 2. Notably, there is only one example with $R^5 = R^6 = H$[12] for which the structure in the solid state is reported. Compound $PhN(CH_2CH_2O)_2SiH_2$ was synthesized by the reaction of the *in situ* generated $PhN(CH_2CH_2OLi)_2$ and SiH_2Cl_2.[12] This chapter reports the synthesis of $MeN(CH_2CMe_2O)_2SiH_2$ by the reaction of $MeN(CH_2CMe_2OH)_2$ with $SiH_2(NEt_2)_2$ at room temperature. $MeN(CH_2CMe_2O)_2SiH_2$ reacts with BH_3·THF complex and HCl in diethyl ether to produce $MeN(CH_2CMe_2O)_2SiHBH_4$ and $MeN(CH_2CMe_2O)_2SiHCl$, respectively.

4.2 RESULTS AND DISCUSSION

4.2.1 The synthesis of $MeN(CH_2CH_2PHR)_2$

The compounds $MeN(CH_2CH_2PHR)_2$ (R = Ph, Mes) were synthesised according to a known method.[13] Bis(2-chloroethyl)methyl ammonium chloride was added to a mixture of the corresponding phosphane and potassium hydroxide in dimethyl sulfoxide at room temperature (Scheme 1). Each reaction mixture was extracted with diethyl ether giving the desired compounds as mixture of diastereomers (δ ^{31}P for **1a/1b**: –58.07/–58.12, δ ^{31}P for **2a/2b:** –92.69/–92.72). In case of the synthesis of **2a/2b** the by-product **3** was also detected (δ ^{31}P for **3**: –94.33; ESI MS *calcd*. for $C_{14}H_{25}O_1N_1P_1$ $[M+H]^+$ 254.1668, *found* 254.1667) For the subsequent reactions described below, the diastereomeric mixtures were used without further purification. Their purification by distillation or crystallisation failed under the experimental conditions used. Notably, the reaction for the preparation of **2** was performed twice. In case (a), there was no by-product while in case (b) there was approximately 20 % of the by-product **3**. The origin for this difference was not established. However, the products from case (a) as well as from case (b) were used for subsequent reactions (see below Scheme 1).

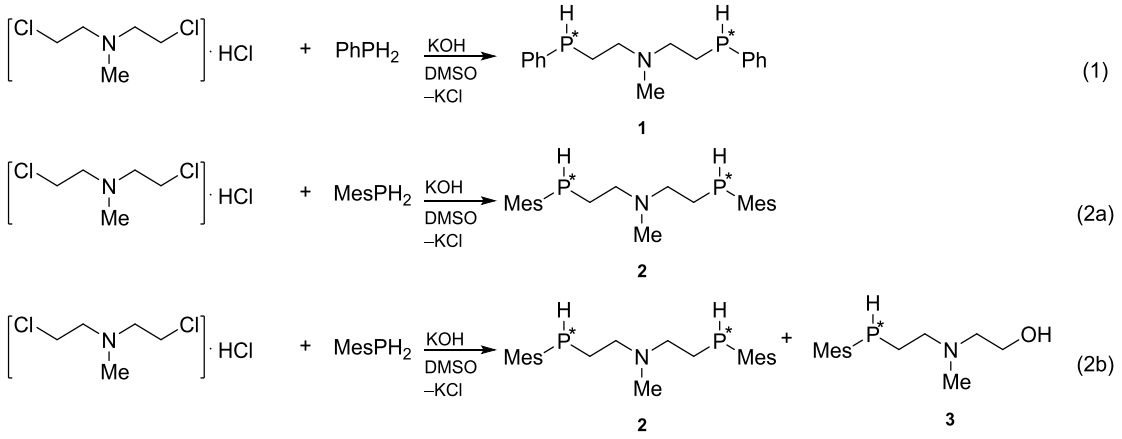

Scheme 1. The synthesis of the ligands **1, 2** and **3**.

The diastereomeric mixtures **1a/1b** and **2a/2b** were isolated in good yields of 82 and 78%, respectively as oxygen-sensitive brown oils. They are soluble in common organic solvents such as hexane, dichloromethane, tetrahydrofuran and toluene. A $^{31}P\{^1H\}$ NMR spectrum of compound **1** in benzene-d_6 shows that the phosphorus atoms resonate at δ –58.07 and –58.12 ppm. They are in agreement with the ^{31}P NMR chemical shift of $HN(CH_2CH_2PHPh)_2$ at δ –59.7.[13] The appearance of two signals in the $^{31}P\{^1H\}$

NMR spectrum is interpreted in terms of compound **1** existing as two diastereomers (RR/SS) and (RS/SR). The upfield shift of compound **2** in its $^{31}P\{^{1}H\}$ NMR spectrum in comparison with compound **1** can be traced back to the relative bulky mesityl substituents.

In a ^{1}H NMR spectrum of **1a/1b** the P-*H* protons appear as a triplet of doublet resonance (δ 4.24, $^{1}J(^{1}H, ^{31}P)$ = 208 Hz, $^{3}J(^{1}H, ^{1}H)$ = 14 Hz). The NCH_2 protons resonate as complex pattern (δ 2.46 - 2.26), while the PCH_2 protons resonate as two different complex patterns (δ 1.98 - 1.94; 1.92 - 1.60).

A ^{1}H NMR spectrum of **2a/2b/3** (obtained from case b) shows for the P-*H* protons a triplet of doublet (δ 4.30, $^{1}J(^{1}H, ^{31}P)$ = 216 Hz, $^{3}J(^{1}H, ^{1}H)$ = 7 Hz). The mesityl protons resonate at δ 6.75 (aromatic), δ 2.41 (*o*-CH_3), and δ 2.10 (*p*-CH_3) while the CH_2 protons appear as three multiplets. The N(CH_2)$_2$ protons resonate at δ 2.35 - 2.27 and the PCH_2 protons resonate as two complex patterns at δ 1.85 - 1.77 and δ 1.66 - 1.58.

4.2.2 The synthesis of the MeN(CH$_2$CH$_2$PR)$_2$Sn

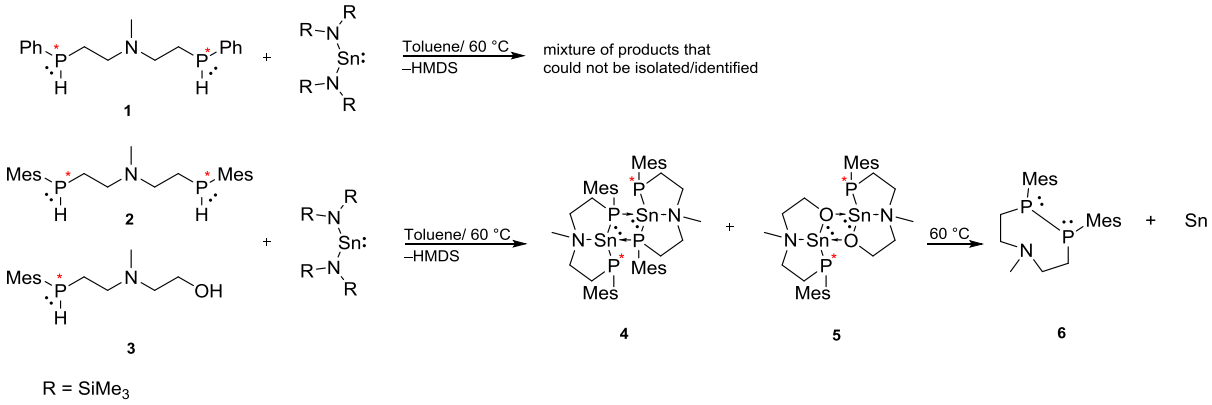

Scheme 2. The reaction of the ligands **1a/1b** and **2a/2b** respectively **2a/2b/3** with tin(II)-amide.

The reaction according to scheme 2 of compound **1** with one molar equivalent Sn[N(SiMe$_3$)]$_2$ in toluene at 60 °C gave a crude reaction mixture a $^{31}P\{^{1}H\}$ NMR spectrum of which appeared to be rather complex (Figure 3) showing resonances at δ –25.3(s), –28.1(s), –32.7(s), –34.6(br), –46.4(d), –50.0(s), from –54.0 to –55.0(m), –58(s), –88.6(t), from –77.0 to –78.0(m). Attempts at isolating a well-defined product from this mixture by crystallization failed. Removal of the solvent in vacuo gave a yellow air- and moisture-sensitive amorphous solid material that was not analysed further. From the data at hand,

we are not able to unambiguously prove the formation of $MeN(CH_2CH_2PPh)_2Sn$ (Scheme 2).

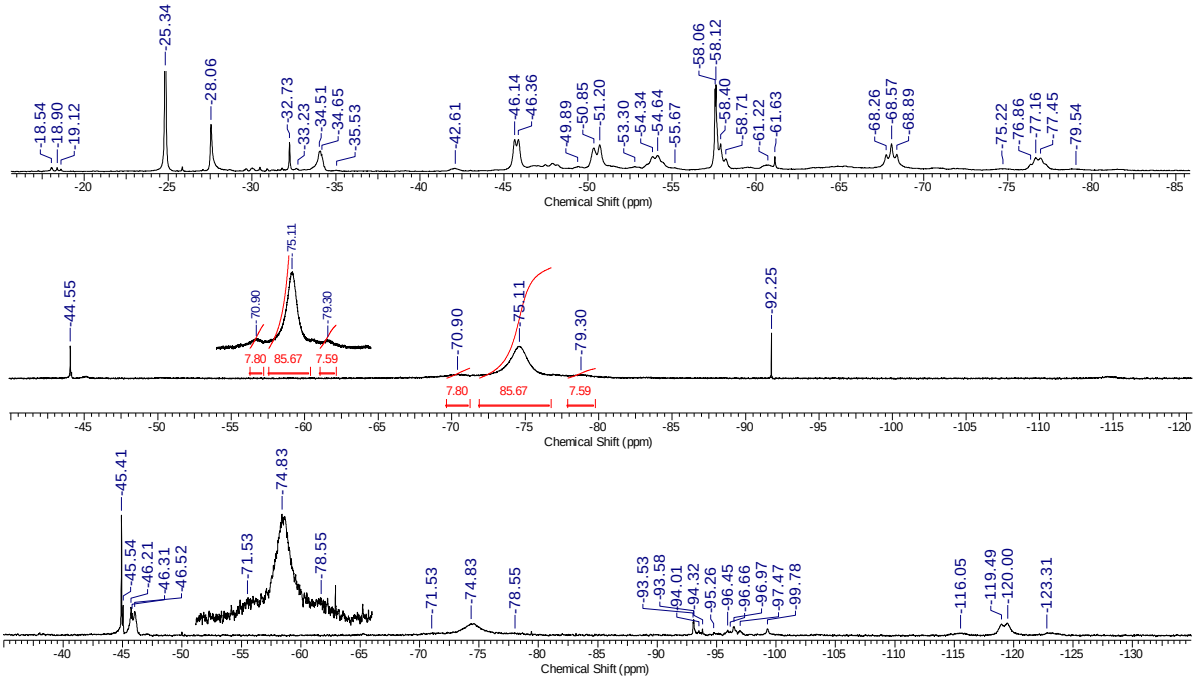

Figure 3. $^{31}P\{^1H\}$ NMR spectra of the reaction mixtures obtained from the reactions of **1a/1b** (top), **2a/2b** (middle), and **2a/2b/3** (bottom) , respectively with Sn(II)amide.

In analogy to the procedure described above, the reaction (Scheme 2) of a mixture consisting of the sterically more demanding ligands **2a/2b** with $Sn[N(SiMe_3)]_2$ gave a crude mixture a $^{31}P\{^1H\}$ NMR spectrum of which (Figure 3) is simpler than that for the product obtained from the reaction involving the sterically less crowded ligand **1**. It shows three resonances at $\delta\,^{31}P$ –75.1 ($\nu_{1/2}$ 341 Hz, **4**), $\delta\,^{31}P$ –45.4 (**6**), and $\delta\,^{31}P$ –46.2 (**6**). The same reaction using a mixture consisting of **2a**, **2b**, **3** (as obtained from case b) showed an additional resonance at $\delta\,^{31}P$ –119.7 ($\nu_{1/2}$ 180 Hz, **5**).

The NMR sample taken from the reaction involving the mixture consisting of **2a**, **2b**, **3** (as obtained from case b) was subjected to ^{31}P NMR at variable temperature (Figure 4). At –60 °C, the broad signal at δ –75.1 (br, $\nu_{1/2}$ = 341 Hz) decoalesces into two equally intense triplet resonances at δ –71.8 ($^2J(^{31}P, ^{31}P)$ = 46 Hz) and δ –78.4 ($^2J(^{31}P, ^{31}P)$ = 46 Hz), both showing unresolved and partially overlapped $^1J(^{31}P, ^{117/119}Sn)$ satellites. At –80 °C the signals shift slightly, become broader, and the triplet splitting is lost. However, the $^{117/119}Sn$ satellites become better visible.

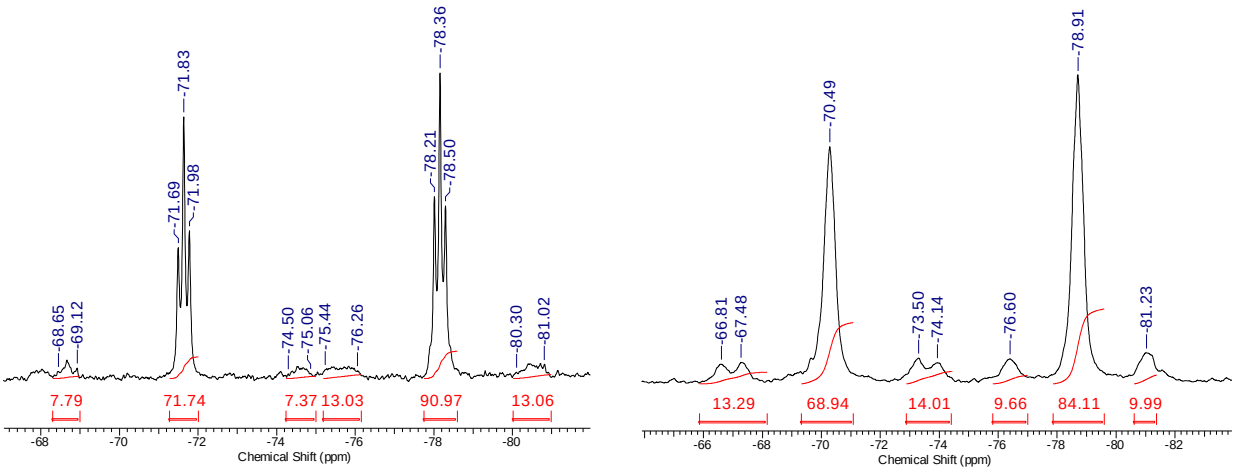

Figure 4. $^{31}P\{^{1}H\}$ NMR spectra of the reaction mixture obtained from the reaction of **2a/2b/3** with Sn(II)amide at –60 °C (left) and –80 °C (right).

The resonance (a) at δ –70.5 shows two $^{1}J(^{31}P, ^{117/119}Sn)$ satellites of 960 and 1180 Hz. The resonance (b) at δ –78.9 shows one unresolved $^{1}J(^{31}P, ^{117/119}Sn)$ of 765 Hz. From the satellite-to-signal-to-satellite integral ratios it is evident, that the signals (a) and (b) belong to the bridging and non-bridging phosphorus atoms, respectively. Attempts at obtaining a reasonable ^{119}Sn NMR spectrum at low temperatures failed.

The temperature-dependent ^{31}P NMR spectra is interpreted in terms of compound **5** being involved in a monomer⇌dimer equilibrium. This equilibrium is fast at room temperature but slow at low temperature on the ^{31}P NMR time scale. The position of this equilibrium could not be established as no ^{119}Sn NMR signal was detected at low temperature. Usually, P(III) compounds are configurationally stable and do not undergo inversion at ambient temperature. However, for certain substituents the inversion barrier can be lowered considerably. Thus, IZOD has shown, that there are two kinds of inversion mechanism, vertex-inversion via trigonal planar transition state and edge inversion via T-shaped transition state (Scheme 3). In the transition state of the vertex-inversion the lone pair of the P^{III} atom locates in a perpendicular pure p-orbital to the plane of the molecule, while the HOMO of the transition state in the edge inversion consists of pure s-orbital and the LUMO is a p-orbital. The pnictines with electronegative σ-withdrawing ligands (F^-) or has a lone pair prefer t-shaped inversion because it can stabilize the empty p-orbital through π-donation and on the other hand the pnictines with electropositive ligands (H^+) prefer vertex-inversion.[16]

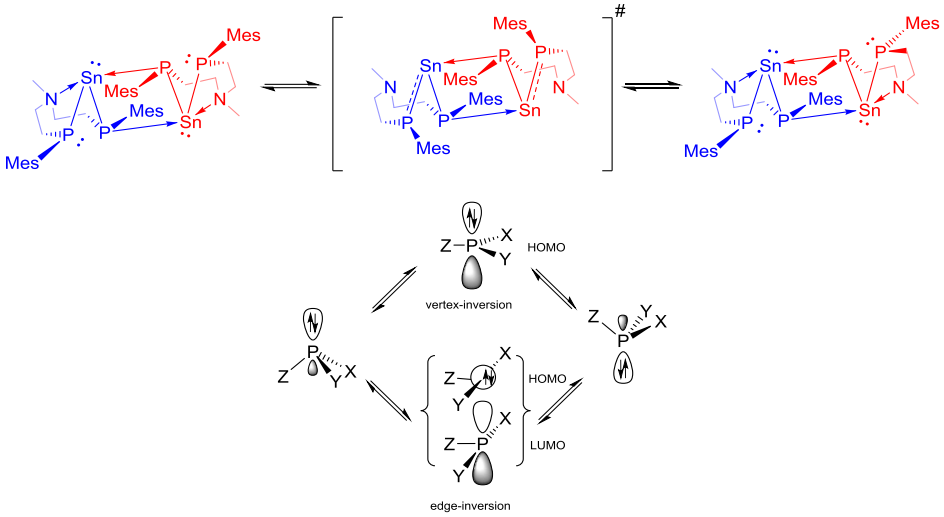

Scheme 3. The inversion of the phosphorus atom.

Attempts to crystallize one or two of the diastereomers of **5** from the reaction mixture failed.

4.2.3 The reactivity of $MeN(CH_2CH_2PR)_2Sn$ toward $W(CO)_5$.thf

The reaction of the product mixture obtained from the reaction with Sn[N(SiMe$_3$)2]2 involving **2a**/**2b**/**3** gave a crude reaction mixture a ^{31}P NMR spectrum of which showed nine signals in the range between –45.3 and –99.2 ppm. Most important are the resonances at δ –53.6 (^1J(^{31}P , $^{117/119}$Sn = 770/803 Hz, integral 1), δ –55.5 (^1J(^{31}P , $^{117/119}$Sn = 998/1042 Hz, integral 2), and δ –59.3 (^1J(^{31}P , $^{117/119}$Sn = 865/903 Hz, integral 2) (Figure 6). The two latter signals are assigned with caution to the complex $[MeN\{CH_2CH_2(Mes)P\}_2SnW(CO)_5]_2$ (**7**) which, despite many attempts, could not be isolated from the reaction mixture. The first signal is assigned to compound **8** (Scheme 5). This assignment gets strong support from the fact that a few crystals of **8** suitable for X-ray diffraction analysis could be isolated.

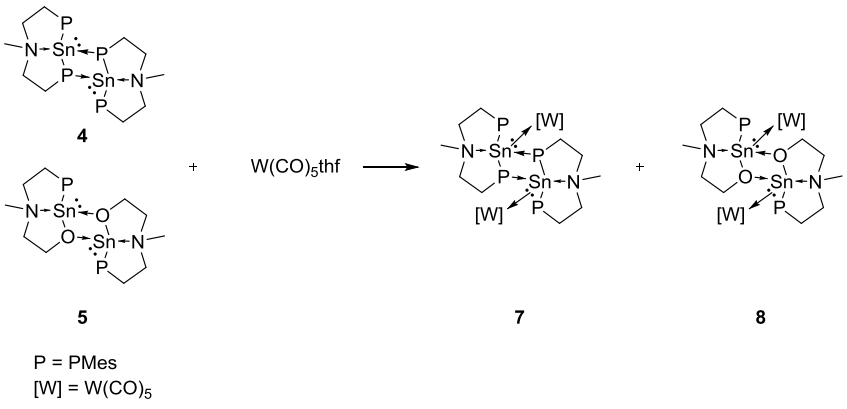

Scheme 4. The reaction of a mixture of **4** and **5** with $W(CO)_5$thf complex.

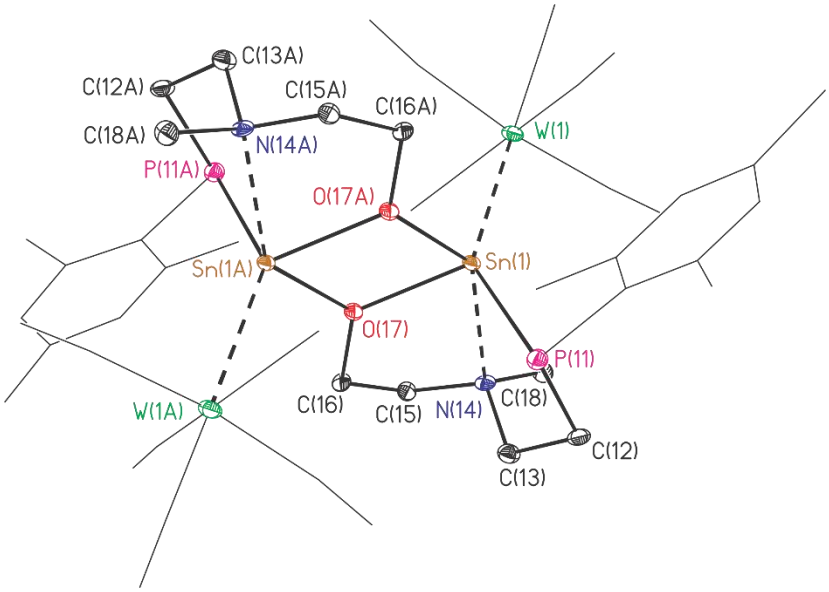

Figure 5: Ellipsoid plot and numbering scheme of the molecular structure of **8.** The hydrogen atoms were omitted for clarity; ellipsoids are set at 30 % probability. Selected bond lengths [Å] and angles [°]: W(1)–Sn(1) 2.7886(7), Sn(1)–P(11) 2.511(2), Sn(1)–N(14) 2.436(7), Sn(1)–O(17A) 2.235(6), Sn(1)–O(17) 2.107(6), W(2)–Sn(2) 2.7883(7), Sn(2)–P(31) 2.512(2), Sn(2)–N(34) 2.432(7), Sn(2)–O(37) 2.097(6), Sn(2)–O(37A) 2.240(7), O(37)–Sn(2A) 2.240(7), P(11)–Sn(1)–W(1) 139.09(6), N(14)–Sn(1)–W(1) 109.44(17), N(14)–Sn(1)–P(11) 80.67(18), O(17)–Sn(1)–W(1) 119.67(17), O(17A)–Sn(1)–W(1) 105.53(15), O(17)–Sn(1)–P(11) 101.24(18), O(17A)–Sn(1)–P(11) 86.83(17), O(17)–Sn(1)–N(14) 74.5(2), O(17A)–Sn(1)–N(14) 139.0(2), O(17)–Sn(1)–O(17A) 169.9(3), P(11)–Sn(2)–W(2) 140.32(6), N(14)–Sn(2)–W(2) 109.11(17), N(14)–Sn(2)–P(11) 80.63(18), O(17A)–Sn(2)–W(2) 105.52(16), O(17)–Sn(2)–W(2) 120.84(18), O(17A)–Sn(2)–P(11) 86.27(17), O(17)–Sn(2)–P(11) 98.83(18), O(17)–Sn(2)–N(14) 74.3(2), O(17A)–Sn(2)–N(14) 139.3(2), O(17)–Sn(2)–O(17A) 90.1(3) and O(2)–C(2)–W(1) 176.7(10).

A suitable single crystal for X-ray analysis of compound 8 crystallizes from toluene in the triclinic crystal system with $P\bar{1}$ space group and two molecules in the unit cell. Figure 4 shows the molecular structure. Selected interatomic distances and angles are given in the figure caption. The Sn(1) atom is five-coordinate by W(1), N(14), O(17), O(17A), P(11) and has a distorted trigonal bipyramidal environment The W(1)–Sn(1) distance of 2.7886(7) is longer than that of the compound reported by Jurkschat with a bond length of 2.737(3) Å.[17] The Sn(1)–P(11) distance of 2.511(2) is shorter than that of the compound reported by IZOD with bond distance of 2.6157(8) Å. [16] The intramolecular Sn(1)–N(14) interaction at a distance of 2.436(7) is longer than that of the compound reported by IZOD with bond distance of 2.422(3) Å.[16] The Sn(1)–O(17) distance of 2.107(6) Å is as expected and comparable with. The W(1) centre shows an octahedral environment coordinated with five carbon monoxide ligands. The dimeric

structure has Sn···O four membered-ring. The average of Sn–O bond distance is 2.171(6)Å.

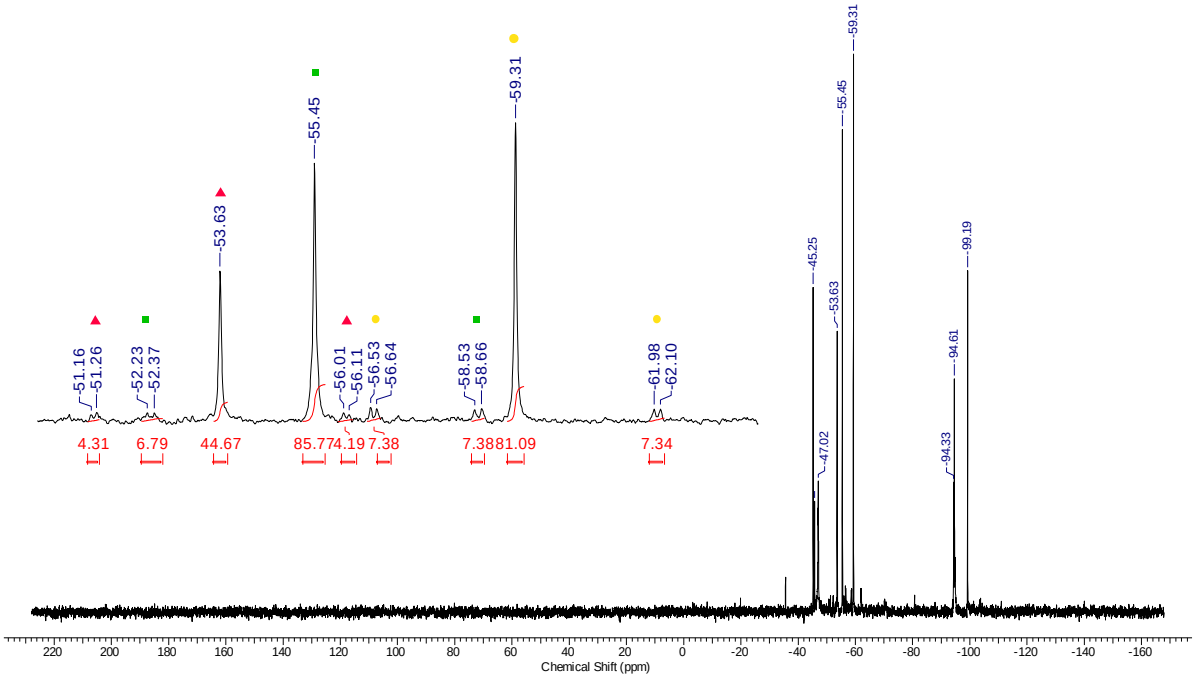

Figure 6. A $^{31}P\{^{1}H\}$ NMR spectra of the reaction mixture obtained according to scheme **4**.

4.2.4 The reactivity of MeN(CH2CH2PR)2Sn toward dihalomethanes

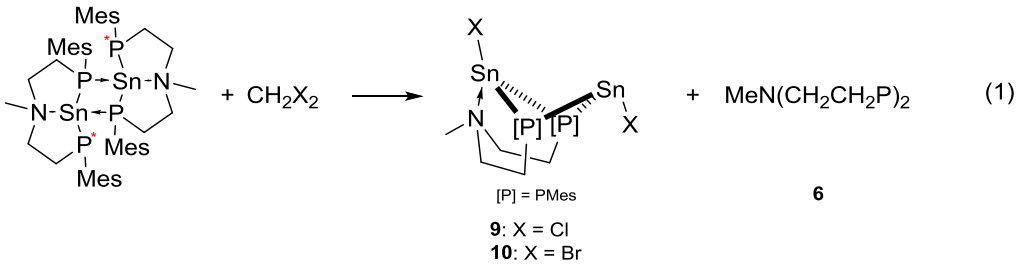

Compound **4** reacts with excess amount of methylene chloride, CH_2Cl_2, and methylene bromide, CH_2Br_2 to give the tin(II) compounds **9,** and **10**, respectively (Equation 1), and the 1,2,-Dimesityl-5-methyl-1,2-diphospha-5-aza-cycloheptan **6.** Compounds **9,** and **10**, are dark yellow crystalline materials. They are soluble in toluene, THF and acetonitrile. Exemplarily, a $^{31}P\{^{1}H\}$ NMR spectrum of the mixture involving the reaction with CH_2Cl_2 shows two equally intense signals at δ –45.7 (**6**) and δ –98.1 ^{1}J (^{31}P , $^{117/119}Sn$) = 1389/1454 Hz, ^{1}J (^{31}P , $^{117/119}Sn$) = 1360/1425 Hz, **10**). A ^{119}Sn NMR spectrum of the same sample shows two triplet resonances at δ 161 (^{1}J (^{119}Sn , ^{31}P) = 1454 Hz, ^{2}J (^{119}Sn , ^{119}Sn) = 288 Hz, Sn1 of **10**) and 48 (^{1}J (^{119}Sn , ^{31}P) = 1425 Hz, ^{2}J (^{119}Sn , ^{119}Sn) = 288 Hz, Sn2 of **10**).

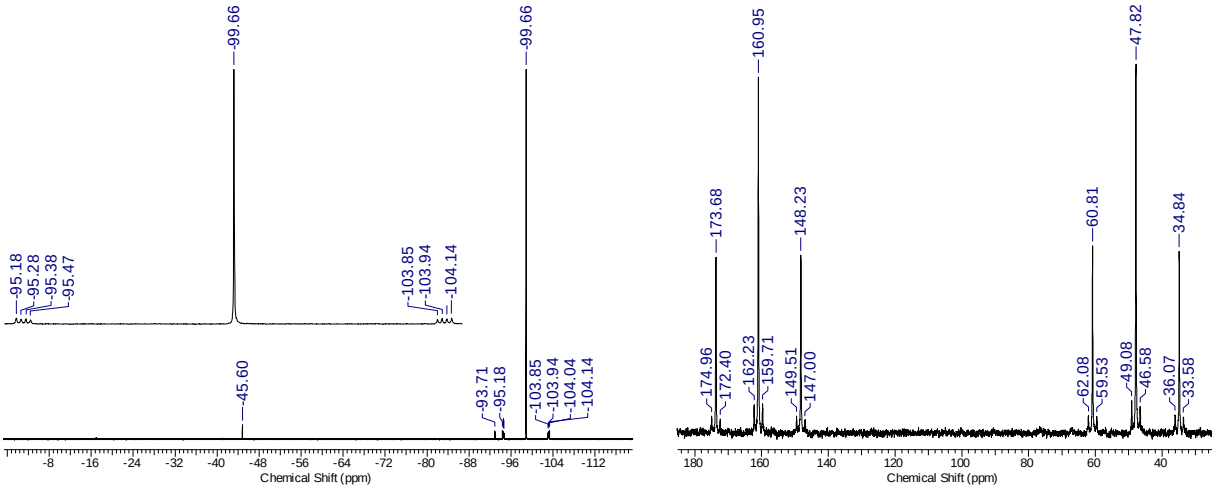

Figure 7. $^{31}P\{^{1}H\}$ NMR (left) and $^{119}Sn\{^{1}H\}$ NMR spectra (right) of compound **9.**

Both the ^{31}P and ^{119}Sn NMR data reveal compound **9** to adopt a similar structure in solution as it was found for the solid state (see below). Apparently, the intramolecular N→Sn coordination is kinetically inert on the NMR time scales. The $^{31}P\{^{1}H\}$ NMR resonance of compound **9** is shifted downfield as compared to **H** (δ –122.4,^{1}J (^{31}P , $^{117/119}Sn$) = 1037 Hz) and shifted upfield as compared to compound **F** and **B**, whit δ –41.1 and –61.2, respectively. In comparison between compounds **9, F** and **B,** compound **F** shows a ^{119}Sn NMR resonance at δ 257 (^{1}J (^{119}Sn, ^{31}P) = 1070 Hz) while **B** shows a resonance at δ 507 (^{1}J (^{119}Sn, ^{31}P) = 1432 Hz).

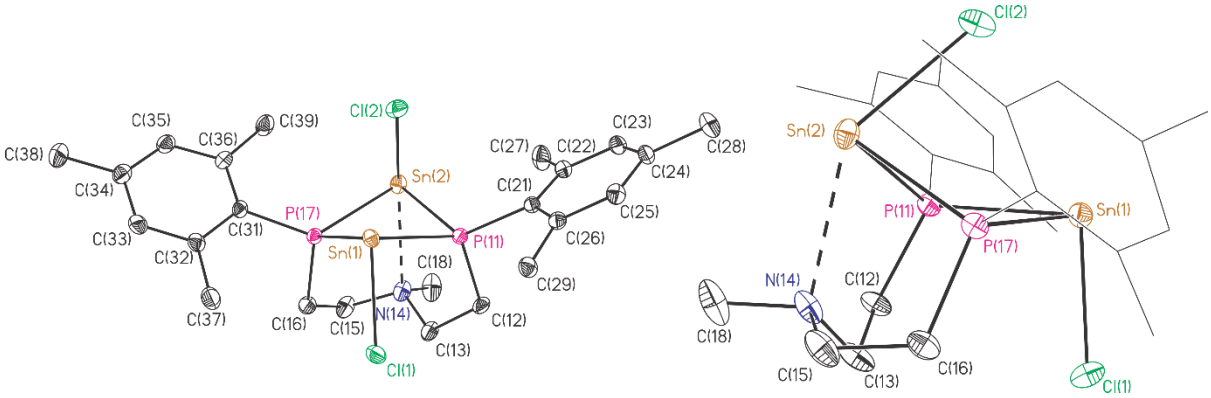

Figure 8: Ellipsoid plot and numbering scheme of the molecular structure of **10.** The hydrogen atoms were omitted for clarity; ellipsoids are set at 30 % probability. Selected bond lengths [Å] and angles [°]: Sn(1)–Cl(1) 2.5159(10), Sn(1)–P(11) 2.6546(9), Sn(1)–P(17) 2.6545(9), Sn(1)–N(14) 4.412(3), Sn(2)–P(11) 2.6273(9), Sn(2)–P(17) 2.6515(10), Sn(2)–Cl(2) 2.6579(11), Sn(2)–N(14) 2.662(3), Cl(1)–Sn(1)–P(11) 91.77(3), Cl(1)–Sn(1)–P(17) 95.66(3), P(11)–Sn(1)–P(17) 79.74(3), Cl(1)–Sn(1)–N(14) 76.43(5), P(11)–Sn(1)–N(14) 43.06(5), P(17)–Sn(1)–N(14) 43.47(4), P(11)–Sn(2)–P(17) 80.29(3), P(11)–Sn(2)–Cl(2) 75.70(3), P(17)–Sn(2)–Cl(2) 84.21(3), P(11)–Sn(2)–N(14) 70.85(7), P(17)–Sn(2)–N(14) 70.98(8), Cl(2)–Sn(2)–N(14) 140.96(8), C(12)–P(11)–Sn(2) 107.25(12), C(21)–P(11)–Sn(2) 121.64(12), C(12)–P(11)–Sn(1) 116.92(14), C(21)–P(11)–Sn(1) 114.93(12) and Sn(2)–P(11)–Sn(1) 93.45(3).

Compound **9** crystallizes from dichloromethane in the hexagonal crystal system with $P6_1$ space group and six molecules in the unit cell. Figure 5 shows its molecular structure and selected interatomic distances and angles are given in the figure caption. The Sn(1) atom is coordinated by Cl(1), P(11), and P(17) and shows a distorted pseudo-tetrahedron, taking the lone electron pair at the tin atom into account. The Sn(2) atom is coordinated by Cl(2), P(11), P(17), and N(14) and shows a pseudo-trigonal-bipyramidal envioronment, when the lone electron pair is considered. The Sn(2)–N(14) distance of 2.662(3) Å is relatively long. Nevertheless, as discussed above, this interaction is kinetically inert on the NMR time scales. As a result of the intramolecular N→Sn(2) interaction, the Sn(2)–Cl(2) distance of 2.6588(11) Å is longer than the Sn(1)–Cl(1) distance of 2.5162(16) Å. The Sn–P distances fall in the narrow range between 2.6544(9) (Sn(2)–P(17)) and 2.6272(10) Å (Sn(1)–P(11)). The Sn(1)–Sn(2) and P(11)–P(17) distances are 3.846(7) and 3.403(5) Å, respectively. The former distance is considerably shorter than twice the van der Waals radius of a tin atom (4.40 Å). DFT calculations have not been performed yet. Such calculations are under way and will help sheding light on the nature of this interaction.

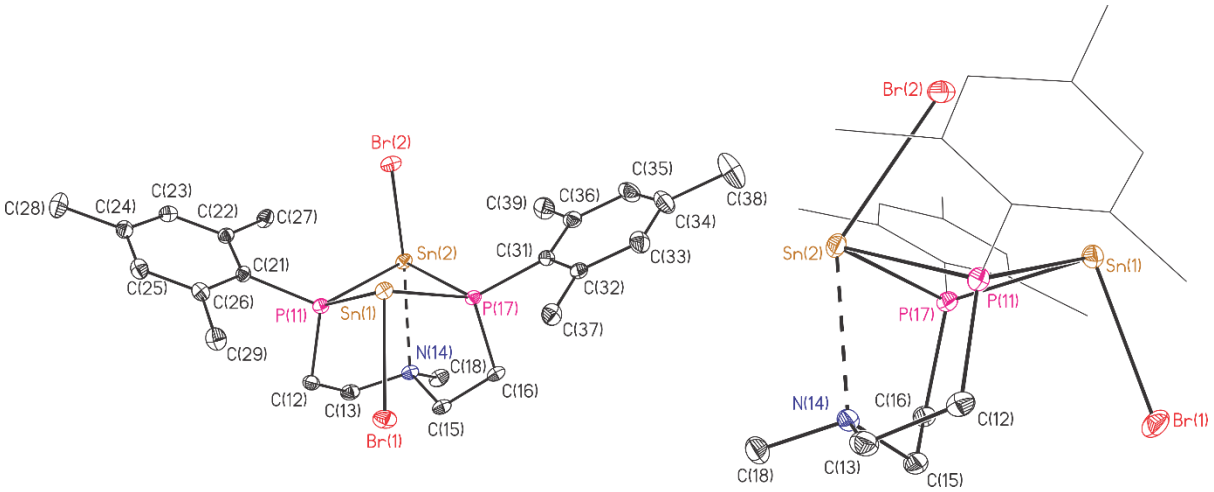

Figure 9. Ellipsoid plot and numbering scheme of the molecular structure of **10.** The hydrogen atoms were omitted for clarity; ellipsoids are set at 30 % probability. Selected bond lengths [Å] and angles [°]: Sn(1)–Br(1) 2.6756(4), Sn(1)–P(11) 2.6741(7), Sn(1)–P(17) 2.6654(8), Sn(2)–Br(2) 2.8434(4), Sn(2)–P(11) 2.6185(8), Sn(2)–P(17) 2.6094(8), Sn(2)–N(14) 2.589(2), P(11)–Sn(1)–Br(1) 92.901(18), P(17)–Sn(1)–Br(1) 94.542(19), P(17)–Sn(1)–P(11) 78.72(2), P(11)–Sn(2)–Br(2) 79.793(19), P(17)–Sn(2)–Br(2) 78.217(19), P(17)–Sn(2)–P(11) 80.75(2), N(14)–Sn(2)–Br(2) 142.18(5), N(14)–Sn(2)–P(11) 72.16(6), N(14)–Sn(2)–P(17) 72.74(5), Sn(2)–P(11)–Sn(1) 94.06(2), C(12)–P(11)–Sn(1) 117.64(10), C(12)–P(11)–Sn(2) 105.32(10), C(12)–P(11)–C(21) 104.98(11), C(21)–P(11)–Sn(1) 112.45(7), C(21)–P(11)–Sn(2) 122.91(6), Sn(2)–P(17)–Sn(1) 94.47(2), C(16)–P(17)–Sn(1) 117.01(10), C(16)–P(17)–Sn(2) 104.39(10), C(31)–P(17)–Sn(1) 114.09(7) and C(31)–P(17)–Sn(2) 122.52(7).

The bromine-substituted compound **10** crystallizes from dichloromethane in monoclinic crystal system with $P2_1/C$ space group and four molecules in the unit cell (Figure 6). Figure 6 shows its molecular structure and selected interatomic distances and angles are given in the figure caption. The overall molecular structure of **10** strongly resembles that of **9**. The The Sn(2)–N(14) distance of 2.589(2) Å is shorter than the corresponding distance in compound **9**. This at first sight unexpected observation might be explaned by a highe ionic character of the Sn–Cl as compared to the Sn–Br bond which in turn causes a stronger Sn–Cl bond and weakens the Sn–N bond. The Sn(1)–Br(1) and Sn(2)–Br(2) distances are 2.6756(4) and 2.8434(4) Å, respectively. The Sn–P distances fall in the range between 2.6742(8) (Sn(1)–P(11) Å) and 2.6093(8) Å (Sn(2)–P(17)) which is slightly bigger than observed for **9**. The Sn(1)–Sn(2) (3.873(3) Å) and P(11)–P(17) (3.386(4) Å) distances are rather similar as compared to those of compound **9**.

4.2.5 A Comparsion between 1, 2 and B

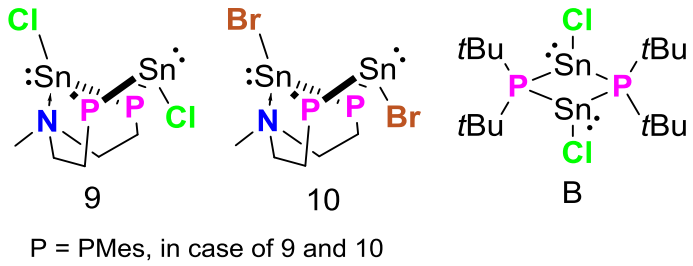

Figure 10. Compounds **9**, **10** and **B**.

Table 3 contains selected interatomic distances and angles of **9**, **10,** and **B** (Figure 10). The Sn–P distances for **B** are within the limits given for compounds **10** and **11**, as discussed in 4.2.4. The same holds for the Sn(1)–Cl(1) and Sn(2)–Cl(2) distances of **B** the P–Sn–P angels vary between 72.73(9) and 96.22(9) °. While the N(14)–Sn(2)–X is bigger in case of **12**; 142.18(5)° than **11**; 140.96(8)°.

Table 1. Comparsion between **10**, **11** and **B**.

	9 (X = Cl)	**10** (X = Br)	**B** (X = Cl)
Sn(1)–X(1)	2.516(1)	2.6756(4)	2.583(3)
Sn(2)–X(2)	2.658(1)	2.8434(4)	2.565(4)
Sn(1)–P(11)	2.6546(9)	2.6741(7)	2.630(3)
Sn(1)–P(17)	2.6545(9)	2.6654(8)	2.620(3)
Sn(2)–P(11)	2.6273(9)	2.6185(8)	2.617(3)

Sn(2)–P(17)	2.651(1)	2.6094(8)	2.614(3)
Sn(2)–N(14)	2.662(3)	2.589(2)	-
X(1)–Sn(1)–P(11)	91.77(3)	92.90(2)	88.59(8)
X(1)–Sn(1)–P(17)	95.66(3)	94.54(2)	88.45(9)
P(11)–Sn(1)–P(17)	79.74(3)	78.72(2)	72.73(9)
P(11)–Sn(2)–P(17)	80.29(3)	80.75(2)	73.06(9)
Sn(2)–P(11)–Sn(1)	93.45(3)	94.06(2)	95.90(9)
Sn(2)–P(17)–Sn(1)	92.90(3)	94.47(2)	96.22(9)
X(2)–Sn(2)–N(14)	140.96(8)	142.18(5)	-

4.2.6 The reactivity of $MeN(CH_2CH_2PR)_2Sn$ toward PhSSPh

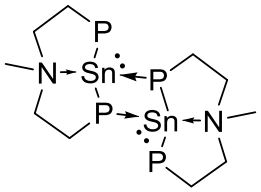

4

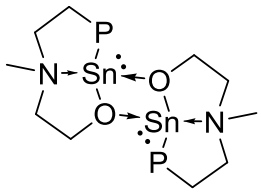

5

+ PhSSPh ⟶ $[Sn(SPh)_2]_2$ + **6** + not identified products

11

Scheme 6. The reaction of a mixture consisting of **4** and **5** with PhSSPh.

The reaction of a mixture consisting of compounds **4** and **5** with PhSSPh in toluene at room temperature gave tin(II) bis(thiophenolate, $[Sn(SPh)_2]_2$, **11**, and 1,2-dimesityl-5-methyl-1,2-diphospha-5-azacycloheptan, **6** (δ = –42.6) (Scheme 6), and not the expected tin(IV) oxidation product $MeN[CH_2CH_2P(Mes)]_2Sn(SPh)_2$. Apparently, a redox reaction took place in which the phosphorus atoms are oxidized from –III to –II and the sulfur atoms are reduced from –I to –II.

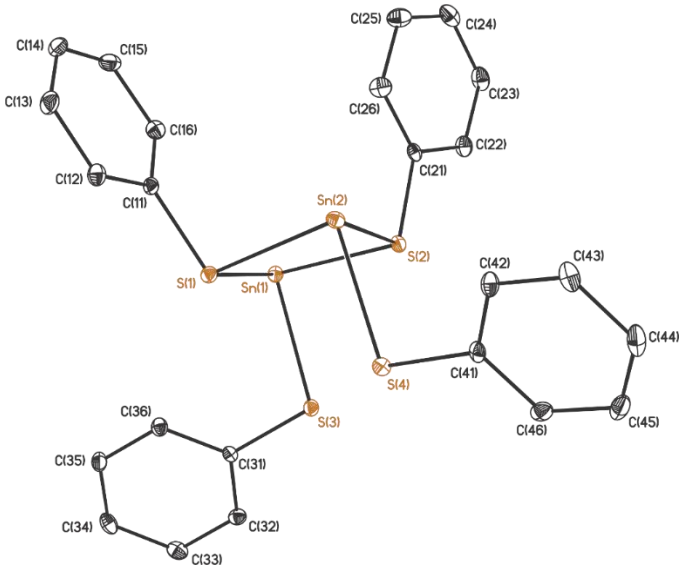

***Figure 11*:** Ellipsoid plot and numbering scheme of the molecular structure of **11.** The hydrogen atoms were omitted for clarity; ellipsoids are set at 30 % probability. Selected bond lengths [Å] and angles [°]: Sn(1)–S(1) 2.8696(6), Sn(1)–S(2) 2.5632(6), Sn(1)–S(3) 2.5416(7), S(1)–Sn(2) 2.5528(6), S(1)–C(11) 1.788(3), Sn(2)–S(2) 2.7895(6), Sn(2)–S(4) 2.5427(7), S(2)–C(21) 1.784(3), S(3)–C(31) 1.782(2), S(4)–C(41) 1.789(2), S(2)–Sn(1)–S(1) 83.116(18), S(3)–Sn(1)–S(1) 84.858(18), S(3)–Sn(1)–S(2) 83.33(2), Sn(2)–S(1)–Sn(1) 94.520(18), C(11)–S(1)–Sn(1) 107.20(8), C(11)–S(1)–Sn(2) 96.59(8), S(1)–Sn(2)–S(2) 84.938(18), S(4)–Sn(2)–S(1) 89.41(2), S(4)–Sn(2)–S(2) 85.786(19), Sn(1)–S(2)–Sn(2) 96.243(19), C(21)–S(2)–Sn(1) 100.69(8), C(21)–S(2)–Sn(2) 104.72(8), C(31)–S(3)–Sn(1) 101.43(9) and C(41)–S(4)–Sn(2) 101.26(9).

Compound **11** crystallizes from toluene at room temperature in the monoclinic crystal system with *P* 1 2_1/n 1 space group and four molecules in the unit cell (Figure 11). Figure 11 shows its molecular structure and selected interatomic distances and angles are given in the figure caption. The molecular structure reveals that the tin and the sulfur atoms have a trigonal pyramidal environment. The average S–C distance is 1.783(3) and the Sn–S distances vary between 2.8696(6) (Sn(1)–S(1)) and 2.5416(7) Å (Sn(1)–S(3)) .

4.3 Amino alcohol derivatives of silicon and lithium

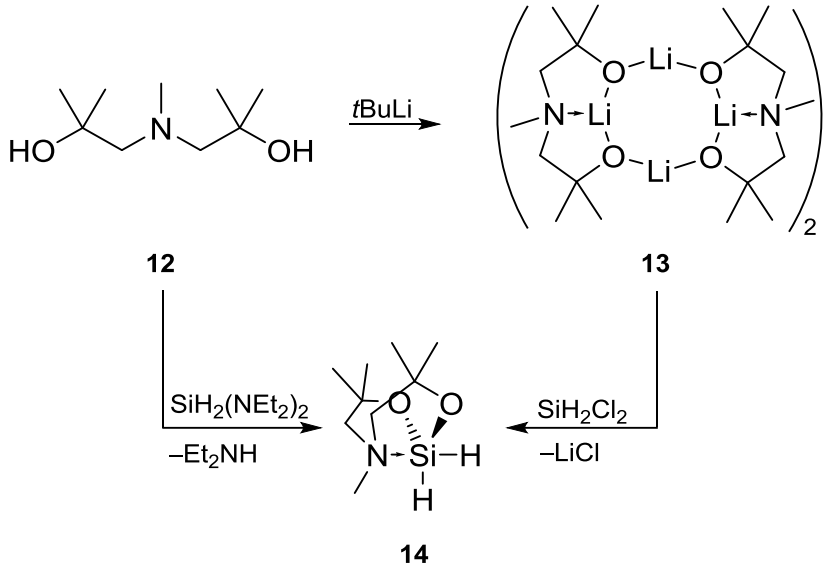

Scheme 7. The reactions of the amino alcohol **1** with *t*BuLi and $SiH_2(NEt_2)_2$, respectevily.

The N-methyl-bis(2-hydroxy-2-methylpropyl)amine (**12**) was deprotonated with *t*BuLi at –60 °C in hexane. After stirring the solution at room temperature for 1h, its volume was concentrated to about 10% giving a precipitate. The latter was isolated by filtration as a white solid. The product is soluble in common organic solvents and reacts with water to give the starting material and lithium hydroxide. ^{1}H, $^{13}C\{^{1}H\}$, and $^{7}Li\{^{1}H\}$ NMR spectra show each broad signals. A ^{1}H NMR spectrum shows resonances at δ 2.49(4H), 2.39(3H), 1.32(m) and 1.21(m). A $^{7}Li\{^{1}H\}$ NMR spectrum displayed three signals at δ 2.2, 1.4 and 0.9.

Compound **13** crystalizes from hexane at room temperature in the triclinic $P\bar{1}$ space group with two molecules per unit cell. Figure 12 shows its molecular structure and selected interatomic distances and angles are given in the figure caption. The molecular structure shows two eight membered rings stacked on each other and define a 16 vertex Li_8O_8 polyhedral cage (Figure 8). The oxygen atoms belong to the corresponding amino alcohol, in which each nitrogen atom coordinates at one lithium center with bond lengths N(14)–Li(4) 2.070(3), N(34)–Li(2) 2.094(3), N(54)–Li(7) 2.046(12) and N(74)–Li(5) 2.103(3) Å. The longest Li–O distance is 1.943(3) and the shortest is 1.847(2) Å for O(77)–Li(5) and O(11)–Li(1), respectively. Four lithium centres are fourfold coordinated by one nitrogen and three oxygen atoms in a distorted

tetrahedral geometry. The other four lithium centres are three-coordinated by three oxygen atoms giving a sort of T-shaped geometry.

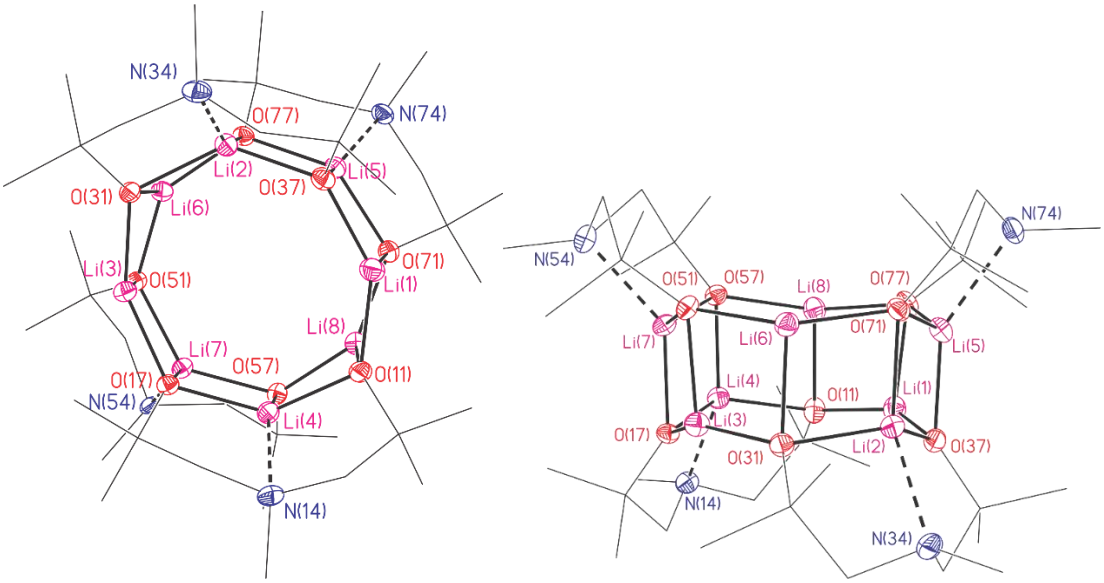

Figure 12. Ellipsoid plot and numbering scheme of the molecular structure of **15.** The hydrogen atoms were omitted for clarity; ellipsoids are set at 30 % probability. Selected bond lengths [Å] and angles [°]: O(11)–Li(1) 1.847(3), O(11)–Li(4) 1.923(3), O(11)–Li(8) 1.943(3), O(17)–Li(3) 1.881(2), O(17)–Li(4) 1.923(3), O(17)–Li(7) 1.912(2), O(31)–Li(2) 1.933(3), O(31)–Li(3) 1.847(2), O(31)–Li(6) 1.936(2), O(37)–Li(1) 1.895(3), O(37)–Li(2) 1.922(3), O(37)–Li(5) 1.918(3), O(51)–Li(3) 1.950(2), O(51)–Li(6) 1.856(2), O(51)–Li(7) 1.909(2), O(57)–Li(4) 1.906(2), O(57)–Li(7) 1.914(2), O(57)–Li(8) 1.878(3), O(71)–Li(1) 1.937(3), O(71)–Li(5) 1.922(3), O(71)–Li(8) 1.856(3), O(77)–Li(2) 1.920(2), O(77)–Li(5) 1.914(3), O(77)–Li(6) 1.871(2), N(14)–Li(4) 2.070(3), N(34)–Li(2) 2.094(3), N(54)–Li(7) 2.046(12), N(74)–Li(5) 2.103(3), Li(1)–O(11)–Li(4) 121.13(12), Li(1)–O(11)–Li(8) 80.55(12), Li(4)–O(11)–Li(8) 78.08(10), Li(3)–O(17)–Li(4) 128.60(11), Li(3)–O(17)–Li(7) 79.34(10), Li(7)–O(17)–Li(4) 76.85(10), Li(2)–O(31)–Li(6) 78.55(10), Li(3)–O(31)–Li(2) 119.76(11), Li(3)–O(31)–Li(6) 80.48(10), Li(1)–O(37)–Li(2) 129.29(11), Li(1)–O(37)–Li(5) 79.92(11), Li(5)–O(37)–Li(2) 78.24(10), Li(6)–O(51)–Li(3) 79.91(10), Li(6)–O(51)–Li(7) 129.07(11), Li(7)–O(51)–Li(3) 77.74(10), Li(4)–O(57)–Li(7) 77.23(10), Li(8)–O(57)–Li(4) 80.11(11), Li(8)–O(57)–Li(7) 123.83(11), Li(5)–O(71)–Li(1) 78.79(11), Li(8)–O(71)–Li(1) 80.51(11), Li(8)–O(71)–Li(5) 127.02(12), Li(5)–O(77)–Li(2) 78.38(11), Li(6)–O(77)–Li(2) 80.48(10) and Li(6)–O(77)–Li(5) 124.94(11).

The synthesis of compound **14** was achieved via two paths (Scheme 7) In path A, compound **12** was reacted with bis(diethylamino)silane in toluene at room temperature according to an acid base reaction. The reaction is exothermic and a gas is developed. In the $^{29}Si\{^{1}H\}$NMR spectrum of the crude reaction mixture, three signals are observed at δ –63.8, –76.9 and –79. In the second path, SiH_2Cl_2 was used as an electrophile and added

to the *in situ* generated compound **12** to give $CH_3N(CH_2CMe_2)_2SiH_2$ **14.** In a $^{29}Si\{^1H\}$ NMR of the reaction mixture appears a singlet at δ –64.2. After the filtration of LiCl and removal of the solvent, the crude product was distilled under reduced pressure (62 °C, 1 mbar) to obtain the product as a colourless oil.

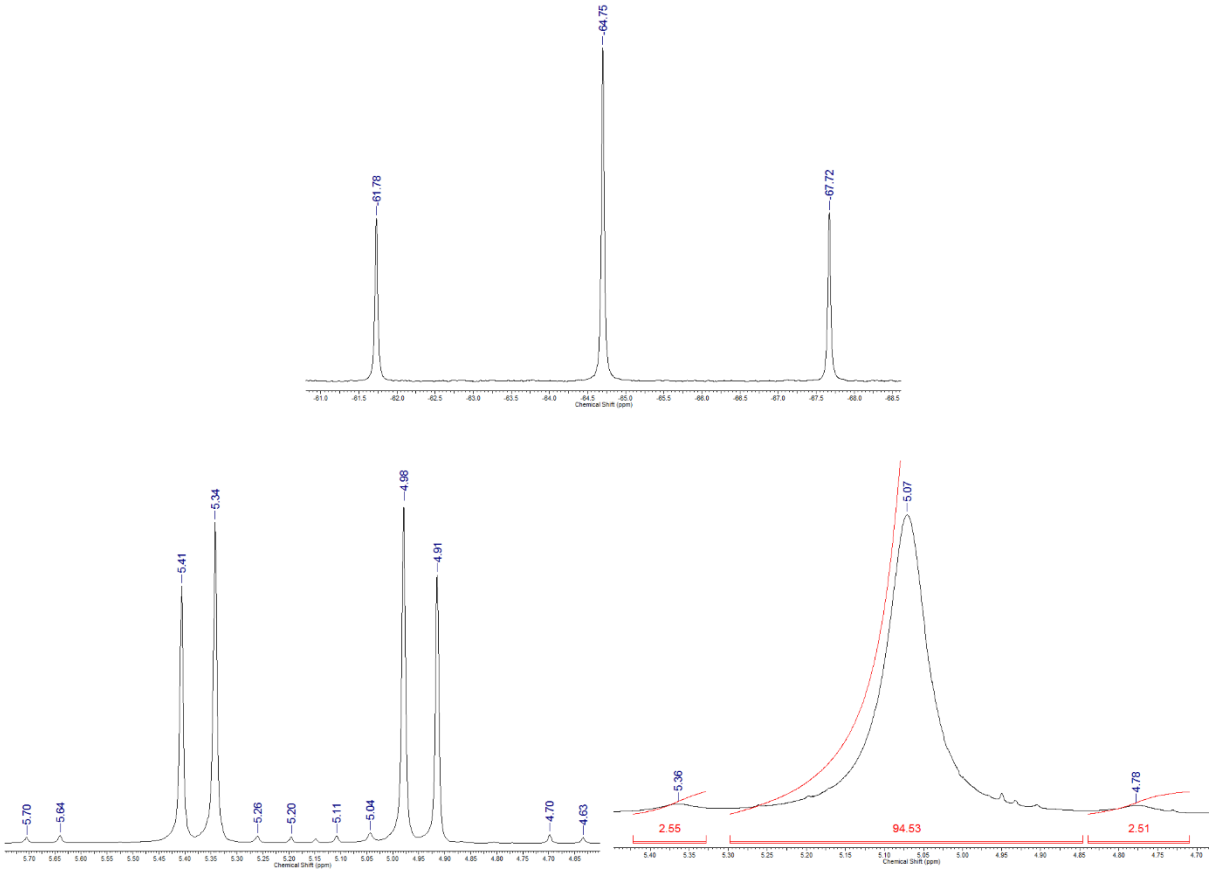

Figure 13. ^{29}Si NMR (top), and ^1H NMR spectra at –80 °C (bottom left), and 25 °C (bottom right) of **16**.

It dissolves in common solvents and hydrolysis in case of contact with water to give the free ligand and not identified product. In a ^1H NMR the SiH_2, N(CH_2)$_2$, CH_3N and C(CH_3)$_2$ resonate at δ 5.08 (^1J(^{1}H , ^{29}Si) = 239 Hz, 5%) (Figure 13, right) 2.23 (4H), 2.15 (3H) and 1.12 (12H), respectively, while in the ^1H NMR at –80 °C the SiH_2 appears as two doublets with ^{29}Si satellites, δ 5.45 (d, ^2J(^{1}H , ^{1}H) = 26 Hz, ^1J(^{1}H , ^{29}Si) = 240 Hz) and 5.35 (d, ^2J(^{1}H , ^{1}H) = 26 Hz, ^1J(^{1}H , ^{29}Si) = 226 Hz) (Figure 13, left). A IR spectrum shows $\bar{\nu}_{SiH}$ at 2126 and 2090 cm^{-1}. A $^{29}Si\{^1H\}$ NMR spectrum reveals a singlet resonance at δ = –64.8 while a ^{29}Si NMR spectrum shows a triplet resonance (δ = –64.8 (t, ^1J (^{29}Si , ^{1}H) = 239 Hz) (Figure 13, top).

The temperature-dependent ^{1}H NMR spectra is interpreted in terms of compound **14** has a labile N→Si interaction and it is in an equilibrium involving N→Si and non-coordinated species (Scheme 8). This equilibrium is fast at room temperature but slow at low temperature on the ^{1}H NMR time scale.

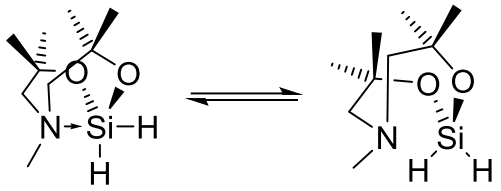

Scheme 8. The suggested equilibrium between coordinated and the non-coordinated species of compound **14**.

Compound **16** crystalizes in the monoclinic C*m* space group with two molecules per unit cell (Figure 10). The Si atom is pentacoordinated and has a distorted trigonal bipyramidal environment with (1A), O(11) and O(11A) occupying the equatorial and H(1B) and N(14) occupy the axial positions. The intramolecular N(14)–Si(1) distance is 2.3551(19) Å. The O(11)–Si(1) distance of 1.6585(12) Å is as expected. The Si(1)–H(1A) (1.38(4) Å) and Si(1)–H(1B) (1.46(4) Å) distances are, within the experimental errors, almost equal. The two $SiONC_2$ five-membered rings show chair-chair conformation.[18] A hydrogen atom H(1B) is pointed along the N(14)→Si(1) axis (axial) the N(14)–Si(1)–H(1B) 171.8(13)° and the other H(1A) is equatorial with N(14)–Si(1)–H(1A) 78.6(18)°.

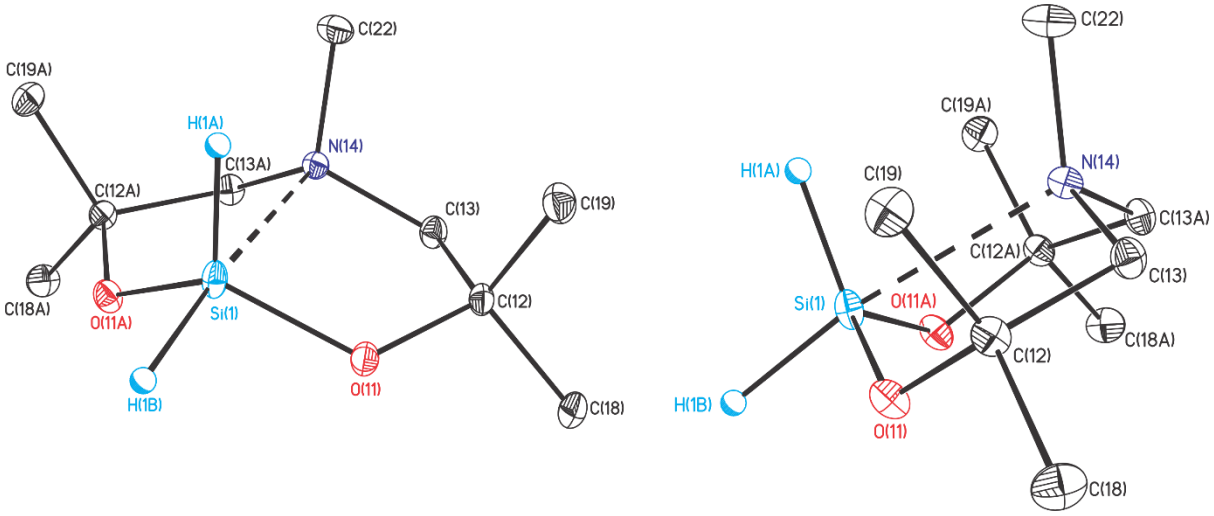

Figure 14. Ellipsoid plot and numbering scheme of the molecular structure of **14.** The hydrogen atoms were omitted for clarity; ellipsoids are set at 30 % probability. Selected bond lengths [Å] and angles [°]: Si(1)–O(11) 1.6585(12), Si(1)–N(14) 2.3551(19), Si(1)–H(1A) 1.38(4), Si(1)–H(1B) 1.46(4), O(11)–Si(1)–O(11A) 123.08(9), O(11)–Si(1)–N(14) 80.69(4), O(11)–Si(1)–H(1A)

114.0(5), O(11)–Si(1)–H(1B) 95.5(6), N(14)–Si(1)–H(1A) 78.6(18), N(14)–Si(1)–H(1B) 171.8(13) and H(1A)–Si(1)–H(1B) 110(2).

Compound **14** reacts with HCl in ether to give $MeN(CH_2CMe_2)SiHCl$, **15**, and hydrogen (Scheme 8). A $^{29}Si\{^1H\}$ NMR spectrum shows a singlet resonance at δ –79. After the solvent had been removed and washed with hexane, the product was isolated as a white solid. It is soluble in diethyl ether, THF and dichloromethane and crystalizes from THF. However, the crystals were too small to perform a X-ray diffraction analysis. A ^1H NMR spectrum displayed for the Si*H* a signal at δ 5.42 $^1J(^1H, ^{29}Si)$ = 333 Hz. A $^{29}Si\{^1H\}$ NMR spectrum shows a singlet at δ –79.9. The reaction of 16 with NHC gave a reaction mixture a ^1H NMR spectrum revealed the presence of unreacted NHC. No signal was observed in a $^{29}Si\{^1H\}$ NMR spectrum of the same sample. Apparently, no reaction had occurred.

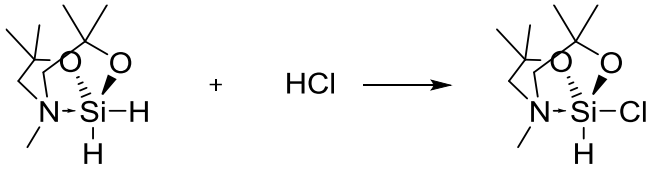

14 **15**

Scheme 8. The synthesis of compound **1** and **2** and their reactivity.

4.4 Experimental section:

All reactions were carried out under argon 4.6 atmosphere using standard Schlenk line technique, unless otherwise specified. The argon was dried by passing through a glass column filled with phosphorus pentoxide and the glassware was dried by flame under reduced pressure. All solvents were dried according to the standard procedures fresh distilled and stored over molecular sieve.[15]

The NMR spectroscopy data was measured on the spectrometers Bruker AV 400 Avance III HD NanoBay, AV 500 Avance III HD, AV 600 Avance III HD, AV 700 Avance III HD and Agilent Technologies DD2. The NMR chemical shifts (δ) are given in ppm and the coupling constants *J* in Hz. ^{1}H and $^{13}C\{^{1}H\}$ NMR were referenced at $SiMe_4$ via the chemical shift of the solvents (C_6D_6 ^{1}H 7.16, ^{13}C 128.39; CD_2Cl_2 ^{1}H 5.32, ^{13}C 54.00; $CDCl_3$ ^{1}H 7.26, ^{13}C 77.16; CD_3CN ^{1}H 1.94, ^{13}C 1.39; CD_3OD ^{1}H 3.31, ^{13}C 49.00). The reference of ^{31}P, 85% H_3PO_4; ^{119}Sn, $SnMe_4$; ^{11}B, $BF_3.OEt_2$ and ^{19}F, $CFCl_3$. The IR spectra (cm^{-1}) are measured as a solid or oil by ATR Perkin Elmer Spectrum two.

The melting point (°C) is measured Büchi M-560 using an opened capillary. The elementary analysis was measured on CHNS-932 of the firm Leco, the measurements were carried out without inert atmosphere. The electrospray-mass spectroscopy was measured by the gadget Thermoquest Finnigan Instrument, which is thermoquest-finnigan device, the mobile phase is acetonitrile or dichloromethane with flow rate 10 µL/min. The concentration is c = 0.1 mg · mL^{-1}, the source voltage is 3.8 kV, the capillary voltage is 41 V (tube lens: 140 V) and the capillary temperature is 275 °C.

$MeN(CH_2CH_2P(H)Ph)_2$ (1):

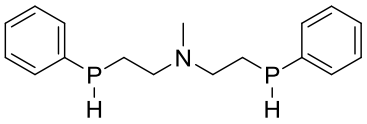

To phenylphosphane (12.5 g, 0.11 mol) in DMSO was added potassium hydroxide (26.3 g, 0.5 mol) and the mixture was stirred for 1h. Bis(2-chloroethyl)methylammonium chloride (11.0 g, 0.06 mol) in DMSO (100 mL) was added dropwise at RT and the reaction mixture stirred for 16h. Water (50 mL) was added and the layers were separated. The aqueous layer was extracted with ether (2x, 100 mL). The combined organic layers were dried over $MgSO_4$ filtered and concentrated to dryness to get (15 g, 82%).

^{1}H NMR (C_6D_6, 300.1 MHz): δ = 7.49 - 7.44 (m, 4H, Ph), 7.19 - 7.10 (m, 6H, Ph), 4.24 (dt, $^1J(^1H , ^{31}P)$= 208 Hz, $^3J(^1H , ^1H)$= 14 Hz, 2H, P*H*), 2.46 - 2.26 (m, 4H, NCH_2), 1.98 (s, 3H, NCH_3), 1.94 - 1.67(m, 4H, PCH_2). **^{13}C{^{1}H} NMR** (C_6D_6, 125.8 MHz): δ = 139.8 (d, $^2J(^{13}C , ^{31}P)$= 19.5 Hz, Ph), 133.6 (d, $^2J(^{13}C , ^{31}P)$= 15.5 Hz, Ph), 130.8 (d, $^2J(^{13}C , ^{31}P)$= 14.8 Hz, Ph), 128.4 (d, $^2J(^{13}C , ^{31}P)$= 4.6 Hz, Ph), 52.7 (s, CH_2), 47.0 (s, CH_2), 12.8 (d, $^4J(^{13}C , ^{31}P)$= 12.8 Hz, NCH_3). **^{31}P{^{1}H} NMR** (C_6D_6, 121.5 MHz): δ = –58.07 (s), –58.12 (s), ESI-MS: *calcd*. for ($L+H^+$) 304.14; *found* 304.13. Elemental analysis is not perform because of the toxicity.

$MeN(CH_2CH_2P(Mes)H)_2$ (2):

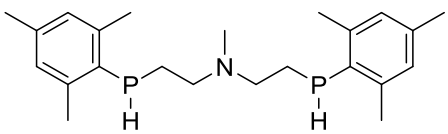

To mesitylphosphane (12.0 g, 0.08 mol) in DMSO was added potassium hydroxide (13.3 g, 0.24 mol) and the mixture was stirred for 1h. Bis(2-chloroethyl)methylammonium chloride (7.6 g, 0.04 mol) in DMSO (100 mL) was added dropwise at room temperature and the reaction mixture stirred for 16h. Water (50 mL) was added and the layers were separated. The aqueous layer was extracted with ether (2x, 100 mL). The combined organic layers were dried over $MgSO_4$ filtered and concentrated to dryness to get (12 g, 78%). **^{1}H NMR** (C_6D_6, 500.1 MHz): δ = 6.75 (s, 4H, *m*-Mes), 4.30 (td, $^1J(^1H , ^{31}P)$= 216.1 Hz, $^2J(^1H , ^{13}C)$= 6.7 Hz, 2H, PH), 2.41 (s, 12H, *o*-Me), 2.27 , 2.35 (m, 4H, NCH_2), 2.10 (s, 6H, *p*-Me), 1.92 (d, $^3J(^1H , ^{13}C)$= 2.3 Hz, 3H, NCH_3), 1.85 - 1.77 (m, 2H, PCH_2), 1.66 - 1.58 (m, 2H, PCH_2). **^{13}C{^{1}H} NMR** (C_6D_6, 125.8 MHz): δ = 142.3 (*i*-Mes), 142.2 (*i*-Mes), 138.0 (*p*-Mes) , 131.1 (*o*-Mes), 131 (*o*-Mes), 129.7 (*m*-Mes), 129.7 (*m*-Mes), 56.5 (NCH_2), 56.5 (NCH_2), 41.6 (NCH_3), 23.6 (*o*-Me), 23.5 (*o*-Me), 21.4 (*p*-Me), 20.2 (PCH_2), 20.1 (PCH_2). **^{31}P{^{1}H} NMR** (C_6D_6, 121.5 MHz): δ = –92.69 (s), –92.72 (s). **IR spectroscopy:** $\bar{\nu}$ = 552 (m), 848 (s), 1455(m) and 2326 (br) cm^{-1}. HRMS: *calcd*. for ($L+H^+$,

$[C_{23}H_{36}N_1P_2]^+$) 388.2317; *found* 388.2324 and *calcd*. for $[C_{14}H_{25}N_1O_1P_1]^+$ 254.1668; *found* 254.1667. Elemental analysis is not perform because of the toxicity.

$MeN(CH_2CH_2P(Mes)SnCl)_2$ (9):

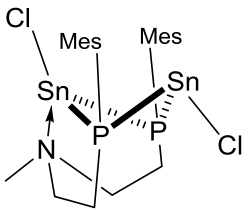

To **4** in Toluene was added methylene chloride at 60 °C for 1h. The volatiles were removed under reduced pressure and the residue was dissolved in toluene. Pale yellow crystals were precipitated upon cooling at –30 °C over 24h.

^{1}H NMR (C_6D_6, 400 MHz): δ = 6.67 (s, 4H, *m*-Mes), 3.41- 3.31 (m, 2H, PCH_{Exo}), 2.96- 2.86 (m, 2H, NCH_{Exo}), 2.66 (br, 12H, *o*-Me), 2.03 (s, 6H, *p*-Me), 1.99 - 1.87 (m, 4H, NCH_{Endo}, PCH_{Endo}), 1.82 (s, 3H, NCH_3). **^{13}C{^{1}H} NMR** (C_6D_6, 100.6 MHz): δ = 140.1 (Mes), 130.6 (*m*-Mes), 129.7(Mes), 126.0 (Mes), 54.42 (NCH_2), 44.5 (NCH_3), 24.0 (PCH2), 24.0 (*o*-Me), 21.2 (*p*-Me). **^{31}P{^{1}H} NMR** (C_6D_6, 121.5 MHz): δ = –99.7 (s, ^1J (^{31}P , $^{117/119}$Sn)= 1389/ 1454 Hz, ^1J (^{31}P , $^{117/119}$Sn)= 1360/ 1425 Hz).**^{119}Sn{^{1}H} NMR** (C_6D_6, 111.9 MHz): δ = 161 (t, ^1J (^{119}Sn , ^{31}P)= 1454 Hz, ^2J (^{119}Sn , ^{119}Sn)= 288 Hz), 48 (t, ^1J (^{119}Sn , ^{31}P)= 1425 Hz, ^2J (^{119}Sn , ^{119}Sn)= 288 Hz). **Elemental analysis** calcd. for $C_{23}H_{33}Cl_2NP_2Sn_2{\cdot}0.5C_7H_8$ 747.88 (g/mol): C, 43.4 %; H, 5.3 %; N 1.9 %. Found: C, 43.0 %; H, 5.3 %; N 1.9 %. **ESI MS:** m/z= 386.2 $[C_{23}H_{34}NP_2+H]^+$, 388.2 $[C_{23}H_{36}NP_2+H]^+$, 574.1 $[C_{23}H_{35}NClP_2Sn+H+MeOH]^+$. **IR spectroscopy:** $\bar{\nu}$ = 807 (m), 725 (m), 647 (vs), 1438 (br) cm^{-1}.

$H_3CN(CH_2CH_2P(Mes)SnBr)_2$ (10):

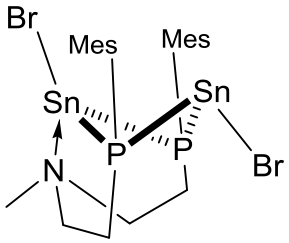

Compound (**5**) was stirred in methylene bromide at RT for 1h. The volatiles were removed under reduced pressure and the residue was dissolved in THF. A yellow crystals were precipitated upon cooling at –30 °C over 24h.

^{1}H NMR (C_6D_6, 400.3 MHz): δ = 6.65 (br, $\Delta\nu_{1/2}$= 23Hz, Mes, 4H), 3.41 - 3.33 (m, CH_2, 2H), 2.98 - 2.91 (m, CH_2, 2H), 2.70 (br, $\Delta\nu_{1/2}$= 23Hz, *O*-CH_3, 6H), 2.57 (br, $\nu_{1/2}$= 23Hz, *O*-CH_3, 6H), 2.01 (s, *P*-CH_3, 6H), 1.98 - 1.85 (m, CH_2, 4H), 1.78 (s, 3H, NCH_3). **^{31}P{^{1}H} NMR** (C_6D_6, 162.0 MHz): δ = –108.3 (s, ^1J (^{31}P , $^{117/119}$Sn)= 1312/ 1322 Hz, ^1J (^{31}P , $^{117/119}$Sn)= 1349/ 1358 Hz).**^{119}Sn{^{1}H} NMR** (C_6D_6, 223.9 MHz): δ = 181 (t, ^1J (^{119}Sn , ^{31}P)= 2849 Hz, ^2J (^{119}Sn , ^{119}Sn)= 287 Hz), 63 (t, ^1J (^{119}Sn , ^{31}P)= 2829 Hz, ^2J (^{119}Sn , ^{119}Sn)= 290 Hz). **Elemental analysis** calcd. for $C_{23}H_{33}Cl_2NP_2Sn_2{\cdot}0.5C_7H_8$ 747.88 (g/mol): C, 43.4 %; H, 5.3 %; N 1.9 %. Found: C, 43.0 %; H, 5.3 %; N 1.9 %. **ESI MS:** *m/z*= 388.2

$[C_{23}H_{36}NP_2+H]^+$, 404.1 $[C_{23}H_{33}NP_2+H+H_2O]^+$, 388.2 $[C_{23}H_{36}NP_2+H+MeOH]^+$, 574.1 $[C_{23}H_{35}NClP_2Sn+H+MeOH]^+$. **IR spectroscopy:** $\bar{\nu}$ = 550, 725, 734, 847, 1438 cm^{-1}.

$MeN(CH_2CMe_2OLi)_2$ (13):

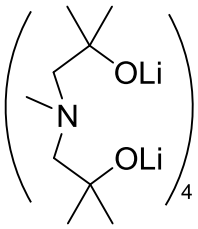

To a hexane solution of (5 g, 28.5 mmol) $H_3CN(CH_2C(CH_3)_2OH)_2$ was added (35 mL, 66 mmol) *t*BuLi at –60 °C. the solution was stirred for two hours and concentered to about 10%. The product was filtrated as a white solid to obtain (4.4 g, 82 %). Second fraction from the product (533.8 mg, 10 %) was collected as colorless crystals from the hexane filtrate at room temperature overnight.

^{1}H NMR (400 MHz, toluene-D_8): δ = 2.45 (br, $\nu_{1/2}$= 60 Hz, 4H, NCH_2), 2.39 (s, 3H, NCH_3), 1.30 (br, $\nu_{1/2}$= 50 Hz, 8H, CCH_3), 1.18 (br, $\nu_{1/2}$= 37 Hz, 4H, CCH_3). **^{7}Li{^{1}H} NMR** (156 MHz, C_6D_6): δ = 2.3(s), 1.25(s), 0.87(s). **^{1}H NMR** (400 MHz, toluene-D_8, –75 °C): δ = 3.10 - 2.17 (m, 7H, NCH_2 and NCH_3), 1.62 - 1.11 (m, CCH_3). **^{7}Li{^{1}H} NMR** (156 MHz, C_6D_6): δ = 2.5 - 1.7(m), 1.2 - 0.5(m). **^{1}H NMR** (400 MHz, THF-D_8): δ = 2.52 (br, $\nu_{1/2}$= 26 Hz, 4H, NCH_2), 2.46 (s, 3H, NCH_3), 1.22 (br, $\nu_{1/2}$= 24 Hz, 3H, CCH_3), 1.08 (br, $\nu_{1/2}$= 32 Hz, 9H, CCH_3). **^{7}Li{^{1}H} NMR** (156 MHz, C_6D_6): δ = 2.0(s), 1.1(s). **^{1}H NMR** (400 MHz, THF-D_8, –75 °C): δ = 2.84 - 2.32 (m, 7H, NCH_2 and NCH_3), 1.24 – 0.91 (m, 12H, CH_3). **^{7}Li{^{1}H} NMR** (156 MHz, THF-D_8, –75 °C): δ = 2.3(s), 1.72(s), 0.65(s), –0.0(s), –0.2(s). Elemental analysis calcd. For $C_9H_{19}Li_2N_1O_2$+2H_2O: C, 48.4%; H, 10.4%; N, 6.3% found C, 48.5%; H, 10.2%; N, 6.7%. The ligand is extremely hygroscopic and the process is not applied under inert conditions.

$MeN(CH_2CMe_2O)_2SiH_2$ (14):

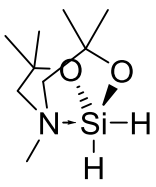

Path A: to (5.2 g, 29.7 mmol) $H_3CN(CH_2C(CH_3)_2OH)_2$ in toluene was added (5.2 g, 30 mmol) $(CH_3CH_2N)_2SiH_2$ at room temperature. **Path B**: to **1** was added $HSiCl_2$ in hexane at –40 °C. The solvent was removed under reduced pressure and the residue was distilled **b**.**p**. 62 °C at 0.9 mbar to obtain the product as a colorless oil (4.0 g, 70 %) **IR:** $\bar{\nu}$ = 543(w), 723(s), 936(vs), 1022(s), 1040(s), 2090(s, SiH_2), 2126(s, SiH_2) and 2974 cm^{-1}. **^{1}H NMR** (400 MHz, C_6D_6): δ = 5.08 (s, ^1J(^{1}H , ^{29}Si) = 237 Hz, 2H, SiH_2) (in the ^{1}H NMR at –80 °C: δ_{SiH_2} = 5.45 (d, ^2J(^{1}H , ^{1}H) = 26 Hz, ^1J(^{1}H , ^{29}Si) = 240 Hz) and 5.35 (d, ^2J(^{1}H , ^{1}H) = 26 Hz, ^1J(^{1}H , ^{29}Si) = 226 Hz)), 2.29 (s, 4H, NCH_2), 2.21 (s, 3H, NCH_3), 1.10 (s, 12H, C(CH_3)$_2$). **^{13}C{^{1}H} NMR** (101 MHz, C_6D_6): δ = 72.8 (s, O*C*(CH_3)$_2$), 72.8 (s, N*C*H_2), 48.5(s, N*C*H_3), 29.7(s, C(*C*H_3)$_2$). **^{29}Si{^{1}H} NMR** (80 MHz, INEPT, C_6D_6): δ = –64.8 and **^{29}Si NMR** (80 MHz, INEPT, C_6D_6): δ = 64.7 (^1J(^{29}Si , ^{1}H) = 237 Hz).

Elemental analysis calcd. For $C_9H_{21}NO_2Si$ 507.3 [g/mol] C, 53.2%; H, 10.4%; N, 7.0% found C, 52.1 %; H, 12.3 %; N, 5.8%. The ligand is extremely hygroscopic and the process is not applied under inert conditions.

$MeN(CH_2CMe_2O)_2SiHCl$ (15):

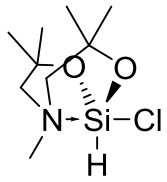

To solution of (4.50 g, 22.1 mmol) $MeN(CH_2CMe_2O)_2SiH_2$ in (50 mL) dichloromethane was added (11.1 mL, 2M) HCl in diethyl ether at 0 °C. The suspension was stirred for 16 h at room temperature after which the white solid was filtered and concentrate to dryness under reduced pressure to obtain (1.2 g, 22%). Another fraction of the product was obtained as crystals from the filtrate at room temperature. The crystals were filtered and dried under reduced pressure to obtain (4.0 g, 75%).

^{1}H NMR (400 MHz, CD_2Cl_2): δ = 5.42 (s, $^1J(^1H, ^{29}Si)$ = 333 Hz, Si*H*), 3.02 (d, $^2J(^1H, ^1H)$ = 13 Hz, NCH_2), 2.83 (d, $^2J(^1H, ^1H)$ = 13 Hz, NCH_2), 2.67 (s, 3H, NCH_3), 1.35 (s, 6H, CCH_3) and 1.33 (s, 6H, CCH_3), **^{13}C{^{1}H} NMR** (101 MHz, CD_2Cl_2): δ = 73.4 (s, *C*Me_2), 70.0 (s, N*C*H_2), 49.6 (s, N*C*H_3) 31.6 (s, *C*H_3) and 30.6 (s, *C*H_3), **^{29}Si{^{1}H} NMR** (80 MHz, INEPT, CD_2Cl_2): δ = –79.9.

4.5 Conclusion

In this chapter the synthesis of novel *P*,*N*,*P*-coordinating ligands $MeN(CH_2CH_2PRH)_2$ (R = Ph **1** and R = Mes **2**) was reported (Scheme 9). These compounds react with $Sn(NR_2)_2$ (R = $SiMe_3$) according to an acid-base reaction to give the corresponding tin(II) compounds $MeN(CH_2CH_2P(Mes))_2Sn$ **5**. The $^{31}P\{^1H\}$ NMR spectrum shows that the corresponding tin(II) compound **5** is dimeric in solution. Compounds **7** and **8** were obtained by the reaction of **4** and **5**, respectively with $W(CO)_5thf$. Compound **4** reacts with excess amount of dihalomethane to give the heteroleptic tin(II) compounds **9** and **10** and the cyclodiphosphane **6.**

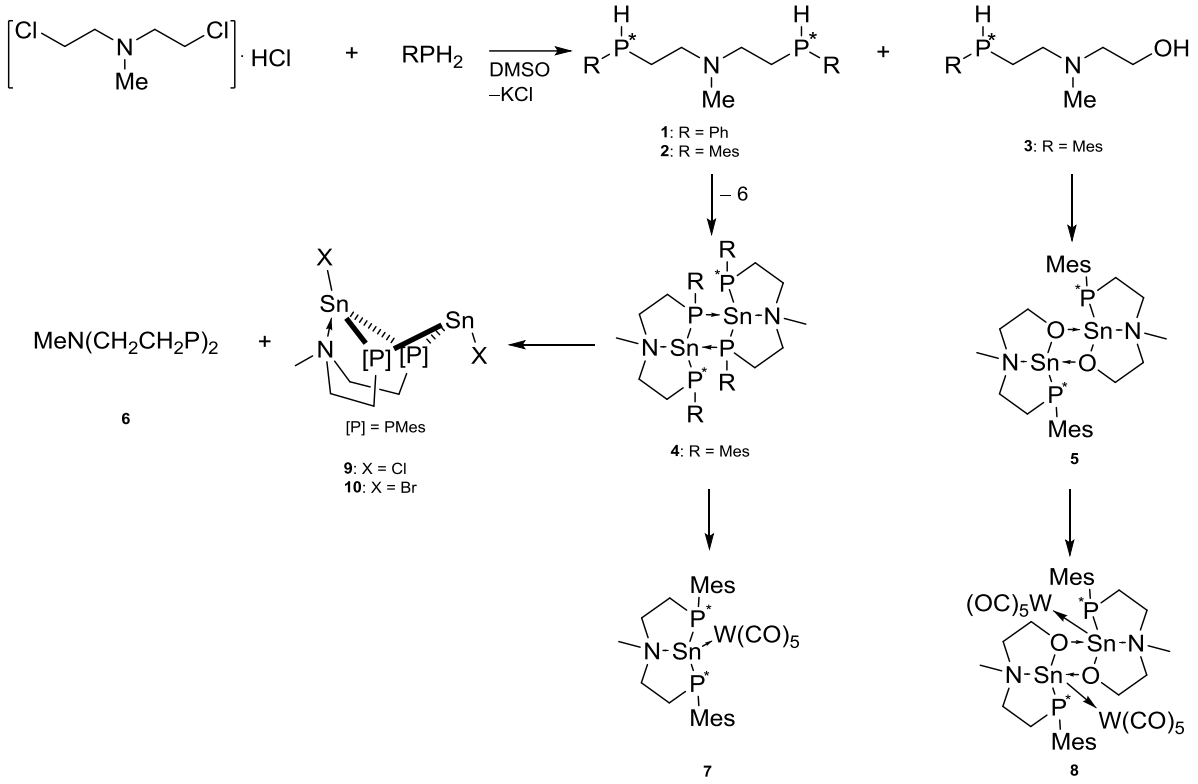

Scheme 9. $MeN(CH_2CH_2PHR)_2$ and their reactivity.

From the reaction of the amino alcohol $MeN(CH_2CMe_2OH)_2$ with *t*BuLi the novel octameric lithium oxocluster **12** was obtained (Scheme 10).

The 1-sila-2,8-dioxa-5-azabicyclooctane derivative **13** was produced by the reaction of **12** with $SiCl_2H_2$ or by the reaction of $MeN(CH_2CMe_2OH)_2$ **11** with $SiH_2(NEt_2)_2$. In the solid state, the silicon atom is pentacoordinated with one H-atom occupying an equatorial and the other H-atom occupying an axial position of a distorted trigonal

bipyramid. This structure is also evident in solution at –80 °C. Compound **14** reacts with HCl giving $MeN(CH_2CMe_2O)_2SiHCl$, **14.**

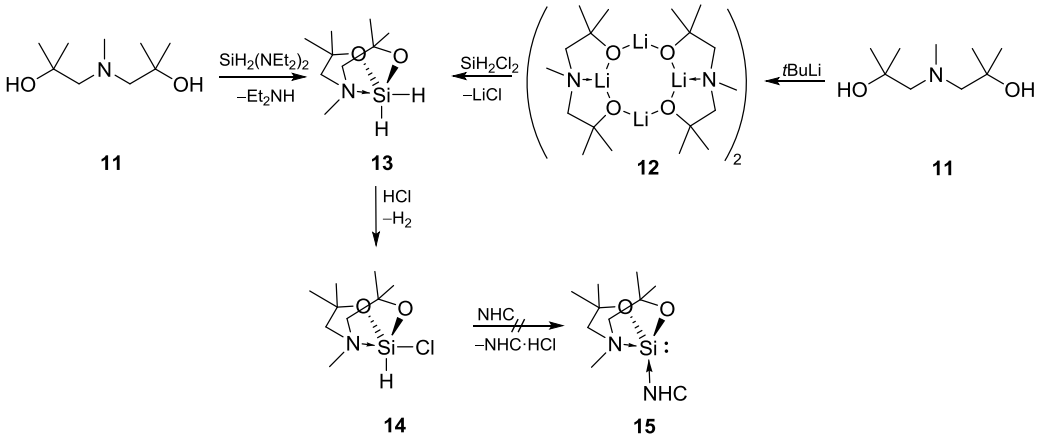

Scheme 10. $MeN(CH_2CH_2OH)_2$, $MeN(CH_2CH_2O)_2SiH_2$ and their reactivity.

4.6 Literature

[1] K. Izod, *Coord. Chem. Rev.* **2012**, *256*, 2972.

[2] M. J. S. Gynane, D. H. Harris, M. F. Lappert, P. P. Power, P. Rividre, M. Rividre-Baudet, *J. CHem. Soc. Dalton Trans.* **1977**, 2004.

[3] W. W. Du Mont, M. Grenz, *Chem. Ber.* **1985**, *118*, 1045.

[4] R. Janoschek, H. Pritzkow, S. Rell, U. Winkler, M. Driess, *Angew. Chem. Int. Ed.* **1995**, *34*, 1614.

[5] K. Izod, J. Stewart, E. R. Clark, W. McFarlane, B. Allen, W. Clegg, R. W. Harrington, *Organometallics* **2009**, *28*, 3327.

[6] K. Izod, J. Stewart, W. Clegg, R. W. Harrington, *Organometallics* **2010**, *29*, 108.

[7] T. Řezníček, L. Dostál, A. Růžička, R. Jambor, *Eur. J. Inorg. Chem.* **2012**, *2012*, 2983.

[8] a) K. Jurkschat, M. Scheer, A. Tzschach, *Z. anorg. allg. Chem.* **1984**, *515*, 147; b) J. Faure, H. Gornitzka, R. Reau, D. Stalke, G. Bertrand, *Eur. J. Inorg. Chem.* **1999**, *1999*, 2295; c) S. M. Mansell, C. A. Russell, D. F. Wass, *Inorganic chemistry* **2008**, *47*, 11367; d) M. Huang, M. M. Kireenko, E. K. Lermontova, A. V. Churakov, Y. F. Oprunenko, K. V. Zaitsev, D. Sorokin, K. Harms, J. Sundermeyer, G. S. Zaitseva et al., *Z. anorg. allg. Chem.* **2013**, *639*, 502.

[9] W. W. du Mont, *Polyhedron* **1988**, *7*, 1317.

[10] M. Driess, S. Martin, K. Merz, V. Pintchouk, H. Pritzkow, H. Griitzmacher, M. Kaupp, *Angew. Chem. Int. Ed.* **1997**, *36*, 1894.

[11] a) M. A. Pudovik, S. A. Terent'eva, A. N. Pudovik, *J. Gen. Chem. USSR (Engl. Transl.)* **1983**, *55*, 2185; b) A. A. Selina, S. S. Karlov, G. S. Zaitseva, *Chem. Heterocycl. Compd.* **2006**, *42*, 1518; c) V. M. D'yakov, A. F. Makarov, A. M. Kir'yanova, S. I. Androsenko, *J. Gen. Chem. USSR (Engl. Transl.)* **1992**, *62*, 285; d) M. G. Voronkov, A. I. Albanov, E. A. Grebneva, O. M. Trofimova, N. F. Chernov, N. N. Chipanina, *Russ. J. Gen. Chem.* **2006**, *76*, 1854.

[12] M. Lutter, L. Iovkova-Berends, C. Dietz, V. Jouikov, K. Jurkschat, *Main Group Metal Chemistry* **2012**, *35*.

[13] A. Helßer, S. Kuchen, O. Stelzer, W. S. Sceldrick, *J. Organomet. Chem.* **1998**, *553*, 39.

[14] S. Molitor, J. Becker, V. H. Gessner, *J. Am. Chem Soc.* **2014**, *136*, 15517.

[15] W. L. F. Armarego, C. L. L. Chai, *Purification of laboratory chemicals*, Elsevier/Butterworth-Heinemann, Amsterdam, Boston, **2009**.

[16] K. Izod, J. Stewart, E. R. Clark, W. McFarlane, B. Allen, W. Clegg, *Organometallics* **2009**, *28*, 3327–3337.

[17] A. Zschunke, M. Scheer, M. Völtzke, K. Jurkschat, A. Tzschach, *J. Organomet. Chem.* **1986**, *308,* 325–334*.*

[18] W. C. Still, I. Galynker, *Tetrahedron*, **1981**, *37*, 3981–3996.

CONCLUSION

In Chapter 1 the syntheses of novel *O*,*C*,*O*-and *O*,*N*,*O*-coordinating pincer-type ligands is reported (Scheme **1**). The compounds were prepared by Hirao cross coupling reactions between the corresponding *di*-bromo pyridine derivate and di*iso*propyl phosphite. The products were isolated in good yields and listed in Scheme **1**.

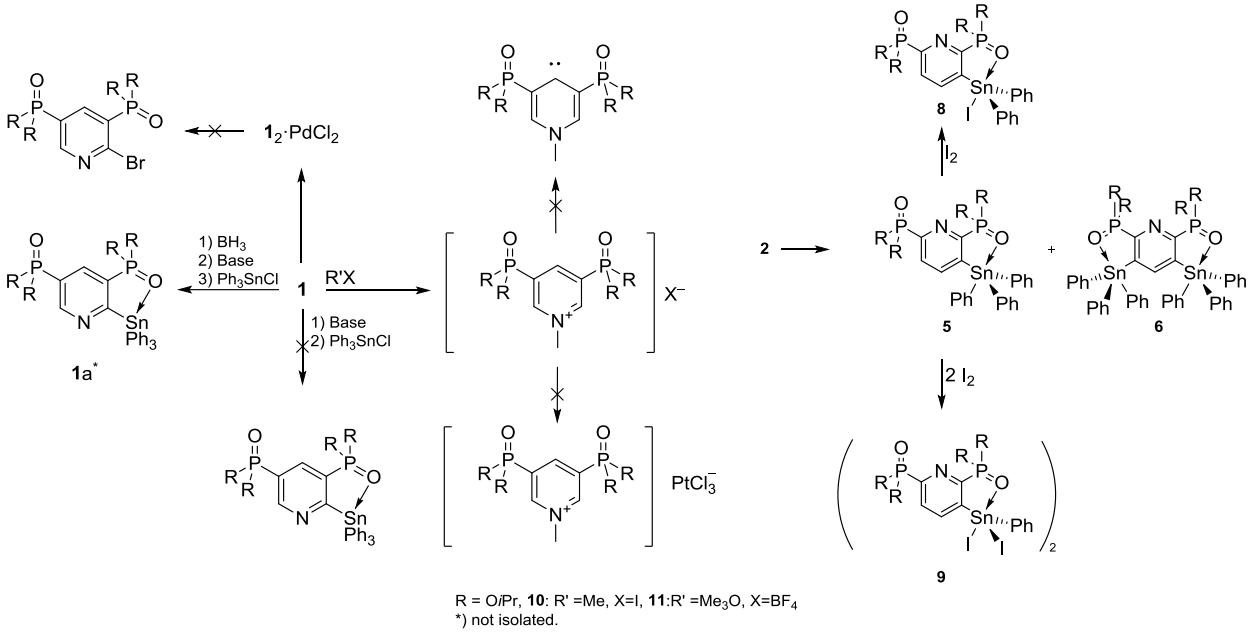

Scheme 7. The reactivity of compounds **1** and **2.**

Compound **1** is stable toward *n*BuLi, *t*BuLi and LDA because it complexes RLi, while the deprotonation of **1**·BH_3 with LDA followed by the addition of $SnPh_3Cl$ gives to **1a** which was, however, not isolated (Scheme 1). The reaction of **1** with alkylation reagents (MeI and Me_3OBF_4) provides the corresponding pyridinium salts **10** and **11**. The reaction of **10** and **11** with base to produce the corresponding carbene, the change of BF_4^- with $PtCl_3^-$, and the addition of elemental bromine to the pyridine ring to achieve selective bromination failed.

Compound **2** reacts with LDA to produce the corresponding lithium compound, which reacts with Ph_3SnCl to give 2,6-di-P(O)(O*i*Pr)$_2$$C_5H_2N$-3-$SnPh_3$ and 2,6-di-P(O)(O*i*Pr)$_2$$C_5H_2N$-3,5-$(SnPh_3)_2$.

In Chapter 2 the reactions of SnX_2 (X = Cl, Br and I) with the phosphorus-substituted pyridine derivatives L_1, L_2, L_3 and L_4 are described giving salts of the type $[(L)SnCl]SnCl_3$ (Scheme 2).

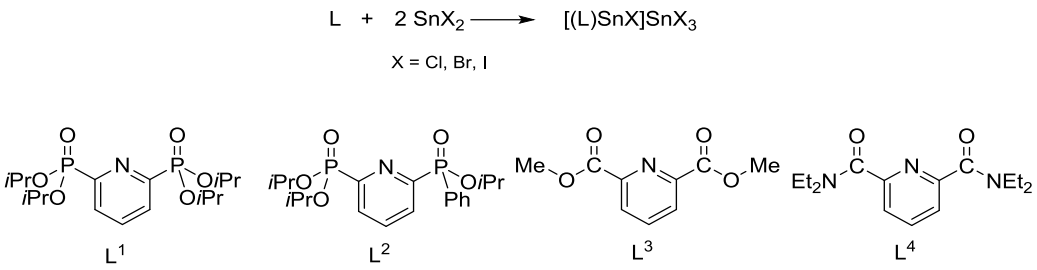

Scheme 2. The reaction of SnX_2 with P-substituted pyridine derivatives.

On the $^{119}Sn\{^1H\}$ NMR time scale, the complexes are kinetically labile with the consequence that no ^{119}Sn resonances were observed. At –80 °C, however, the exchange processes are slow and single resonances are observed for both the cation $[(L)SnCl]^+$ (δ –701) and the anion $SnCl_3^-$ (δ –90). Two diastereomers are observed for $[(L\_2)SnCl]SnCl_3$. The reaction of $[(L)SnCl]SnCl_3$ with $[W(CO)_5(thf)]$ gave the unprecedented $[(L)SnCl]W(CO)_4SnCl_3$, in which not only the anion $SnCl_3^-$ but also the cation $[(L_1)SnCl]^+$coordinate to the $W(CO)_4$ moiety.

The results of the polymerization reaction of polyurethane using compounds [(L)SnCl]SnCl (Scheme 2) as catalysts are shown in Chapter 3.

In Chapter 4 the synthesis of novel *P,N,P*-coordinating ligands $MeN(CH_2CH_2PRH)_2$ (R = Ph **1** and R = Mes **2**) is reported (Scheme 3). These compounds react with $Sn(NR_2)_2$ (R = $SiMe_3$) according to an acid-base reaction to give the corresponding tin(II) compounds $MeN(CH_2CH_2P(Mes))_2Sn$ **5**. The $^{31}P\{^1H\}$ NMR spectrum shows that the corresponding tin(II) compound **4** is dimeric in solution. Compounds **7** and **8** were obtained by the reaction of the mixture of **4** and **5**, respectively with $W(CO)_5$thf . Compound **4** reacts with excess amount of dihalomethane to give the heteroleptic tin(II) compounds **9** and **10** and the cyclodiphosphane **6.**

From the reaction of the amino alcohol $MeN(CH_2CMe_2OH)_2$ with *t*BuLi the novel octameric lithium oxocluster **12** was obtained (Scheme 3). The 1-sila-2,8-dioxa-5-azabicyclooctane derivative **13** was produced by the reaction of **12** with $SiCl_2H_2$ or by the reaction of $MeN(CH_2CMe_2OH)_2$ **11** with $SiH_2(NEt_2)_2$. In the solid state, the silicon atom is pentacoordinated with one H-atom occupying an equatorial and the other H-atom

occupying an axial position of a distorted trigonal bipyramid. This structure is also evident in solution at –80 °C. Compound **13** reacts with HCl giving $MeN(CH_2CMe_2O)_2SiHCl$, **14.**

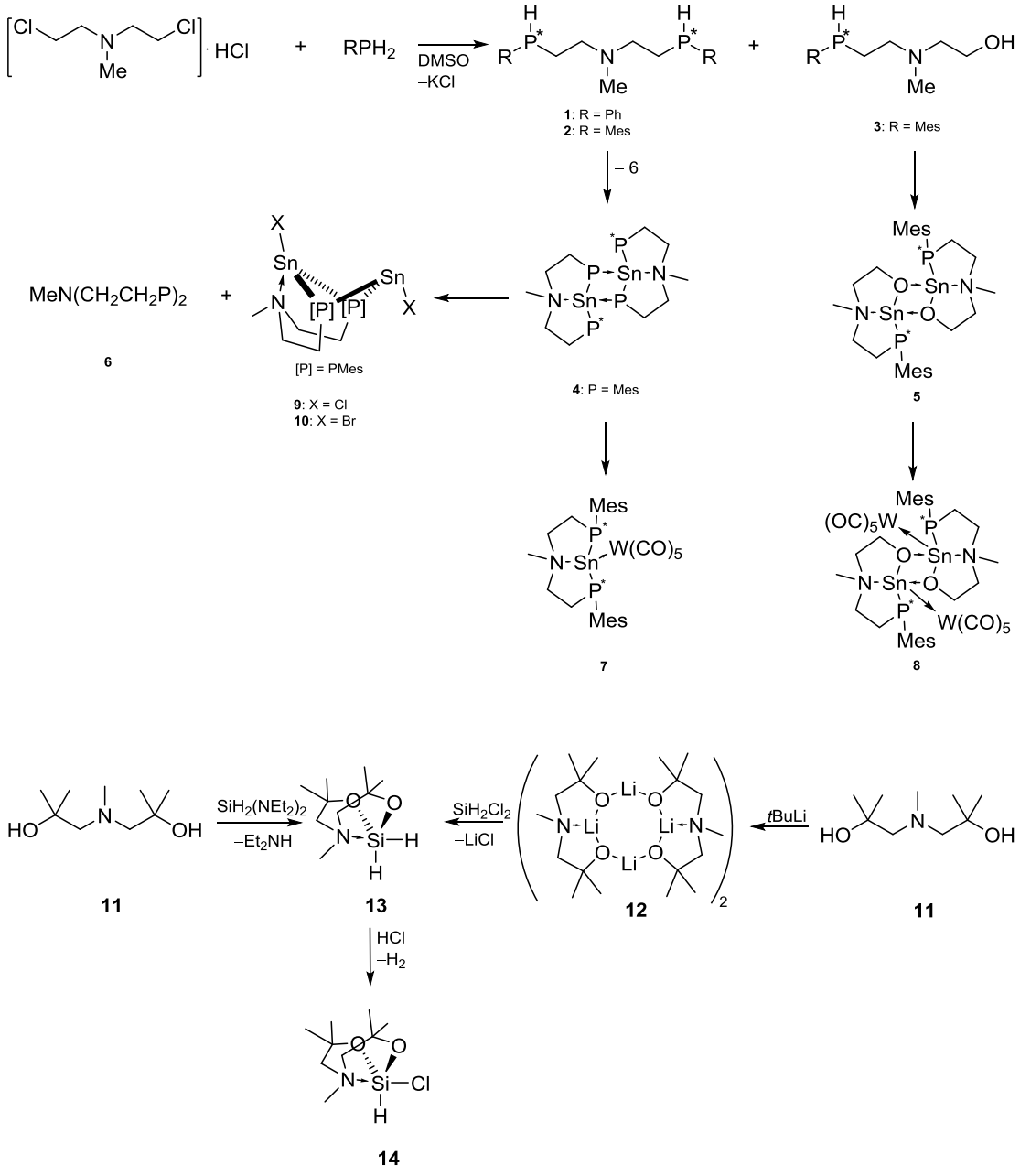

Scheme 3. The synthesis of compound **4** and its reactivity (top). The synthesis of the octamer Li-O cluster, compound **13** and its reactivity toward HCl.

ZUSAMMENFASSUNG

In Kapitel 1 ist die Synthese der neuartigen, potentiell *O*,*C*,*O*- und *O*,*N*,*O*-koordinierenden Zangenliganden ausgehend von den entsprechenden Dibromopyridinen und Di*iso*propylphosphit beschrieben (Schema 1).

Aufgrund der Komplexbildung des Li→N-Addukts ist Verbindung **1** stabil gegenüber *n*BuLi, *t*BuLi and LDA. **1**·BH_3 kann hingegen mittels LDA deprotoniert werden. Nachfolgende Zugabe von Ph_3SnCl zur lithierten Spezies liefert Verbindung **1a**, dessen Isolierung nicht erfolgte (Schema 1). Die Reaktion von **1** mit MeI bzw. $Me_3O{\cdot}BF_4$ ergibt die entsprechenden Pyridiniumsalze **10** und **11**. Versuche zur Darstellung der analogen Carbene durch Umsetzung von **10** und **11** mittels einer Base, ebenso wie die Überführung in das entsprechende Chloroplatinatsalz schlugen fehl. Bromierungsversuche von **1** und **1**$_2$·$PdCl_2$ mittels elementarem Brom waren unter den im Rahmen dieser Arbeit gewählten Bedingungen ebenfalls nicht erfolgreich.

Verbindung **2** reagiert mit LDA und nachflogende Zugabe von Ph_3SnCl zu 2,6-[P(O)(O*i*Pr)$_2$]$_2$$C_5H_2N$-3-$SnPh_3$ und 2,6-[P(O)(O*i*Pr)$_2$]$_2$$C_5H_2N$-3,5-($SnPh_3$)$_2$.

In Kapitel 2 wird die Darstellung von Salzen des Typs [(L)SnX]SnX_3 vorgestellt, in welchen SnX_2 mit den entsprechenden phosphorsubstituierten Pyridin-Derivaten **L_1**, **L_2**, **L_3** und **L_4** reagiert (Schema 2).

Bei Raumtemperatur sind die dargestellten Komplexe auf der $^{119}Sn\{^1H\}$-NMR-Zeitskala kinetisch labil, weshalb keine ^{119}Sn Resonanzen beobachtet werden. Bei –80 °C ist der Austauschprozess verlangsamt, wodurch im analogen $^{119}Sn\{^1H\}$-NMR-Spektrum zwei Signale aufgelöst sind, welche dem Kation $SnCl^+$ bei δ –701 bzw. dem Anion $SnCl_3^-$ bei δ –90 zugeordnet werden. Das $^{119}Sn\{^1H\}$-NMR-Spektrum bei –80 °C zeigt zwei Diastereomere für [(L_2)SnCl]$SnCl_3$. Bedingt durch die stereogenität eines der beiden Phosphorzentren wird im entsprechenden [(L_2)SnCl]$SnCl_3$ Salz ein Diastereomerpaar beobachtet.

Die in diesem Zusammenhang durchgeführte Umsetzung von [(L_1)SnCl]$SnCl_3$ mit $W(CO)_5$thf liefert überraschenderweise die Koordinationsverbindung [(L)SnCl]$W(CO)_4SnCl_3$, in welcher sowohl das Anion $SnCl_3^-$ als auch das Kation $SnCl^+$ mit der $W(CO)_4$-Funktionalität wechselwirkt.

In Kapital 3 wurde die Katalysatoraktivität von [(L)SnCl]$SnCl_3$ (Schema 2) in Polymerisationsreaktionen zu Polyurethan untersucht und diskutiert.

In Kapitel 4 wird die Synthese der neuartigen *P*,*N*,*P* koordinierenden Liganden $MeN(CH_2CH_2PRH)_2$ (R = Ph **1** and R = Mes **2**) beschrieben (Schema 3). Verbindungen **1** und **2** reagieren hierbei in einer Säure-Base-Reaktion mit $Sn(NR_2)_2$ (R = $SiMe_3$) zu den entsprechenden Zinn(II) amiden **4** und **5**, wobei **4** nicht isoliert wurde. Das $^{31}P\{^1H\}$-NMR-Spektrum deutet auf eine dimere Struktur von **4** in Lösung. Verbindungen **7** und **8** wurden durch Reaktion von **4** und **5** mit $W(CO)_5$thf erhalten. Verbindung **4** reagiert mit einem Überschuss von Dihalomethanen zu den heteroleptischen Zinn(II)-Verbindungen **9**, **10** und dem Cyclodiphosphan **6**.

Aus der Reaktion des Aminoalkohols $MeN(CH_2CMe_2OH)_2$ mit *t*BuLi resultiert die oktamere Lithium-Oxoclusterverbindung **12** (Schema 3). Das 1-Sila-2,8-dioxa-5-azabicyclooctane Derivat **13** ist durch Umsetzung von **12** mit H_2SiCl_2 oder durch Reaktion von $MeN(CH_2CMe_2OH)_2$ **11** mit $SiH_2(NEt_2)_2$ isolierbar. Im Festkörper liegt das entsprechende Siliciumatom pentakoordiniert vor und weist eine verzerrt trigonal-bipyramidale Umgebung auf, in welcher ein H-Atom die äquatoriale Position besetzt und das andere H-Atom sich in axialer Position befindet. Die im Festkörper getätige Interpretation konvergiert mit analogen NMR-spektroskopischen Untersuchungen von **13** bei –80 °C. Verbindung **13** reagiert zudem mit HCl zum Chlorosilan $MeN(CH_2CMe_2O)_2SiHCl$, **14**.

CRYSTALLOGRAPHIC DATA

Chapter 1

Compound	**1**	**3**
Empirical formula	$C_{17}H_{31}N_1O_6P_2$	$C_{11}H_{17}Br_1N_1O_3P_1$
Formula weight	407.37	322.13
Temperature [K]	173	173
Crystal size [mm]	0.16 x 0.15 x 0.10	0.6 x 0.275 x 0.203
Crystal system	Triclinic	Monoclinic
Space group	$P\bar{1}$	$P\ 1\ 2_1/\ n\ 1$
a [Å]	6.2005(5)	6.2233(3)
b [Å]	12.316(2)	26.2564(16)
c [Å]	14.5095(18)	8.8466(5)
α [°]	101.789(13)	90
β [°]	90.696(8)	107.540(6)
ɣ [°]	103.584(10)	90
Volume [Å^3]	1052.2(2)	1378.34(15)
Z	2	4
F(000)	436	656
Density (calculated) [Mg/m^3]	1.286	1.552
μ [mm^{-1}]	0.237	3.095
Absorption correction	Semi-empirical	Semi-empirical
Θ range for data collection [°]	2.483 to 25.500	2.536 to 30.952
h values	–7≤h≤7	–8≤h≤8
k values	–14≤k≤14	–37≤k≤36
l values	–17≤l≤17	–12≤l≤12
Scan method	ω- and ψ-Scan	ω- and ψ-Scan
Reflections collected	10833	11509
Data [$I > 2\sigma(I)$]	3917	3953
Parameters	236	216
R_{int}	0.0614	0.0291
R1	0.1571	0.0495
wR2	0.413	0.0741
GooF (F^2)	1.21	1.030
Largest diff. peak and hole e.Å^{-3}	1.316 and –0.939	0.825 and –0.867

Compound	**5**	**6**
Empirical formula	$C_{35}H_{45}N_1O_6P_2Sn_1$	$C_{46}H_{70}I_4N_2O_{12}P_4Sn_2$
Formula weight	756.35	1711.90
Temperature [K]	173	173
Crystal size [mm]	0.39 x 0.300 x 0.080	0.200 x 0.070 x 0.050
Crystal system	Triclinic	Monoclinic
Space group	$P\bar{1}$	$P2_1/c$
a [Å]	11.7129(4)	14.8747(12)
b [Å]	12.9475(5)	10.9899(8)
c [Å]	13.4239(4)	20.7043(17)
α [°]	98.139(3)	90
β [°]	102.026(3)	109.277(9)
ɣ [°]	112.863(4)	90
Volume [Å^3]	1777.86(12)	3194.8(5)
Z	2	2
F(000)	780	1656
Density (calculated) [Mg/m^3]	1.413	1.780
μ [mm^{-1}]	0.852	2.866
Absorption correction	Semi-empirical	Semi-empirical
Θ range for data collection [°]	2.475 to 25.498	2.353 to 25.499
h values	–14≤h≤14	–17≤h≤17
k values	–15≤k≤15	–13≤k≤13
l values	–16≤l≤16	–25≤l≤25
Reflections collected	14903	44381
Scan method	ω- and ψ-Scan	ω- and ψ-Scan
Data [$I > 2\sigma(I)$]	6609	5938
Parameters	388	361
R_{int}	0.0269	0.0907
R1	0.0319	0.1080
wR2	0.1019	0.2069
GooF (F^2)	0.875	1.096
Largest diff. peak and hole e.Å^{-3}	1.310 and –0.868	1.000 and –2.659

Compound	**7**	**8**
Empirical formula	$C_{34}H_{62}Cl_2N_2O_{12.50}P_4Pd_1$	$C_{18}H_{34}I_2N_1O_6P_2$
Formula weight	1000.03	549.30
Temperature [K]	173(2)	173.15
Crystal size [mm]	0.580 x 0.260 x 0.050	0.459 x 0.114 x 0.037
Crystal system	Triclinic	Monoclinic
Space group	$P\bar{1}$	P 1 21/n
a [Å]	11.3540(3)	9.5890(3)
b [Å]	14.7147(4)	22.5240(8)
c [Å]	15.9171(4)	12.8067(5)
α [°]	113.877(3)	90
β [°]	90.006(2)	109.607(4)
ɣ [°]	104.598(2)	90
Volume [Å^3]	2337.47(12)	2605.65(17)
Z	2	4
F(000)	1040	1120
Density (calculated) [Mg/m^3]	1.421	1.400
μ [mm^{-1}]	0.704	1.381
Absorption correction	Semi-empirical	Semi-empirical
Θ range for data collection [°]	2.253 to 25.499	2.319 to 25.498
h values	–13≤h≤13	–11≤h≤11
k values	–17≤k≤17	–27≤k≤27
l values	–19≤l≤19	–15≤l≤15
Reflections collected	35273	25629
Scan method	ω- and ψ-Scan	ω- and ψ-Scan
Data [$I > 2\sigma(I)$]	8703	4846
Parameters	540	300
R_{int}	0.0272	0.0363
R1	0.0316	0.0313
wR2	0.0759	0.0588
GooF (F^2)	1.053	1.041
Largest diff. peak and hole e.Å^{-3}	0.687 and –0.571	0.402 and –v0.294

Chapter 2

Compound	**1**	**1·C7H8**
Empirical formula	$C_{17}H_{31}Cl_4N_1O_6P_2Sn_2$	$C_{17}H_{31}Cl_4N_1O_6P_2Sn_2$
Formula weight	786.55	786.55
Temperature [K]	173.15	173.15
Crystal size [mm]	0.216 x 0.154 x 0.049	0.19 x 0.145 x 0.067
Crystal system	Orthorhombic	Triclinic
Space group	Pbca	$P\bar{1}$
a [Å]	16.0153(7)	9.8170(3)
b [Å]	17.3377(7)	11.2738(4)
c [Å]	20.9922(11)	15.5274(5)
α [°]	90	72.235(3)
β [°]	90	85.570(3)
ɣ [°]	90	76.991(3)
Volume [Å^3]	5828.8(5)	1596.11(9)
Z	8	2
F(000)	3088	722
Density (calculated) [Mg/m^3]	1.793	1.637
μ [mm^{-1}]	2.221	2.028
Absorption correction	Semi-empirical	Semi-empirical
Θ range for data collection [°]	2.320 to 25.998	2.127 to 31.290
h values	–19≤h≤19	–13≤h≤13
k values	–20≤k≤21	–16≤k≤15
l values	–25≤l≤25	–21≤l≤21
Reflections collected	31296	26214
Scan method	ω- and ψ-Scan	ω- and ψ-Scan
Data [$I > 2\sigma(I)$]	5715	9271
Parameters	267	297
R_{int}	0.0945	0.0270
R1	0.0888	0.0262
wR2	0.1226	0.0535
GooF (F^2)	0.870	1.039
Largest diff. peak and hole e.Å^{-3}	1.087 and –0.704	0.684 and –0.470

Compound	**1a**	**2**
Empirical formula	$C_{17}H_{31}Br_4N_1O_6P_2Sn_2$	$C_{20}H_{26}Cl_4N_1O_5P_2Sn_2$
Formula weight	964.39	801.54
Temperature [K]	173.15	173.15
Crystal size [mm]	0.173 x 0.114 x 0.112	0.157 x 0.154 x 0.153
Crystal system	Monoclinic	Monoclinic
Space group	C 1 2/c 1	P 1 c 1
a [Å]	34.2885(8)	8.4467(5)
b [Å]	8.36075(17)	8.8740(6)
c [Å]	21.1992(4)	20.0213(11)
α [°]	90	90
β [°]	101.555(2)	93.316(5)
ɣ [°]	90	90
Volume [Å^3]	5954.2(2)	1498.20(16)
Z	8	2
F(000)	3664	782
Density (calculated) [Mg/m^3]	2.152	1.777
μ [mm^{-1}]	7.184	2.160
Absorption correction	Semi-empirical	Semi-empirical
Θ range for data collection [°]	2.089 to 25.500	2.295 to 25.500
h values	–41≤h≤41	–10≤h≤10
k values	–10≤k≤10	–10≤k≤10
l values	–25≤l≤25	–24≤l≤24
Reflections collected	46986	15196
Scan method	ω- and ψ-Scan	ω- and ψ-Scan
Data [$I > 2\sigma(I)$]	5547	5508
Parameters	297	296
R_{int}	0.0433	0.0570
R1	0.0235	0.0687
wR2	0.0411	0.1193
GooF (F^2)	1.093	0.972
Largest diff. peak and hole e.Å^{-3}	0.368 and –0.387	1.100 and –0.597

Compound	**3**	**4**
Empirical formula	$C_{21}H_{31}Cl_4N_1O_{10}P_2Sn_2W_1$	$C_9H_9Cl_4N_1O_4Sn_2$
Formula weight	1082.44	574.35
Temperature [K]	173.15	173.15
Crystal size [mm]	0.144 x 0.134 x 0.09	0.144 x 0.094 x 0.058
Crystal system	Triclinic	Orthorhombic
Space group	$P\bar{1}$	Pbca
a [Å]	10.5910(4)	14.5495(6)
b [Å]	11.5327(4)	10.2315(4)
c [Å]	16.9449(6)	21.8290(8)
α [°]	102.515(3)	90
β [°]	95.617(3)	90
ɣ [°]	117.087(4)	90
Volume [Å^3]	1752.30(12)	3249.5(2)
Z	2	8
F(000)	1032	2160
Density (calculated) [Mg/m^3]	2.052	2.348
μ [mm^{-1}]	5.131	3.740
Absorption correction	Semi-empirical	Semi-empirical
Θ range for data collection [°]	2.217 to 25.499	2.333 to 25.498
h values	–12≤h≤12	–16≤h≤17
k values	–13≤k≤13	–4≤k≤12
l values	–20≤l≤20	–24≤l≤26
Reflections collected	17602	10477
Scan method	ω- and ψ-Scan	ω- and ψ-Scan
Data [$I > 2\sigma(I)$]	6511	3031
Parameters	395	183
R_{int}	0.0300	0.0383
R1	0.0372	0.0363
wR2	0.0616	0.0543
GooF (F^2)	1.065	1.012
Largest diff. peak and hole e.Å^{-3}	1.308 and –0.588	0.711 and –0.685

Compound	**4a**	**5**
Empirical formula	$C_{11}H_{12}Br_4N_1O_4Sn_2$	$C_{15}H_{23}Cl_4N_3O_2Sn_2$
Formula weight	793.25	656.54
Temperature [K]	123.15 K	173.15
Crystal size [mm]	0.132 x 0.119 x 0.062	0.111 x 0.079 x 0.022
Crystal system	Monoclinic	Monoclinic
Space group	P 1 21/c 1	P 1 21/n 1
a [Å]	9.1735(5)	12.9207(4)
b [Å]	15.7590(7)	9.2863(2)
c [Å]	14.6729(7)	19.6602(6)
α [°]	90	90
β [°]	104.734(5)	106.427(3)
ɣ [°]	90	90
Volume [Å^3]	2051.44(18)	2262.64(13)
Z	4	4
F(000)	1456	1272
Density (calculated) [Mg/m^3]	2.568	1.927
μ [mm^{-1}]	10.241	2.695
Absorption correction	Semi-empirical	Semi-empirical
Θ range for data collection [°]	2.296 to 29.185	2.160 to 25.498
h values	–10≤h≤11	–15≤h≤15
k values	–21≤k≤16	–11≤k≤11
l values	–19≤l≤18	–23≤l≤23
Reflections collected	13789	25529
Scan method	ω- and ψ-Scan	ω- and ψ-Scan
Data [$I > 2\sigma(I)$]	4840	4222
Parameters	211	239
R_{int}	0.0406	0.0368
R1	0.0500	0.0252
wR2	0.0610	0.0528
GooF (F^2)	1.053	1.090
Largest diff. peak and hole e.Å^{-3}	0.652 and –0.650	1.518 and –0.486

Compound	**5a**	**7**
Empirical formula	$C_{15}H_{23}Br_4N_3O_2Sn_2$	$C_{17}H_{22}Cl_3NO_5P_2Sn_2$
Formula weight	834.38	726.02
Temperature [K]	173.15	173.15
Crystal size [mm]	0.128 x 0.067 x 0.04	0.055 x 0.042 x 0.041
Crystal system	Monoclinic	Triclinic
Space group	P 1 21/n 1	$P\bar{1}$
a [Å]	12.9993(8)	9.1669(3)
b [Å]	9.6551(5)	11.4948(5)
c [Å]	19.8783(12)	13.0032(5)
α [°]	90	114.176(4)
β [°]	105.036	94.573(3)
ɣ [°]	90	95.669(3)
Volume [Å^3]	2409.5(3)	1232.93(9)
Z	4	2
F(000)	1560	704
Density (calculated) [Mg/m^3]	2.3	1.956
μ [mm^{-1}]	8.721	2.509
Absorption correction	Semi-empirical	Semi-empirical
Θ range for data collection [°]	2.122 to 29.166	2.252 to 25.497
h values	−16≤h≤17	−13≤k≤13
k values	−13≤k≤12	−13≤k≤13
l values	−25≤l≤25	−15≤l≤15
Reflections collected	16216	20016
Scan method	ω- and ψ-Scan	ω- and ψ-Scan
Data [$I > 2\sigma(I)$]	5593	4570
Parameters	239	275
R_{int}	0.0484	0.0352
R1	0.0624	0.0306
wR2	0.0666	0.0663
GooF (F^2)	1.028	1.052
Largest diff. peak and hole e.Å^{-3}	0.827 and −0.747	1.002 and −0.449

Compound	**8**
Empirical formula	$C_{16}H_{12}Cl_2N_2O_8Sn_2$
Formula weight	668.56
Temperature [K]	173.15
Crystal size [mm]	0.052 x 0.046 x 0.022
Crystal system	Triclinic
Space group	$P\bar{1}$
a [Å]	6.2734(10)
b [Å]	8.7969(16)
c [Å]	9.5351(14)
α [°]	74.154(15)
β [°]	105.036
ɣ [°]	84.642(14)
Volume [Å^3]	498.87(15)
Z	1
F(000)	320
Density (calculated) [Mg/m^3]	2.225
μ [mm^{-1}]	2.82
Absorption correction	Semi-empirical
Θ range for data collection [°]	2.243 to 25.492
h values	−7≤h≤7
k values	−10≤k≤10
l values	−11≤l≤11
Reflections collected	5755
Scan method	ω- and ψ-Scan
Data [$I > 2\sigma(I)$]	1859
Parameters	137
R_{int}	0.0827
R1	0.0603
wR2	0.0666
GooF (F^2)	0.1074
Largest diff. peak and hole e.Å^{-3}	1.519 and −1.263

Chapter 4

Compound	**8**	**9**
Empirical formula	$C_{38}H_{44}N_2O_{12}P_2Sn_2W_2$	$C_{25}H_{37}Cl_2N_1P_2Sn_2$
Formula weight	1387.77	729.78
Temperature [K]	173.15	173.15
Crystal size [mm]	0.112 x 0.072 x 0.023	0.19 x 0.18 x 0.13
Crystal system	Triclinic	Hexagonal
Space group	$P\bar{1}$	$P6_1$
a [Å]	9.7794(3)	18.2524(3)
b [Å]	14.5288(6)	18.2524(3)
c [Å]	17.9768(8)	17.1600(5)
α [°]	90.138(4)	90
β [°]	97.748(3)	90
ɣ [°]	101.139(3)	120
Volume [Å^3]	2482.12(18)	4950.94(18)
Z	2	6
F(000)	1320	2330
Density (calculated) [Mg/m^3]	1.857	1.561
μ [mm^{-1}]	5.732	1.792
Absorption correction	Semi-empirical	Semi-empirical
Θ range for data collection [°]	2.286 to 31.108	2.23 to 25.50
h values	–13≤h≤13	–22≤k≤22
k values	–19≤k≤19	–22≤k≤22
l values	–26≤l≤25	–20≤l≤20
Reflections collected	33962	47829
Scan method	ω- and ψ-Scan	ω- and ψ-Scan
Data [$I > 2\sigma(I)$]	14160	6145
Parameters	531	278
R_{int}	0.051	0.043
R1	0.0588	0.0217
wR2	0.1498	0.0564
GooF (F^2)	1.067	1.056
Largest diff. peak and hole e.Å^{-3}	6.150 and –2.318	0.426 and –0.279

Compound	**10**	**11**
Empirical formula	$C_{23}H_{33}Br_2N_1P_2Sn_2$	$C_{24}H_{20}S_4Sn_2$
Formula weight	782.64	674.02
Temperature [K]	173.15	173.15
Crystal size [mm]	0.15 x 0.13 x 0.08	0.192 x 0.16 x 0.018
Crystal system	Monoclinic	Monoclinic
Space group	$P\,1\,2_1/c\,1$	$P\,1\,2_1/n\,1$
a [Å]	13.3482(4)	11.6430(3)
b [Å]	17.6295(5)	11.5627(3)
c [Å]	15.5576(4)	18.0182(4)
α [°]	90	90
β [°]	99.415(3)	92.912(2)
ɣ [°]	90	90
Volume [Å^3]	3611.74(18)	2422.56(10)
Z	4	4
F(000)	1512	1312
Density (calculated) [Mg/m^3]	1.439	1.848
μ [mm^{-1}]	3.693	2.417
Absorption correction	Semi-empirical	Semi-empirical
Θ range for data collection [°]	2.194 to 25.499	2.094 to 30.914
h values	–16≤h≤16	–16≤h≤16
k values	–19≤k≤21	–16≤k≤15
l values	–18≤l≤18	–20≤l≤24
Reflections collected	30032	20423
Scan method	ω- and ψ-Scan	ω- and ψ-Scan
Data [$I > 2\sigma(I)$]	6735	6991
Parameters	254	271
R_{int}	0.0411	0.0338
R1	0.0248	0.0262
wR2	0.0543	0.063
GooF (F^2)	1.004	1.100
Largest diff. peak and hole e.Å^{-3}	0.543 and –0.401	0.750 and –0.603

Compound	**13**	**14**
Empirical formula	$C_{36}H_{75}Li_8N_4O_8$	$C_9H_{21}NO_2Si_1$
Formula weight	747.52	203.36
Temperature [K]	173.15	173.15
Crystal size [mm]	0.15 x 0.13 x 0.08	0.065 × 0.033 × 0.017
Crystal system	Triclinic	monoclinic
Space group	*P*-1	*C*m
a [Å]	12.3281(5)	10.6538(9)
b [Å]	12.6875(6)	10.2666(8)
c [Å]	18.2704(7)	5.9310(5)
α [°]	72.943(4)	90
β [°]	87.840(3)	116.775(8)
ɣ [°]	61.456(5)	90
Volume [Å^3]	2382.0(2)	90
Z	2	2
F(000)	814	224.0
Density (calculated) [Mg/m^3]	1.042	1.166
μ [mm^{-1}]	0.069	0.177
Absorption correction	Semi-empirical	Semi-empirical
Θ range for data collection [°]	2.348 to 31.066	5.838 to 64.952
h values	–17≤h≤17	–15 ≤h ≤ 15
k values	–18≤k≤18	–15 ≤k ≤15
l values	–24≤l≤26	–8 ≤ l ≤ 8
Reflections collected	38953	5820
Scan method	ω- and ψ-Scan	ω- and ψ-Scan
Data [$I > 2\sigma(I)$]	13721	1975
Parameters	576	73
R_{int}	0.0366	0.0243
R1	0.0548	0.0306
wR2	0.1547	0.0799
GooF (F^2)	1.021	1.072
Largest diff. peak and hole e.Å^{-3}	0.364 and –0.281	0.56 and –0.15

LIST OF CHARACTERIZED COMPOUNDS

Chapter 1

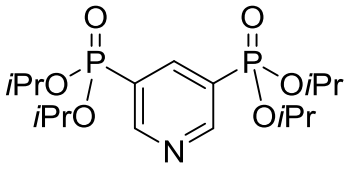

1

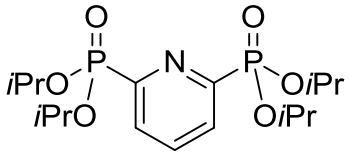

2

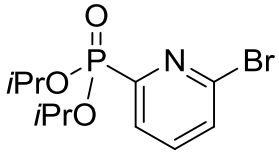

3

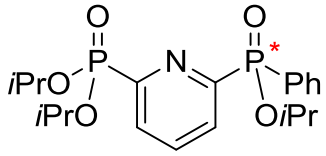

4

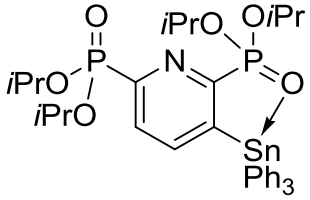

5

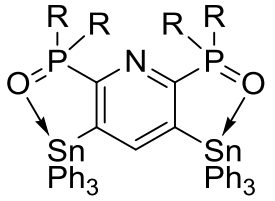

R = O*i*Pr

6

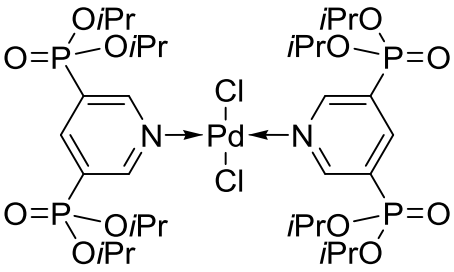

7

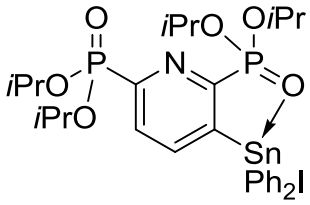

8

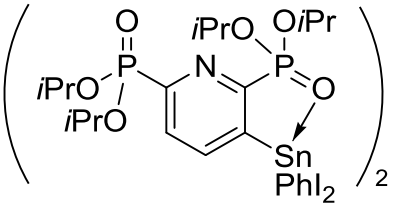

9

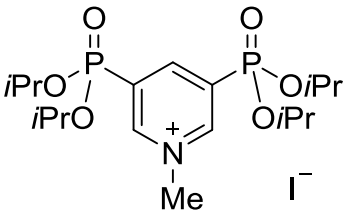

10

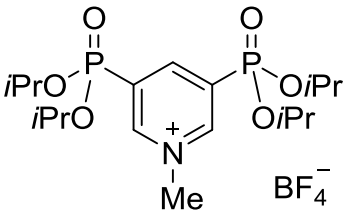

11

Chapter 2

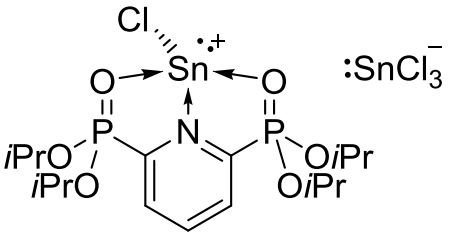

1

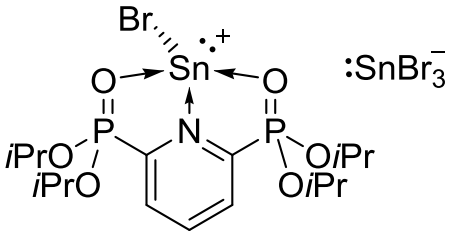

1a

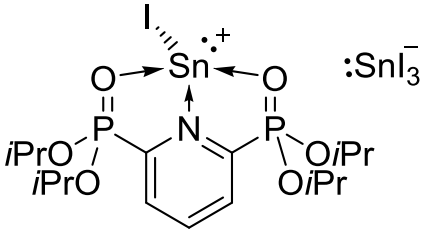

1b

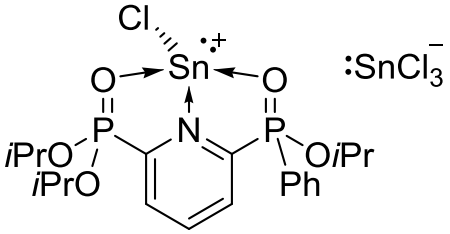

2b

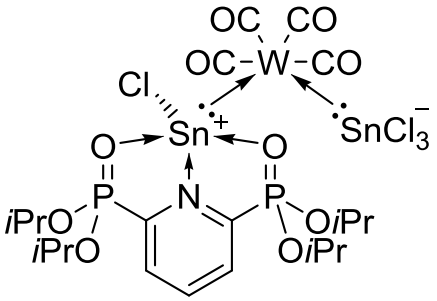

3

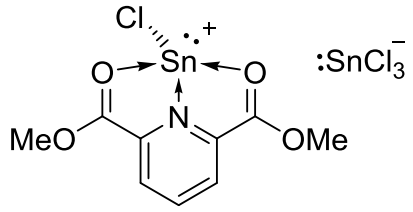
Cl
Sn
O
O
N
MeO
OMe
:SnCl3−

4

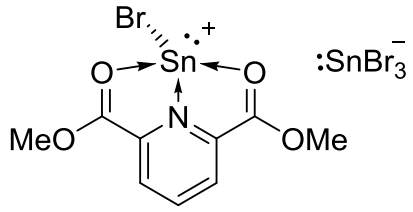
Br
Sn
O
O
N
MeO
OMe
:SnBr3−

4a

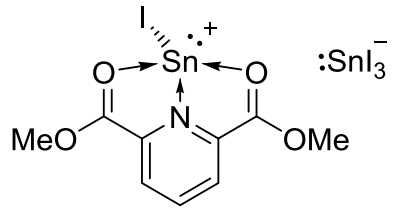
I
Sn
O
O
N
MeO
OMe
:SnI3−

4b

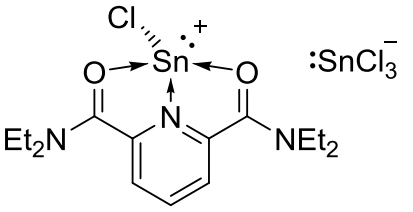
Cl
Sn
O
O
N
Et2N
NEt2
:SnCl3−

5

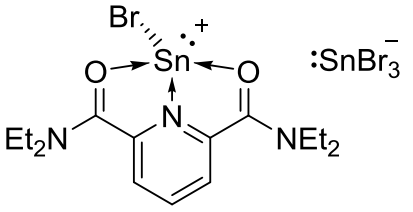
Br
Sn
O
O
N
Et2N
NEt2
:SnBr3−

5a

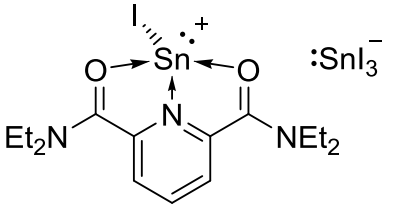
I
Sn
O
O
N
Et2N
NEt2
:SnI3−

5b

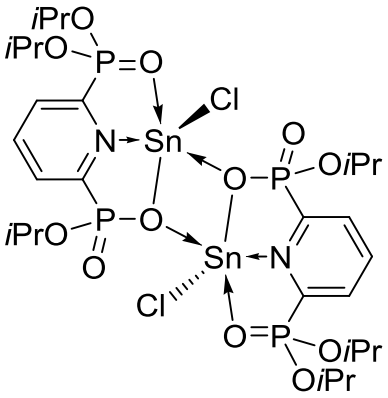
iPrO
iPrO
P=O
Cl
N
Sn
O
O
P
OiPr
iPrO
P
O
O
Sn
N
Cl
O
P
OiPr
OiPr

6

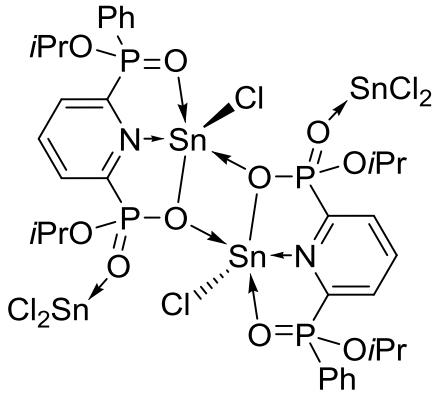
Ph
iPrO
P=O
Cl
SnCl2
N
Sn
O
O
P
OiPr
iPrO
P
O
O
Sn
N
Cl2Sn
Cl
O
P
OiPr
Ph

7

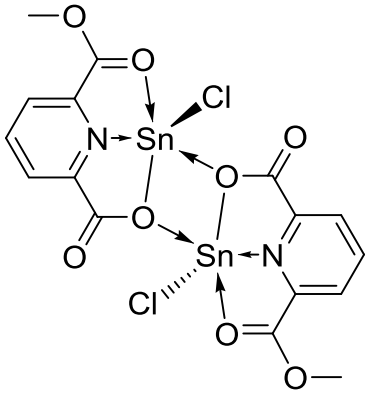
O
O
Cl
N
Sn
O
O
O
O
Sn
N
Cl
O
O

8

Chapter 4

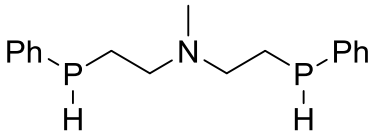

1

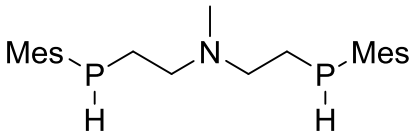

2

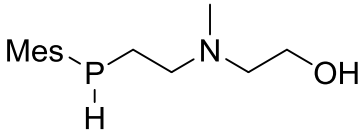

3

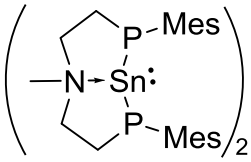

4

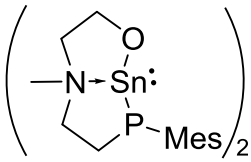

5

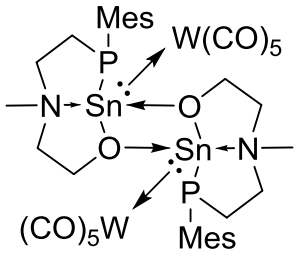

8

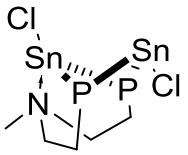

9

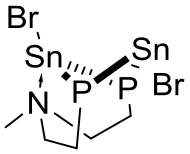

10

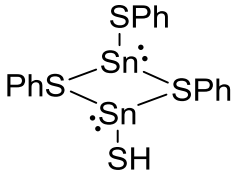

11

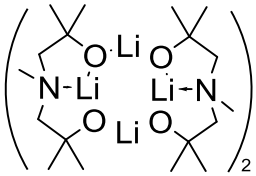

13

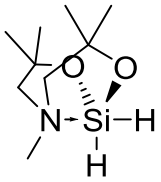

14

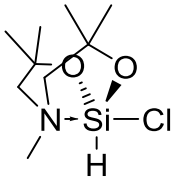

15

CURRICULUM VITAE

Personal details: Born 07.09.1985 in Syria

Citizenship: German and Syrian.

Employment to date:

Nov. 2012 – Scientific assistant at the Technische Universität Dortmund, Germany.

- Supervision of bachelor thesis, apprentices and undergraduates. In addition to teaching activities.

Nov. 2011 – Aug. 2012 Laboratory assistant at Taros Chemicals GmbH & Co. KG.

- Synthesis and purification of organic compounds.

Education:

Apr. 2013 – Preparation for Doctorate Thesis at the Technische Universität Dortmund, Germany.

Oct. 2010 – Apr. 2013 M.Sc. Chemistry at the Technische Universität Dortmund, Germany.

Sep. 2003 – Mar. 2008 B.Sc. Chemistry at the University of Damascus department of Applied Chemistry, Syria.

Further education:

Mar. 23 – 26.2017 Structure analysis of incommensurately modulated crystals and composite crystals. A practical introduction using JANA 2006. Bayreuth, Germany.

Feb. 23, Mar. 26.2017 Project Management.

Sep. 2013 – Apr. 2014 Innovation management.

Apr. 2013 – Jul. 2013 Allgemeine Betriebswirtschaftslehre.

Jan. 2009 – May 2010 DSH (Deutsche Sprachprüfung für den Hochschulzugang) with a total score 74 %.

Jan. 2008 – May 2008 TOEFL (Test of English as a Foreign Language) with a total score 517.

Skills:

Languages: German: good written and spoken.

English: good written and spoken.

	Arabic: native language.
Computer:	Good knowledge in Word, Excel and PowerPoint.
	Good knowledge in ChemOffice (Cambridge molecule editor software package), ShelX, PLATON, Olex^2 (crystal structures) and GaussView (theoretical chemistry).
Chemistry:	Working with air and moisture-sensitive compounds such as lithium organics under inert atmosphere using schlenk-line technique.
	Chromatographic purification.
	Molecule characterization using NMR, ESI/MS, MALDI, IR and X-ray.
Leadership:	Supervision of apprentices, undergraduates (up to 30 students) and bachelor thesis.

School:

Sep. 2000 – Jun 2003	High school in Damascus, Syria.
Sep. 1997 – Jun. 2000	Middle school in Damascus, Syria.
Sep. 1991 – Jun. 1997	Elementary school in Damascus, Syria.

Hobbies:

Outdoor sports specially, climbing.

PUBLICATION LIST

1. „**Neue Anorganische Zinnverbindungen als Katalysatoren für Polyurethaneherstellung**“

Hazem Alnasr, Andre Platzek, Klaus Jurkschat. Patent no. 5441975.

2. “**Introducing Stereogenic Centers to Group XIV Metallatranes**”

B. Glowacki, M. Lutter, H. Alnasr, R. Seymen, W. Hiller, K. Jurkschat, *Inorg. Chem.* **2017**, *56*, 4937–4949.

3. “**A Ferrocenyl-Backboned Unsymmetric O,C-Coordinating Ligand and Its Tin Derivatives**”

B. Janssen, H. Alnasr, M. Lutter, I. Krossing, K. Jurkschat, *ChemistryOpen* **2016**, *5*, 319 – 324.

The structure of about 200 compounds were determined by single-crystal X-ray Diffraction analysis for the Jurkschat research team.

Erklärung

Hiermit versichere ich, dass ich die vorliegende Arbeit selbst verfasst und keine außer den angegebenen Hilfsmitteln und Quellen benutzt habe, und dass die Arbeit in dieser oder ähnlicher Form noch bei keiner anderen Universität eingereicht wurde.

Hazem Alnasr